IEEE Guide for Bus Design in Air Insulated Substations

IEEE Power & Energy Society

Sponsored by the
Substations Committee

605™

IEEE
3 Park Avenue
New York, NY 10016-5997, USA

14 May 2010

IEEE Std 605™-2008
(Revision of
IEEE Std 605-1998 /
Incorporates
IEEE Std 605a-2010)

Copyright The Institute of Electrical and Electronics Engineers, Inc.
Provided by IHS under license with IEEE
No reproduction or networking permitted without license from IHS

Order Number: 02120914
Sold to:EGAT [700166108393] - VARRIS.Y@EGAT.CO.TH,
Not for Resale,2016-09-15 03:57:47 UTC

--`,,,,,,`,```,,``,,`,,`,-`-`,```,,,`---
Copyright The Institute of Electrical and Electronics Engineers, Inc.
Provided by IHS under license with IEEE
No reproduction or networking permitted without license from IHS
Order Number: 02120914
Sold to:EGAT [700166108393] - VARRIS.Y@EGAT.CO.TH,
Not for Resale,2016-09-15 03:57:47 UTC

IEEE Std 605™-2008
(Revision of
IEEE Std 605-1998 /
Incorporates
IEEE Std 605a-2010)

IEEE Guide for Bus Design in Air Insulated Substations

Sponsor

Substations Committee

of the

IEEE Power & Energy Society

Approved 10 December 2008

IEEE-SA Standards Board

Copyright The Institute of Electrical and Electronics Engineers, Inc.
Provided by IHS under license with IEEE
No reproduction or networking permitted without license from IHS

Order Number: 02120914
Sold to:EGAT [700166108393] - VARRIS.Y@EGAT.CO.TH,
Not for Resale,2016-09-15 03:57:47 UTC

The following permissions have been granted for material reprinted in this standard:

The author thanks the International Electrotechnical Commission (IEC) for permission to reproduce information from its International Standard 60076-10-1. All such extracts are copyright of IEC, Geneva, Switzerland. All rights reserved. Further information on the IEC is available from www.iec.ch. IEC has no responsibility for the placement and context in which the extracts and contents are reproduced by the author, nor is IEC in any way responsible for the other content or accuracy therein. Royalty-free permission to use this material is granted for world rights distribution, with permission to modify (with the appropriate notification to IEC in writing) and reprint in all future revisions and editions in all media known or hereinafter known. Copyright © 1993 IEC, Geneva, Switzerland.www.iec.ch.

Material reprinted with permission from CIGRE, Publication: "Calculated values of dynamic short circuit stress in a high voltage test structure with and without reclosure," ELECTRA 63, © 1979 CIGRE.

Royalty-free permission to use this material is granted for world rights distribution, with permission to modify (with the appropriate notification to IEC in writing) and reprint in all future revisions and editions in all media known or hereinafter known.

Information is extracted from ASCE 7-02; for further information, the complete text of the manual should be referenced at the following link: http://~vww.pubs.asce.or~/ASCE7.l1tml1?393909. The Structural Engineering Institute (SET) of ASCE has issued Errata to ASCE 7-02, which can be viewed at their website: http://www.seinstitite.or~/pdf/errata0204.

Abstract: A proper design of the substation bus ensures a safe and reliable operation of the substation and the power system. Two different types of buses are used in substations, the rigid bus and the strain (cable). This guide provides information on the different bus arrangements used in substations stating the advantages and disadvantages of each. Also it provides information as related to each bus type and construction. Once the bus type is selected, this guide provides the calculation tools for each bus type. Based on these calculations, the engineer can specify the bus size, forces acting on the bus structure, number of mounting structures required, and hardware requirements.

Keywords: ampacity, bus support, corona, electromagnetic, finite-element, forces, ice, mounting structure, rigid bus structures, short circuit, strain-bus structures, substation design, wind

The Institute of Electrical and Electronics Engineers, Inc.
3 Park Avenue, New York, NY 10016-5997, USA

Copyright © 2010 by the Institute of Electrical and Electronics Engineers, Inc.
All rights reserved. Published 14 May 2010. Printed in the United States of America.

Corrections were made to Clause 8, Clause 11, Clause 12, Annex C, Annex H, and Annex I as required by
IEEE Std 605a™-2010.

IEEE, National Electrical Safety Code, and NESC are a registered trademark in the U.S. Patent & Trademark Office, owned by The Institute of Electrical and Electronics Engineers, Incorporated.

National Electrical Code and NEC are registered trademarks in the U.S. Patent & Trademark Office, owned by The National Fire Protection Association.

PDF: ISBN 978-0-7381-5857-0 **STD95855**
Print: ISBN 978-0-7381-5858-7 **STDPD95855**

IEEE prohibits discrimination, harassment and bullying. For more information, visit http://www.ieee.org/web/aboutus/whatis/policies/p9-26.html.
No part of this publication may be reproduced in any form, in an electronic retrieval system or otherwise, without the prior written permission of the publisher.

Copyright The Institute of Electrical and Electronics Engineers, Inc.
Provided by IHS under license with IEEE
No reproduction or networking permitted without license from IHS

Order Number: 02120914
Sold to:EGAT [700166108393] - VARRIS.Y@EGAT.CO.TH,
Not for Resale,2016-09-15 03:57:47 UTC

IEEE Standards documents are developed within the IEEE Societies and the Standards Coordinating Committees of the IEEE Standards Association (IEEE-SA) Standards Board. The IEEE develops its standards through a consensus development process, approved by the American National Standards Institute, which brings together volunteers representing varied viewpoints and interests to achieve the final product. Volunteers are not necessarily members of the Institute and serve without compensation. While the IEEE administers the process and establishes rules to promote fairness in the consensus development process, the IEEE does not independently evaluate, test, or verify the accuracy of any of the information or the soundness of any judgments contained in its standards.

Use of an IEEE Standard is wholly voluntary. The IEEE disclaims liability for any personal injury, property or other damage, of any nature whatsoever, whether special, indirect, consequential, or compensatory, directly or indirectly resulting from the publication, use of, or reliance upon this, or any other IEEE Standard document.

The IEEE does not warrant or represent the accuracy or content of the material contained herein, and expressly disclaims any express or implied warranty, including any implied warranty of merchantability or fitness for a specific purpose, or that the use of the material contained herein is free from patent infringement. IEEE Standards documents are supplied "**AS IS**."

The existence of an IEEE Standard does not imply that there are no other ways to produce, test, measure, purchase, market, or provide other goods and services related to the scope of the IEEE Standard. Furthermore, the viewpoint expressed at the time a standard is approved and issued is subject to change brought about through developments in the state of the art and comments received from users of the standard. Every IEEE Standard is subjected to review at least every five years for revision or reaffirmation, or every ten years for stabilization. When a document is more than five years old and has not been reaffirmed, or more than ten years old and has not been stabilized, it is reasonable to conclude that its contents, although still of some value, do not wholly reflect the present state of the art. Users are cautioned to check to determine that they have the latest edition of any IEEE Standard.

In publishing and making this document available, the IEEE is not suggesting or rendering professional or other services for, or on behalf of, any person or entity. Nor is the IEEE undertaking to perform any duty owed by any other person or entity to another. Any person utilizing this, and any other IEEE Standards document, should rely upon his or her independent judgment in the exercise of reasonable care in any given circumstances or, as appropriate, seek the advice of a competent professional in determining the appropriateness of a given IEEE standard.

Interpretations: Occasionally questions may arise regarding the meaning of portions of standards as they relate to specific applications. When the need for interpretations is brought to the attention of IEEE, the Institute will initiate action to prepare appropriate responses. Since IEEE Standards represent a consensus of concerned interests, it is important to ensure that any interpretation has also received the concurrence of a balance of interests. For this reason, IEEE and the members of its societies and Standards Coordinating Committees are not able to provide an instant response to interpretation requests except in those cases where the matter has previously received formal consideration. A statement, written or oral, that is not processed in accordance with the IEEE-SA Standards Board Operations Manual shall not be considered the official position of IEEE or any of its committees and shall not be considered to be, nor be relied upon as, a formal interpretation of the IEEE. At lectures, symposia, seminars, or educational courses, an individual presenting information on IEEE standards shall make it clear that his or her views should be considered the personal views of that individual rather than the formal position, explanation, or interpretation of the IEEE.

Comments for revision of IEEE Standards are welcome from any interested party, regardless of membership affiliation with IEEE. Suggestions for changes in documents should be in the form of a proposed change of text, together with appropriate supporting comments. Recommendations to change the status of a stabilized standard should include a rationale as to why a revision or withdrawal is required. Comments and recommendations on standards, and requests for interpretations should be addressed to:

Secretary, IEEE-SA Standards Board
445 Hoes Lane
Piscataway, NJ 08854
USA

Authorization to photocopy portions of any individual standard for internal or personal use is granted by The Institute of Electrical and Electronics Engineers, Inc., provided that the appropriate fee is paid to Copyright Clearance Center. To arrange for payment of licensing fee, please contact Copyright Clearance Center, Customer Service, 222 Rosewood Drive, Danvers, MA 01923 USA; +1 978 750 8400. Permission to photocopy portions of any individual standard for educational classroom use can also be obtained through the Copyright Clearance Center.

Copyright The Institute of Electrical and Electronics Engineers, Inc.
Provided by IHS under license with IEEE
No reproduction or networking permitted without license from IHS

Order Number: 02120914
Sold to:EGAT [700166108393] - VARRIS.Y@EGAT.CO.TH,
Not for Resale,2016-09-15 03:57:47 UTC

Introduction

This introduction is not part of IEEE Std 605-2008, IEEE Guide for Bus Design in Air Insulated Substations.

This introduction provides some background on the rationale used to develop this guide. This information is meant to aid in the understanding and usage of this guide.

Buses consisting of conductor structures and the associated hardware comprise a large percentage of the substation equipment investment. The proper design of substation bus structures contributes to the safe and reliable operation of the substation and the power system. Two different types of buses are most commonly used in substations: rigid bus and strain bus (cable). This guide provides information on the different bus arrangements used in substations stating the advantages and disadvantages of each. Also, it provides information on each bus type and construction. Once the bus type is selected, this guide provides the calculation tools for each bus type. Based on these calculations, the engineer can specify the bus size, the forces acting on the bus structure, the number of mounting structures required, and the hardware requirements. However, this guide does not provide any guidance on the seismic design of bus structures, which is given in IEEE Std 693™-2005[a] and IEEE Std 1527™-2006.

Incorporate corrections were made to Clause 8, Clause 11, Clause 12, Annex C, Annex H, and Annex I as required by IEEE Std 605a™-2010.

Notice to users

Laws and regulations

Users of these documents should consult all applicable laws and regulations. Compliance with the provisions of this standard does not imply compliance to any applicable regulatory requirements. Implementers of the standard are responsible for observing or referring to the applicable regulatory requirements. IEEE does not, by the publication of its standards, intend to urge action that is not in compliance with applicable laws, and these documents may not be construed as doing so.

Copyrights

This document is copyrighted by the IEEE. It is made available for a wide variety of both public and private uses. These include both use, by reference, in laws and regulations, and use in private self-regulation, standardization, and the promotion of engineering practices and methods. By making this document available for use and adoption by public authorities and private users, the IEEE does not waive any rights in copyright to this document.

[a]Information on references can be found in Clause 2.

Copyright © 2010 IEEE. All rights reserved.

Copyright The Institute of Electrical and Electronics Engineers, Inc.
Provided by IHS under license with IEEE
No reproduction or networking permitted without license from IHS

Order Number: 02120914
Sold to:EGAT [700166108393] - VARRIS.Y@EGAT.CO.TH,
Not for Resale,2016-09-15 03:57:47 UTC

Updating of IEEE documents

Users of IEEE standards should be aware that these documents may be superseded at any time by the issuance of new editions or may be amended from time to time through the issuance of amendments, corrigenda, or errata. An official IEEE document at any point in time consists of the current edition of the document together with any amendments, corrigenda, or errata then in effect. In order to determine whether a given document is the current edition and whether it has been amended through the issuance of amendments, corrigenda, or errata, visit the IEEE Standards Association web site at http://ieeexplore.ieee.org/xpl/standards.jsp, or contact the IEEE at the address listed previously.

For more information about the IEEE Standards Association or the IEEE standards development process, visit the IEEE-SA web site at http://standards.ieee.org.

Errata

Errata, if any, for this and all other standards can be accessed at the following URL: http://standards.ieee.org/reading/ieee/updates/errata/index.html. Users are encouraged to check this URL for errata periodically.

Interpretations

Current interpretations can be accessed at the following URL: http://standards.ieee.org/reading/ieee/interp/index.html.

Patents

Attention is called to the possibility that implementation of this guide may require use of subject matter covered by patent rights. By publication of this guide, no position is taken with respect to the existence or validity of any patent rights in connection therewith. A patent holder or patent applicant has filed a statement of assurance that it will grant licenses under these rights without compensation or under reasonable rates, with reasonable terms and conditions that are demonstrably free of any unfair discrimination to applicants desiring to obtain such licenses. Other Essential Patent Claims may exist for which a statement of assurance has not been received. The IEEE is not responsible for identifying Essential Patent Claims for which a license may be required, for conducting inquiries into the legal validity or scope of Patents Claims, or determining whether any licensing terms or conditions are reasonable or non-discriminatory. Further information may be obtained from the IEEE Standards Association.

Copyright © 2010 IEEE. All rights reserved.
--`,,,,,,`,```,,``,,,,`,-`-`,```,,,`---
Copyright The Institute of Electrical and Electronics Engineers, Inc.
Provided by IHS under license with IEEE
No reproduction or networking permitted without license from IHS
Order Number: 02120914
Sold to:EGAT [700166108393] - VARRIS.Y@EGAT.CO.TH,
Not for Resale,2016-09-15 03:57:47 UTC

Participants

IEEE Std 605-2008

At the time this guide was submitted to the IEEE-SA Standards Board, the Substation Bus Design Working Group had the following membership:

Hanna Abdallah, *Chair*
Jean-Bernard Dastous, *Vice Chair*
Charles Haahr, *Secretary*

Ken Aldrige
Scott Andries
Radoslav Barac
Thomas B. Barnes
Joseph Bell
Romulus Berzescu
Robert Brown
Steven Brown
Mohamed Chaaban
Chih-Hung Chen
John Clayton
Randy Clelland
Alton Comans
Richard N. Crowdis
Brad Davis
Dennis DeCosta
Jeff Dicharry
Gary Engmann
William Esposito
D. Lane Garrett
John Havlik
Jim M. Hogan
William B. Kahanek
Richard P. Keil
Dave Kelley
Charles Koenig
Donald N. Laird
Jean Leduc
Debra Longtin
Julie Martin
A. P. Sakis Meliopoulos
Jeffrey Merryman
Robert Nowell
Edward J. O'Donnell
John Randolph
Steve Reiter
Ryland Revelle
Bruce Rockwell
Donald R. Rogers
Jerzy W. Salamon
John Casey Scoggins
Hamid Sharifnia
Devki Sharma
Steven Shelton
Borid Shvarstberg
Douglas Smith
David Stamm
Ryan Stargel
Brian Stephens
Brian K. Story
William R. Thompson
Brian Wallace
Keith Wallace
Diane Watkins
Don Wengerter
Kenneth White
Allen Xi
Roland Youngberg

Copyright © 2010 IEEE. All rights reserved.

Copyright The Institute of Electrical and Electronics Engineers, Inc.
Provided by IHS under license with IEEE
No reproduction or networking permitted without license from IHS

Order Number: 02120914
Sold to:EGAT [700166108393] - VARRIS.Y@EGAT.CO.TH,
Not for Resale,2016-09-15 03:57:47 UTC

The following members of the balloting committee voted on this guide. Balloters may have voted for approval, disapproval, or abstention.

William J. Ackerman
Steven Alexanderson
Stan Arnot
Ali Al Awazi
David Bassett
W. J. Bill Bergman
Steven Bezner
Wallace Binder
Michael Bio
Steven Brockshink
Chris Brooks
Steven Brown
Terry Burley
Michael Champagne
Chih-Hung Chen
Randy Clelland
Tommy Cooper
Jean-Bernard Dastrous
F. A. Denbrock
Donald Dunn
Gary Engmann
Rulon R. Fronk
D. Lane Garrett
Waymon Goch
Jalal Gohari
James Graham
Randall Groves
Charles Haahr
Kenneth S. Hanus
Steven Hensley
Lee S. Herron
Gary Heuston
Scott Hietpas
R. Jackson
Clark Jacobson
Mark Jurgemeyer
Gael Kennedy
Kamran Khan
Joseph L. Koepfinger
David W. Krause
Jim Kulchisky
Donald N. Laird
Chung-Yiu Lam
Thomas La Rose
Gerald Lee
Albert Livshitz
Debra Longtin
Federico Lopez
Keith Malmedal
Frank Mayle
Omar Mazzoni
Susan Mcnelly
Jeffrey Merryman
Gary Michel
Jerry Murphy
Jeffrey Nelson
Michael S. Newman
Robert Nowell
T. Olsen
Christopher Petrola
Paulette Payne Powell
Iulian Profir
John Randolph
Ryland Revelle
Michael Roberts
Charles Rogers
Thomas Rozek
Anne-Marie Sahazizian
Jerzy W. Salamon
Steven Sano
Bartien Sayogo
Devki Sharma
Douglas Smith
James E. Smith
Jerry Smith
John Spare
Ryan Stargel
Brian Stephens
Brian K. Story
Malcolm Thaden
James Timperley
John Vergis
Kenneth White
James Wilson
Larry Yonce
Roland Youngberg
Ahmed Zobaa

When the IEEE-SA Standards Board approved this guide on 10 December 2008, it had the following membership:

Robert M. Grow, *Chair*
Tom A. Prevost, *Vice Chair*
Steve M. Mills, *Past Chair*
Judith Gorman, *Secretary*

Victor Berman
Richard DeBlasio
Andrew Drozd
Mark Epstein
Alexander Gelman
William R. Goldbach
Arnold M. Greenspan
Kenneth S. Hanus
James Hughes
Richard H. Hulett
Young Kyun Kim
Joseph L. Koepfinger*
John Kulick
David J. Law
Glenn Parsons
Ronald C. Petersen
Chuck Powers
Narayanan Ramachandran
Jon Walter Rosdahl
Anne-Marie Sahazizian
Malcolm V. Thaden
Howard L. Wolfman
Don Wright

*Member Emeritus

Also included are the following nonvoting IEEE-SA Standards Board liaisons:

Satish K. Aggarwal, *NRC Representative*
Michael Janezic, *NIST Representative*

Copyright © 2010 IEEE. All rights reserved.
Copyright The Institute of Electrical and Electronics Engineers, Inc.
Provided by IHS under license with IEEE
No reproduction or networking permitted without license from IHS
Order Number: 02120914
Sold to:EGAT [700166108393] - VARRIS.Y@EGAT.CO.TH,
Not for Resale,2016-09-15 03:57:47 UTC

At the time this guide was submitted to the IEEE-SA Standards Board, the Substation Bus Design Working Group had the following membership:

Hanna Abdallah, *Chair*
Jean-Bernard Dastous, *Vice Chair*
Charles Haahr, *Secretary*

Ken Aldrige
Scott Andries
Radoslav Barac
Thomas B. Barnes
Joseph Bell
Romulus Berzescu
Robert Brown
Steven Brown
Mohamed Chaaban
Chih-Hung Chen
John Clayton
Randy Clelland
Alton Comans
Richard N. Crowdis
Brad Davis
Dennis DeCosta
Jeff Dicharry
Gary Engmann
William Esposito
D. Lane Garrett
John Havlik
Jim M. Hogan
William B. Kahanek
Richard P. Keil
Dave Kelley
Charles Koenig
Donald N. Laird
Jean Leduc
Debra Longtin
Julie Martin
A. P. Sakis Meliopoulos
Jeffrey Merryman
Robert Nowell
Edward J. O'Donnell
John Randolph
Steve Reiter
Ryland Revelle
Bruce Rockwell
Donald R. Rogers
Jerzy W. Salamon
John Casey Scoggins
Hamid Sharifnia
Devki Sharma
Steven Shelton
Borid Shvarstberg
Douglas Smith
David Stamm
Ryan Stargel
Brian Stephens
Brian K. Story
William R. Thompson
Brian Wallace
Keith Wallace
Diane Watkins
Don Wengerter
Kenneth White
Allen Xi
Roland Youngberg

The following members of the balloting committee voted on this guide. Balloters may have voted for approval, disapproval, or abstention.

Hanna Abdallah
William J. Ackerman
Steven Alexanderson
Stan Arnot
W. J. Bill Bergman
Steven Bezner
Wallace Binder
Michael Bio
A. James Braun
Steven Brown
Michael Champagne
Robert Christman
Randy Clelland
Robert Damron
Jean-Bernard Dastrous
Gary L. Donner
Michael Dood
Randall Dotson
Douglas J. Edwards
Gary Engmann
Eric Fujisaki
D. Lane Garrett
Jalal Gohari
Edwin Goodwin
James Graham
Randall Groves
David Harris
Steven Hensley
Lee S. Herron
Gary Heuston
Clark Jacobson
Gael Kennedy
Yuri Khersonsky
James Kinney
Joseph L. Koepfinger
Jim Kulchisky
Donald N. Laird
Chung-Yiu Lam
Debra Longtin
G. Luri
Daleep Mohla
Georges Montillet
Jerry Murphy
Arthur Neubauer
Michael S. Newman
Robert Nowell
T. Olsen
Lorraine Padden
Alexandre Parisot
Iulian Profir
John Randolph
Michael Roberts
Charles Rogers
Thomas Rozek
Anne-Marie Sahazizian
Bartien Sayogo
Dennis Schlender
Devki Sharma
Gil Shultz
Douglas Smith
James E. Smith
Jerry Smith
John Spare
Ryan Stargel
Brian Stephens
Gary Stoedter
Brian K. Story
Malcolm Thaden
John Vergis
Jane Verner
Kenneth White
James Wilson
Alexander Wong
Larry Yonce
Roland Youngberg

Copyright © 2010 IEEE. All rights reserved.

Copyright The Institute of Electrical and Electronics Engineers, Inc.
Provided by IHS under license with IEEE
No reproduction or networking permitted without license from IHS

Order Number: 02120914
Sold to:EGAT [700166108393] - VARRIS.Y@EGAT.CO.TH,
Not for Resale,2016-09-15 03:57:47 UTC

When the IEEE-SA Standards Board approved this amendment on 25 March 2010, it had the following membership:

Robert M. Grow, *Chair*
Richard H. Hulett, *Vice Chair*
Steve M. Mills, *Past Chair*
Judith Gorman, *Secretary*

Karen Bartleson
Victor Berman
Ted Burse
Clint Chaplin
Andy Drozd
Alexander Gelman
Jim Hughes
Young Kyun Kim
Joseph L. Koepfinger*
John Kulick
David J. Law
Hung Ling
Oleg Logvinov
Ted Olsen
Ronald C. Petersen
Thomas Prevost
Jon Walter Rosdahl
Sam Sciacca
Mike Seavey
Curtis Siller
Don Wright

*Member Emeritus

Also included are the following nonvoting IEEE-SA Standards Board liaisons:

Satish K. Aggarwal, *NRC Representative*
Richard DeBlasio, *DOE Representative*
Michael Janezic, *NIST Representative*

Lorraine Patsco
IEEE Standards Program Manager, Document Development

Soo Kim
IEEE Standards Program Manager, Technical Program Development

Copyright © 2010 IEEE. All rights reserved.

Copyright The Institute of Electrical and Electronics Engineers, Inc.
Provided by IHS under license with IEEE
No reproduction or networking permitted without license from IHS

Order Number: 02120914
Sold to:EGAT [700166108393] - VARRIS.Y@EGAT.CO.TH,
Not for Resale,2016-09-15 03:57:47 UTC

Contents

1. Overview 1
1.1 Scope 1
1.2 Purpose 2

2. Normative references 2

3. Definitions 3

4. Bus arrangements 4
4.1 Single Bus Single Breaker Arrangement (SBSB) 5
4.2 Main and Transfer Bus Arrangement (MTB) 6
4.3 Double Bus Single Breaker Arrangement (DBSB) 6
4.4 Ring Bus Arrangements (RB) 7
4.5 Breaker and Half Bus Arrangement (B-1/2) 8
4.6 Double Bus Double Breaker Arrangement (DBDB) 9
4.7 Bus Arrangements Comparison 10

5. Bus Design Considerations 12
5.1 Preliminary Bus Design Considerations 12
5.2 Construction Type 13
5.3 Disconnect Switches 15

6. Conductors 15
6.1 General 15
6.2 Materials 15
6.3 Rigid Conductors 18
6.4 Flexible Conductors 19
6.5 Field Bending of Rigid Conductors 20
6.6 Connections 21

7. Design procedure 25
7.1 Design specification 25
7.2 Select bus arrangement 25
7.3 Design considerations 25
7.4 Select conductor type 25
7.5 Structure design 26
7.6 Review calculations 27
7.7 Select materials 27

8. Ampacity 27
8.1 Heat Balance 27
8.2 Conductor Temperature Limits 29
8.3 Ampacity Tables 30

9. Corona and Radio Interference 30
9.1 Determination of corona performance 30
9.2 EMI tolerance of substation equipment 31
9.3 Reducing EMI 31
9.4 Reducing corona generated radiated and conductor signal interference 32

Copyright © 2010 IEEE. All rights reserved.

Copyright The Institute of Electrical and Electronics Engineers, Inc.
Provided by IHS under license with IEEE
No reproduction or networking permitted without license from IHS

Order Number: 02120914
Sold to:EGAT [700166108393] - VARRIS.Y@EGAT.CO.TH,
Not for Resale,2016-09-15 03:57:47 UTC

10. Overview of mechanical design of bus structures 33
10.1 Introduction 33
10.2 General mechanical design procedure 33
10.3 Calculation methods 35

11. Loads on bus structure 36
11.1 Gravitational loads 36
11.2 Wind loads 42
11.3 Short circuit loads 53
11.4 Thermal Loads 80

12. Dimensional, strength and other design considerations 83
12.1 Maximum allowable span based on vertical deflection limits 83
12.2 Maximum allowable span length based on conductor fiber stress 86
12.3 Simplified evaluation of insulator cantilever force 88
12.4 Strength of porcelain insulators 96
12.5 Induced vibrations 98
12.6 Natural frequency of rigid conductors 99
12.7 Vibration attenuation 100
12.8 Clearances considerations 102
12.9 Rigid bus fittings 102

Annex A (informative) Bibliography 103

Annex B (informative) Rigid bus connector ampacity 105

Annex C (informative) Thermal considerations for outdus bus-conductor design 115

Annex D (informative) Corona and substation bus design 139

Annex E (informative) Physical properties of common bus conductors 153

Annex F (informative) Calculation example of short circuit analysis on rigid bus systems 176

Annex G (informative) Calculation example of short circuit analysis on strain bus systems 183

Annex H (informative) Example rigid bus design 190

Annex I (informative) Example strain bus design 211

Copyright © 2010 IEEE. All rights reserved.

Copyright The Institute of Electrical and Electronics Engineers, Inc.
Provided by IHS under license with IEEE
No reproduction or networking permitted without license from IHS

Order Number: 02120914
Sold to:EGAT [700166108393] - VARRIS.Y@EGAT.CO.TH,
Not for Resale,2016-09-15 03:57:47 UTC

Copyright The Institute of Electrical and Electronics Engineers, Inc.
Provided by IHS under license with IEEE
No reproduction or networking permitted without license from IHS

Order Number: 02120914
Sold to:EGAT [700166108393] - VARRIS.Y@EGAT.CO.TH,
Not for Resale,2016-09-15 03:57:47 UTC

IEEE Guide for Bus Design in Air Insulated Substations

IMPORTANT NOTICE: This guide is not intended to ensure safety, security, health, or environmental protection. Implementers of the guide are responsible for determining appropriate safety, security, environmental, and health practices or regulatory requirements.

This IEEE document is made available for use subject to important notices and legal disclaimers. These notices and disclaimers appear in all publications containing this document and may be found under the heading "Important Notice" or "Important Notices and Disclaimers Concerning IEEE Documents." They can also be obtained on request from IEEE or viewed at http://standards.ieee.org/IPR/disclaimers.html

1. Overview

1.1 Scope

The information in this design guide is applicable to both rigid bus and strain bus designs for outdoor and indoor, air-insulated, alternating current substations. Ampacity, radio influence, vibration, and electromechanical forces resulting from gravity, wind, fault current, and thermal expansion are considered. Design criteria for conductor and insulator strength calculations are included.

This guide does not consider the following:

a) The electrical criteria for the selection of insulators (see IEEE Std 1313.2™-1999 [B22])

b) The seismic forces to which the substation may be subjected (see IEEE Std 693™-2005 and IEEE Std 1527™-2006)

c) The design of mounting structures

d) Design considerations for contaminated environments (see IEEE Std 1313.2-1999 [B22])

e) Installation methods

f) Design of direct current buses

Copyright © 2010 IEEE. All rights reserved.

Copyright The Institute of Electrical and Electronics Engineers, Inc.
Provided by IHS under license with IEEE
No reproduction or networking permitted without license from IHS

Order Number: 02120914
Sold to:EGAT [700166108393] - VARRIS.Y@EGAT.CO.TH,
Not for Resale,2016-09-15 03:57:47 UTC

1.2 Purpose

Substation rigid and strain bus structure design involves electrical, mechanical, and structural considerations. It is the purpose of this guide to integrate these considerations into one document. Special considerations are given to fault current force calculations. The factors considered include the decrement of the fault current, the flexibility of supports, and the natural frequency of the bus. These factors are mentioned in ANSI C37.32-1996 but are not taken into consideration in the equations presented in that standard, including intended users and benefits to users.

2. Normative references

The following referenced documents are indispensable for the application of this document (i.e., they must be understood and used, so that each referenced document is cited in text and its relationship to this document is explained). For dated references, only the edition cited applies. For undated references, the latest edition of the referenced document (including any amendments or corrigenda) applies.

AA-ADM-1, Aluminum Design Manual, 2005.[1]

Accredited Standards Committee C-2, National Electrical Safety Code® (NESC®).[2]

ANSI C29.9-1983 (Reaff 2002), American National Standard for Wet-Process Porcelain Insulators (Apparatus, Post Type).[3]

ANSI C37.32-1996, American National Standard for High-Voltage Air Disconnect Switches Interrupter Switches, Fault Initiating Switches, Grounding Switches, Bus Supports and Accessories Control Voltage Ranges—Schedule of Preferred Ratings, Construction Guidelines and Specifications.

ASCE 7-05, Minimum Design Loads for Buildings and Other Structures.[4]

ASTM B188-02, Standard Specification for Seamless Copper Bus Pipe and Tube.[5]

ASTM B241/B241M-02, Standard Specification for Aluminum and Aluminum-Alloy Seamless Pipe and Seamless Extruded Tube.

AWS D1.2-2003, Structural Welding Code–Aluminum.[6]

IEEE Std C37.30™-1997, IEEE Standard Requirements for High-Voltage Switches.[7,8]

[1]Aluminum Association publications are available from The Aluminum Association, 1525 Wilson Boulevard, Suite 600, Arlington, VA 22209 (www.aluminum.org).
[2]The NESC is available from the Institute of Electrical and Electronics Engineers, 445 Hoes Lane, Piscataway, NJ 08854, USA (http://standards.ieee.org).
[3]ANSI publications are available from the Sales Department, American National Standards Institute, 25 West 43rd Street, 4th Floor, New York, NY 10036, USA (http://www.ansi.org/).
[4]ASCE publications are available from the American Society of Civil Engineers, 1801 Alexander Bell Drive, Reston, VA 20191-4400, USA (www.asce.org).
[5]ASTM publications are available from the American Society for Testing and Materials, 100 Barr Harbor Drive, West Conshohocken, PA 19428-2959, USA (http://www.astm.org/).
[6]AWS publications are available from the American Welding Society, 2671 W. 81st Street, Hialeah, FL 33016 (www.awspubs.com).
[7]The IEEE standards or products referred to in this clause are trademarks of the Institute of Electrical and Electronics Engineers, Inc.

Copyright © 2010 IEEE. All rights reserved.

Copyright The Institute of Electrical and Electronics Engineers, Inc.
Provided by IHS under license with IEEE
No reproduction or networking permitted without license from IHS

Order Number: 02120914
Sold to:EGAT [700166108393] - VARRIS.Y@EGAT.CO.TH,
Not for Resale,2016-09-15 03:57:47 UTC

IEEE Std 693™-2005, IEEE Recommended Practice for Seismic Design of Substations.

IEEE Std 1527™-2006, IEEE Recommended Practice for the Design of Flexible Buswork Located in Seismically Active Areas.

NEMA CC 1-2005, Electric Power Connectors for Substations.[9]

NFPA 70, 2007 Edition, National Electrical Code® (NEC®).[10]

3. Definitions

For the purposes of this document, the following terms and definitions apply. *The IEEE Standards Dictionary: Glossary of Terms & Definitions* should be referenced for terms not defined in this clause.[11]

aeolian vibration: The vibration of a structure induced by the flow of air around or through it.

ampacity: The current-carrying capacity, expressed in amperes, of an electric conductor under stated thermal conditions.

annealing: The sustained heating of a material, such as metal or glass, at a known high temperature, followed by the gradual cooling of the material; a process that is carried out to reduce hardness or brittleness, to eliminate various stresses and weaknesses, or to produce other qualities.

bus: A conductor or group of electrical conductors serving as common connections between circuits, generally in the form of insulated cable, rigid rectangular or round bars, or stranded overhead cables held under tension.

bus structure: An assembly of bus conductors, with associated connection joints and insulating supports.

bus support: An insulating support for a bus.

NOTE—A bus support includes one or more insulator units with fittings for fastening to the mounting structure and for receiving the bus.[12]

conduction: The transfer of heat through a medium while the medium itself experiences no mass movement as a whole. *Contrast*: **convection; radiation**.

convection: The transfer of heat that occurs when a fluid flows over a solid body (like wind around a conductor), when the temperature of the fluid and the solid boundary are different. *Contrast*: **conduction; radiation**.

corona: A luminous discharge due to ionization of the air surrounding a conductor, caused by a voltage gradient exceeding a certain critical value.

---

[8]IEEE publications are available from the Institute of Electrical and Electronics Engineers, 445 Hoes Lane, Piscataway, NJ 08854, USA (http://standards.ieee.org).
[9]NEMA publications are available from Global Engineering Documents, 15 Inverness Way East, Englewood, CO 80112, USA (http://global.ihs.com/).
[10]NFPA publications are available from Publication Sales, National Fire Protection Association, 1 Batterymarch Park, P.O. Box 9101, Quincy, MA 02269-9101, USA (http://nfpa.org/codes/index.html).
[11] *The IEEE Standards Dictionary: Glossary of Terms & Definitions* is available at http://shop.ieee.org/.
[12]Notes in text, tables, and figures are given for information only and do not contain requirements needed to implement the standard.

Copyright © 2010 IEEE. All rights reserved.

Copyright The Institute of Electrical and Electronics Engineers, Inc.
Provided by IHS under license with IEEE
No reproduction or networking permitted without license from IHS

Order Number: 02120914
Sold to:EGAT [700166108393] - VARRIS.Y@EGAT.CO.TH,
Not for Resale,2016-09-15 03:57:47 UTC

damping: (1) The temporal decay of the amplitude of a free oscillation of a system, associated with energy loss from the system. (2) A dynamic property of a vibrating structure that indicates its ability to dissipate mechanical energy. (3) An energy dissipation mechanism that reduces the response amplification and broadens the vibratory response over frequency in the region of resonance.

drag: The force acting on a body when a fluid flows around it (like wind around a conductor).

drag coefficient: A factor representing the effect of drag on a body.

emissivity: The ratio of power radiated by a material body to the power radiated by a blackbody at the same temperature.

mounting structure: A structure for mounting an insulating support.

natural frequency: A frequency at which a body or system vibrates due to its own physical characteristics (mass and stiffness) when the body or system is distorted and then released.

radiation: (1) The action of emitting radiant energy in the form of waves or particles. (2) The transfer of heat by radiation. *Contrast*: **conduction; convection**.

rigid-bus structure: A bus structure composed of rigid conductors supported by rigid insulators.

spring constant: A constant representing the equivalent resistance to displacement of a support under a load in a given direction.

strain-bus structure: A bus structure composed of flexible conductors supported by strain insulators.

tensile strength: The maximum tensile stress (stretching) that a material can withstand without failure.

yield strength: The stress level at which a material attains a specified permanent (plastic) deformation, usually 0.2% of the original gauge length, indicative of when a material begins to deform permanently (plastically) under loading.

Young's modulus: A mechanical property of a material representing its resistance to elongation in the elastic range of deformation. Specifically, Young's modulus is the elastic modulus for tension or tensile stress, and it is the force per unit cross section of the material divided by the fractional increase in length resulting from the stretching of a standard rod or wire of the material.

4. Bus arrangements

Several important factors affect the selection of bus arrangements. These factors include but are not limited to cost, safety, reliability, simplicities of relaying, flexibility of operation, ease of maintenance, available ground area, location of connecting lines, provision for expansion, and appearance.

In general, bus arrangements require disconnect switches to be installed on each side of the breaker to provide a visual opening when a breaker is taken out of service during maintenance or repair. For safety and reliability, the electric clearances must meet appropriate codes and recommendations. Insulation coordination studies should be performed to calculate the voltage levels that result from lightning surge, switching surge, or due to temporary fault conditions. To improve reliability, the electric connections should be simple; the more complex the connections, the more chances that a faulty condition will occur.

Copyright © 2010 IEEE. All rights reserved.

Copyright The Institute of Electrical and Electronics Engineers, Inc.
Provided by IHS under license with IEEE
No reproduction or networking permitted without license from IHS

Order Number: 02120914
Sold to:EGAT [700166108393] - VARRIS.Y@EGAT.CO.TH,
Not for Resale,2016-09-15 03:57:47 UTC

Buses are typically arranged to allow access to equipment for maintenance or replacement due to failure or upgrades. In addition, bus arrangements should provide for future growth, including consideration of disconnect switches that allow for continuity of service during construction.

This subclause consists of descriptions of substation bus arrangements that are used today.

4.1 Single bus single breaker arrangement (SBSB)

The single bus single breaker arrangement shown in Figure 1 consists of one main bus that contains positions for several circuits. The circuits are normally connected via circuit breakers but can be connected via circuit switchers, which are motor or manually operated switches. The single bus single breaker arrangement is generally applied in substations from distribution voltage through 121 kV to 161 kV and in locations where system reliability is not critical.

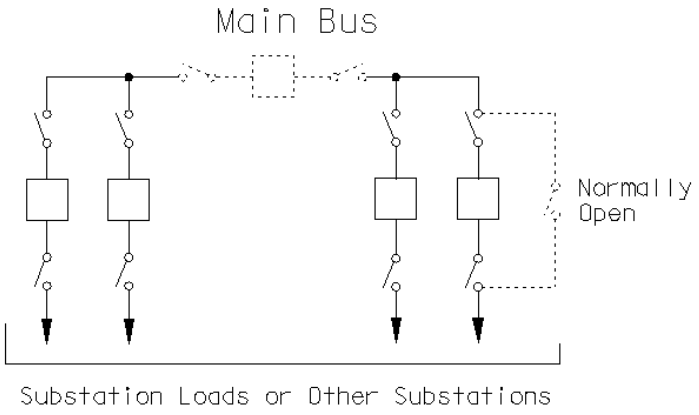

Figure 1—Single bus breaker

The single bus single breaker arrangement is the simplest to operate but offers the least reliability and operational flexibility.

A breaker failure or bus fault condition will require the tripping of all breakers connected to the bus causing power loss to all the circuits connected to that bus.

To increase the reliability of a single bus single breaker arrangement, a bus-sectionalizing breaker can be installed on the bus, as shown in Figure 1 with dashed lines. As a result, a bus fault or breaker failure will lead to the loss of only part of the substation.

To improve operating flexibility, a normally open bypass circuit may be installed in parallel with the breaker (see Figure 1). The bypass may be a switch or fuse, depending on voltage and current levels. When the bypass is closed, the breaker may be taken out of service for maintenance or replacement without disrupting the circuit. While the breaker is bypassed, the associated protective relays will be disabled, and a fault on the circuit may result in the loss of the entire bus. See Table 1 for the advantages and disadvantages of a single bus single breaker arrangement.

Copyright © 2010 IEEE. All rights reserved.

Copyright The Institute of Electrical and Electronics Engineers, Inc.
Provided by IHS under license with IEEE
No reproduction or networking permitted without license from IHS

Order Number: 02120914
Sold to:EGAT [700166108393] - VARRIS.Y@EGAT.CO.TH,
Not for Resale,2016-09-15 03:57:47 UTC

4.2 Main and transfer bus arrangement (MTB)

The main and transfer bus arrangement is a modification to the single bus arrangement as shown in Figure 2. This arrangement consists of two buses, a main and a transfer. Each circuit bay consists of one breaker and three switches, except the transfer breaker bay, which requires only two switches. The main bus is normally energized, and all circuits are serviced from the main bus as shown in Figure 2(a).

The addition of the transfer bus and transfer breaker allows taking any breaker out of service while the associated circuit remains in service. When a breaker is taken out of service, the transfer breaker and its normally open switches are closed, the circuit breaker and its switches are opened. Figure 2(b) shows circuit #1 breaker out of service and circuit #1 serviced by the transfer breaker.

The use of a transfer breaker for more than one circuit requires a selector switch to select the appropriate protective and control scheme. The selector switch arrangement complicates the protective and control schemes, which result in additional work during the initial construction period and operation.

The main and transfer bus arrangement shown in Figure 2(a) requires a considerable amount more of bus conductor, insulators, and material for bus and switch mounting structures as compared with the single breaker arrangement (Figure 1). This increases the foundation requirements and therefore drives the cost high. See Table 1 for the advantages and disadvantages of a main and transfer bus arrangement.

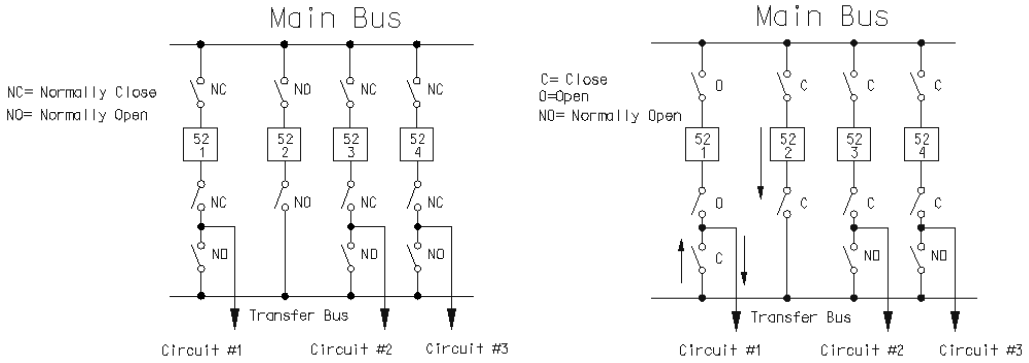

(a) Normal operation (b) Transfer breaker sparing circuit#1 breaker

Figure 2—Main and transfer bus arrangement

4.3 Double bus single breaker arrangement (DBSB)

The double bus single breaker arrangement shown in Figure 3 is a modification of the sectionalized radial single bus. This arrangement consists of two main buses connected together through a circuit breaker. Each circuit uses a circuit breaker and three disconnect switches and can be connected to either bus through disconnect switches. This arrangement allows all circuits to be connected to one bus in case of an outage on the other bus.

This arrangement is used in areas where high contamination is expected. Buses are taken out of service to clean the insulators. It also allows split bus operation if system conditions require it. A bus tie breaker may be added to increase the system flexibility by allowing split bus operation. A transfer breaker may be added, as shown in Figure 3(b), to allow bypassing a circuit breaker: Additional disconnect allows for connecting circuits #1 or #2 directly to the main bus #1, if a corresponding circuit breaker should be taken out of service. For example, to spare circuit #1 breaker, we should open all three disconnects adjacent to the breaker and close a normally open

Copyright © 2010 IEEE. All rights reserved.

Copyright The Institute of Electrical and Electronics Engineers, Inc.
Provided by IHS under license with IEEE
No reproduction or networking permitted without license from IHS

Order Number: 02120914
Sold to:EGAT [700166108393] - VARRIS.Y@EGAT.CO.TH,
Not for Resale,2016-09-15 03:57:47 UTC

disconnect between circuit #1 and the main bus #1. After this is done, circuit #1 may stay in service; it will be switched by a breaker installed between main buses #1 and #2. During this period of time, circuit #2 should be fed from main bus #2; see Table 1 for the advantages and disadvantages of a double bus single breaker arrangement.

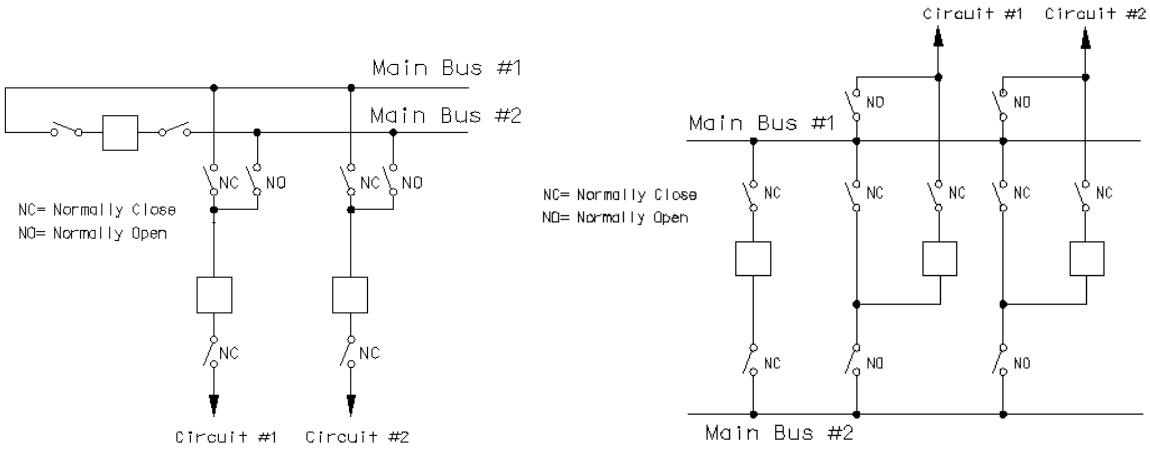

(a) Option 1 (b) Option 2

Figure 3—Double bus single breaker arrangement

4.4 Ring bus arrangements (RB)

In the ring bus arrangement, each circuit is connected between two breakers. The breakers are arranged in a series connection to form the "ring." In the ring bus arrangement, one breaker per circuit is possible as shown in Figure 4. The switchyard is normally operated with all breakers in the closed position. Power flow is evenly distributed because the ring bus operates as a single node.

Copyright © 2010 IEEE. All rights reserved.

Copyright The Institute of Electrical and Electronics Engineers, Inc.
Provided by IHS under license with IEEE
No reproduction or networking permitted without license from IHS

Order Number: 02120914
Sold to:EGAT [700166108393] - VARRIS.Y@EGAT.CO.TH,
Not for Resale,2016-09-15 03:57:47 UTC

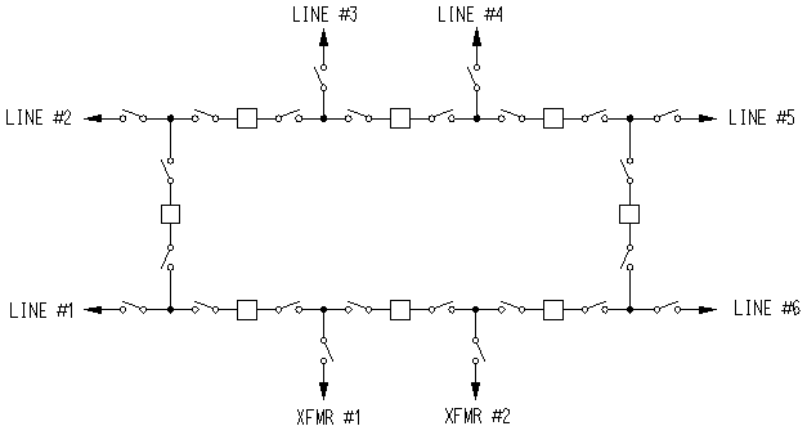

Figure 4—Ring bus arrangement (eight breakers—eight circuits[13])

By opening selected breakers, any circuit can be removed from service without affecting service to the other lines. Line disconnect switches are often applied to allow a circuit to be removed from service and to allow the remaining elements to remain in service with the ring partially open. Sources of generation or redundant circuits should not be terminated on adjacent positions of the ring bus; this strategy will prevent a failed circuit breaker from removing two sources of generation or two feeds to the same load from service.

The bus is reduced to connections between equipment; therefore, typically it requires much less bus, insulators, and mounting structures than the other arrangements discussed previously except the single bus single breaker arrangement. The protective and operating schemes are simple compared with the main transfer bus arrangement.

Breaker maintenance is easily accomplished without taking a line out of service by opening that breaker and associated disconnect switches. Portions of the bus can be de-energized, but a circuit would also have to be taken out of service at the same time. Power flow may be restricted during maintenance and emergency operations.

The ring bus arrangement is very reliable when all breakers are closed and the ring is intact. Typically, the breakers on either side of a circuit are opened when the circuit is taken out of service, opening the ring. Under this scenario, a fault on a second circuit may split the remaining circuits into two isolated operating systems. A similar situation may occur if a single breaker is taken out of service for maintenance. However, with breakers becoming more maintenance free, the ring bus arrangement is becoming more popular. See Table 1 for the advantages and disadvantages of a ring bus arrangement.

4.5 Breaker and half bus arrangement (B-1/2)

The breaker and half bus arrangement shown in Figure 5 consists of two main buses that are normally energized. Three breakers are required to serve two circuits. The middle breaker is common between two circuits and, hence, the name breaker and half bus arrangement. Any breaker or bus can be taken out of service without interruption of service. Faults on one circuit do not affect the other circuit unless the associated breaker fails to trip.

[13]Usually a ring bus is limited to eight breakers in a ring, but there may be more than eight breakers depending on particular conditions, which include loading of the circuits, reliability constraints, and so on.

Copyright © 2010 IEEE. All rights reserved.

Copyright The Institute of Electrical and Electronics Engineers, Inc.
Provided by IHS under license with IEEE
No reproduction or networking permitted without license from IHS

Order Number: 02120914
Sold to:EGAT [700166108393] - VARRIS.Y@EGAT.CO.TH,
Not for Resale,2016-09-15 03:57:47 UTC

This arrangement is costly due to the number of breakers and switches needed, and it requires a large ground area. However, it uses approximately 25% less equipment than the double bus double breaker arrangement for each circuit.

This arrangement is used for substations where reliability and service continuity is important. This arrangement is used extensively for voltage levels above 345 kV and some 230 kV substations due to the importance of these substations. Line switches can be added if required.

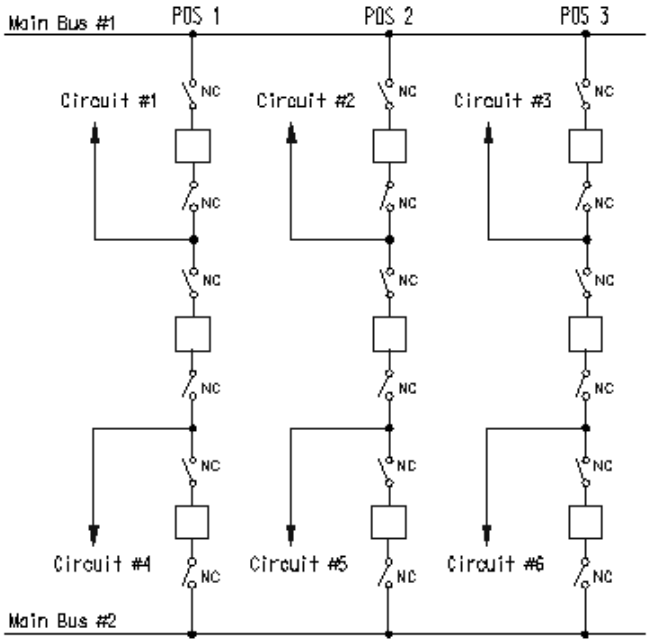

Figure 5—Breaker and half bus arrangement

4.6 Double bus double breaker arrangement (DBDB)

This bus arrangement, shown in Figure 6, consists of two main buses with two breakers and four switches per circuit. Any breaker or bus can be taken out of service for maintenance without an interruption to service. Split bus operation is possible. This bus arrangement is considered to be the most reliable.

This arrangement requires a large ground area. It is the most expensive one because it requires the most equipment per circuit. This bus arrangement requires a considerable amount of material for mounting structures.

This bus arrangement is rarely used at this time due to its cost and the space required.

Copyright © 2010 IEEE. All rights reserved.

Copyright The Institute of Electrical and Electronics Engineers, Inc.
Provided by IHS under license with IEEE
No reproduction or networking permitted without license from IHS

Order Number: 02120914
Sold to:EGAT [700166108393] - VARRIS.Y@EGAT.CO.TH,
Not for Resale,2016-09-15 03:57:47 UTC

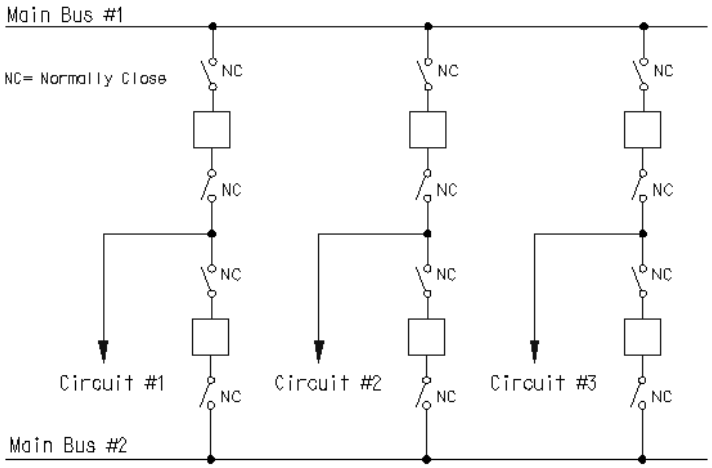

Figure 6—Double bus double breaker arrangement

4.7 Bus arrangements comparison

The advantages and disadvantages of each of the arrangements are listed in Table 1.

Copyright © 2010 IEEE. All rights reserved.

Copyright The Institute of Electrical and Electronics Engineers, Inc.
Provided by IHS under license with IEEE
No reproduction or networking permitted without license from IHS

Order Number: 02120914
Sold to:EGAT [700166108393] - VARRIS.Y@EGAT.CO.TH,
Not for Resale,2016-09-15 03:57:47 UTC

Table 1—Bus arrangements comparison

Bus arrangements	Advantages	Disadvantages	Cost (NOTE 1)	Land (m^2) (NOTE 2)
SBSB	Lowest cost Small land area Easy to expand Simple to operate Simple protective schemes	Low reliability Bus or breaker fault causes loss of entire station Breaker maintenance requires the associated circuit outage	100% 120% (with sect. breaker)	3160 3810 (with sect. breaker)
MTB	Easy to expand Allows for breaker maintenance Increased flexibility over single bus	Low reliability Bus or breaker fault causes loss of entire station Increased complexity over single bus Complex protective scheme Large land area required	140%	5960
DBSB	Allows for outage on any one of the buses Increased flexibility over single bus May allow for breaker maintenance	Low reliability Bus or breaker fault causes loss of entire station Increased complexity over single bus High cost Very large land area required	175% (Opt.1) 190% (Opt.2)	9290 (Opt.1) 11 520 (Opt.2)
RB	High reliability Flexible operation Allows for breaker maintenance Bus fault does not affect continuity of operation	Extensive relaying and control schemes Breaker failure results in loss of two circuits Large land area required May split into two operating systems	125%	5720
B-1/2	Easy to expand High reliability Flexible operation Allows for breaker maintenance Bus fault does not affect continuity of operation	High cost Extensive relaying and control schemes Large land area required	145%	4600
DBDB	Easy to expand Very high reliability Very flexible operation Allows for breaker maintenance Bus fault does not affect continuity of operation Breaker failure results in loss of only one circuit	High cost Large land area required Extensive relaying and control schemes	190%	5810

NOTE 1—Cost in percent is given to illustrate the cost relationship among the different bus arrangements with the SBSB design as the base.

NOTE 2—Metric values have been rounded to the nearest square meter.

NOTE 3—System voltage is 230 kV.

NOTE 4—Number of circuits in all bus arrangements is 4.

NOTE 5—Similar protective schemes have been used for each bus and line as required.

NOTE 6—Cost of land or control house is not included in the estimate.

NOTE 7—Unit costs used in this table to obtain estimates for each arrangements are installed costs, including cost of equipment, foundation, steel, design, engineering, construction supervision, control circuits, and so on.

Copyright © 2010 IEEE. All rights reserved.

Copyright The Institute of Electrical and Electronics Engineers, Inc.
Provided by IHS under license with IEEE
No reproduction or networking permitted without license from IHS

Order Number: 02120914
Sold to:EGAT [700166108393] - VARRIS.Y@EGAT.CO.TH,
Not for Resale,2016-09-15 03:57:47 UTC

5. Bus design considerations

Substation bus systems provide the following functions:

a) The means to allow more than one electric circuit to connect to the substation

b) The means for incoming and outgoing circuit termination

c) The means for electrically interconnecting switching and other equipment such as transformers, capacitors banks, reactors, and so on

Today, several types of bus systems are used in substations: rigid bus, strain (flexible) bus, and gas-insulated bus. The rigid bus is a common type of bus system in use in North America. The strain conductor bus is often used in high- and extra-high-voltage substations (230 kV and higher) where either high-capacity or increased seismic withstand capability is required, and the area is available. The gas-insulated bus is suitable for unique environmental or space-constrained applications. The gas bus may be suitable when available ground area in a substation is very small, requiring only 10% of the area of air-insulated substations. Also, it is used in urban and industrial locations subject to space constraints and pollution, mountainous areas (extra site preparation, altitude, snow, and ice concerns), coastal areas (salt associated problems), underground substations, and areas where aesthetics are major concerns.

5.1 Preliminary bus design considerations

Prior to the start of a bus design, several design conditions need consideration. These design conditions shall establish the minimum electrical and structural requirements for the type of bus being considered. Preliminary design considerations are as follows:

a) Number and type of circuits served by the bus, and the reliability desired or required for these circuits

a) Site location and size

b) Seismic activity

c) Conductor ampacity

d) Maximum anticipated fault current

e) Maximum operating voltage

f) Fault clearing time

g) Electrical and safe working clearances

h) Phase spacing

i) Bus conductor temperature

j) Maximum and minimum ambient temperature

k) Maximum anticipated wind speed

l) Maximum anticipated icing conditions combined with wind

m) Altitude and latitude of the substation

n) Basic substation layout

o) Standard design practices

p) Hardware and equipment availability

Copyright © 2010 IEEE. All rights reserved.

Copyright The Institute of Electrical and Electronics Engineers, Inc.
Provided by IHS under license with IEEE
No reproduction or networking permitted without license from IHS

Order Number: 02120914
Sold to:EGAT [700166108393] - VARRIS.Y@EGAT.CO.TH,
Not for Resale,2016-09-15 03:57:47 UTC

In addition to these preliminary design considerations, the local public may have input concerning the noise and aesthetics of the substation and surrounding area.

The bus design can begin after all of the design conditions are firmly established and the bus arrangement has been determined. Several factors must be considered to determine the appropriate bus arrangement for a substation. These factors may include the following:

— Construction type

— Material type

— Type of disconnect switches

The following subclauses discuss the above factors.

5.2 Construction type

5.2.1 Box structure

The box structure is generally applied at 138 kV and below. It requires the least amount of land area and uses layers of bus, disconnect switches, and related equipment, one above the other, connected with vertical bus runs and supported on a common structure. Rigid or strain bus can be used. The bus configurations most easily applied to a box structure are single bus, split single bus, main and transfer, and single breaker double bus. This construction is generally considered the least attractive and is predominantly installed in rural or industrial locations.

5.2.2 Low-profile rigid bus

Low-profile rigid bus construction can be used for all voltage levels. The main and cross buses run horizontally on two relatively low levels supported by insulators on mounting structures. Other substation equipment, such as switches and fuses, are supported on individual structures.

The advantages and disadvantages of this type of bus construction are as follows:

Advantages

a) Use low-level mounting structures. This will result in a low profile bus, which is important in populated areas.

b) The conductors are not under strain, which improves the reliability by reducing the probability of breakage.

c) The station post insulators are more accessible for cleaning in an area of high contamination.

d) A rigid bus requires less area because the phase-to-phase clearance is less for the rigid bus than for the strain bus.

Copyright © 2010 IEEE. All rights reserved.

Copyright The Institute of Electrical and Electronics Engineers, Inc.
Provided by IHS under license with IEEE
No reproduction or networking permitted without license from IHS

Order Number: 02120914
Sold to:EGAT [700166108393] - VARRIS.Y@EGAT.CO.TH,
Not for Resale,2016-09-15 03:57:47 UTC

Disadvantages

e) Due to the span length limitation, the rigid bus requires more mounting structures than the strain bus. As a result, more foundations and grounding will be required.

f) Additional design features may be needed to allow access to equipment for maintenance.

g) Experience shows that in seismic areas, the rigid bus is less reliable than the strain bus and may break during earthquakes. Expansion fittings may create impact loads during an earthquake, because the thermal expansion fitting gap is too small to allow for relative displacements at the top of insulators. Conductors may also pull out of the expansion fittings during an earthquake. Cast bus fittings may be brittle and lack sufficient strength to resist earthquake loads; forged fittings should then be considered. Other aspects may also influence the seismic behavior of rigid bus assemblies. Therefore, careful considerations should be given to the behavior of rigid bus assemblies on insulators in areas subjected to earthquakes.

5.2.3 Strain bus

Strain bus construction uses one or more flexible conductors attached to supporting structures via insulator and hardware assemblies. The main bus conductors are normally under medium-to-high tension. Bus taps and equipment jumpers are under low tension. Strain bus may be used at any voltage level, but it has typically been used at extra-high-voltage (EHV) and ultra-high-voltage (UHV) levels due to the very large phase-phase and phase-to-ground clearances required.

The advantages and disadvantages of the strain bus construction are as follows:

Advantages

a) Less mounting structures are used, and therefore, the substation area is open and clear to allow access to equipment for maintenance.

b) Strain bus may be more effective to earthquake loads.

c) Fewer insulators and less hardware are used in the strain bus.

d) Strain bus requires fewer man-hours to construct than the rigid bus.

Disadvantages

e) Strain bus requires larger phase-to-phase clearance to allow for conductor swing due to wind and short circuit forces. This will result in a larger substation area.

f) Strain bus requires a higher structure to allow for phase-to-ground clearance due to conductor sag.

g) The strain bus uses a larger structure than rigid bus.

h) Careful consideration should be given to strain bus between interconnected equipment subjected to earthquakes, to allow enough slack to permit differential displacement (see IEEE Std 1527-2006).

5.2.4 Gas insulated bus

This type of bus construction consists of completely enclosed rigid bus conductors and equipment insulated with pressurized SF_6 gas. Because of the excellent insulating properties of this gas phase, spacing can be very compact to allow construction in a much smaller physical space than an open-air insulated bus. SF_6 gas bus construction is

Copyright © 2010 IEEE. All rights reserved.

Copyright The Institute of Electrical and Electronics Engineers, Inc.
Provided by IHS under license with IEEE
No reproduction or networking permitted without license from IHS

Order Number: 02120914
Sold to:EGAT [700166108393] - VARRIS.Y@EGAT.CO.TH,
Not for Resale,2016-09-15 03:57:47 UTC

typically used at EHV and UHV levels where land costs or environmental hazards offset the much higher SF_6 equipment costs.

Advantages

a) Require minimum land area
b) Enclosed live parts not exposed to the environment
c) Modularized designs minimize construction man-hours

Disadvantages

d) Requires very expensive specialized equipment
e) Pressurized bus may create potential safety issues

5.3 Disconnect switches

The clearance requirements for each switch must be determined. For example, if the available phase-to-phase clearance is 3 m, a switch that requires 4.5 m clearances cannot be used. The installation, operation, and adjustment of a switch must be evaluated.

Considerations must be given to switch maintenance requirements and to the availability of spare parts.

The mechanical loads that can be applied to a switch must be considered and evaluated. Similarly the effect on the switch of thermal expansion and contraction of the rigid bus must be considered.

6. Conductors

6.1 General

Conductors are available in a wide variety of materials, alloys, and types of construction. The intent of this subclause is to describe the more common types of conductors that are installed in outdoor, air-insulated substations.

6.2 Materials

6.2.1 General

Overhead conductors used for transmitting electrical power are normally constructed of copper or aluminum materials. If greater strength is required, then alloys or steel reinforcing may be added to the copper or aluminum material to increase the strength of the overall conductor assembly.

Alternative metals such as gold, silver, and other materials may be applied for special applications, but these materials are generally not used in the power industry based on economic or physical considerations. In contrast,

Copyright © 2010 IEEE. All rights reserved.
Copyright The Institute of Electrical and Electronics Engineers, Inc.
Provided by IHS under license with IEEE
No reproduction or networking permitted without license from IHS
Order Number: 02120914
Sold to:EGAT [700166108393] - VARRIS.Y@EGAT.CO.TH,
Not for Resale,2016-09-15 03:57:47 UTC

copper and aluminum metals are readily available and provide a relatively good blend of electrical, mechanical, and economic properties.

6.2.2 Copper

Copper is a highly conductive metal with tensile and ductile strengths that can be altered to achieve the desired properties. There are three basic types of copper conductor: hard-drawn copper, medium-hard-drawn copper, and annealed copper, also known as soft-drawn copper.

Copper rod drawn into wire without heat treatment will provide relatively high-strength wire with low elongation properties. Such wire is known as hard-drawn copper and is suitable for overhead transmission line applications.

Heat treatment of the copper conductor will anneal the material to a more ductile metal that is easier to form and shape. However, the heating process will also lower the tensile strength of the conductor. This type of conductor is known as soft-drawn copper. Typical applications for soft-drawn copper wire include ground wire, insulated conductors, and other locations where it is necessary to bend and shape the conductor.

Medium-hard-drawn copper is annealed copper drawn to a slightly smaller diameter. The characteristics of this conductor tend to approach hard-drawn copper, but a uniform tensile strength is difficult to obtain. As a result, the tensile strength of medium-hard-drawn copper is typically specified in ranges. Typical applications for medium-hard-drawn copper include overhead distribution lines.

The resistivity of copper increases slightly with increasing hardness. Other properties of copper conductors are listed in Table 2.

Copyright © 2010 IEEE. All rights reserved.

Copyright The Institute of Electrical and Electronics Engineers, Inc.
Provided by IHS under license with IEEE
No reproduction or networking permitted without license from IHS

Order Number: 02120914
Sold to:EGAT [700166108393] - VARRIS.Y@EGAT.CO.TH,
Not for Resale,2016-09-15 03:57:47 UTC

Table 2—Properties of common bus materials

Metal	Alloy and temper	ASTM reference standard	Minimum tensile strength MPa (ksi)	Minimum yield strength MPa (ksi)	Minimum Conductivity at 20 °C in % of IACS (NOTE 1)	Modulus of elasticity GPa (ksi)
Copper tube	H80 Hard (<4" OD)	B-188	275 (40.0)	172 (25.0) (NOTE 6)	96.6 (NOTE 2)	110 (16 000)
	H80 Hard (>4" OD)	B-188	260 (38.0)	163 (23.8) (NOTE 6)	97.4 (NOTE 2)	110 (16 000)
	O60 Soft	B-188	—	—	100 (NOTE 2)	110 (16 000)
Copper wire	Hard	B-1	430 (62.1) (NOTE 3)	—	96.16	110 (16 000)
	Medium-hard	B-2	340 (49.0) (NOTE 3)	—	96.66	110 (16 000)
	Soft	B-3	—	—	100	110 (16 000)
Aluminum tubes and shapes	6061-T6	B-241	260 (38.0)	240 (35.0)	40 (typical)	69 (10 000)
	6063-T6	B-241	205 (30.0)	170 (25.0)	53 (typical)	69 (10 000)
	6101-T6	B-317	200 (29.0)	172 (25.0)	55.00	69 (10 000)
	6101-T61	B-317	138 (20.0)	103 (15.0)	57.00	69 (10 000)
	6101-T63	B-317	186 (27.0)	152 (22.0)	56.00	69 (10 000)
	6101-T64	B-317	103 (15.0)	55 (8.0)	59.50	69 (10 000)
	6101-T65	B-317	172 (25.0)	138 (20.0)	56.50	69 (10 000)
Aluminum wire	1350-H19 (NOTE 5)	B-230	180 (26) (NOTE 4)	—	61.00	69 (10 000)
	6201-T81	B-398	315 (46) (NOTE 4)	—	52.50	69 (10 000)

NOTE 1—The international standard for the resistivity of annealed copper is 0.15328 Ω-g/m^2 at 68 °F (20 °C). This value represents 100% of the International Annealed Copper Standard (IACS).

NOTE 2—Applicable to copper UNS nos. C10200, C10400, C10500, C10700, C11000, C11300, C11400, and C11600.

NOTE 3—Nominal value, see ASTM B-1, B-2, or B-3 as applicable.

NOTE 4—Nominal value, see ASTM B-230 or B-398 as applicable.

NOTE 5—Prior to 1975, aluminum alloy 1350 was identified as EC aluminum.

NOTE 6—The *Chase Electrical Handbook* [B11] states on page 47 that, "Copper has no true elastic limit, its stress-strain diagram having no section which is a perfectly straight line. For a practical engineering figure it is common practice to use as the yield strength of copper the stress which will produce an elongation under load of ½ of one percent." The yield strength values listed in the Table 1 are based on 62.5% of the ASTM minimum tensile strength as indicated in Tables 8 and 9 of the *Chase Electrical Handbook.*

6.2.3 Aluminum

Aluminum is generally considered to be more cost effective than copper and has become the standard of most utilities for overhead transmission lines and substation bus applications. Copper and copper-based materials are still in use but are primarily associated with high-current and grounding applications, short equipment jumpers or spans, and substation expansion projects to match the existing conductor.

The tensile strength and conductivity of aluminum is less than hard-drawn copper. However, if the cross-sectional area of aluminum is increased to match the electrical conductivity of a copper conductor, the resulting breaking strength of equivalent conductors will be about the same, except the aluminum conductor will weigh only about

Copyright © 2010 IEEE. All rights reserved.

Copyright The Institute of Electrical and Electronics Engineers, Inc.
Provided by IHS under license with IEEE
No reproduction or networking permitted without license from IHS

Order Number: 02120914
Sold to:EGAT [700166108393] - VARRIS.Y@EGAT.CO.TH,
Not for Resale,2016-09-15 03:57:47 UTC

55% of its copper counterpart. This fact gives aluminum conductors a definite advantage over equivalent copper conductors to reduce loadings on substation structures or to increase span lengths on transmission lines.

Pure aluminum has a conductivity of about 65% of IACS. Alloying the material or adding other elements to the metal typically reduces the conductivity.

Aluminum is available in a wide variety of alloys and tempers. Electrical-grade (Type EC) conductors are defined as aluminum materials that exhibit a minimum conductivity of 61% of IACS. Various tempers of EC conductors are available. EC-H12 and EC-H112 have greater conductivity but lower strength and tend to be applied in low-voltage, high-current applications. Tempers EC-H13 and EC-H17 provide slightly lower conductivity but have greater strength.

In recent years, a second grade of aluminum was developed for the electrical industry and was designated as No. 2 EC. No. 2 EC is an aluminum-magnesium-silicone alloy with minimum conductivity ranging from 55% to 57% of IACS, depending on the applied tempering.

The selection of an outdoor, high-voltage substation tubular bus is typically governed by mechanical strength considerations rather than by electrical characteristics. As a result, structural aluminum alloys have been commonly applied for substation bus applications. Aluminum alloys 6061, 6063, and 6101 are the most common alloys used for tubular bus applications.

Aluminum alloys can also be hardened by tempering the metal, with the most common temper classifications being T6, T61, and T63. The characteristics of various aluminum alloys and tempers is shown in Table 2.

Aluminum alloys 6063-T6 and 6101-T6 have a typical conductivity of 53% to 55% of IACS and provide an excellent blend of mechanical, electrical, and economic properties. If greater strength is required, 6061-T6 is also a common substation bus with a typical conductivity of 40% of IACS, but it is stiffer and more difficult to shape in the field.

6.3 Rigid conductors

Rigid conductors may take several forms but are generally flat rectangular bars, angles, tubes, or another structural shape. Flat bars can be bent easily and joined together but tend to lack the mechanical strength necessary for long spans. Stiffer cross sections such as angles increase the structural strength of the conductor and may be installed in distribution substations, but the application may be limited to lower voltages under certain conditions due to corona and radio noise considerations. A structural shape such as an integral web bus might be used for high-current applications or to gain added mechanical strength for long spans in EHV substations. The load capability of substation equipment may not be adequately addressed by connection with rigid buses, which can transmit loads directly to them; flexible conductors are more appropriate because they generally provide more flexiblity and thus diminish the loads transmitted.

Tubular buses have gained wide acceptance in the utility industry because they possess good conductive, mechanical, and corona characteristics. A tubular bus may be either square or round, but a round tubular bus is much more common because cylindrical shapes have the following characteristics:

a) Maintain equal rigidity in all directions, which is an inherent advantage for withstanding wind, short circuit, and ice loading conditions

b) Bend easier than other shapes when forming bends or offsets

c) Minimize corona, audible noise, and radio noise

d) Avoid large sags to provide a more pleasing appearance

Copyright © 2010 IEEE. All rights reserved.

Copyright The Institute of Electrical and Electronics Engineers, Inc.
Provided by IHS under license with IEEE
No reproduction or networking permitted without license from IHS

Order Number: 02120914
Sold to:EGAT [700166108393] - VARRIS.Y@EGAT.CO.TH,
Not for Resale,2016-09-15 03:57:47 UTC

The mechanical strength and stiffness of the rigid bus also allows the conductor spacing and height to be decreased when compared with flexible conductor alternatives. This can be an important factor if there are height restrictions or if a low-profile or very low-profile substation is desired for aesthetic considerations.

An aluminum bus may be purchased as a structural pipe or seamless pipe. A structural pipe is intended only for structural applications and is not suitable for situations where the pipe is repeatedly flexed. The reason is that the structural pipe is manufactured with a continuous die-welded seam located along the length of the pipe that tends to split during vibration. In the case of a substation bus, aeolian vibration is common, which means that structural pipes are not recommended for substation applications. Splitting of a structural pipe can also be a problem during field bending operations.

An aluminum bus installed in substations is normally designated as extruded, seamless round pipes or tubes fabricated from the hollow ingot process in conformance with ASTM B-241 or ASTM B-317. Extruded seamless round tubes are defined as an extruded hollow product having a round cross section and a uniform wall thickness.

Pipes and tubes are similar, but a subtle difference does exist between the two. Pipes are manufactured to nominal diameters with wall thicknesses defined by a schedule. In contrast, tubes are defined or described by a specific outside diameter and by a specific wall thickness.

6.4 Flexible conductors

6.4.1 Stranding

Conductors are generally categorized as being either solid or stranded. A solid conductor is a conductor with a solid, circular, cross section. As the size of the conductor increases, solid conductors become stiff and difficult to handle and can be damaged more easily during installation. As a result, larger conductor sizes tend to be stranded.

ASTM stranding classifications for power cable applications are generally indicated with an AA, A, or B designation. Bare outdoor cables used for overhead transmission line applications are typically Class AA. Class A cables are generally covered with weather-resistant materials and are sometimes specified for bare conductors where greater flexibility is needed. Class B stranded conductors are typically applied in insulated power cables or where additional flexibility is required.

6.4.2 Types of flexible conductors

Although copper is a very good conductor material, economics have tended to favor aluminum. As a result, most utilities install aluminum bus in outdoor substation locations.

An all-aluminum conductor (AAC) is manufactured with 1350-H19 grade aluminum. An AAC is a relatively low-cost conductor that has good conductivity and moderate strength characteristics. Substation buses and transmission lines with relatively short spans are ideal applications for an AAC.

Aluminum conductor, steel-reinforced (ACSR) cables consist of a solid or stranded galvanized steel core surrounded by one or more layers of 1350-H19 aluminum wires. The size of an ACSR cable is determined by the cross-sectional area of the aluminum contained in the ACSR cable. Stranding for ACSR cables is indicated by the number of aluminum wires followed by the number of galvanized steel wires. For example, a 795 kcmil 26/7 ACSR cable has 26 aluminum wires totaling 795 kcmil of aluminum cross-sectional area placed over a steel core composed of

Copyright © 2010 IEEE. All rights reserved.

Copyright The Institute of Electrical and Electronics Engineers, Inc.
Provided by IHS under license with IEEE
No reproduction or networking permitted without license from IHS

Order Number: 02120914
Sold to:EGAT [700166108393] - VARRIS.Y@EGAT.CO.TH,
Not for Resale,2016-09-15 03:57:47 UTC

seven galvanized steel wires. The presence of a steel core in ACSR conductors provides a high mechanical-strength-to-weight ratio that makes it well suited for long-span applications.

An all-aluminum alloy conductor (AAAC) was developed as a replacement for 6/1 and 26/7 ACSR conductors. The AAAC is constructed from 6201-T81 aluminum alloy, giving it characteristics similar to ACSR but with improved corrosion characteristics. As a result, an AAAC can be a good choice for coastal locations or other corrosive environments.

An aluminum conductor, aluminum-alloy reinforced conductor (ACAR) mixes 6201-T81 and 1350-H19 aluminum strands of the same diameter. The strands of the conductor are therefore interchangeable to allow the conductor assembly to be designed to optimize the mechanical and electrical properties of the aluminum and aluminum alloy.

An aluminum conductor, steel-supported conductor (ACSS) is similar to standard ACSR cables except the aluminum is fully annealed. Because the aluminum is already annealed, the conductor can be operated at temperatures in excess of 200 °C. However, care should be taken when applying ACSS inside a substation to be sure the conductor does not exceed the temperature rating of equipment that may be connected to the conductor.

Other types of construction such as trapezoidal-shaped wire (TW), vibration-resistant wire (VR), self-damping conductor (SD), and many more variations are possible but are seldom found in substations.

6.5 Field bending of rigid conductors

Rigid conductors are normally routed in relatively straight lines, but occasional turns and offsets are required. Bus fittings can be used to accomplish the turns or offsets, but rigid conductors can also be bent. The following factors must be considered when bus conductors are bent:

a) Ductile properties of the metal
b) Size and shape of the conductor
c) Bending method
d) Bending equipment to be used

The metal must be ductile, which means that the metal must be soft enough to allow sufficient stretching or compressing without fracturing as the conductor is bent. Ideally, the conductor should have a high elongation value and a low ratio of yield strength to tensile strength.

The size and shape of the conductor should also be considered. For example, rectangular bars can be bent flatwise to form a 90° elbow without cracking, but the minimum bending radius is dependent on the ductility of the bar and the ratio of bar width to bar thickness. The minimum flatwise bending radius of aluminum rectangular bus bars required to avoid visible cracks or ruptures is indicated in Table 3.

Aluminum bus bars can also be bent edgewise. Typically, the minimum edgewise bending radius of the rectangular bar is equal to the width of the bar. An edgewise bend is considered successful if no cracks or ruptures are visible and the bar at the outer radius is not thinned to less than 90% of bar thickness.

Copyright © 2010 IEEE. All rights reserved.

Copyright The Institute of Electrical and Electronics Engineers, Inc.
Provided by IHS under license with IEEE
No reproduction or networking permitted without license from IHS

Order Number: 02120914
Sold to:EGAT [700166108393] - VARRIS.Y@EGAT.CO.TH,
Not for Resale,2016-09-15 03:57:47 UTC

Table 3—Minimum flatwise bending radius of rectangular aluminum bus

Alloy and temper	Maximum bar width mm (in)	Bar thickness mm (in)	Minimum bending radius
6101-T6	150 (6)	3–9 (0.125–0.375)	2.0 × thickness
		10–13 (0.376–0.500)	2.5 × thickness
6101-T61	150 (6)	3–13 (0.125–0.500)	1.0 × thickness
		14–19 (0.501–0.749)	2.0 × thickness
		20–25 (0.750–1.000)	3.0 × thickness
		26–41 (1.001–1.625)	4.0 × thickness
6101-T63	150 (6)	3–9 (0.125–0.375)	1.0 × thickness
		10–13 (0.376–0.500)	1.5 × thickness
6101-T64	300 (12)	3–19 (0.125–0.750)	1.0 × thickness
		19–25 (0.751–1.000)	2.0 × thickness
6101-T65	150 (6)	3–13 (0.125–0.500)	1.0 × thickness
		13–19 (0.501–0.749)	2.0 × thickness

6.6 Connections

6.6.1 General

An electrical connector is any device that joins two or more conductors for the purpose of providing a continuous electrical path. Connectors may be the bolted, compression, swaged, welded, or brazed type and should conform to NEMA CC 1-2005. Care is required when specifying connectors to be sure the maximum rated operating temperature of the connector is not exceeded, corona and audible noise requirements are within acceptable limits, mechanical strength is sufficient, dissimilar metals are properly interfaced; and so on.

6.6.1.1 Bolted

Bolted connections normally require no special tools and are easier to install with an unskilled workforce than other connectors. The common types of bolting hardware for joining various bus materials are indicated in Table 4.

Table 4—Common bolting hardware

Bus bar materials to be joined	Bolting hardware
Copper to copper	1. Silicon bronze 2. Stainless steel 3. Galvanized steel
Aluminum to copper	Stainless steel or galvanized steel. Usually, either a bimetallic transition plate is inserted between the two flat-to-flat pads of the dissimilar metals or tinned connectors are used for the transition.
Aluminum to aluminum	1. Aluminum 2. Stainless steel
Galvanized steel to copper	1. Silicon bronze 2. Stainless steel or galvanized steel
Galvanized steel to aluminum	1. Aluminum 2. Stainless steel or galvanized steel

A good mechanical connection between two conductors is often assumed to be a good electrical connection. However, this may not be a good assumption because the electrical characteristics of the connection will largely be determined by the condition of the contact surfaces. Metallic surfaces, if exposed to air and not properly cleaned,

Copyright © 2010 IEEE. All rights reserved.
Copyright The Institute of Electrical and Electronics Engineers, Inc.
Provided by IHS under license with IEEE
No reproduction or networking permitted without license from IHS
Order Number: 02120914
Sold to:EGAT [700166108393] - VARRIS.Y@EGAT.CO.TH,
Not for Resale,2016-09-15 03:57:47 UTC

may contain surface oxides that are semiconductive, resulting in a relatively high contact resistance. In addition, contact surfaces may appear to be smooth, but microscopic hills and valleys are present that will reduce the actual contact area to a small percentage of the total mating surface area. By applying pressure, the initial contact points will be deformed to gain additional contact area, but even under maximum pressure, the actual contact area will be only a fraction of the total mating surface area.

Bolt hole sizes are oversized, and the bearing area of a hex-head bolt or nut is very small. As a result, the bolt head or nut may slowly embed itself into the conductor under normal bolting pressures. This is typically avoided by placing two large flat washers, one on each outer side of the joint, to distribute pressure uniformly as the bolt is tightened. Table 5 provides typical torque values for bolted power connections installed without spring washers.

Table 5—Typical torque values for bolted connectors

Diameter of bolt mm (in)	Silicon bronze N-m (ft-lbs)	Stainless and galvanized steel N-m (ft-lbs)	Aluminum N-m (ft-lbs)
8 (5/16)	20 (15)	20 (15)	—
10 (3/8)	27 (20)	27 (20)	19 (14)
13 (1/2)	54 (40)	54 (40)	34 (25)
16 (5/8)	75 (55)	75 (55)	54 (40)
19 (3/4)	95 (70)	95 (70)	—

It is important for bus bolting hardware to apply a relatively constant pressure as the joint heats and cools. If the bolting hardware and bus bars being connected contain dissimilar metals, then it is important to accommodate the differential expansion and contraction of the dissimilar metals as the connector cycles through cold and hot temperatures. In such applications, a spring washer, such as a Belleville washer, is typically installed to accommodate the expansion and contraction. Belleville washers are a specialized type of spring washer that are round but slightly conical in shape unless flattened under pressure. In practice, the bolt assembly is tightened until the Belleville washer is flattened and then the nut is backed off slightly, not to exceed a quarter turn. This practice ensures the best possible result because the washer is firmly seated on the bus, and the washer exerts a force that is very close to its maximum capacity.

6.6.1.2 Compression

Compression fittings are intended to be installed on stranded conductors. The fitting typically consists of a hollow sleeve into which a bare conductor is inserted. A hand, pneumatic, or hydraulic press will then crimp the sleeve onto the conductor one or more times as recommended by the manufacturer. A properly crimped compression fitting will deform the conductor strands slightly to provide good electrical continuity and mechanical strength. Close attention to coordinating compression dies with compression fittings and conductors is required to assure the crimp is installed properly. In some instances, it may be desirable to perform a sample compression and then to cut through the compression to confirm the compression die is truly coordinated with the compression fitting.

In most cases, compression accessories are filled with a specified amount of compound prior to installing the conductor. The compound is intended to seal the accessory from water that may otherwise corrode or possibly damage the accessory over time. Whenever possible, the compressed area of the accessory should be oriented down to prevent the entrance of moisture into the barrel of the connector. If the compressed area of the accessory is oriented up, then the manufacturer of the accessory should be contacted to determine whether a special fitting is recommended to allow periodic filling of the connector barrel.

Copyright © 2010 IEEE. All rights reserved.

Copyright The Institute of Electrical and Electronics Engineers, Inc.
Provided by IHS under license with IEEE
No reproduction or networking permitted without license from IHS

Order Number: 02120914
Sold to:EGAT [700166108393] - VARRIS.Y@EGAT.CO.TH,
Not for Resale,2016-09-15 03:57:47 UTC

Compression joints require special tools to crimp or indent the connector. However, the material cost of the connector is lower than bolted connectors so that a properly equipped and skilled workforce can make the selection of compression joints economical.

6.6.1.3 Swage

Swage fittings are similar to traditional compression fittings but can be applied to tubular bus or stranded conductors. The compression technique produces a 360° radial swage on the connector with dies that are slotted to collapse on each other to maintain equal pressure on all sides. Swage fittings approach the characteristics of welded fittings but do not require the degree of skill required for welded fittings. As a result, swage fittings can be an economical alternative to welded fittings.

6.6.1.4 Welded

Welded joints melt the conductors to form a solid, homogeneous union. Welded joints that are properly installed are generally considered to be the most reliable type of connector from an electrical viewpoint because there is no contact resistance to generate heat when high currents are present.

Workmanship is a key element to attain a properly installed welded connection. Welders should be qualified in accordance with AWS D1.2-2003. To ensure good weld penetration, all welds on the aluminum bus should be made with the gas metal-arc (MIG) welding process. The shielding gas should be welding grade argon, helium, or a mixture of the two. Filler alloy 4043 should be used for 6061-T6 base metal.

The heat applied during welding will anneal the base metal and weaken the conductor. The Aluminum Electrical Conductor Handbook [B1] recommends an allowable yield stress of 50% of the yield stress for welded conductors. This accounts for not only the annealing but also for possible weld defects. Couplers typically use internal sleeves to overcome the annealing problem.

Welded joints may be relatively expensive in situations where there are few joints to be installed, and access to equipment and qualified welders is limited. However, welded joints can be economical if there are a large number of joints to be installed, and a qualified workforce is available.

6.6.1.5 Brazed

Brazed joints are similar to welded joints except the brazing does not require melting of the metals being joined. Brazing does require a uniform heating of the joint to the temperature that will allow all of the brazing filler material to flow into the joint. Although brazing can be successfully applied to smaller tubes and shapes, it is generally not applied in outdoor substations.

6.6.2 Aluminum-to-copper connections

Aluminum-to-copper connections require care because of the corrosion that can occur between dissimilar metals. Over time, corrosion will cause increased joint resistance, which will result in heating during periods of high current and will ultimately lead to failure of the joint. In certain clean applications, it is possible to connect copper to aluminum directly with a suitable joint compound, but this practice is generally not recommended. Typically, one of the following methods is recommended for connecting aluminum to copper:

a) Tin-plate or copper-line the aluminum contact surface

Copyright © 2010 IEEE. All rights reserved.

Copyright The Institute of Electrical and Electronics Engineers, Inc.
Provided by IHS under license with IEEE
No reproduction or networking permitted without license from IHS

Order Number: 02120914
Sold to:EGAT [700166108393] - VARRIS.Y@EGAT.CO.TH,
Not for Resale,2016-09-15 03:57:47 UTC

b) Tin-plate the copper contact surface

c) Install a bimetallic transition plate between the contact surfaces

d) Silver-plate the copper contact surface

Whenever possible, copper should not be placed above aluminum. Rain will wash copper salts down onto the aluminum metal and cause discoloration.

6.6.3 Joint compounds

Joint compound or sealants are generally not applied to bolted copper connections unless the connector is placed in a highly corrosive environment. However, it is prudent to install a sealant inside the barrel of a copper or bronze compression connector to seal out moisture that may otherwise infiltrate the connection.

Aluminum-to-aluminum and aluminum-to-copper joints should be coated with a suitable joint compound. In fact, the primary cause of aluminum conductor accessory failures in high-voltage transmission line applications involves inadequate or improper application of joint compounds.

Joint compounds are installed to do the following:

a) Protect the compressed steel barrels or sleeves of conductor accessories from corrosion. During compression, galvanizing is removed from the accessory and the filler compound acts as a barrier to corrosion.

b) Clean conductor strands during compression. Filler compounds applied to aluminum conductors often contain aluminum particles that abrade the conductors during the compression.

c) Fill the conductor strands to block moisture infiltration into the conductor.

d) Enhance the ultimate holding strength of the conductor accessory.

Particular care is required with aluminum because nonconducting surface oxides develop very quickly when the metal is exposed to air. In most instances, the manufacturer of the joint compound will recommend that the metal be cleaned, coated with a joint compound, and wire brushed through the compound, with the compound remaining in place while the connector is installed. The wire brushing abrades the oxide layers, and the compound forms a barrier to minimize the creation of new surface oxides that can lead to a high resistive joint.

If solid-dielectric cable insulation such as PVC, polyethylene, or rubber is present, the joint compound should be a nonpetroleum base to avoid adverse chemical reactions.

Joint compounds used to connect flat surfaces do not require grit in the compound. Gritted joint compounds should be applied only in compressive joints that will be placed under tension. Grit normally refers to hard metallic particles mixed into the compound that are intended to increase the holding strength of the joint when tension is applied.

6.6.4 Maintenance

Periodic inspection of substation conductors is generally recommended to assess the condition of the conductors and the associated electrical connections. Normally, maintenance activities will consist of an infrared scan of the substation to identify locations where the operating temperature is higher than adjacent areas. Areas of high temperature should be investigated to verify that the conductors are properly sized and that the electrical connectors are properly installed.

Copyright © 2010 IEEE. All rights reserved.

Copyright The Institute of Electrical and Electronics Engineers, Inc.
Provided by IHS under license with IEEE
No reproduction or networking permitted without license from IHS

Order Number: 02120914
Sold to:EGAT [700166108393] - VARRIS.Y@EGAT.CO.TH,
Not for Resale,2016-09-15 03:57:47 UTC

7. Design procedure

The recommended design procedure in this guide is summarized in Figure 7, and its main steps are described in 7.1 through 7.7.

7.1 Design specification

The specification for a station required to design bus includes a one-line diagram as well as station capacity (MVA), fault level (kA), and continuous and emergency bus ratings (A). The one-line diagram should indicate the required station equipment and connections for both the initial and the future stages of development.

7.2 Select bus arrangement

Clause 4 covers various bus arrangements that may be considered. Bus layouts should be prepared for the various stages of the station development. This is to ensure that there is minimal disruption to the station operation when going from one stage to another.

7.3 Design considerations

Additional considerations must be made to finalize the design. These include the following items:

a) Clearances (12.8).

b) Transitions between different bus type and/or heights.

c) Bus to equipment connections.

d) Grade changes. A large station may have a grade change. To minimize bus bends, the footing height may be varied to maintain a constant bus elevation. Footing elevation changes can compensate for a certain amount of elevation change, and beyond this, bus transitions will be required.

e) Access to the equipment and bus during construction and maintenance.

7.4 Select conductor type

There are many types of conductors that may be used, and they are detailed in Clause 6. Factors considered include the following:

a) Ampacity (Clause 8)

b) Corona (Clause 9)

c) Mechanical strength and deflection (Clause 12)

d) Seismic withstand

e) Cost

Multiple conductor types may be required to accommodate the design. For example, rigid and flexible conductors may both be used in a design.

Copyright © 2010 IEEE. All rights reserved.

Copyright The Institute of Electrical and Electronics Engineers, Inc.
Provided by IHS under license with IEEE
No reproduction or networking permitted without license from IHS

Order Number: 02120914
Sold to:EGAT [700166108393] - VARRIS.Y@EGAT.CO.TH,
Not for Resale,2016-09-15 03:57:47 UTC

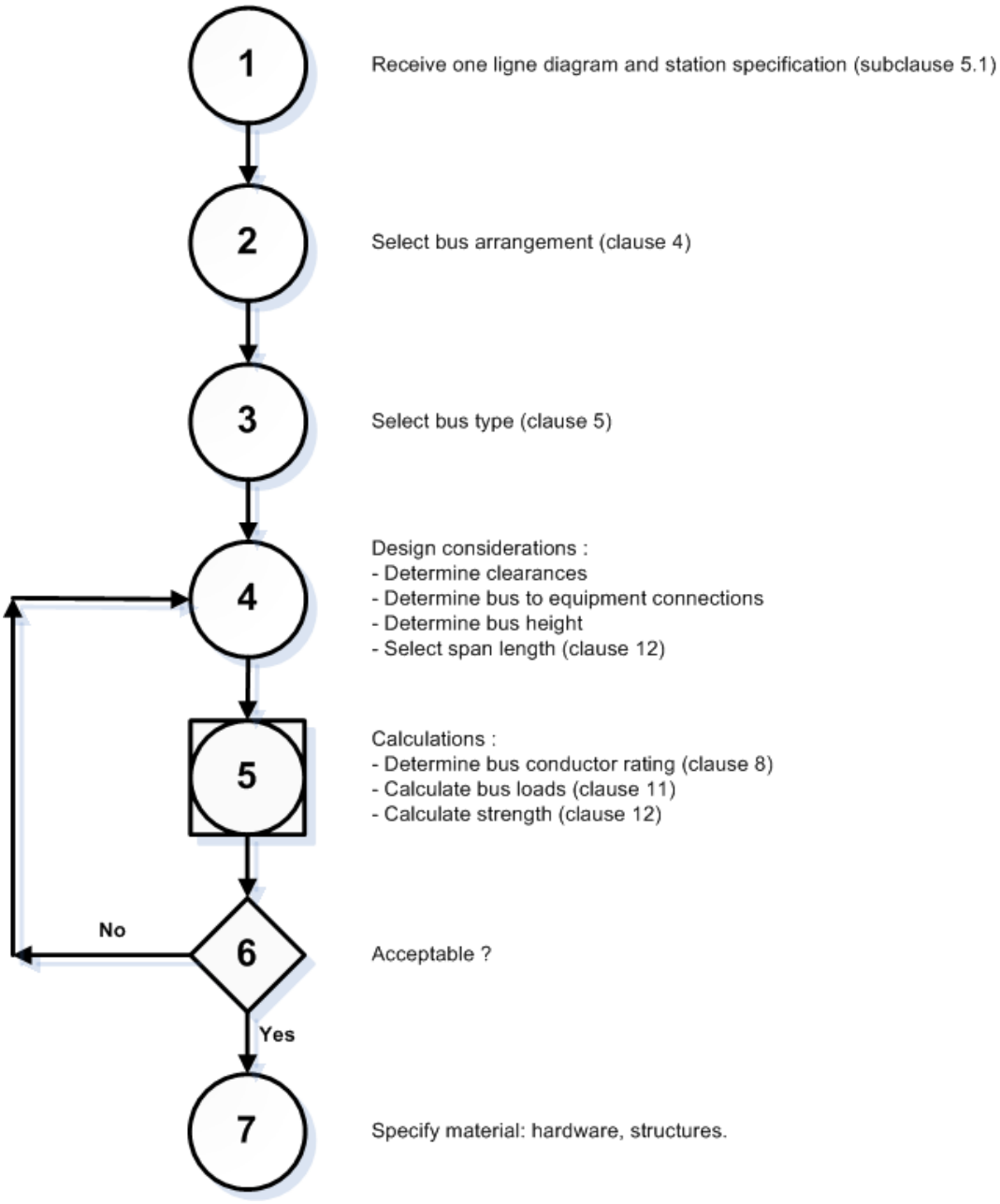

Figure 7—Bus design procedure flow chart

7.5 Structure design

Design the support structures to withstand permanent and exceptional loads on them. The calculation methods are presented in Clause 10, the loads to consider in Clause 11, and the strength and other considerations in Clause 12.

Copyright © 2010 IEEE. All rights reserved.

Copyright The Institute of Electrical and Electronics Engineers, Inc.
Provided by IHS under license with IEEE
No reproduction or networking permitted without license from IHS

Order Number: 02120914
Sold to:EGAT [700166108393] - VARRIS.Y@EGAT.CO.TH,
Not for Resale,2016-09-15 03:57:47 UTC

7.6 Review calculations

Verify that the structures are able to withstand the design loads in an acceptable manner. If the structures are found to be unacceptable, then they must be redesigned.

7.7 Select materials

Based on the calculations performed, materials such as insulators, bus conductors, fittings, and other components will be selected. The information from the design would then be provided to the civil engineer to design support structures and foundations for the bus design.

8. Ampacity

The ampacity requirement of the bus conductor is usually determined by either the electrical system requirements or the ampacity of the connected equipment. The conductor ampacity is limited by the conductor's maximum operating temperature. Excessive conductor temperatures may anneal the conductor, thereby reducing its strength, or may damage connected equipment by the transfer of heat. Excessive temperatures may also cause rapid oxidation of the copper conductor.

8.1 Heat balance

The temperature of a conductor depends on the balance of heat input and output. For balance, the heat input due to ohmic losses (I^2R) and solar radiation equals the heat output due to convection, radiation, and conduction. The heat balance may be expressed as follows:

$$I^2 R F + q_s = q_c + q_r + q_{\text{cond}} \tag{1}$$

where

I is the current through the bus conductor, A
R is the direct-current resistance at the operating temperature, □Ω/m [Ω/ft]
F is the skin-effect coefficient
q_s is the solar heat gain, W/m [W/ft]
q_c is the convective heat loss, W/m [W/ft]
q_r is the radiation heat loss, W/m [W/ft]
q_{cond} is the conductive heat loss, W/m [W/ft]

Solving the current for a given conductor temperature rise is as follows:

$$I = \sqrt{\frac{q_c + q_r + q_{\text{cond}} - q_s}{R F}} \tag{2}$$

Copyright © 2010 IEEE. All rights reserved.

Copyright The Institute of Electrical and Electronics Engineers, Inc.
Provided by IHS under license with IEEE
No reproduction or networking permitted without license from IHS

Order Number: 02120914
Sold to:EGAT [700166108393] - VARRIS.Y@EGAT.CO.TH,
Not for Resale,2016-09-15 03:57:47 UTC

NOTE—Values for convective or conductive heat transfer into the conductor element on the right side of Equation (2) are entered as negative numbers. Heat transfer out of the conductor element are entered as positive numbers.

8.1.1.1 Effective resistance, *RF*

A conductor's effective resistance at a given temperature and frequency is the direct-current resistance *R* modified by the skin-effect coefficient *F*. These values may be obtained from published data.

8.1.2 Solar heat gain, q_s

The amount of solar heat gained is a function of the following:

a) The total solar and sky radiation
b) The coefficient of solar absorption for the conductor's surface
c) The projected area of the conductor
d) The altitude of the conductor above sea level
e) The orientation of the conductor with respect to the sun's rays

8.1.3 Convective heat loss, q_c

A bus conductor loses heat through natural or forced convection.

8.1.3.1 Natural convective heat loss

Natural convective heat loss is a function of the following:

a) The temperature difference between the conductor surface and the ambient air temperature
b) The orientation of the conductor's surface
c) The width of the conductor's surface
d) The conductor's surface area

8.1.3.2 Forced convective heat loss

Forced convective heat loss is a function of the following:

a) The temperature difference between the conductor's surface and the ambient air temperature
b) The length of flow path over the conductor
c) The wind speed and direction
d) The conductor's surface area

8.1.4 Radiation heat loss, q_r

A conductor loses heat through the emission of radiated heat. The heat lost is a function of the following:

Copyright © 2010 IEEE. All rights reserved.
Copyright The Institute of Electrical and Electronics Engineers, Inc.
Provided by IHS under license with IEEE
No reproduction or networking permitted without license from IHS
Order Number: 02120914
Sold to:EGAT [700166108393] - VARRIS.Y@EGAT.CO.TH,
Not for Resale,2016-09-15 03:57:47 UTC

a) The difference in the absolute temperature of the conductor and surrounding bodies

b) The emissivity of the conductor's surface

c) The conductor's surface area

8.1.5 Conductive heat loss, q_{cond}

Conduction is a minor method of heat transfer because the contact surface is usually very small. Conduction may cause an increase in the temperature of the equipment attached to the bus conductor. Conductive heat loss is usually neglected in bus-ampacity calculations.

8.2 Conductor temperature limits

8.2.1 Continuous (see IEEE Std C37.30-1997)

Aluminum alloy and copper conductors may be operated continuously at 90 °C without appreciable loss of strength. They may also be operated at 100 °C under emergency conditions with some annealing. Copper may, however, suffer excessive oxidation if operated at or above 80 °C. Conductors should not be operated at temperatures high enough to damage the connected equipment.

8.2.2 Fault conditions (see ANSI C37.32-1996)

A conductor's temperature will rise rapidly under fault conditions. This is due to the inability of the conductor to dissipate the heat as rapidly as it is generated. Annealing of conductor alloys may occur rapidly at these elevated temperatures. The maximum fault current that can be allowed for copper and aluminum alloy conductors may be calculated using Equation (3) and Equation (4). Refer to 11.3.1 of IEEE Std 80™-2000 [B19] for other materials. In general, the final temperature of the conductor is limited to the maximum temperature considered for thermal expansion.

For aluminum conductors (40% to 65% IACS conductivity):

$$I = C \times 10^6 A_c \sqrt{\frac{1}{t} \log_{10}\left(\frac{T_f - 20\,^{\circ}\mathrm{C} + (15\,150/G)}{T_i - 20\,^{\circ}\mathrm{C} + (15\,150/G)} \right)} \qquad (3)$$

where

C is 2.232×10^{-4} A $s^{0.5}$ /mm^2 for A_c in mm^2 (0.144 A $s^{0.5}$ /in^2 for A_c in in^2)
I is the maximum allowable root-mean-square (RMS) value of fault current, A
A_c is the conductor cross-sectional area, mm^2 (in^2)
G is the conductivity in percent International Annealed Copper Standard (IACS)
t is the duration of fault, s
T_f is the allowable final conductor temperature, °C
T_i is the conductor temperature at fault initiation, °C

Copyright © 2010 IEEE. All rights reserved.

Copyright The Institute of Electrical and Electronics Engineers, Inc.
Provided by IHS under license with IEEE
No reproduction or networking permitted without license from IHS

Order Number: 02120914
Sold to:EGAT [700166108393] - VARRIS.Y@EGAT.CO.TH,
Not for Resale,2016-09-15 03:57:47 UTC

And for copper conductors (95% to 100% IACS conductivity):

$$I = C \times 10^6 A_c \sqrt{\frac{1}{t} \log_{10}\left(\frac{T_f - 20\,^{\circ}\mathrm{C} + (25400/G)}{T_i - 20\,^{\circ}\mathrm{C} + (25400/G)}\right)} \tag{4}$$

where

C is 3.410×10^{-4} A $s^{0.5}$ /mm^2 for A_c in mm^2 (0.220 A $s^{0.5}$ /$in^2$for A_c in in^2)

8.2.3 Attached equipment

Because heat generated in the bus conductor may be conducted to attached equipment, allowable conductor temperatures may be governed by the temperature limitations of attached equipment. Equipment temperature limitations should be obtained from the applicable specification or the manufacturer. High-voltage air switches and bus supports are described in IEEE Std C37.30-1997.

8.3 Ampacity tables

The ampacity for most aluminum-alloy and copper bus-conductor shapes are included in Annex B, which are based on calculations neglecting conductive heat loss.

9. Corona and radio interference

Corona discharges occur on air insulated conductors when the electric field intensity at the conductor surface causes ionization in air. The field intensity at the initiation of the discharges is known as “corona onset gradient.” Electromagnetic interference (EMI) is caused by the corona.

However, the rigid-bus designer should be aware that EMI can be produced at any voltage by arcing due to poor bonding between bus conductors and associated hardware.

Substation bus corona will probably occur. There is no physical law that supports any specific onset voltage. The probability that corona will occur depends on many factors (e.g., bus contamination, weather, surface nicks, and field voltage gradient).

The designer’s problem is to select a bus conductor and to specify bus hardware that will have acceptable corona performance.

9.1 Determination of corona performance

The onset of corona can only be treated statistically. The corona and EMI performance of a substation bus design could be evaluated to determine the “excedence level” (the probability that EMI will exceed a reference level) and the EMI magnitude and frequency spectrum.

Copyright © 2010 IEEE. All rights reserved.

Copyright The Institute of Electrical and Electronics Engineers, Inc.
Provided by IHS under license with IEEE
No reproduction or networking permitted without license from IHS

Order Number: 02120914
Sold to:EGAT [700166108393] - VARRIS.Y@EGAT.CO.TH,
Not for Resale,2016-09-15 03:57:47 UTC

There is a tradition of treating the corona as a deterministic value. Peek's equation, published in 1929, has been used in corona onset voltage, and more information about Peek's equation is given in Annex D.

However, Peek's equation has no mechanism to calculate the probability of corona below the calculated voltage. Also, Peek's equation has no mechanism to calculate the magnitude and frequency spectrum of radiated EMI due to the design of the substation bus.

Four basic factors determine the maximum surface voltage gradient of a smooth bus-conductor Em. They are as follows:

a) Conductor diameter or shape
b) Distance from ground
c) Phase spacing
d) Applied voltage

Although electric field intensity is an important variable, the corona onset gradient is affected by many other variables. The relationship between the onset of corona and these other variables is difficult to determine, and the occurrence of these variables is difficult to predict. In Juette [B27], test data show a 16-to-1 variation in EMI from "very clean conductors" to "very polluted conductors," as well as a 16-to-1 variation from dry weather to heavy rain EMI. Research has shown that corona and EMI will occur at voltage gradients from 10 kV/cm to more than 30 kV/cm.

9.2 EMI tolerance of substation equipment

The principal concern for EMI in substations is interference with station relaying, control, and communications equipment. Protection equipment is a particular concern. Five IEEE standards do include some treatment of radiated EMI and conducted signal interference. However, CISPR 24 [B12] is the only standard that provides broadband radiated and conductor EMI tolerance limits for equipment that bears some resemblance to the type of equipment that is used in substations.

9.3 Reducing EMI

There is some probability that corona generated interference will occur. Following good practices in design and specification of substation bus hardware assemblies, and proper installation of the hardware, will reduce the probability.

9.3.1 Conductor selection

Circular bus shapes will generally give the best performance. A smooth surface condition is important if operating near the allowable surface voltage gradient.

Formulas are provided in Annex D for calculating the maximum surface voltage gradient for a smooth, circular bus-conductor Em. The calculation should be 110% of the nominal line-to-ground voltage to provide for an operating margin.

Copyright © 2010 IEEE. All rights reserved.
Copyright The Institute of Electrical and Electronics Engineers, Inc.
Provided by IHS under license with IEEE
No reproduction or networking permitted without license from IHS
Order Number: 02120914
Sold to:EGAT [700166108393] - VARRIS.Y@EGAT.CO.TH,
Not for Resale,2016-09-15 03:57:47 UTC

The allowable surface voltage gradient for equal radio-influence generation Eo for smooth, circular bus conductors is a function of bus diameter, barometric pressure, and operating temperature. Annex D gives a method for determining the allowable surface voltage gradient.

9.3.2 Hardware specification

Bus fittings and hardware for use in rigid-bus structures should be specified as being free of corona under fair-weather conditions at the intended operating voltage, altitude, and temperature.

It should be noted that the testing methods discussed below do not require the control of air temperature and air pressure during testing. The reader should refer to Annex D to determine the difference between the allowable voltage gradients under expected operating conditions and possible laboratory conditions. If the difference is significant, the designer may specify that the testing voltage be increased according to the methods of Annex D to compensate for the test pressure and temperature.

9.3.2.1 Hardware testing methods

Bus fittings and hardware should be tested by the manufacturer in a laboratory under a simulated field configuration. All bus fittings and hardware should be tested while attached to a section of the bus conductor for which they are to be used.

The visual corona extinction voltage should be tested according to NEMA CC 1-2005.

IEC 61284 [B17] provides guidance for testing of some fittings that may be used in substation bus design.

9.3.2.2 Hardware test acceptance criteria

The following performance should be specified for fittings and hardware under fair-weather conditions.

The extinction voltage for visual corona should be at least 110% of nominal operating voltage or at least 110% of the testing voltage adjusted to compensate for pressure and temperature.

The specified radio-influence voltage (RIV) limits for various bus system components should match those given in the following standards:

a) For fittings and connectors, see NEMA CC 1-2005.

b) For insulators and hardware assemblies, see ANSI C29.9-1983.

9.4 Reducing corona generated radiated and conductor signal interference

Enclose switchyard and control house protection control and communications equipment in grounded metal enclosures to reduce the corona radiated EMI exposure of the equipment.

Proven methods to reduce conducted corona generated signal interference are given in the recommendations given in IEEE Std 525™-2007 [B20].

Copyright © 2010 IEEE. All rights reserved.
Copyright The Institute of Electrical and Electronics Engineers, Inc.
Provided by IHS under license with IEEE
No reproduction or networking permitted without license from IHS
Order Number: 02120914
Sold to:EGAT [700166108393] - VARRIS.Y@EGAT.CO.TH,
Not for Resale,2016-09-15 03:57:47 UTC

10. Overview of mechanical design of bus structures

10.1 Introduction

Bus structures should be designed to withstand the permanent and exceptional loads that act on them during their operational lives. They should also be designed so that their operational behavior is acceptable and in accordance with expectations, such as to have deflections and sags within a permissible range, to have an acceptable strength and level of vibrations, and so on.

The purpose of this clause is to introduce the loads applied to bus structures to consider in design, as well as the available calculation methods to evaluate their effects on structure. Clause 11 describes the loads in detail, and Clause 12 describes the required design considerations such as insulator strength, deflection criteria, induced vibrations, and clearances.

10.2 General mechanical design procedure

To design a bus structure:

a) Assume preliminary design data: choice of dimensions (span lengths), material, and section properties.

b) Evaluate the loads applied on the bus structure.

c) Combine these loads in a statistically coherent manner since they cannot generally all happen at the same time. The load combination may be determined by utility design standards or published guidelines applicable to substation bus structures

d) Calculate the structure's response to the load combination established in item c).

e) Verify that the structure can withstand the load combination and has an acceptable operational behavior.

Note that at item e), one can also decide to redesign the structure (or parts of it) in order to optimize it and save on construction costs.

Both the load-resistant factor design (LRFD) methodology (also called the ultimate strength design (USD) methodology) and the allowable stress design (ASD) methodology are design approaches acceptable as per this guide. The LRFD methodology is the current predominate method used in the design of steel structures in the United States and Canada.

10.2.1 Loads to consider in design

The loads to consider are the permanent loads and the exceptional loads. Note that the loads as well as their intensity vary generally according to substation location and according to design and application requirements. The loads described herein are preceded by the abbreviation under which they will be referred to in the next subclauses.

The permanent loads are as follows:

a) *D*: dead load: weight of the structure, of components and of rigid/strain buses

--`,,,,,,`-`-`,,`,,`,`,,`-`-`,,`,,`,`---
Copyright © 2010 IEEE. All rights reserved.
Copyright The Institute of Electrical and Electronics Engineers, Inc.
Provided by IHS under license with IEEE
No reproduction or networking permitted without license from IHS
Order Number: 02120914
Sold to:EGAT [700166108393] - VARRIS.Y@EGAT.CO.TH,
Not for Resale,2016-09-15 03:57:47 UTC

b) T_c: tension loads from strained conductors

c) T: thermal loads from thermal expansion of the material

The exceptional loads are as follows:

a) W: wind loads

b) W_I: wind load including effects of augmented section by ice (wind-on-ice)

c) I_w: ice weight load

d) SC: electromagnetic loads (short circuits)

e) E: earthquakes

f) WS: wet snow loads

NOTE 1—Earthquake loads are not defined in this guide. See IEEE Std 693-2005 and IEEE Std 1527-2006 for the evaluation of seismic loads acting on rigid and flexible bus, as well as their seismic design requirements.

NOTE 2—The wind speed for load W_I is not the same as for W. W_I acts on an augmented section due to the ice thickness. For the United States, W_I can be obtained from Figure 8 to Figure 13, whereas W is obtained from Figure 14 to Figure 18.

NOTE 3—The tension load from strain conductors T_c will be increased under low-temperature and/or transverse wind.

NOTE 4—Wet snow or rain-on-snow loads may be significant in regions such as Colorado, Northern California, and some areas in Canada (and possibly elsewhere). This load is not described in this guide but will be considered in the next revision. See ASCE 7-05 for details.

10.2.2 Nominal strength

The nominal strength for the conductors and structural members should be defined according to the design methodology retained (LRFD or ASD) based on the yield and ultimate strength of the material used.

Typical values of strengths used in bus design are presented in Table 6 for informative purposes, in addition to the values for aluminum and copper already presented in Table 2. Precise values based on the alloy use or rated strength of porcelain shall be used in design.

Table 6—Typical material properties for support and insulators

Material	Young's modulus E	Yield strength (F_y)	Ultimate tensile strength (F_u)
Steel (note that there are large variations according to alloy type—values here are for structural steel)	200 GPa ($2.9 \cdot 10^4$ ksi)	250 MPa (36 ksi)	395 MPa (58 ksi)
Porcelain	70–100 GPa ($10 \cdot 10^6$ psi to $15 \cdot 10^6$ psi)	30–100 MPa (4 ksi to 15 ksi) or per manufacturer's recommendation.	Porcelain is brittle: Ultimate strength is the same as yield strength.

NOTE 1—Usually, porcelain strength is defined not as stress but as cantilever rating, which is defined as the maximum horizontal load that can be applied at the top of insulator with its base fixed.

NOTE 2—Porcelain strength may vary greatly depending on the composition and manufacturing. The exact properties from the supplier shall be used in the design.

Copyright © 2010 IEEE. All rights reserved.
Copyright The Institute of Electrical and Electronics Engineers, Inc.
Provided by IHS under license with IEEE
No reproduction or networking permitted without license from IHS
Order Number: 02120914
Sold to:EGAT [700166108393] - VARRIS.Y@EGAT.CO.TH,
Not for Resale,2016-09-15 03:57:47 UTC

10.3 Calculation methods

10.3.1 Introduction

Today, different calculation methods are available to calculate both the loads and the corresponding response of the structure. These range from simplified calculations to the use of finite-element software. This guide will describe both the use of simplified calculations and finite-element calculations, whenever they apply.

In general, simplified calculations are conservative and are limited to specific design cases such as simple beam assemblage with given boundary conditions. Finite-element calculations permit generally a more detailed and precise analysis of a structure, especially under three-dimensional (3D) dynamic loading such as short circuits, and are more suitable to design optimization. However, either methods (or a combination of them) should lead to a proper design if used in accordance with the recommendation of this guide.

10.3.2 Calculation steps

To evaluate a structure's response to the applied loads (and/or different combinations of them), the following calculation steps are necessary, either by hand and/or numerically:

a) Evaluate the loads and their combinations

b) Calculate the resulting internal forces and displacements in the members to the external applied loads

c) Analyze the members' strength from the results of item b) and compare with corresponding nominal strength according to the design methodology used (LRFD or ASD)

10.3.3 Simplified calculations

Simplified calculations consist of calculating manually the response of a structure to the applied loads. For an isostatic structure, this requires the use of static analysis principles and basic notions of strength of material as described in many textbooks on the subject. A civil, structural, or mechanical engineer is required for such calculations for rigid and strain bus structures.

10.3.4 Finite-element calculations

Finite-element calculations require describing the geometry in the program by specifying end points for each structural member such as supports, conductors, and insulators. Then, one creates lines between these points and assigns to them the corresponding structural and material properties of the existing members. One divides such lines into a finite number of elements as to discretize the structure; this step is called meshing, and the mesh should be reasonably fine so as to represent correctly the structural behavior.

Different types of elements are generally available in a program such as beams, plates, solids, and so on. In the case of rigid and strain bus structures, the use of beam elements was found to be representative and of sufficient precision. One may use more refined elements such as plates and solids in order to refine the stress analysis in a specific area.

Once the structure has been described in the program, that is, in technical terms, the structure has been "meshed," and it is ready for analysis. One then specifies the loads acting on the structure in the program, either implicitly for the dead weight using the density specified in the description of the material properties of a given member plus the

Copyright © 2010 IEEE. All rights reserved.

Copyright The Institute of Electrical and Electronics Engineers, Inc.
Provided by IHS under license with IEEE
No reproduction or networking permitted without license from IHS

Order Number: 02120914
Sold to:EGAT [700166108393] - VARRIS.Y@EGAT.CO.TH,
Not for Resale,2016-09-15 03:57:47 UTC

specification of gravitational acceleration in the vertical direction or manually, to specify for example the pressure on a given section and direction corresponding to the wind speed considered.

The calculation of the structural response to the loads is the final step in the program. Depending on the type of loads as well as on the structure flexibility, static or dynamic analysis is required, either through linear or nonlinear analysis as described in the following clauses. It is recommended that a structural, mechanical or substation engineer who understands the principle of finite-element methodology shall be the key user to run the program for such analysis.

Usually, linear static analysis is adequate to calculate the response to dead (weight and tension loads), climatic loading (wind and ice), and thermal loads. Linear dynamic analysis is adequate to calculate the dynamic response to short circuit and earthquakes for rigid buses. Nonlinear dynamic analysis is mandatory to calculate the response to short circuit for strain buses.

11. Loads on bus structure

Unless otherwise noted, the loads defined in this clause apply to both rigid and strain buses. Also note that gravitational loads, which include ice and wind loads, apply to the insulators and bus supporting structure.

11.1 Gravitational loads

Gravitational loads consist of the weight of the conductor, insulators, supporting structure, ice, damping material, and concentrated loads (equipment attachments, tap conductors, etc.).

11.1.1 Weight of the conductor

The unit weight of circular rigid bus conductors, which includes pipes and tubes, is given as follows:

$$F_c = \frac{\pi w_c}{4}\left(D_o^2 - D_i^2\right) = \pi\ w_c\ t_c\ (D_o - t_c) \tag{5}$$

where

F_c is the conductor unit weight (N/m) [lbf/in]
w_c is the specific conductor weight (N/m^3) [lbf/in^3], (for aluminum w_c = 26 500 N/m^3 [0.0977 lbf/in^3])
D_o is the conductor outside diameter (m) [in]
D_i is the conductor inside diameter (m) [in]
t_c is the conductor wall thickness (m) [in]

The weight of other conductor types should be obtained from manufacturer's specifications.

NOTE—Multiply the result in lbf/in by 12 to get results in lbf/ft.

Copyright © 2010 IEEE. All rights reserved.

Copyright The Institute of Electrical and Electronics Engineers, Inc.
Provided by IHS under license with IEEE
No reproduction or networking permitted without license from IHS

Order Number: 02120914
Sold to:EGAT [700166108393] - VARRIS.Y@EGAT.CO.TH,
Not for Resale,2016-09-15 03:57:47 UTC

11.1.2 Weight of the damping material, concentrated masses, and mounting structure

The weight of the material used to damp vibration of the conductor should be included in the computation of the gravitational forces. If a cable or chain is used inside the bus conductor, then the weight of the vibration damping material should be given as a continuous unit weight.

The gravitational forces due to concentrated masses (commercial vibration dampers, equipment attachments, and tap conductors) should be included in the summation of gravitational forces.

The weight of supporting structure should be evaluated using the section properties of the structure.

11.1.3 Ice load

For engineering design purposes, it is assumed that the conductors, insulators, and supporting structure are covered with a uniform ice thickness. The ice weight on a circular conductor is given as follows:

$$F_I = \pi w_I r_I (D_o + r_I) \tag{6}$$

where

F_I is the ice unit weight (N/m) [lbf/in]
w_I is the ice weight (8820 N/m^3) [0.0330 lbf/in^3]
r_I is the equivalent uniform radial thicknesses of ice due to freezing rain (m) [in]
D_o is the conductor outside diameter (m) [in]

NOTE—Multiply the result in lbf/in by 12 to get results in lbf/ft.

For sections other than circular, the ice weight is given as follows:

$$F_I = w_I A_I \tag{7}$$

where

A_I is the area covered by ice on the section considered (m^2) [in^2]

The ice thickness used by the utility for transmission line design should be considered as the criteria for the loading on rigid or strain bus conductors. The thickness of ice will depend on the user's standard; it could be 6.4 mm (1/4 in) to 12.7 mm (1/2 in) or higher depending on the winter conditions or the location of the installation, for it cannot always be assumed that ice will not accumulate even with a conductor temperature above 0 °C. The only exceptions to this general rule of thumb are regions where the ambient temperature does not fall below 0 °C and regions that are too dry to prevent ice from forming.

Alternatively, the minimum ice thickness for the United States can be determined according to the 50 YR mean recurrence interval uniform ice thickness due to freezing rain with concurrent 3 s gust wind speeds used in ASCE 7-05. These are shown in Figure 8 through Figure 13 for the contiguous Unites States. Thicknesses for Hawaii, and for ice accretions due to other sources in all regions, shall be obtained from local meteorological studies. Note that in those figures, the ice thickness is given in inches and must be converted to the proper units used in calculations. For other countries, refer to national codes and related maps.

Copyright © 2010 IEEE. All rights reserved.

Copyright The Institute of Electrical and Electronics Engineers, Inc.
Provided by IHS under license with IEEE
No reproduction or networking permitted without license from IHS

Order Number: 02120914
Sold to:EGAT [700166108393] - VARRIS.Y@EGAT.CO.TH,
Not for Resale,2016-09-15 03:57:47 UTC

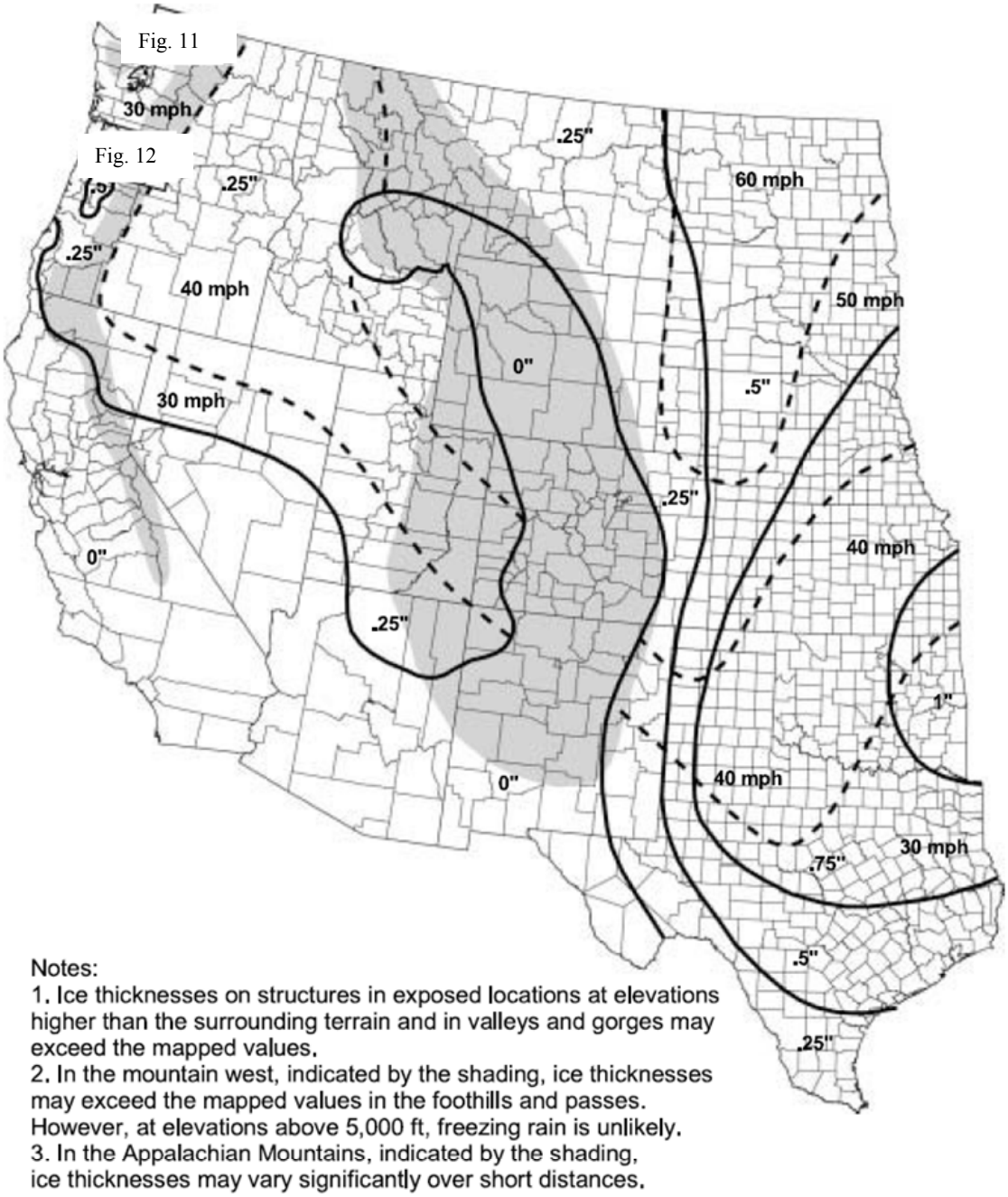

Figure 8—Extreme radial glaze ice thickness (in) Western United States (except the Pacific Northwest), 50-year return period with concurrent 3 s wind speeds[14]

[14]This figure is reproduced from ASCE 7-05 Figure 10.2a with permission.

Copyright © 2010 IEEE. All rights reserved.

Copyright The Institute of Electrical and Electronics Engineers, Inc.
Provided by IHS under license with IEEE
No reproduction or networking permitted without license from IHS

Order Number: 02120914
Sold to:EGAT [700166108393] - VARRIS.Y@EGAT.CO.TH,
Not for Resale,2016-09-15 03:57:47 UTC

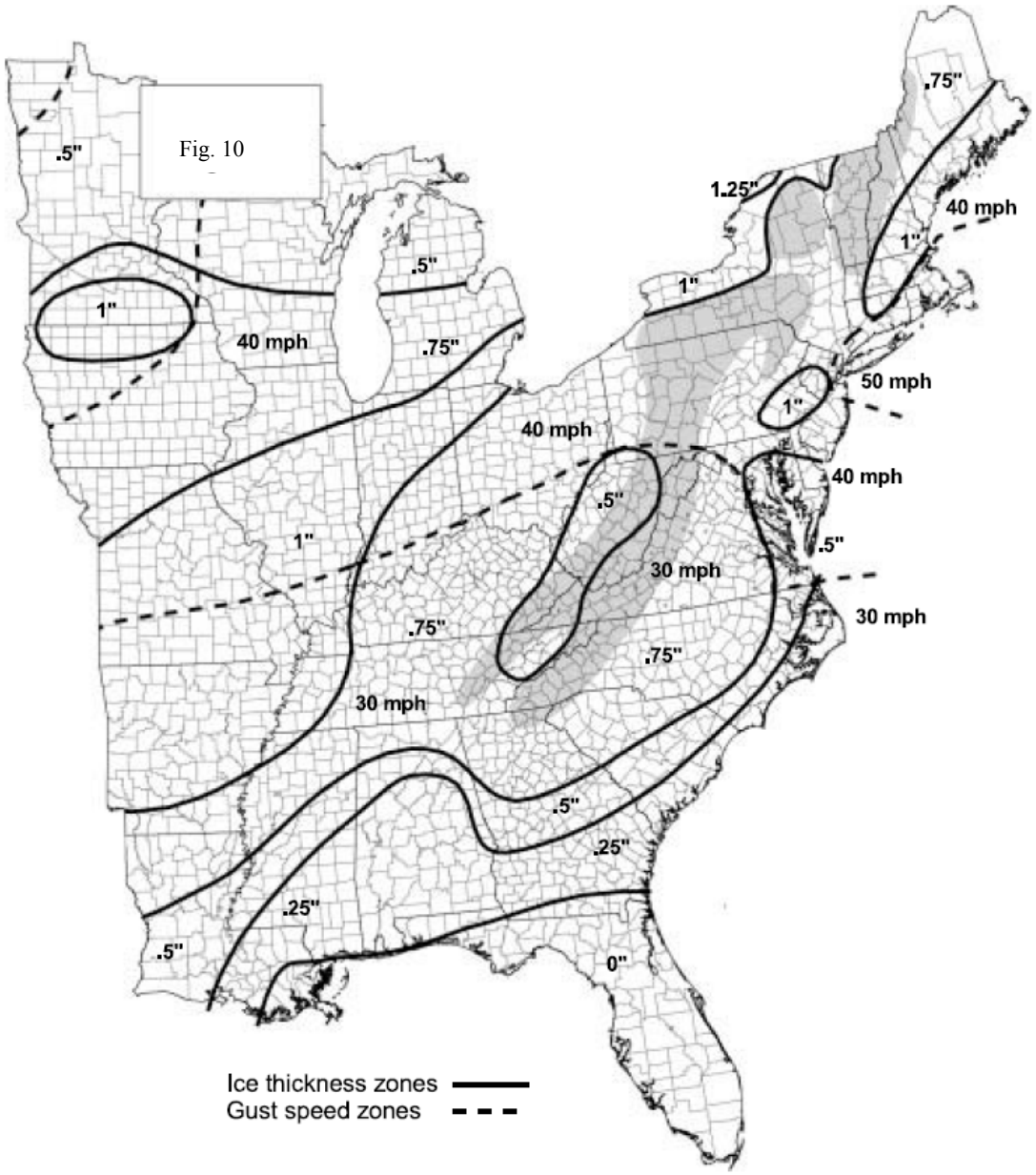

Figure 9—Extreme radial glaze ice thickness (in), Eastern United States, 50-year return period with concurrent 3 s wind speed[15]

[15]This figure is reproduced from ASCE 7-05 Figure 10.2b with permission.

Copyright © 2010 IEEE. All rights reserved.

Copyright The Institute of Electrical and Electronics Engineers, Inc.
Provided by IHS under license with IEEE
No reproduction or networking permitted without license from IHS

Order Number: 02120914
Sold to:EGAT [700166108393] - VARRIS.Y@EGAT.CO.TH,
Not for Resale,2016-09-15 03:57:47 UTC

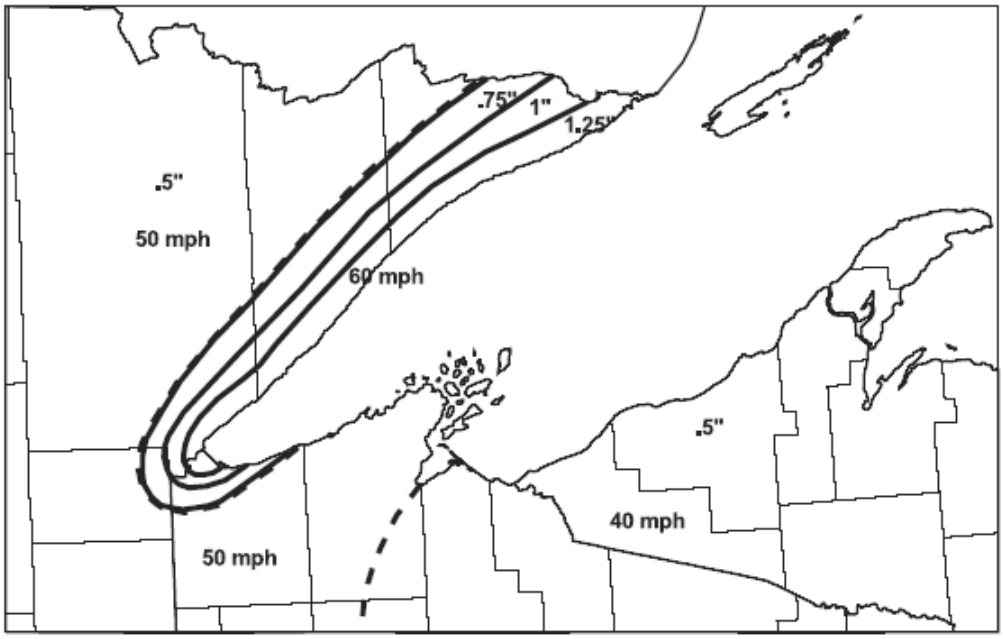

Figure 10—Extreme radial glaze ice thickness (in), Lake Superior, 50-year return period with concurrent 3 s wind speeds[16]

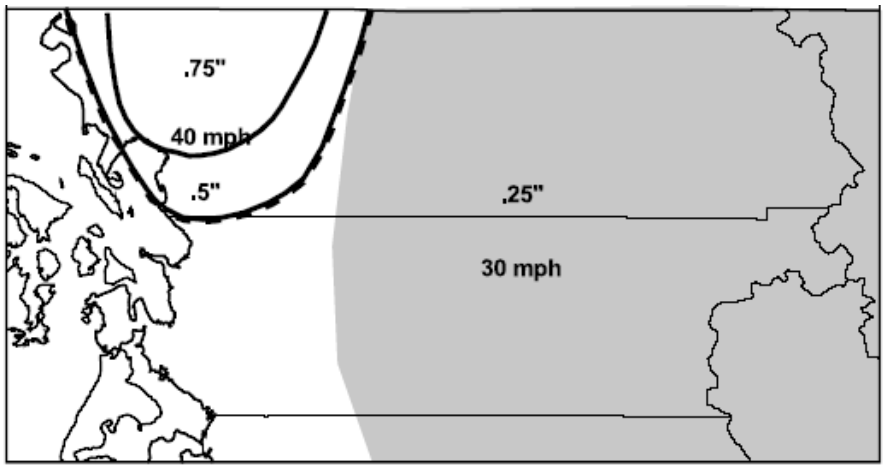

Figure 11—Extreme radial glaze ice thickness (in), Fraser Valley, 50-year return period with concurrent 3 s wind speeds[17]

[16]This figure is reproduced from ASCE 7-05 Figure 10.3 with permission.
[17]This figure is reproduced from ASCE 7-05 Figure 10.4 with permission.

Copyright © 2010 IEEE. All rights reserved.

Copyright The Institute of Electrical and Electronics Engineers, Inc.
Provided by IHS under license with IEEE
No reproduction or networking permitted without license from IHS

Order Number: 02120914
Sold to:EGAT [700166108393] - VARRIS.Y@EGAT.CO.TH,
Not for Resale,2016-09-15 03:57:47 UTC

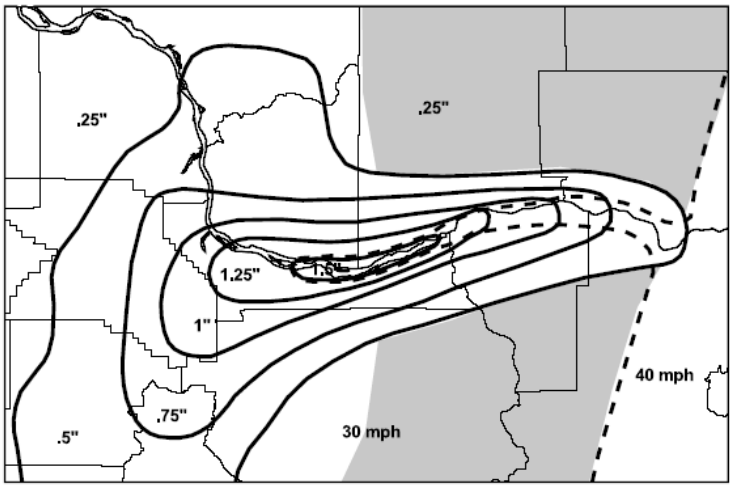

Figure 12—Extreme radial glaze ice thickness (in), Columbia River Gorge, 50-year return period with concurrent 3 s wind speeds[18]

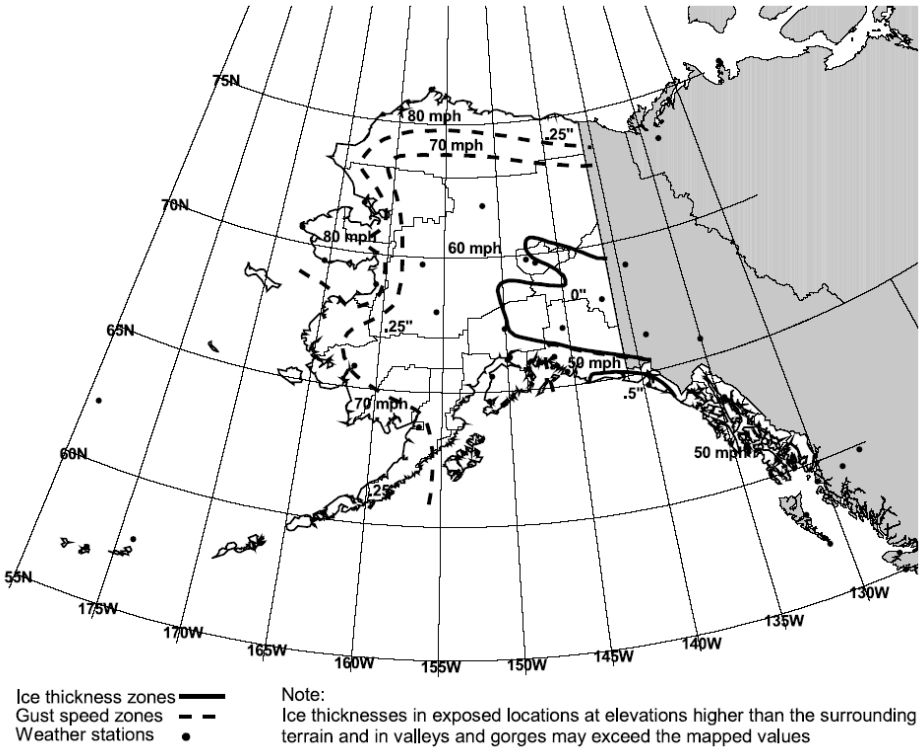

Figure 13—Extreme radial glaze ice thickness (in), Alaska, 50-year return period with concurrent 3 s wind speeds[19]

[18]This figure is reproduced from ASCE 7-05 Figure 10.5 with permission.
[19]This figure is reproduced from ASCE 7-05 Figure 10.6 with permission.

Copyright © 2010 IEEE. All rights reserved.
Copyright The Institute of Electrical and Electronics Engineers, Inc.
Provided by IHS under license with IEEE
No reproduction or networking permitted without license from IHS
Order Number: 02120914
Sold to:EGAT [700166108393] - VARRIS.Y@EGAT.CO.TH,
Not for Resale,2016-09-15 03:57:47 UTC

11.2 Wind loads

The maximum force due to wind may occur during extreme wind conditions with no ice or high wind conditions with ice. In general, the extreme wind conditions result in higher loads than the high wind conditions with ice. However, it is recommended to calculate wind loads with both types of wind in order to evaluate the maximum scenario, as it might not always be the case depending on particular local conditions.

Factors that affect wind forces are the speed and gust of wind, the conductor size and shape, the height and exposure of the conductor, and the radial thickness of ice. Wind loads should be evaluated in the horizontal direction that produces the maximum load.

In the case of extreme wind speed (without ice), the wind load by unit length on a conductor (or a slender structure such as support or isolator) is given as follows:

$$F_W = C V^2 D_o C_f K_Z G_f I \tag{8}$$

where

F_w is the wind load by unit length (N/m) [lbf/ft]
C is a constant (SI: 0.613, British: 2.132×10^{-4})
V is the extreme wind speed without ice (m/s) [mi/h]
D_o is the conductor outside diameter or the height of the profile used as conductor (m) [in]
C_f is the force coefficient
K_z is the height and exposure factor
G_f is the gust response factor
I is the importance factor of the structure.

NOTE—The results in British units are directly in lbf/ft (divide the result by 12 to get results in lbf/in).

In the case of high wind with ice, the wind load by unit length on a conductor is given as follows:

$$F_{WI} = C V_I^2 \left(D_o + 2r_I\right) C_f K_Z G_f I \tag{9}$$

where

F_{WI} is the wind load with ice by unit length (N/m) [lbf/ft]
V_I is the high wind speed with ice (m/s) [mi/h]
r_I is the equivalent uniform radial thicknesses of ice due to freezing rain (m) [in]
G_f is the gust response factor which is equal to 1.0 for ice and concurrent wind

The evaluation of the different quantities required in Equation (8) and Equation (9) is presented in 11.2.1 to 11.2.4.

Copyright © 2010 IEEE. All rights reserved.

Copyright The Institute of Electrical and Electronics Engineers, Inc.
Provided by IHS under license with IEEE
No reproduction or networking permitted without license from IHS

Order Number: 02120914
Sold to:EGAT [700166108393] - VARRIS.Y@EGAT.CO.TH,
Not for Resale,2016-09-15 03:57:47 UTC

11.2.1 Extreme wind speed, *V*

The extreme wind speed used by the utility for transmission line design should be used as the criteria for the loading on rigid or strain bus conductors. This wind speed will depend on the location of the substation considered. For the United States, the extreme wind speed can be determined according to the Basic Wind Speed used in ASCE 7-05, as presented in Figure 14 through Figure 18. Note that in those figures, the wind speed is given in miles per hour followed in parentheses by the speed in m/s. For other countries, refer to national codes and related maps.

11.2.2 High wind speed with ice, V_i

The high wind speed with ice used by the utility for transmission line design should be used as the criteria for the loading on rigid or strain bus conductors. This wind speed will depend on the location of the substation considered. For the United States, the high wind speed with ice can be determined according to the 50 YR mean recurrence interval uniform ice thickness due to freezing rain with concurrent 3 s gust wind speeds given in Figure 8 through Figure 13. Note that in those figures, the wind speed is given in miles per hour and must be converted to the proper units used in SI calculations. For other countries, refer to national codes and related maps.

11.2.3 Force coefficient, C_f

The wind force exerted on a conductor varies with the shape of the conductor and the orientation of the wind. The variation with the shape is reflected in the force coefficient C_f. The force coefficient is 1.0 for rigid tubular conductors and strain bus conductors and approximated to 2.0 for other shapes such as channels, I-beam, square and rectangular sections, and so on. The C_f values are for the wind normal to the conductor. More precise values of C_f can be obtained from handbooks or published guidelines applicable to substation bus structures.

Copyright © 2010 IEEE. All rights reserved.

Copyright The Institute of Electrical and Electronics Engineers, Inc.
Provided by IHS under license with IEEE
No reproduction or networking permitted without license from IHS

Order Number: 02120914
Sold to:EGAT [700166108393] - VARRIS.Y@EGAT.CO.TH,
Not for Resale,2016-09-15 03:57:47 UTC

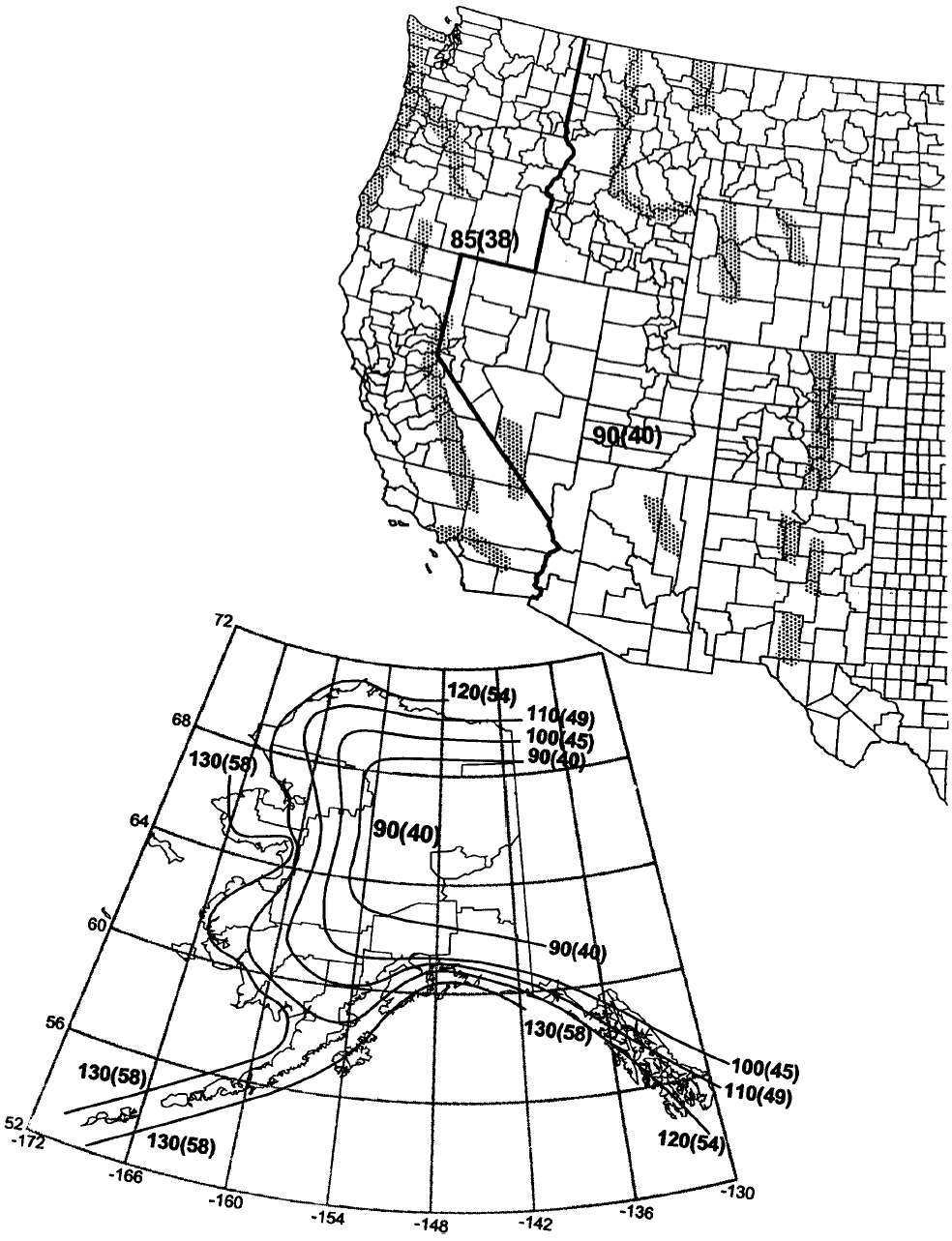

Figure 14—Basic wind speed in miles per hour (m/s)—Western United States and Alaska[20]

[20]This figure is reproduced from ASCE 7-05 Figure 6-1 with permission.

Copyright © 2010 IEEE. All rights reserved.

Copyright The Institute of Electrical and Electronics Engineers, Inc.
Provided by IHS under license with IEEE
No reproduction or networking permitted without license from IHS

Order Number: 02120914
Sold to:EGAT [700166108393] - VARRIS.Y@EGAT.CO.TH,
Not for Resale,2016-09-15 03:57:47 UTC

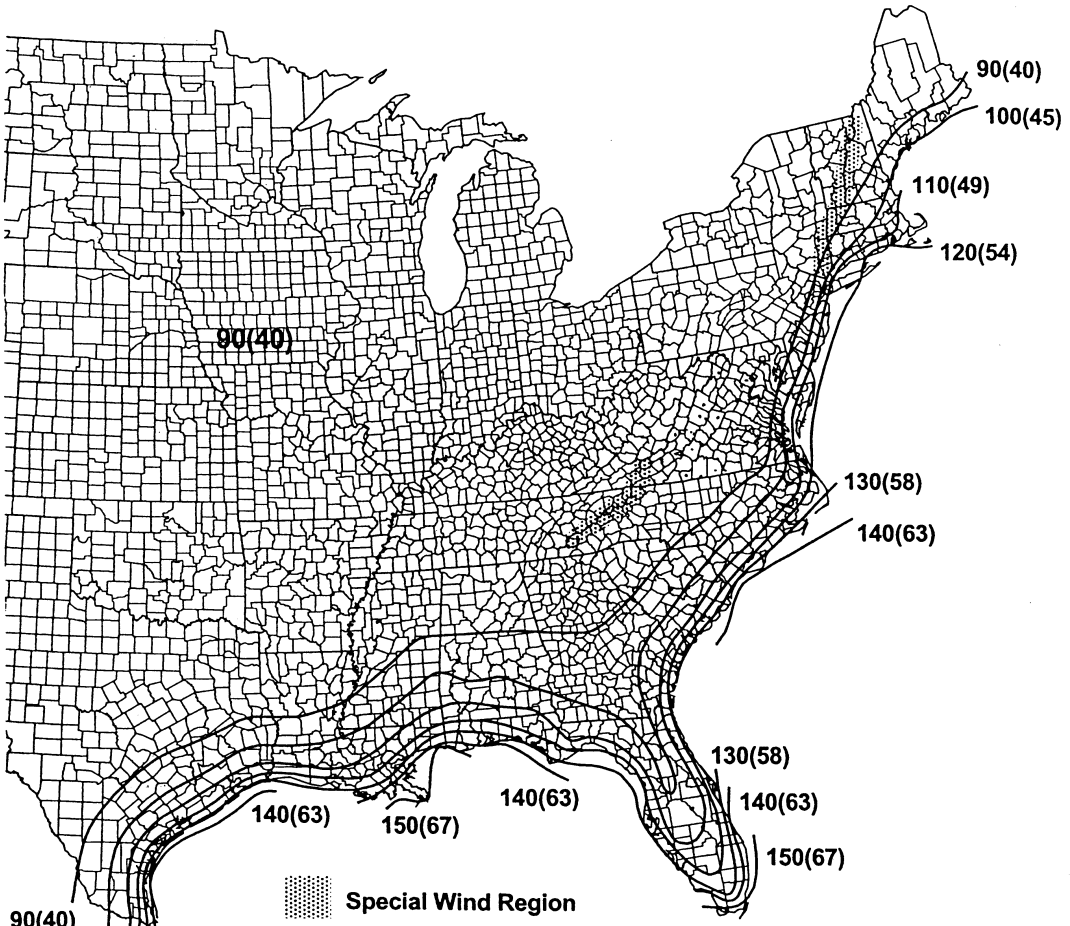

Notes:

1. Values are nominal design 3-second gust wind speeds in miles per hour (m/s) at 33 ft (10 m) above ground for Exposure C category.
2. Linear interpolation between wind contours is permitted.
3. Islands and coastal areas outside the last contour shall use the last wind speed contour of the coastal area.
4. Mountainous terrain, gorges, ocean promontories, and special wind regions shall be examined for unusual wind conditions.

Figure 15—Basic wind speed in miles per hour (m/s)—Eastern United States[21]

[21]This figure is reproduced from ASCE 7-05 Figure 6-1 continued with permission.

Copyright © 2010 IEEE. All rights reserved.

Copyright The Institute of Electrical and Electronics Engineers, Inc.
Provided by IHS under license with IEEE
No reproduction or networking permitted without license from IHS

Order Number: 02120914
Sold to:EGAT [700166108393] - VARRIS.Y@EGAT.CO.TH,
Not for Resale,2016-09-15 03:57:47 UTC

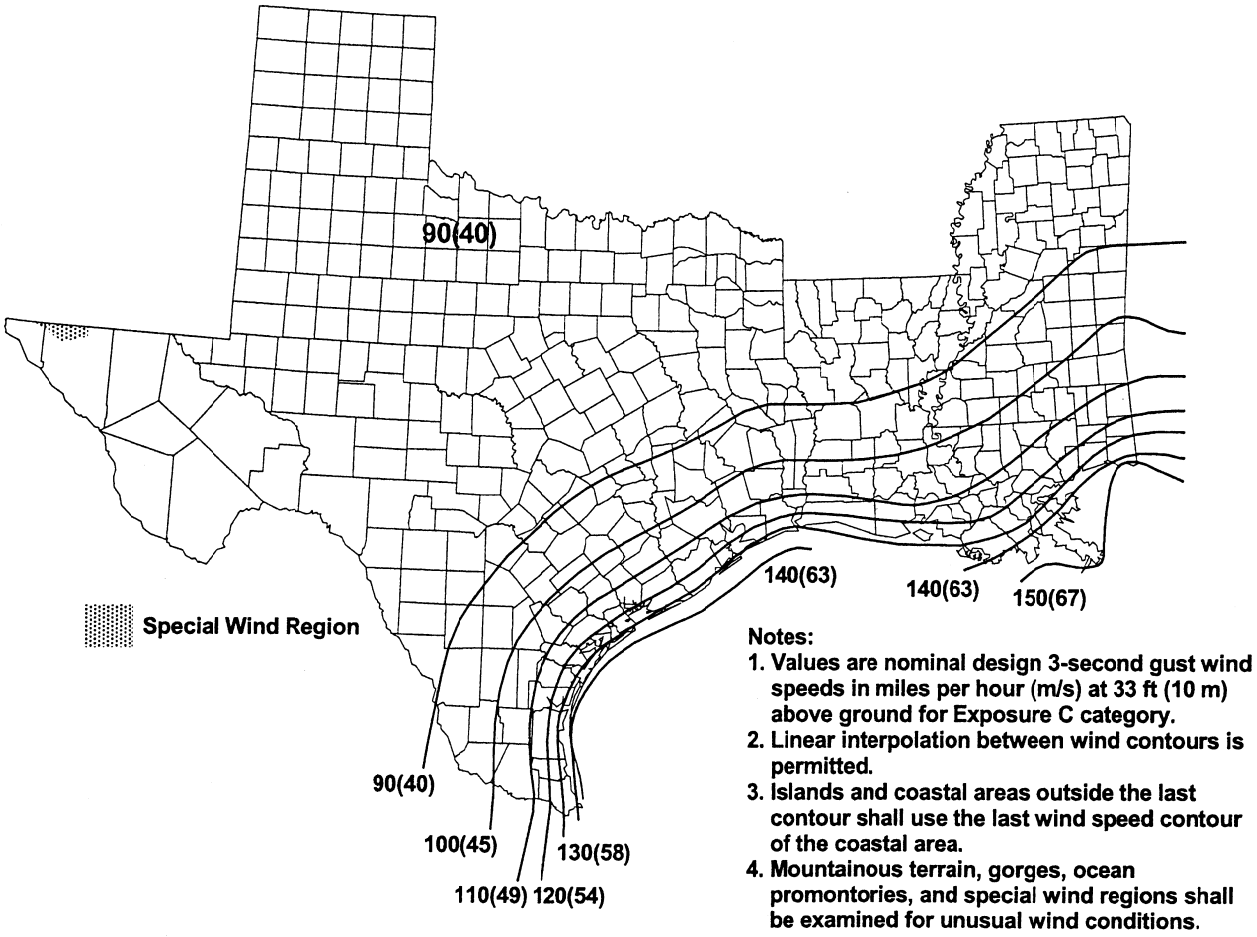

Figure 16—Basic wind speed in miles per hour (m/s)—Western Gulf of Mexico hurricane coastline[22]

[22] Reproduced from ASCE 7-05 Figure 6-1A with permission.

Copyright © 2010 IEEE. All rights reserved.

Copyright The Institute of Electrical and Electronics Engineers, Inc.
Provided by IHS under license with IEEE
No reproduction or networking permitted without license from IHS

Order Number: 02120914
Sold to:EGAT [700166108393] - VARRIS.Y@EGAT.CO.TH,
Not for Resale,2016-09-15 03:57:47 UTC

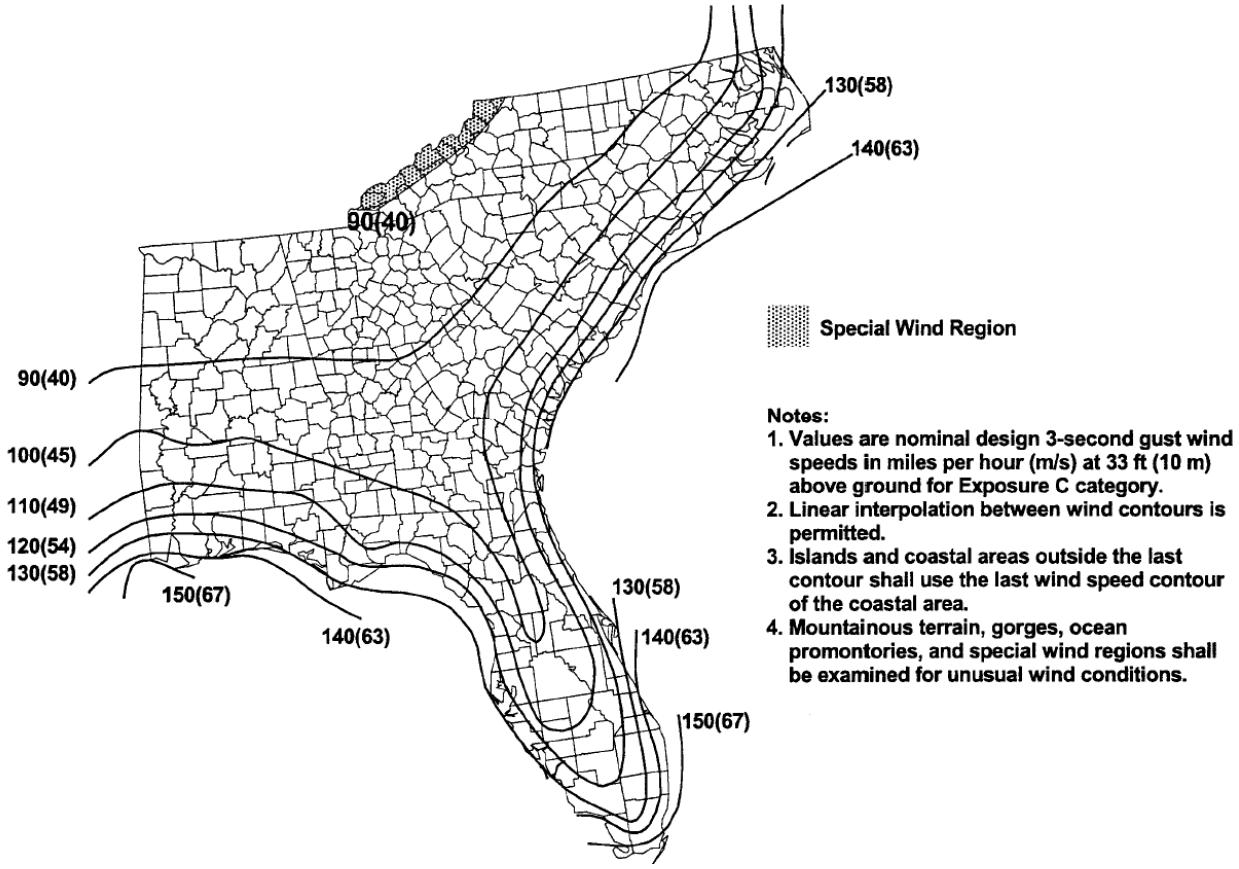

Figure 17—Basic wind speed in miles per hour (m/s)—Eastern gulf of Mexico and southeastern US hurricane coastline[23]

[23] Reproduced from ASCE 7-05 Figure 6-1B with permission.

Copyright © 2010 IEEE. All rights reserved.

Copyright The Institute of Electrical and Electronics Engineers, Inc.
Provided by IHS under license with IEEE
No reproduction or networking permitted without license from IHS

Order Number: 02120914
Sold to:EGAT [700166108393] - VARRIS.Y@EGAT.CO.TH,
Not for Resale,2016-09-15 03:57:47 UTC

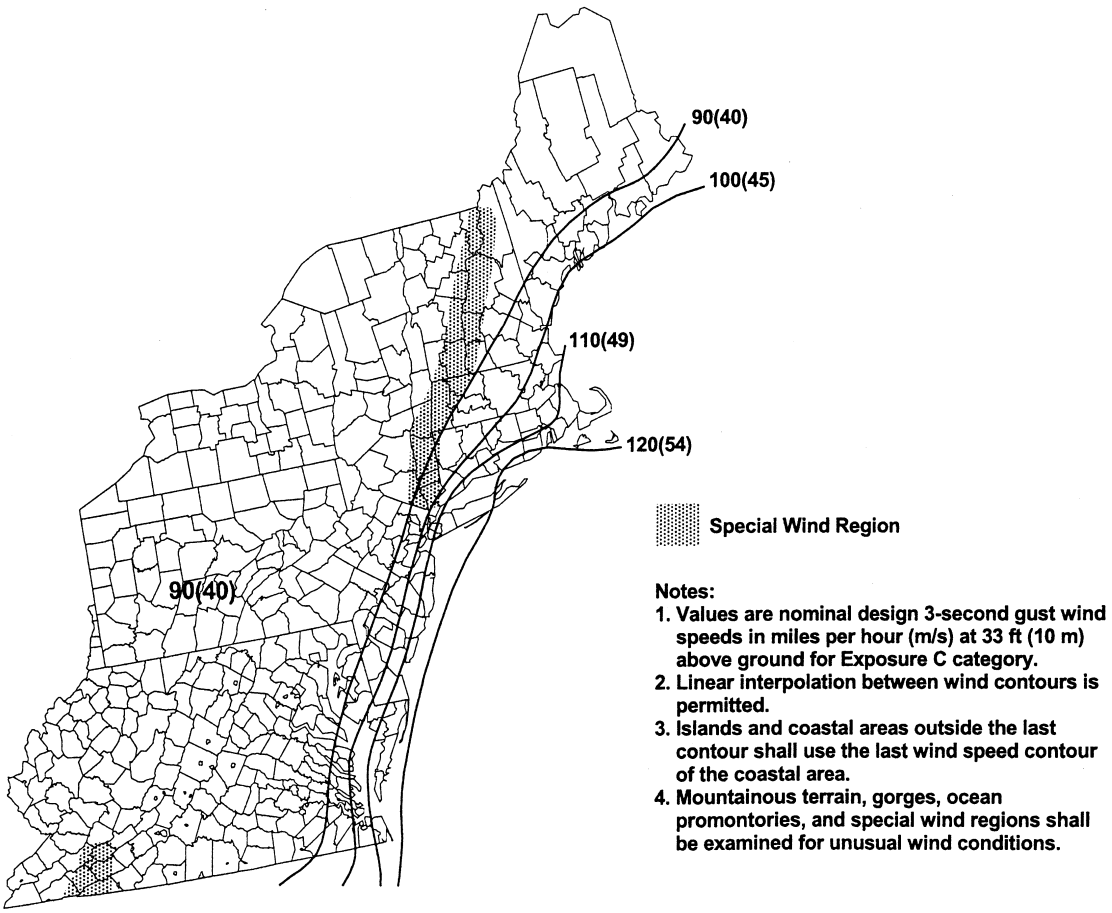

Figure 18—Basic wind speed in miles per hour (m/s)—Mid and Northern Atlantic hurricane coastline[24]

[24] Reproduced from ASCE 7-05 Figure 6-1C with permission.

Copyright © 2010 IEEE. All rights reserved.

Copyright The Institute of Electrical and Electronics Engineers, Inc.
Provided by IHS under license with IEEE
No reproduction or networking permitted without license from IHS

Order Number: 02120914
Sold to:EGAT [700166108393] - VARRIS.Y@EGAT.CO.TH,
Not for Resale,2016-09-15 03:57:47 UTC

11.2.4 Height and exposure factor, K_Z

The height and exposure factor, K_Z, takes into account the effect of the following elements:

a) The structure height above ground
b) The characteristics of the ground roughness for the site
c) The surface irregularities for the site

The height and exposure factor K_Z should be selected from Table 7. K_Z factors in Table 7 are based on surface roughness and exposure categories as described in ASCE 7-05. The summarized definitions for surface roughness and exposure categories are as follows:

Surface Roughness B: Urban or suburban areas with closely spaced obstructions such as wooded areas, single-family homes, or larger structures.

Surface Roughness C: Open terrain with scattered obstructions having heights generally less than 9.1 m (30 ft) including open country, grasslands, and water surfaces in hurricane-prone regions.

Surface Roughness D: Flat, unobstructed areas and water surfaces outside hurricane-prone regions including smooth mud flats, salt flats, and unbroken ice.

Exposure B: Exposure B shall apply where the ground conditions as described by surface roughness B exist prevailing in the upwind direction a distance of at least 800 m (2630 ft).

Exposure C: Exposure C shall apply for all cases where exposures B or D do not apply.

Exposure D: Exposure D shall apply where the ground conditions as described by surface roughness D exist prevailing in the upwind direction a distance of at least 1525 m (5000 ft). Exposure D shall extend inland a distance of 200 m (660 ft) or 10 times height of the structure, whichever is greater.

Copyright © 2010 IEEE. All rights reserved.

Copyright The Institute of Electrical and Electronics Engineers, Inc.
Provided by IHS under license with IEEE
No reproduction or networking permitted without license from IHS

Order Number: 02120914
Sold to:EGAT [700166108393] - VARRIS.Y@EGAT.CO.TH,
Not for Resale,2016-09-15 03:57:47 UTC

Table 7—Height and exposure factor K_Z

Height above ground		Exposure B	Exposure C	Exposure D
(m)	(ft)			
0–4.6	0–15	0.57	0.85	1.03
6.1	20	0.62	0.90	1.08
7.6	25	0.66	0.94	1.12
9.1	30	0.70	0.98	1.16
12.2	40	0.76	1.04	1.22
15.2	50	0.81	1.09	1.27
18	60	0.85	1.13	1.31
21.3	70	0.89	1.17	1.34
24.4	80	0.93	1.21	1.38
27.4	90	0.96	1.24	1.40
30.5	100	0.99	1.26	1.43

The values of the height and exposure factor K_Z are listed in Table 7 for heights up to 30.5 m (100 ft) above ground. The values for K_Z can also be determined for any values of height z as

$$K_z = 2.01(z/z_g)^{2/\alpha} \tag{10}$$

for 4.6 m (15ft) < z < z_g

and

$$K_z = 2.01(4.6/z_g)^{2/\alpha} \tag{11}$$

for z < 4.6 m (15 ft),

where

z is the effective height at which the wind is being evaluated
z_g is the gradient height as determined in Table 8
α is the power law coefficient for 3-s gust wind as determined in Table 8

NOTE 1—Both z and z_g must be expressed in the same units in Equation (10).

NOTE 2—The z_g value must be in meters (m). Alternatively, the value of 4.6 m in Equation (11) can be replaced by 15 to use z_g in ft.

Copyright © 2010 IEEE. All rights reserved.

Copyright The Institute of Electrical and Electronics Engineers, Inc.
Provided by IHS under license with IEEE
No reproduction or networking permitted without license from IHS

Order Number: 02120914
Sold to:EGAT [700166108393] - VARRIS.Y@EGAT.CO.TH,
Not for Resale,2016-09-15 03:57:47 UTC

Table 8—Gradient height z_g and power law coefficient α

Exposure	z_g		α
	(m)	(ft)	
B	366	1200	7.0
C	274	900	9.5
D	213	700	11.5

11.2.5 Gust response factor, G_f

11.2.5.1 Gust response factor on rigid bus conductors

A gust response factor of 0.85 shall be used on rigid bus conductors used in rigid bus structures for all exposure categories.

11.2.5.2 Gust response factor on strain bus conductors

A wire gust response factor G_{WRF} should be used in lieu of G_f in Equation (8) or Equation (9) to determine wind loads acting on strain bus conductors. This factor is a function of the exposure category, span between structures, and wire effective height; this factor accounts for the horizontal variation, wind span, and the wind profile.

For exposures B, C, and D, the wire gust response factor is given in Table 9 through Table 11, respectively. In these tables, the wire effective height is the height above the ground to the wire (strain bus) attachment point. For other heights or for a wire bus effective height over 30.5 m (100 ft) or a span over 229 m (750 ft), G_{WRF} can be evaluated using Equation (12).

Table 9—Wire gust response factor G_{WRF}, exposure B

Wire effective height, h		Wire span, L			
(m)	(ft)	L < 30.5 m L < 100 ft	30.5 < L ≤ 76 m 100 < L ≤ 250 ft	76 < L ≤ 153 m 250 < L ≤ 500 ft	153< L ≤ 230 m 500 < L ≤ 750 ft
< 10	≤ 33	1.17	1.11	1.00	0.90
> 10 to 12	> 33 to 40	1.07	1.02	0.93	0.84
> 12 to 15	> 40 to 50	1.05	1.00	0.91	0.83
> 15 to 18	> 50 to 60	1.02	0.98	0.89	0.81
> 18 to 21	> 60 to 70	1.00	0.96	0.87	0.80
> 21 to 24.4	> 70 to 80	0.98	0.94	0.86	0.79
> 24.4 to 27.5	> 80 to 90	0.97	0.93	0.85	0.78
> 27.5 to 30.5	> 90 to 100	0.95	0.92	0.84	0.77

Copyright © 2010 IEEE. All rights reserved.

Copyright The Institute of Electrical and Electronics Engineers, Inc.
Provided by IHS under license with IEEE
No reproduction or networking permitted without license from IHS

Order Number: 02120914
Sold to:EGAT [700166108393] - VARRIS.Y@EGAT.CO.TH,
Not for Resale,2016-09-15 03:57:47 UTC

Table 10—Wire gust response factor G_{WRF}, exposure C

Wire effective height, h		Wire span, L			
(m)	(ft)	L < 30.5 m L < 100 ft	30.5 < L ≤ 76 m 100 < L ≤ 250 ft	76 < L ≤ 153 m 250 < L ≤ 500 ft	153< L ≤ 230 m 500 < L ≤ 750 ft
< 10	≤ 33	0.95	0.92	0.86	0.79
> 10 to 12	> 33 to 40	0.91	0.88	0.82	0.76
> 12 to 15	> 40 to 50	0.90	0.87	0.81	0.75
> 15 to 18	> 50 to 60	0.89	0.86	0.80	0.75
> 18 to 21	> 60 to 70	0.88	0.85	0.80	0.74
> 21 to 24.4	> 70 to 80	0.87	0.84	0.79	0.73
> 24.4 to 27.5	> 80 to 90	0.86	0.83	0.78	0.73
> 27.5 to 30.5	> 90 to 100	0.85	0.83	0.78	0.73

Table 11—Wire gust response factor G_{WRF}, exposure D

Wire effective height, h		Wire span, L			
(m)	(ft)	L < 30.5 m L < 100 ft	30.5 < L ≤ 76 m 100 < L ≤ 250 ft	76 < L ≤ 153 m 250 < L ≤ 500 ft	153< L ≤ 230 m 500 < L ≤ 750 ft
< 10	≤ 33	0.85	0.82	0.77	0.72
> 10 to 12	> 33 to 40	0.82	0.80	0.75	0.71
> 12 to 15	> 40 to 50	0.81	0.79	0.75	0.70
> 15 to 18	> 50 to 60	0.80	0.78	0.74	0.70
> 18 to 21	> 60 to 70	0.80	0.78	0.74	0.70
> 21 to 24.4	> 70 to 80	0.79	0.78	0.73	0.69
> 24.4 to 27.5	> 80 to 90	0.79	0.77	0.73	0.69
> 27.5 to 30.5	> 90 to 100	0.79	0.77	0.73	0.69

$$G_{WRF} = \frac{1 + 2.7\, E_W B_W^{1/2}}{k_v^2} \tag{12}$$

where

E_W is $4.9\ (\kappa)^{1/2}\ (33/h)_{1/\alpha_s}$
B_W is $1/[1 + (0.8L/L_S)]$
h is the wire of strain bus effective height, in feet
k_v is 1.43
L is the wire horizontal span length, in feet
L_s is the turbulence scale, Table 12
κ is the surface drag coefficient, Table 12
α_s is the power law coefficient (10 min average wind), Table 12

Table 12—Exposure category constants for determination of G_{WRF}

Exposure category	Surface drag coefficient κ	Power law coefficient α_s (10 min average wind)	Turbulence scale L_s (ft)
B	0.010	4.5	170
C	0.005	7.0	220
D	0.003	10.0	250

Copyright © 2010 IEEE. All rights reserved.

Copyright The Institute of Electrical and Electronics Engineers, Inc.
Provided by IHS under license with IEEE
No reproduction or networking permitted without license from IHS

Order Number: 02120914
Sold to:EGAT [700166108393] - VARRIS.Y@EGAT.CO.TH,
Not for Resale,2016-09-15 03:57:47 UTC

11.2.5.3 Gust response factor on other structures

For other structures with a fundamental frequency greater or equal to 1Hz, the gust response factor is equal to 0.85. For structures with a fundamental frequency lower than 1 Hz, see ASCE 7-05.

11.2.6 Importance factor for basic wind speed

The return period, also called the mean recurrence interval, is approximately the reciprocal of the annual probability of occurrence. A 50-year mean recurrence interval signifies an approximately 2% annual probability of occurrence of wind loading that will exceed or equal the design value, and it corresponds to an importance factor I = 1.0. For substation structures that require a higher level of reliability, a recurrence interval of 100-year mean recurrence interval may be desirable, and it corresponds to an importance factor I = 1.15.

The selection of the importance factor provides a method of adjusting the level of structural reliability. The use of an importance factor equal to 1.0 does not imply that the structures are not important. Rather, it represents a good understanding of the probabilities of failure and required structural reliability. It is the owner's responsibility to select the appropriate importance factor for their substation structures.

11.3 Short circuit loads

The magnetic fields produced by fault current cause forces on the bus conductors. The bus conductors and bus supports must be strong enough to withstand these forces.

The force imparted to the bus structure by fault current is dependent on conductor spacing, magnitude of fault current, type of short circuit, and degree of short circuit asymmetry. Other factors to be considered are support flexibility as well as corner and end effects.

The behavior of a bus structure made of rigid conductors can be considered linear. For such structures, the electromagnetic loads do not vary with the conductor's displacements, which are assumed to be small. Therefore, a linear analysis either by simplified or finite-element method is suitable for such analysis.

The behavior of a bus structure made of strained conductors (flexible) to short circuits is nonlinear. For such structures, the electromagnetic loads do vary with the displacements of the conductors such as when two strain buses are attracted or repelled by each other. Therefore, a nonlinear analysis either by simplified calculation approximations or nonlinear finite-element method is suitable for such analysis.

The short circuit loads can be evaluated either by simplified calculations or more precisely using finite-element software with the ability to calculate automatically the spatial and temporal distribution of such loads. In general, simplified calculations present a high degree of conservatism, whereas the finite-element methodology provides a more refined and representative calculation.

11.3.1 Generalities on short circuit current and forces

A short circuit generates electric current that in general consists of a sinusoidal waveform and a direct current (dc) component that is varying with time (decaying). For faults near generating units, the RMS value of the alternating current (ac) component may also vary with time. Faults may be three phase, phase to phase, phase to ground, and so on.

Copyright © 2010 IEEE. All rights reserved.

Copyright The Institute of Electrical and Electronics Engineers, Inc.
Provided by IHS under license with IEEE
No reproduction or networking permitted without license from IHS

Order Number: 02120914
Sold to:EGAT [700166108393] - VARRIS.Y@EGAT.CO.TH,
Not for Resale,2016-09-15 03:57:47 UTC

The flow of high levels of current generates forces on the current carrying conductors. The basic physical law is expressed with the *Biot-Savart* equation as below, which is explained with the aid of Figure 19. The figure shows two segments of conductors of lengths d_1 and d_2, respectively and carrying electric current i_1 and i_2, respectively. The force that will act on each one of these two segments is as follows:

$$F(t)=\frac{\mu}{4\pi r^2} i_1(t) i_2(t)\left[d_1 \otimes (u_r \otimes d_2)\right] \tag{13}$$

where

μ	is the magnetic permeability equal to $4\pi \times 10^{-7}$ V-s/(A-m)
r	is the distance between the two conductor segments
u_r	is the unit directional vector in the direction r
d_1	is a vector of length d_1 in the direction of the current flow in conductor segment 1
d_2	is a vector of length d_2 in the direction of the current flow in conductor segment 2

NOTE—The symbol ⊗ is the vectorial cross product.

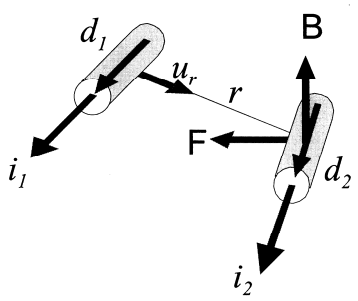

Figure 19—Illustration of two conductor segments carrying electric current

In the case of two parallel conductor segments, the cross products simply become the product of the conductor segment lengths and the force is along the line between the two segment centers, either attracting the two conductor segments or repelling them depending on the direction of the current.

This physical law is applicable to rigid bus structures as well as flexible bus structures. In the case of a rigid bus, the geometry of the bus remains practically invariant as the displacements tend to be very small. In the case of a flexible bus, the geometry of the bus varies as the forces from the fault current move the conductors around. As the distances between conductors change, so do the forces from the currents.

11.3.2 Maximum fault condition parameters

In the design process, one must consider the worst possible scenario. In terms of forces from fault currents, the fault initiation instance with respect to the source waveform is very important. Depending on the type of fault considered (phase to phase or three phased), appropriate electrical parameters need to be fixed in numerical calculations as to generate maximum fault conditions for design. The voltage angle at the initiation of fault is random in nature and should thus be fixed to:

a) 0 for phase-to-phase fault for any conductor geometry

Copyright © 2010 IEEE. All rights reserved.

Copyright The Institute of Electrical and Electronics Engineers, Inc.
Provided by IHS under license with IEEE
No reproduction or networking permitted without license from IHS

Order Number: 02120914
Sold to:EGAT [700166108393] - VARRIS.Y@EGAT.CO.TH,
Not for Resale,2016-09-15 03:57:47 UTC

b) π/4 for three-phased fault for parallel conductors; for other arrangements, the angle producing the maximum result must be found by trial and error. This value is valid for rigid buses; for flexible buses, the value producing the maximum result must be found by trial and error if the finite-element method is used.

11.3.3 Simplified calculations for short circuit loads on rigid buses

11.3.3.1 Basic force equation between infinitely long parallel conductors

The equation for the force between parallel, infinitely long conductors in a flat configuration due to a fully asymmetrical short circuit current is as follows.

For metric units:

$$F_{sc} = \frac{16\Gamma I_{sc}^2}{10^7 D} \tag{14}$$

For English units:

$$F_{sc} = \frac{3.6\Gamma I_{sc}^2}{10^7 D} \tag{15}$$

where

F_{sc} is the fault current force by unit length, N/m (lbf/ft)
I_{sc} is the symetrical RMS fault current, A
D is the conductor spacing center-to-center, m (ft)
Γ is a constant based on type of fault and conductor location (Table 13)

Equation (14) and Equation (15) assume that the fault is initiated to produce the maximum current offset. Specifically, it has been assumed that the dc offset current is $\sqrt{2}I_{sc}$, which is the same as the peak ac current. Thus, the maximum current through the conductor is $2\sqrt{2}I_{sc}$.

The magnitudes of the fault current I_{SC} for each type of fault (three phase, phase to phase, etc.) do not assume their peak values at the same time, and the dc offset is in general different for each phase. The effect of these variations is expressed in the factor Γ. This factor is tabulated in Table 13.

Copyright © 2010 IEEE. All rights reserved.
Copyright The Institute of Electrical and Electronics Engineers, Inc.
Provided by IHS under license with IEEE
No reproduction or networking permitted without license from IHS
Order Number: 02120914
Sold to:EGAT [700166108393] - VARRIS.Y@EGAT.CO.TH,
Not for Resale,2016-09-15 03:57:47 UTC

Table 13—Γ constant for simplified calculation short circuit basic force equation

Type of short circuit	Configuration	Conductor	Γ
Phase to phase	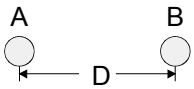	A or B	1.000
Three phase	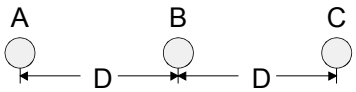	B	0.866
Three phase	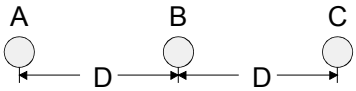	A or C	0.808
Phase to phase	Triangular arrangement—equilateral triangle—side D	A or B	1.0
Three phase	Triangular arrangement—equilateral triangle—side D	A or B or C	0.5

NOTE—For a three-phase fault, this table indicates that the maximum force is on the central conductor B. However, results from finite-element calculations (which provide a much closer estimation of the maximum forces than the preceding equation) indicate that in most cases, the maximum stresses and transmitted effects on the support structure are in either conductor A or C.

11.3.3.2 Corrected basic force equation between parallel conductors

Equation (14) [or Equation (15)] for the basic force by unit length between infinitely long conductors provides in most cases an overly conservative estimate of the maximum force that will occur in practice. Many inherent hypotheses underlying this equation are not realistic in practice, among others:

a) Infinite conductor length; in practice, the conductors are of finite length.

b) The peak current is twice the RMS value; in practice, the peak current is a function of the time constant of the circuit.

c) The structure responds instantaneously to the electromagnetic load and reaches its maximum response at the same time the current is at its peak; in practice the maximum response of the structure is attained after the current has reach its peak value, due to the flexibility of the supporting structure and of the conductors themselves.

d) Damping of the insulator, supporting structure, and conductors is not accounted for in these equations.

The following corrected basic force equation is proposed to alleviate some of the conservatism present in the basic force equation for infinitely long conductors:

$$F_{sc\_\text{corrected}} = D_f^2 K_f F_{sc} \tag{16}$$

Copyright © 2010 IEEE. All rights reserved.

Copyright The Institute of Electrical and Electronics Engineers, Inc.
Provided by IHS under license with IEEE
No reproduction or networking permitted without license from IHS

Order Number: 02120914
Sold to:EGAT [700166108393] - VARRIS.Y@EGAT.CO.TH,
Not for Resale,2016-09-15 03:57:47 UTC

where

D_f is the half-cycle decrement factor to account for the momentary peak factor effect
K_f is the mounting structure flexibility factor to account for the structure's flexibility
F_{sc} is the basic force Equation (14) [or Equation (15) in British units].

The evaluation of the constants D_f and K_f is presented in the following discussion. It is to be underlined that even with these factors, the resulting force equation is still a conservative estimate of the force acting on the structure, as compared with finite-element calculations that provide a more realistic estimate as supported by correlations with tests. Also, this equation is valid only for parallel conductors and cannot take into account 3D effects, corner effects, etc, which are present in most cases in practice.

a) Half-cycle decrement factor D_f

A typical short circuit current comprises of an ac (power frequency) component and a dc decreasing component. The typical short circuit current time variation $i_{sc}(t)$is given by

$$i_{sc}(t) = \sqrt{2}\, I_{sc} \left[\cos(2\pi f t + \delta) - e^{-t/T_a} \cos(\delta)\right] \tag{17}$$

where

f is the system frequency
δ is the angle between current and tension at establishment of fault
t is the time

where

$$T_a = \frac{X}{R}\frac{1}{2\pi f} \tag{18}$$

where

X is the system reactance at the location of the fault
R is the system resistance at the location of the fault

Note that the worst condition occurs for $\delta = 0$.

Due to the dc decreasing component, the maximum force on the conductor will theoretically occur during the first half cycle of the fault current if the dynamic response of the bus and supporting structure is not taken into account. The peak value of the force in the first half cycle, assuming fully offset fault current is expressed with the aid of the half cycle decrement factor D_f:

$$D_f = \frac{1 + e^{-\frac{1}{2fT_a}}}{2} \tag{19}$$

Copyright © 2010 IEEE. All rights reserved.

Copyright The Institute of Electrical and Electronics Engineers, Inc.
Provided by IHS under license with IEEE
No reproduction or networking permitted without license from IHS

Order Number: 02120914
Sold to:EGAT [700166108393] - VARRIS.Y@EGAT.CO.TH,
Not for Resale,2016-09-15 03:57:47 UTC

For convenience, Table 14 provides values of the decrement factor. Note that the half-cycle decrement factor will be 0.5 if the dc component of the current is not present.

Table 14—Half-cycle decrement factor D_f for various values of *X/R* ratio

60 Hz				50 Hz			
X/R	T_a	D_f	D_f^2	***X/R***	T_a	D_f	D_f^2
30	0.0796	0.950	0.903	30	0.0955	0.950	0.903
20	0.0531	0.927	0.860	20	0.0637	0.927	0.860
10	0.0265	0.865	0.749	10	0.0318	0.865	0.749
5	0.0133	0.767	0.588	5	0.0159	0.767	0.588
2	0.0053	0.604	0.365	2	0.0064	0.604	0.365
1	0.0027	0.522	0.272	1	0.0032	0.522	0.272

Equation (19) gives the maximum decrement factor in the first half cycle of the fault. The actual correction when maximum conductor span deflection occurs is usually less because of the following:

— Most conductor spans will not reach maximum deflection until after the first quarter-cycle.

— Additional current decrement occurs as the fault continues, especially for low *X/R* ratios.

The combination of these two factors results in a lower maximum deflection than the deflection caused by steady-state force equal to the maximum force in the first quarter cycle.

Tests have demonstrated that conductor spans with natural frequencies of 1/10 of the power frequency or less, and in a system with an *X/R* ratio of 13 or less, will have fault current forces that will be typically less than one half the calculated first half-cycle force when the conductor span reaches full deflection.

b) Mounting structure flexibility factor K_f

Because of their flexibility, the bus and mounting structures are capable of absorbing energy during a fault. Thus, depending on the type of mounting structures and their heights, the effective fault current forces will be lower than the half-cycle maximum value. The effect of the structure flexibility is accounted with the mounting-structure flexibility factor, K_f.

Values of K_f for single-phase mounting structures are given in Figure 20. K_f is usually assumed to be unity for three-phase mounting structures.

Copyright © 2010 IEEE. All rights reserved.

Copyright The Institute of Electrical and Electronics Engineers, Inc.
Provided by IHS under license with IEEE
No reproduction or networking permitted without license from IHS

Order Number: 02120914
Sold to:EGAT [700166108393] - VARRIS.Y@EGAT.CO.TH,
Not for Resale,2016-09-15 03:57:47 UTC

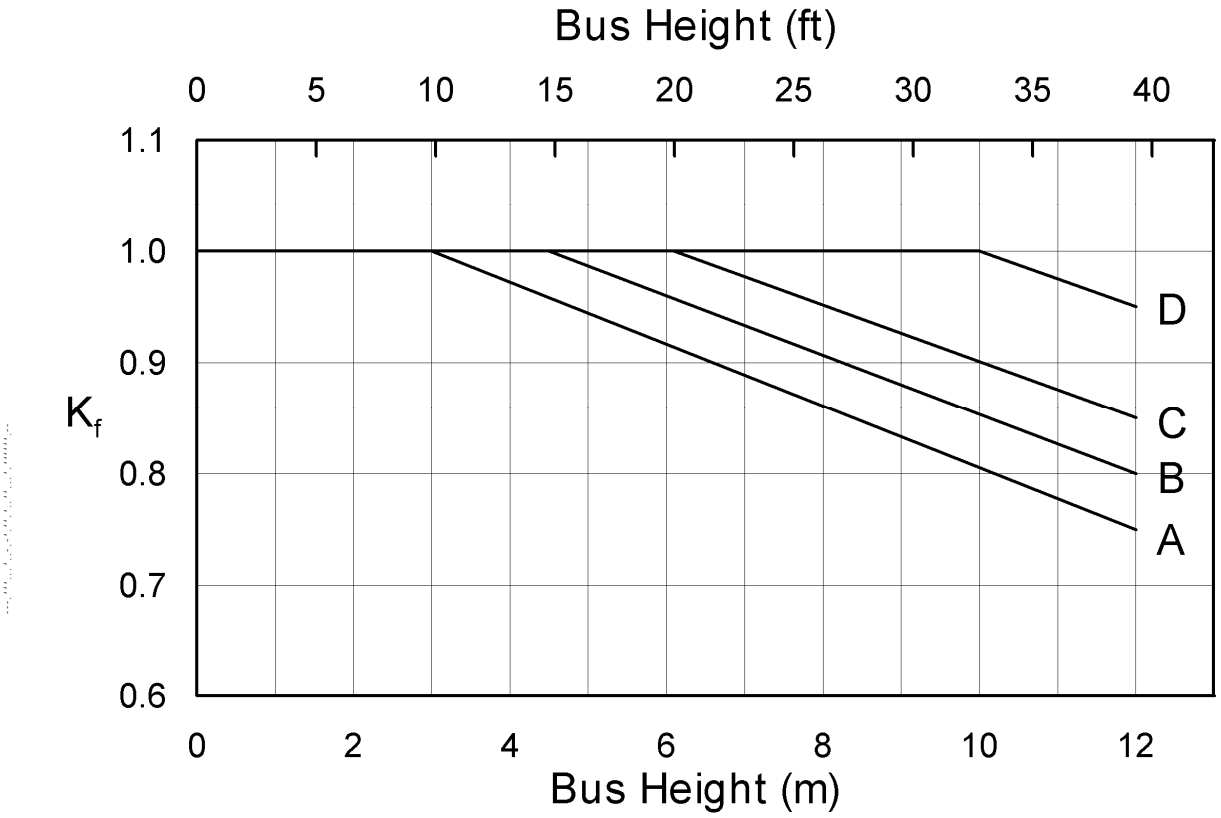

NOTE—A, lattice and tubular aluminum; B, tubular and wide-flange steel and wood pole; C, lattice steel; D, solid concrete.

Figure 20—K_f for various types of single-phase mounting structures

There have been fault current tests conducted on specific combinations of rigid-bus structures with mounting structures that indicate lower values of K_f than those shown in Figure 20. Where the structures are similar to those tested, the lower values of K_f may apply. Future work is expected to produce methods for determining values of K_f for specific mounting structures.

11.3.3.3 Bundle conductor pinch factor for rigid buses

Forces from short circuit currents are also developed on the subconductors of bundle conductors. Because of the close proximity of the subconductors, these forces could be substantial. Simplified expressions of the forces on subconductors are given below under the following assumptions: (1) the fault current will be equally distributed among the subconductors of the bundle and (2) the forces of the other phases are neglected.

Metric units:

$$F_{sc-b} = \frac{16\Gamma_b I_{sc}^2}{10^7 D_b N^2} \tag{20}$$

Copyright © 2010 IEEE. All rights reserved.

Copyright The Institute of Electrical and Electronics Engineers, Inc.
Provided by IHS under license with IEEE
No reproduction or networking permitted without license from IHS

Order Number: 02120914
Sold to:EGAT [700166108393] - VARRIS.Y@EGAT.CO.TH,
Not for Resale,2016-09-15 03:57:47 UTC

English units:

$$F_{sc-b} = \frac{3.6\,\Gamma_b\,I_{sc}^2}{10^7\,D_b\,N^2} \tag{21}$$

where

F_{sc-b} is the short circuit force in bundle conductors by unit length, N/m (lbf/ft)
Γ_b is a constant based on type of fault and conductor configuration (Table 15)
D_b is the distance between subconductors, m (ft)
N is the number of subconductors in the bundle

Table 15—Γ_b constant for simplified calculation short circuit force equation in bundle subconductors

Configuration	Γ_b
Two subconductors—separation distance D_b	1.000
Three subconductors—equilateral triangle—separation distance D_b	1.73
Four subconductors—square—separation distance D_b	1.91

11.3.3.4 Precision of simplified calculations for rigid bus and other effects

The values for the short circuit forces calculated by all equations in the preceding subclause are for parallel and infinitely long conductors. The results will be conservative because of end effects and because, as stated earlier, such equations do not take into account the transient dynamic response of the conductors, insulators, and supporting structures in regard to the relatively short duration of short circuits, as well as of the inherent damping in insulators and structures. Furthermore, these equations cannot be used for special cases such as corners and nonparallel conductors. Subclause 11.3.4 describes a modern and advanced method leading to a more precise evaluation of forces that can also be used to deal with any type of geometry, including corner and end effects.

11.3.4 Finite-element calculations for short circuit loads on rigid buses

11.3.4.1 Description of the method

The use of finite-element software with the ability to calculate electromagnetic loads permits evaluation of their variation in time automatically according to short circuit current waveform, its type (phase to phase or three phased), as well as their spatial distribution. To do so, linear dynamic analysis is required in the software as well. Such software does not generally provide the loads directly to the user but does provide their effect by calculation of the dynamic response of the complete structure (conductors, insulators, and supports) to them. This latter characteristic also permits more precisely evaluation of the response of the structure.

Generally, such software divides each conductor in a finite number of small elements and calculates the electromagnetic interaction between each (within a phase and between each phase). This latter characteristic thus permits evaluation of the spatial distribution of such loads in a precise way and consideration of complex 3D conductor arrangements, without the limitations and conservatism implied in the use of the infinitely long parallel simplified calculations presented in the preceding subclauses. For example, corner effects can be evaluated precisely as well as the situation where more than three conductors are implied, such as when 2 three-phased structures cross each other at different heights.

Copyright © 2010 IEEE. All rights reserved.

Copyright The Institute of Electrical and Electronics Engineers, Inc.
Provided by IHS under license with IEEE
No reproduction or networking permitted without license from IHS

Order Number: 02120914
Sold to:EGAT [700166108393] - VARRIS.Y@EGAT.CO.TH,
Not for Resale,2016-09-15 03:57:47 UTC

Another advantage of this method is to easily permit the realization of parametric studies in order to study effects of variation of different parameters (e.g., spans, type, and size of conductors and/or insulators) as to optimize a design.

To produce accurate results with such a method, a relatively precise knowledge of all structural characteristics and boundary conditions must first be obtained.

The finite-element method has been validated experimentally by various investigators and has been shown to provide accurate results. Hosemann and Tsanakas [B14] as well as Iordanescu et al. [B25] describe some comparisons with actual tests.

11.3.4.2 Finite-element calculation examples

Finite-element calculation examples of a short circuit for rigid bus structures are given in Annex F. Comparisons with simplified calculations are provided as well. It is observed that simplified calculations are conservative.

11.3.5 Simplified calculations for short circuit loads on strain bus

11.3.5.1 Generalities

The methods described below use simple analytical representations of short circuit effects. They give maximum values and no information about the time history of the phenomena. These methods require only general data, for example, span length, static tension, distance between phases, structure stiffness, cable mass, short circuit current, and duration. They apply only for specific general cases. These methods are valid for spans that are long enough so that flexural conductor stiffness does not play a significant role, which is generally 10–15 m and over. They do not apply to flexible buses interconnecting substation equipment over short spans (generally below 7–8 m; e.g., between a disconnect switch and a circuit breaker). Stranded conductors as used in substation bus systems are hence assumed to have no flexural strength and are therefore normally under tensile force only, in static equilibrium with the load imposed by their own weight.

The simplified methods of calculating mechanical short circuit effects are based on the configurations illustrated in Figure 21 and Figure 22. The short circuit loads act in the horizontal x-direction and cause the spans to swing out of the vertical *yz* plane. Because of the inertia of the system, the response of the bus is much slower than the time function of the short circuit forces, and the electromagnetic force can be computed in the undeformed initial position of the conductors.

Copyright © 2010 IEEE. All rights reserved.
Copyright The Institute of Electrical and Electronics Engineers, Inc.
Provided by IHS under license with IEEE
No reproduction or networking permitted without license from IHS
Order Number: 02120914
Sold to:EGAT [700166108393] - VARRIS.Y@EGAT.CO.TH,
Not for Resale,2016-09-15 03:57:47 UTC

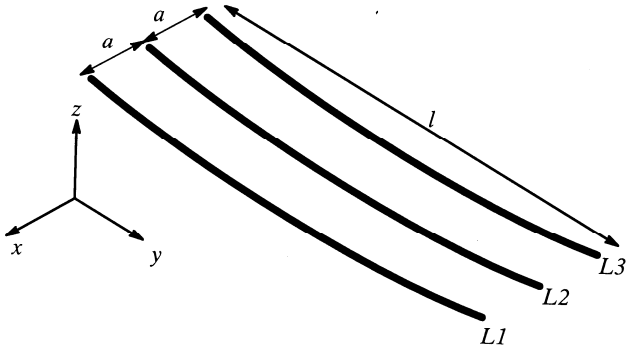

Figure 21—Schematic configuration for three-phase short circuit or line-to-line short circuit

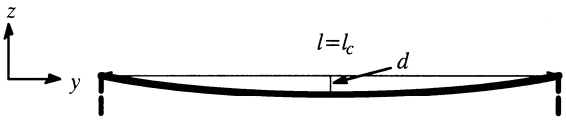

a) strained conductor with vertical support insulators

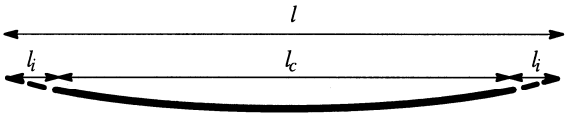

b) strained conductor with insulator chains

Figure 22—Dimensions of strain bus for two basic support conditions

Three types of forces can be calculated with the simplified calculation methods as follows:

a) The maximum tensile force during the short circuit, denoted by F_t

b) The maximum tensile force after the short circuit when the conductor drops back, denoted by F_f

c) The maximum tensile force caused by the pinch effect when conductors in a bundle clash together under the short circuit, denoted by F_{pi}

These forces are applied in the horizontal direction of the line (direction y in Figure 21 and Figure 22), at the attachment points of the conductor.

In addition, the simplified methods permit calculation of the following:

a) The maximum horizontal displacement of the span, denoted by b_h

b) The minimum air clearance between conductors, denoted by a_{min}

In installations with strain buses, the stresses occurring in line-to-line short circuits and balanced three-phase short circuits are approximately equal. However, for line-to-line short circuits, the conductor swing out typically results in the maximum decrease of clearance (when adjacent conductors carrying short circuit current move toward one another

Copyright © 2010 IEEE. All rights reserved.
Copyright The Institute of Electrical and Electronics Engineers, Inc.
Provided by IHS under license with IEEE
No reproduction or networking permitted without license from IHS
Order Number: 02120914
Sold to:EGAT [700166108393] - VARRIS.Y@EGAT.CO.TH,
Not for Resale,2016-09-15 03:57:47 UTC

after the short circuit). In the case of a balanced three-phase short circuit, the center conductor (*L*2 in Figure 21 moves only slightly because of its inertia and the alternating bidirectional forces that act on it, thus leading to a lesser decrease of clearance than the former case).

Note that the calculations of the maximum forces and minimum clearances shall be carried on the basis of the static tensile force F_{st}, as described in the following subclause, existing at the local minimum winter temperature (e.g., –20 °C), and on the basis of F_{st} at the maximum operating temperature (e.g., 60 °C). To evaluate them at those temperatures, it is necessary to know the corresponding sag *d*.

11.3.5.2 Origin of simplified calculation method for strain bus

The simplified calculation method presented below is derived from IEC 60865-1 Ed. 2-1993 [B16] and uses with permission many equations and figures from this standard.[24]

11.3.5.3 Preliminary calculations

To obtain the forces and geometric quantities discussed in the previous subclause, several preliminary calculations are necessary, which are described below. In what follows, the term "conductor" is used for a bundle of *n* subconductors.

Characteristic electromagnetic load

Let *F'* be the characteristic electromagnetic load per unit length (N/m) on a flexible conductor in three-phase systems on the outer conductors:

$$F' = \frac{\mu_o}{2\pi} 0.75 \frac{I_{k3}^2}{a} \frac{l_c}{l} \tag{22}$$

where for SI units

μ_0 is the magnetic permeability constant given by $1.257 \cdot 10^{-6}$ V-s/A-m
I_{k3} is the RMS value of the three-phase symmetrical short circuit current (A) in the conductor
a is the center-line distance between conductor mid-points (Figure 21), m
l is the conductor span, m
l_c is the distance between the two supports, m

NOTE—For strained conductors that exert bending forces on the support insulators (vertical insulators), the span l is equal to the conductor span l_c (Figure 22(a). For spans with strained conductors attached to the structure with insulator chains, $l = l_c + 2l_i$, where l_i is the length of one insulator chain [Figure 22(b)].

In the case of two-line single-phase systems, *F'* is given by:

$$F' = \frac{\mu_o}{2\pi} \frac{I_{k2}^2}{a} \frac{l_c}{l} \tag{23}$$

[24]The authors thank the International Electrotechnical Commission (IEC) for permission to reproduce information from its International Standard IEC 60865-1 Ed. 2.0-1993 [B16] All such extracts are copyright of the IEC, Geneva, and Switzerland. All rights reserved. Further information on the IEC is available from the World Wide Web at www.iec.ch. The IEC has no responsibility for the placement and context in which the extracts and contents are reproduced by the authors, nor is the IEC in any way responsible for the other content or accuracy therein.

Copyright © 2010 IEEE. All rights reserved.

Copyright The Institute of Electrical and Electronics Engineers, Inc.
Provided by IHS under license with IEEE
No reproduction or networking permitted without license from IHS

Order Number: 02120914
Sold to:EGAT [700166108393] - VARRIS.Y@EGAT.CO.TH,
Not for Resale,2016-09-15 03:57:47 UTC

where

I_{k2} is the RMS value of the two-phase symmetrical short circuit current.

It is to be recognized that Equation (22) and Equation (23) are of the same order because typically

$$I_{k2} = \frac{\sqrt{3}}{2} \times I_{k3}$$

Ratio of electromagnetic force to gravitational force

Let r be the ratio of F' to the gravitational force (F_g) on a conductor:

$$r = \frac{F'}{F_g} = \frac{F'}{n\overline{m}\,g} \tag{24}$$

where

n is the number of subconductors in the bundle
$\overline{m}$ is the linear mass of a single subconductor in the bundle (kg/m)
g is the gravitational acceleration (9.8 m/s^2)

The direction of the resulting force exerted on the conductor is given by:

$$\delta_1 = \arctan(r) \tag{25}$$

Static tensile force

Let F_{st} be the static tensile force (N) of a conductor made of n subconductors under its own weight at mid span, in its normal operating configuration. For a conductor with both ends at equal height and for which the ratio of sag to span is smaller than 1/8, a good approximation is given by:

$$F_{st} = \frac{n\overline{m}\,g\,l^2}{8d} \tag{26}$$

where

l is the span (m)
d is the sag (m)

NOTE—If instead of the sag d the static tensile force F_{st} is provided as input, then Equation (26) can be inversed to provide the value of sag d.

Copyright © 2010 IEEE. All rights reserved.

Copyright The Institute of Electrical and Electronics Engineers, Inc.
Provided by IHS under license with IEEE
No reproduction or networking permitted without license from IHS

Order Number: 02120914
Sold to:EGAT [700166108393] - VARRIS.Y@EGAT.CO.TH,
Not for Resale,2016-09-15 03:57:47 UTC

Natural period of conductor oscillation

Let T be the natural period (s) of the conductor oscillation (pendulum or free oscillation) assuming a small oscillating angle δ around the *y*-axis from the vertical plane *y*-*z* (Figure 21):

$$T = 2\pi\sqrt{0.8\frac{d}{g}} \tag{27}$$

Period of oscillation during short circuit

Let T_{res} be the resulting period(s) of the conductor oscillation during the short circuit flow:

$$T_{res} = \frac{T}{\sqrt[4]{1+r^2}\left[1-\frac{\pi^2}{64}\left(\frac{\delta_1}{90^o}\right)^2\right]} \tag{28}$$

NOTE— The value δ_1 is in degrees.

Maximum swing-out angle

During phase-to-phase or three-phase short circuits, two of the spans swing away from each other (the two external spans in the case of a three-phase system). Assuming that they remain evenly shaped, they can be considered to act as rigid pendulums. During the short circuit duration T_{k1}, a theoretical maximum angle $\delta=\delta_k$ is attained and the distance between the centers of gravity of the conductors is higher than the equilibrium position given by *2a* (Figure 21) in the case of a three-phase system and *a* in case of a line-to-line fault (Figure 21). The theoretical maximum angle δ_k is given by:

$$\delta_k = \begin{cases} \delta_1\left[1-\cos\left(360^\circ\frac{T_{k1}}{T_{\text{res}}}\right)\right] & \text{for } 0 \le \frac{T_{k1}}{T_{\text{res}}} \le 0.5 \\ 2\delta_1 & \text{for } \frac{T_{k1}}{T_{\text{res}}} > 0.5 \end{cases} \tag{29}$$

where

T_{k1} is the duration of the short circuit(s)

However, spans during short circuits do not behave like free, ideal pendulums (or free oscillators); they sustain radial displacements for some time within the δ_k range. For this reason, the maximum swing-out angle, denoted by δ_m, will be different from the theoretical value δ_k.

Copyright © 2010 IEEE. All rights reserved.

Copyright The Institute of Electrical and Electronics Engineers, Inc.
Provided by IHS under license with IEEE
No reproduction or networking permitted without license from IHS

Order Number: 02120914
Sold to:EGAT [700166108393] - VARRIS.Y@EGAT.CO.TH,
Not for Resale,2016-09-15 03:57:47 UTC

The maximum swing-out angle is obtained as follows:

$$\delta_m = \begin{cases} 1.25 \arccos \chi & \text{for } 0.766 \le \chi \le 1 \\ 10° + \arccos \chi & \text{for } -0.985 \le \chi \le 0.766 \\ 180° & \text{for } \chi \le -0.985 \end{cases} \quad (30)$$

where

$$\chi = \begin{cases} 1 - r \sin \delta_k & \text{for } 0 \le \delta_k \le 90° \\ 1 - r & \text{for } \delta_k > 90° \end{cases} \quad (31)$$

In the case where T_{k1} is unknown or is greater than 0.4 T, then the value 0.4 T shall be used for T_{k1} in Equation (29), Equation (39), and Equation (44).

Flexibility norm of the conductor-insulator system

Let N be the flexibility norm of the conductor-insulator system:

$$N = \frac{1}{k_{eq}\, l} \quad (32)$$

where

k_{eq} is the equivalent axial rigidity of the system, N/m, which calculation is obtained as follows.

The axial rigidity of a conductor of span l_c (approximately equal to the conductor length for small sag) is given for a conductor made of one material by:

$$k_c = n \frac{E_s\, A_s}{l_c} \quad (33)$$

where

n is the number of subconductors
E_s is the Young modulus of the subconductor material, N/m^2
A_s is the subconductor cross section area, m^2

For a conductor made of two material (e.g., aluminium/steel), the axial rigidity is given by:

$$k_c = n \left(\frac{E_{s1}\, A_{s1} + E_{s2}\, A_{s2}}{l_c} \right) \quad (34)$$

Copyright © 2010 IEEE. All rights reserved.

Copyright The Institute of Electrical and Electronics Engineers, Inc.
Provided by IHS under license with IEEE
No reproduction or networking permitted without license from IHS

Order Number: 02120914
Sold to:EGAT [700166108393] - VARRIS.Y@EGAT.CO.TH,
Not for Resale,2016-09-15 03:57:47 UTC

where the indices 1 and 2 refer to the two respective materials used.

The axial rigidity of an insulator string of length l_i is given by:

$$k_i = \frac{E_i A_i}{l_i} \tag{35}$$

where

E_i is the Young modulus of the insulator string material, N/m^2
A_i is the insulator effective cross section, m^2

To evaluate k_{eq}, two cases are now given, considering that each component acts together as serial springs.

a) Strained conductor attached to the structure with two insulator chains (one on each side)

For this case, the equivalent axial rigidity k_{eq} is calculated from:

$$\frac{1}{k_{eq}} = \frac{1}{k_c} + \frac{2}{k_i} \tag{36}$$

b) Strained conductor attached to the structure with vertical support insulators

For this case, the equivalent axial rigidity k_{eq} is calculated from:

$$\frac{1}{k_{eq}} = \frac{1}{k_c} + \frac{1}{S} \tag{37}$$

where

S is an empirical value given by 10^5 N/m

Stress factor

The stress factor of the conductor used below in Figure 23 and in Equation (40) and Equation (42), is given by:

$$\zeta = \frac{(n g \overline{m} l)^2}{24 F_{st}^3 N} \tag{38}$$

Copyright © 2010 IEEE. All rights reserved.
Copyright The Institute of Electrical and Electronics Engineers, Inc.
Provided by IHS under license with IEEE
No reproduction or networking permitted without license from IHS
Order Number: 02120914
Sold to:EGAT [700166108393] - VARRIS.Y@EGAT.CO.TH,
Not for Resale,2016-09-15 03:57:47 UTC

11.3.5.4 Maximum tensile force during the short circuit

The maximum tensile force during the short circuit, F_t , is calculated using the load parameter φ given by:

$$\phi = \begin{cases} 3\left(\sqrt{1+r^2}-1\right) & \text{for } T_{k1} \geq \dfrac{T_{\text{res}}}{4} \\ 3\left(r\sin\delta_k + \cos\delta_k - 1\right) & \text{for } T_{k1} < \dfrac{T_{\text{res}}}{4} \end{cases} \tag{39}$$

and the factor ψ from Figure 23 or calculated as the real solution of the equation:

$$\varphi^2\psi^3 + \varphi(2+\zeta)\psi^2 + (1+2\zeta)\psi - \zeta(2+\varphi) = 0 \tag{40}$$

with $0 \leq \psi \leq 1$.

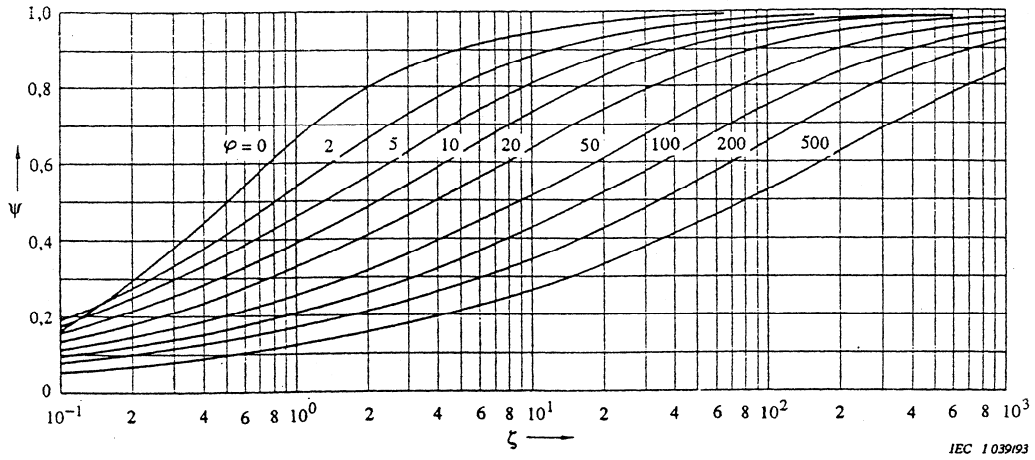

Figure 23—Factor ψ for maximum tensile force during short circuit[25]

The maximum tensile force, F_t (N/m) is given by:

$$F_t = \begin{cases} F_{st}\,(1+\varphi\,\psi) & \text{for } n = 1 \\ 1.1\,F_{st}\,(1+\varphi\,\psi) & \text{for } n \geq 2 \end{cases} \tag{41}$$

[25]Copyright © 1993 IEC, Geneva, Switzerland. www.iec.ch.

Copyright © 2010 IEEE. All rights reserved.
Copyright The Institute of Electrical and Electronics Engineers, Inc.
Provided by IHS under license with IEEE
No reproduction or networking permitted without license from IHS
Order Number: 02120914
Sold to:EGAT [700166108393] - VARRIS.Y@EGAT.CO.TH,
Not for Resale,2016-09-15 03:57:47 UTC

11.3.5.5 Maximum tensile force after the short circuit when the conductor drops back

On termination of the short circuit, the bus oscillates or drops back. The maximum value of the corresponding tensile F_f on termination of the drop is only significant for $r > 0.6$ and $\delta_m \geq 70°$. In this case, F_f (N/m) is given by:

$$F_f = 1.2 F_{st} \sqrt{1 + 8\zeta \frac{\delta_m}{180^o}} \tag{42}$$

11.3.5.6 Maximum horizontal displacement of the span and minimum air clearance

To calculate the maximum horizontal displacement of the span during the short circuit and the resulting minimum air clearance, account is taken of the elastic elongation due to the change of tension during the short circuit and to the thermal expansion.

The elastic deformation (nonpermanent elongation) due to the change of the tension load in the bus is given by:

$$\varepsilon_{\text{elas}} = N (F_t - F_{st}) \tag{43}$$

The elastic deformation due to thermal expansion is given by:

$$\varepsilon_{th} = \begin{cases} c_{th} \left[\dfrac{I_{k3}}{n A_s} \right]^2 \dfrac{T_{res}}{4} & \text{for } T_{k1} \geq T_{res}/4 \\ c_{th} \left[\dfrac{I_{k3}}{n A_s} \right]^2 T_{k1} & \text{for } T_{k1} < T_{res}/4 \end{cases} \tag{44}$$

where

c_{th} is a constant depending on the conductor material as described in Table 16.

NOTE—In the case of two-line single-phase systems, replace I_{k3} in Equation (44) by I_{k2}.

Table 16—Constant c_{th} (in SI units)

Material	c_{th} $m^4/(A^2s)$
Aluminium, aluminium alloy, and aluminium/steel conductors with a cross-section ratio of Al / St > 6	0.27×10^{-18}
Aluminium/steel conductors with a cross-section ratio of Al / St ≤ 6	0.17×10^{-18}
Copper	0.088×10^{-18}

The maximum horizontal displacement within a span, b_h (m), is given according to the two following cases:

Copyright © 2010 IEEE. All rights reserved.

Copyright The Institute of Electrical and Electronics Engineers, Inc.
Provided by IHS under license with IEEE
No reproduction or networking permitted without license from IHS

Order Number: 02120914
Sold to:EGAT [700166108393] - VARRIS.Y@EGAT.CO.TH,
Not for Resale,2016-09-15 03:57:47 UTC

a) Strained conductor attached to the structure with two insulator chains ($l_c = l - 2l_i$)

$$b_h = \begin{cases} C_F\, C_D\, d \sin\delta_1 & \text{for } \delta_m \geq \delta_1 \\ C_F\, C_D\, d \sin\delta_m & \text{for } \delta_m < \delta_1 \end{cases} \quad (45)$$

b) Strained conductor attached to the structure with vertical support insulators ($l_c = l$)

$$b_h = \begin{cases} C_F\, C_D\, d & \text{for } \delta_m \geq 90^o \\ C_F\, C_D\, d \sin\delta_m & \text{for } \delta_m < 90^o \end{cases} \quad (46)$$

where

C_D is the sag increase factor from the elastic and thermal elongation, given by:

$$C_D = \sqrt{1 + \frac{3}{8}\left[\frac{l}{d}\right]^2 (\varepsilon_{elas} + \varepsilon_{th})} \quad (47)$$

and

C_F is a factor that allows for a possible increase in the dynamic sag of the conductor caused by a change in shape of the conductor curve and is given by:

$$C_F = \begin{cases} 1.05 & \text{for } r \leq 0.8 \\ 0.97 + 0.1\, r & \text{for } 0.8 < r < 1.8 \\ 1.15 & \text{for } r \geq 1.8 \end{cases} \quad (48)$$

Due to a short circuit, conductors in a single-plane configuration are displaced at the midpoint of the span in the worst case in a circle of radius b_h about a straight line connection of the two adjacent anchor points. The reduced phase-to-phase clearance or minimum distance a_{min} (m) between the midpoints of the two main conductors during a line-to-line two-phase short circuit is given in the worst case by:

$$a_{min} = a - 2b_h \quad (49)$$

11.3.5.7 Maximum tensile force caused by the pinch effect

The following applies to regular bundle configurations, where the midpoints of the subconductors are located on a circle with equal distances a_s (m) between adjacent subconductors (Figure 24).

If the clearance between subconductors and the configuration of the spacers are such that the subconductors of the bundle effectively clash during a short circuit, the maximum tensile force due to the pinch effect, F_{pi}, may be ignored in contrast to the maximum tensile force F_t during the short circuit for regular bundle configurations of up to four subconductors.

Copyright © 2010 IEEE. All rights reserved.

Copyright The Institute of Electrical and Electronics Engineers, Inc.
Provided by IHS under license with IEEE
No reproduction or networking permitted without license from IHS

Order Number: 02120914
Sold to:EGAT [700166108393] - VARRIS.Y@EGAT.CO.TH,
Not for Resale,2016-09-15 03:57:47 UTC

Subconductors are considered to clash effectively, that is without a significant pinch effect, if the clearance a_s between the midpoints of adjacent subconductors, as well as the distance l_s (m) between two adjacent spacers (Figure 24) fulfill *either* of the following two equations:

$$a_S / d_S \leq 2 \quad \text{and} \quad l_S \geq 50 a_S \tag{50}$$

or

$$a_s / d_s \leq 2.5 \quad \text{and} \quad l_s \geq 70 a_s \tag{51}$$

where

d_s is the diameter of a subconductor, m

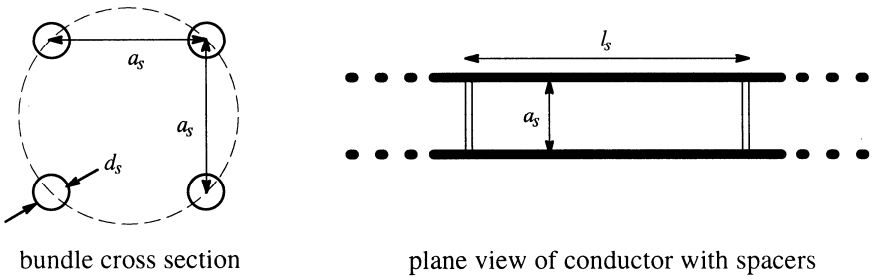

Figure 24—Bundle configuration of flexible conductors

If the bundle configurations under examination do not fulfill either Equation (50) or Equation (51), then the conductors do not clash effectively (that is the pinch effect is significant) and the following apply for calculating the maximum tensile force due to the pinch effect.

The short circuit current force F_v (N) is given by:

$$F_v = (n-1)\frac{\mu_o}{2\pi}\left(\frac{I_{k3}}{n}\right)^2 \frac{l_s}{a_s}\frac{\nu_2}{\nu_3} \tag{52}$$

NOTE—In the case of two-line single-phase systems, replace I_{k3} in Equation (52), Equation (53), Equation (60), and Equation (63) by I_{k2}.

Copyright © 2010 IEEE. All rights reserved.
Copyright The Institute of Electrical and Electronics Engineers, Inc.
Provided by IHS under license with IEEE
No reproduction or networking permitted without license from IHS
Order Number: 02120914
Sold to:EGAT [700166108393] - VARRIS.Y@EGAT.CO.TH,
Not for Resale,2016-09-15 03:57:47 UTC

The factor ν_2 is given in Figure 25, as a function of:

$$\nu_1 = f \cdot \frac{1}{\left(\sin\frac{180^{\circ}}{n}\right)}\sqrt{\frac{\left(a_s - d_s\right)\bar{m}}{\frac{\mu_o}{2\pi}\left(\frac{I_{k3}}{n}\right)^2 \frac{n-1}{a_s}}} \tag{53}$$

where

f is the system frequency (60 Hz)
ν_3 is given by Figure 26 where κ is the peak current factor given by:

$$\kappa = 1.02 + 0.98 \times e^{-3\frac{R}{X}} \tag{54}$$

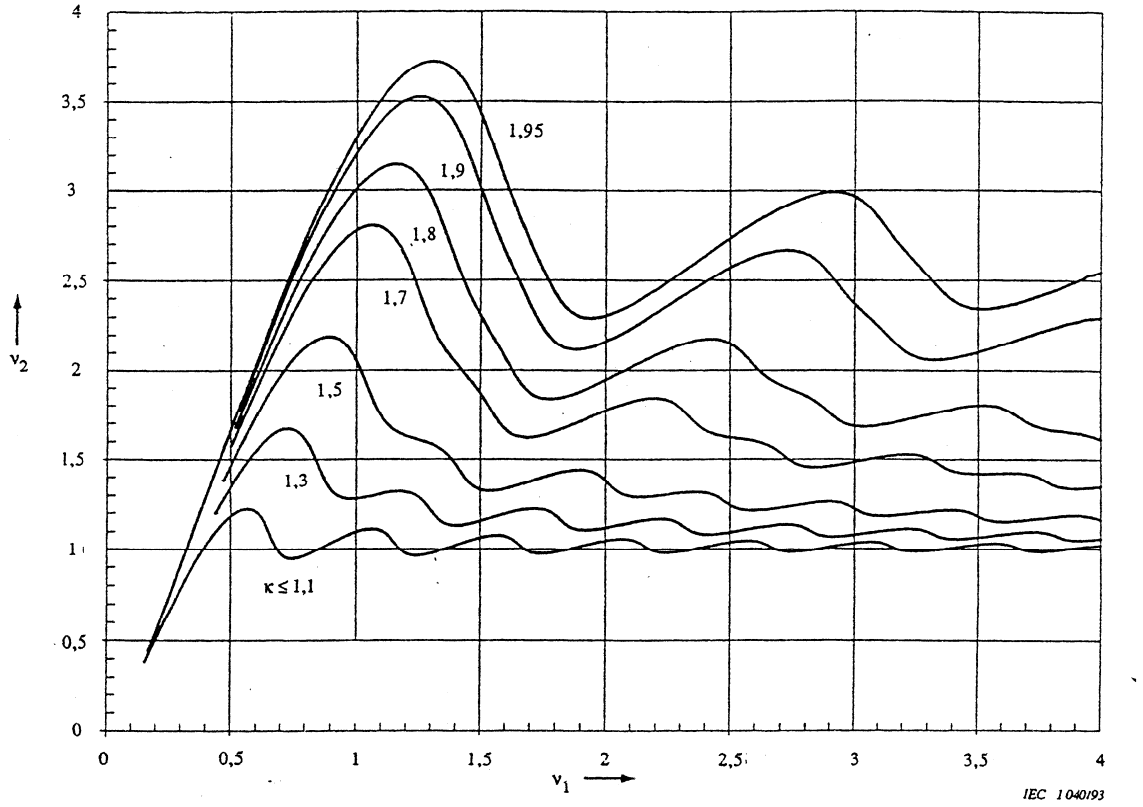

Figure 25—ν_2 as a function of ν_1 and κ[26]

[26]Copyright © 1993 IEC, Geneva, Switzerland. www.iec.ch.

Copyright © 2010 IEEE. All rights reserved.
Copyright The Institute of Electrical and Electronics Engineers, Inc.
Provided by IHS under license with IEEE
No reproduction or networking permitted without license from IHS
Order Number: 02120914
Sold to:EGAT [700166108393] - VARRIS.Y@EGAT.CO.TH,
Not for Resale,2016-09-15 03:57:47 UTC

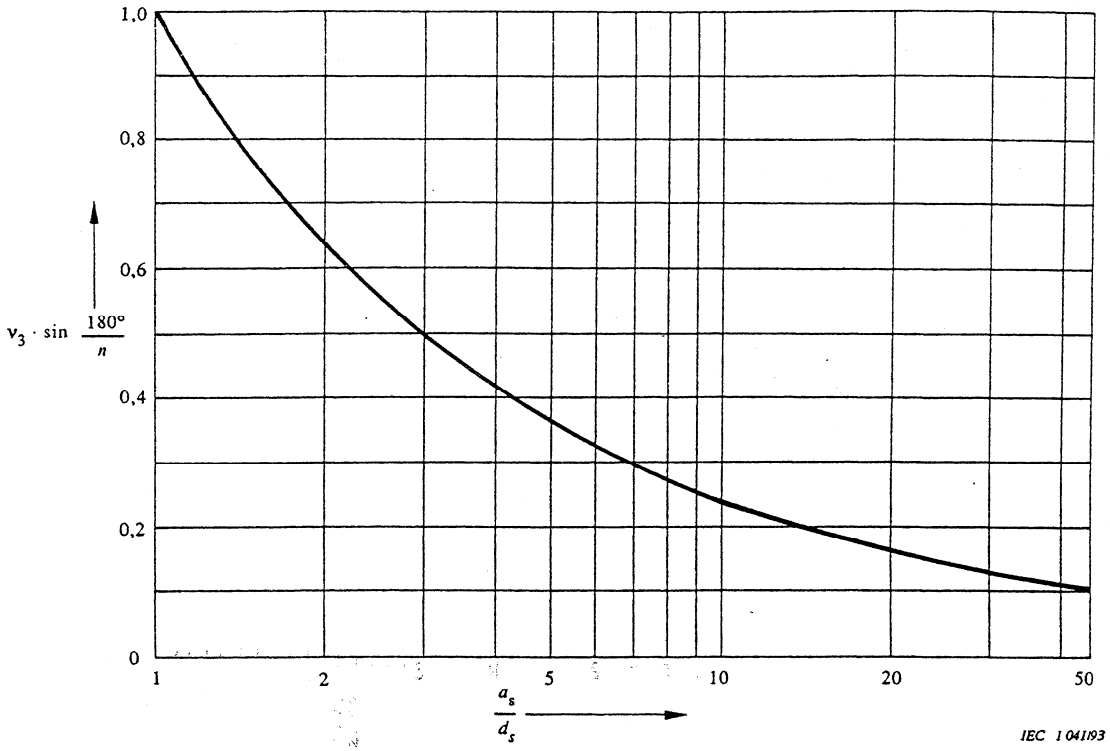

Figure 26—$\nu_3 \cdot \sin\frac{180^o}{n}$ as a function of a_s/d_s[27]

The strain factors characterizing the contraction of the bundle are calculated from

$$\varepsilon_{st} = 1.5\frac{F_{st} l_s^2 N}{(a_s - d_s)^2}\left(\sin\frac{180^o}{n}\right)^2 \tag{55}$$

and

$$\varepsilon_{pi} = 0.375\frac{F_v l_s^3 N}{(a_s - d_s)^3}\left(\sin\frac{180^o}{n}\right)^3 \tag{56}$$

[27]Copyright © 1993 IEC, Geneva, Switzerland, www.iec.ch.

Copyright © 2010 IEEE. All rights reserved.
Copyright The Institute of Electrical and Electronics Engineers, Inc.
Provided by IHS under license with IEEE
No reproduction or networking permitted without license from IHS
Order Number: 02120914
Sold to:EGAT [700166108393] - VARRIS.Y@EGAT.CO.TH,
Not for Resale,2016-09-15 03:57:47 UTC

According to the bundle configuration during the short circuit current flow, the maximum force due to the pinch effect is calculated differently. The bundle configuration is determined according to the parameter *j* defined as follows:

$$j = \sqrt{\frac{\varepsilon_{pi}}{1+\varepsilon_{st}}} \tag{57}$$

if $j \geq 1$ the subconductors clash and F_{pi} is given by:

$$F_{pi} = F_{st}\left(1+\frac{\nu_e}{\varepsilon_{st}}\xi\right) \tag{58}$$

where

ξ is given by the real solution of

$$\xi^3 + \varepsilon_{st}\,\xi^2 - \varepsilon_{pi} = 0 \tag{59}$$

with $j^{2/3} \leq \xi \leq j$, which shall be determined analytically or shall be taken from Figure 27.

Copyright © 2010 IEEE. All rights reserved.

Copyright The Institute of Electrical and Electronics Engineers, Inc.
Provided by IHS under license with IEEE
No reproduction or networking permitted without license from IHS

Order Number: 02120914
Sold to:EGAT [700166108393] - VARRIS.Y@EGAT.CO.TH,
Not for Resale,2016-09-15 03:57:47 UTC

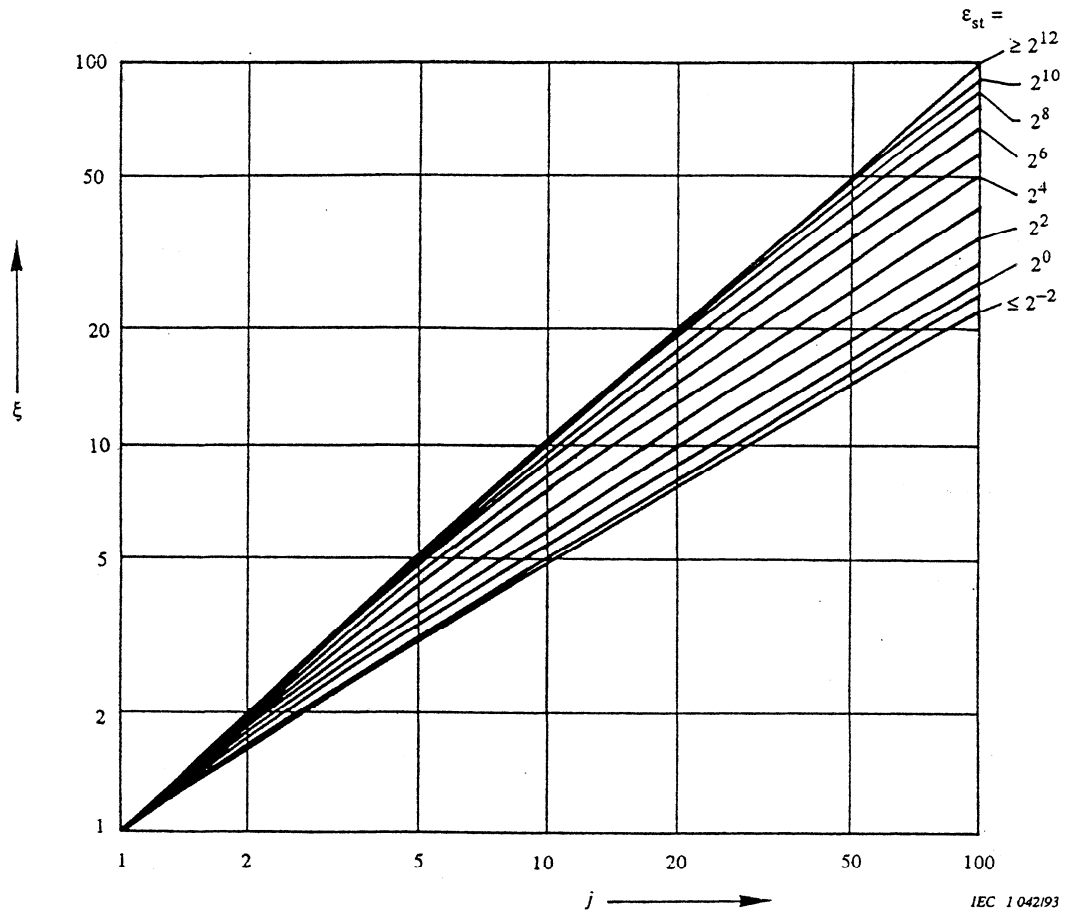

Figure 27—ξ as a function of *j* and ε_{st}[28]

v_e is given by:

$$v_e = \frac{1}{2} + \left[\frac{9}{8} n(n-1) \frac{\mu_o}{2\pi} \left(\frac{I_{k3}}{n} \right)^2 N v_2 \left(\frac{l_s}{a_s - d_s} \right)^4 \frac{\left(\sin \frac{180^o}{n} \right)^4}{\xi^3} \left\{ 1 - \frac{\arctan \sqrt{v_4}}{\sqrt{v_4}} \right\} - \frac{1}{4} \right]^{1/2} \tag{60}$$

NOTE— $\arctan \sqrt{v_4}$ in Equation (60) must be expressed in radians.

[28] Copyright © 1993 IEC, Geneva, Switzerland, www.iec.ch.

Copyright © 2010 IEEE. All rights reserved.
Copyright The Institute of Electrical and Electronics Engineers, Inc.
Provided by IHS under license with IEEE
No reproduction or networking permitted without license from IHS
Order Number: 02120914
Sold to:EGAT [700166108393] - VARRIS.Y@EGAT.CO.TH,
Not for Resale,2016-09-15 03:57:47 UTC

with

$$v_4 = \frac{a_s - d_s}{d_s} \tag{61}$$

if j <1 the subconductors do not clash and F_{pi} is given by:

$$F_{pi} = F_{st}\left(1 + \frac{v_e'}{\varepsilon_{st}}\eta^2\right) \tag{62}$$

where

η is given in Figure 28, Figure 29, or Figure 30 according to the parameter a_s/d_s

v_e' is given by:

$$v_e' = \frac{1}{2} + \left[\frac{9}{8}n(n-1)\frac{\mu_o}{2\pi}\left(\frac{I_{k3}}{n}\right)^2 N v_2 \left(\frac{l_s}{a_s - d_s}\right)^4 \frac{\left(\sin\frac{180^o}{n}\right)^4}{\eta^4}\left\{1 - \frac{\arctan\sqrt{v_4'}}{\sqrt{v_4'}}\right\} - \frac{1}{4}\right]^{1/2} \tag{63}$$

NOTE— $\arctan\sqrt{v_4'}$ in Equation (63) must be expressed in radians.

with

$$v_4' = \eta\left[\frac{a_s - d_s}{a_s - \eta(a_s - d_s)}\right] \tag{64}$$

Copyright © 2010 IEEE. All rights reserved.

Copyright The Institute of Electrical and Electronics Engineers, Inc.
Provided by IHS under license with IEEE
No reproduction or networking permitted without license from IHS

Order Number: 02120914
Sold to:EGAT [700166108393] - VARRIS.Y@EGAT.CO.TH,
Not for Resale,2016-09-15 03:57:47 UTC

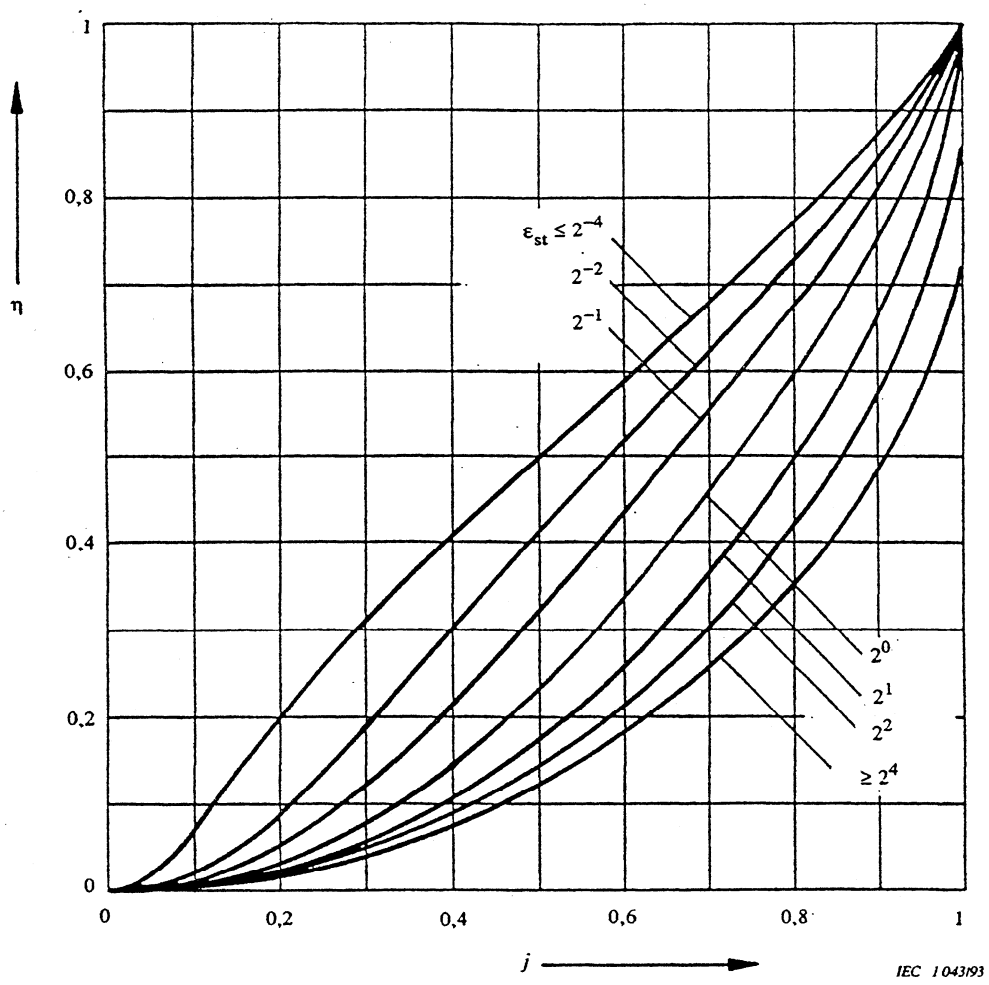

Figure 28—η as a function of *j* and ε_{st} for 2.5 < $a_s/d_s \leq 5.029$[29]

[29] Copyright © 1993 IEC, Geneva, Switzerland, www.iec.ch.

Copyright © 2010 IEEE. All rights reserved.

Copyright The Institute of Electrical and Electronics Engineers, Inc.
Provided by IHS under license with IEEE
No reproduction or networking permitted without license from IHS

Order Number: 02120914
Sold to:EGAT [700166108393] - VARRIS.Y@EGAT.CO.TH,
Not for Resale,2016-09-15 03:57:47 UTC

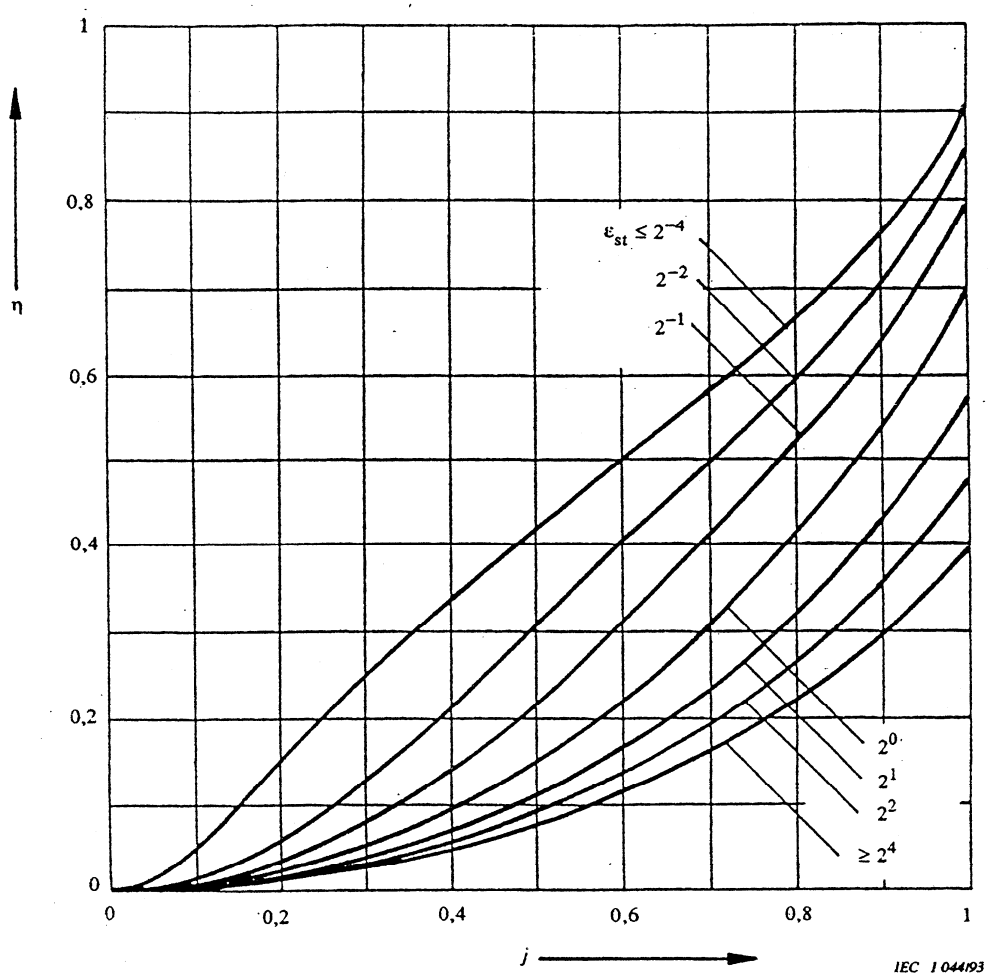

Figure 29—η as a function of *j* and ε_{st} for 5.0 < $a_s/d_s \leq$ 10.0[30]

[30] Copyright © 1993 IEC, Geneva, Switzerland, www.iec.ch.

Copyright © 2010 IEEE. All rights reserved.

Copyright The Institute of Electrical and Electronics Engineers, Inc.
Provided by IHS under license with IEEE
No reproduction or networking permitted without license from IHS

Order Number: 02120914
Sold to:EGAT [700166108393] - VARRIS.Y@EGAT.CO.TH,
Not for Resale,2016-09-15 03:57:47 UTC

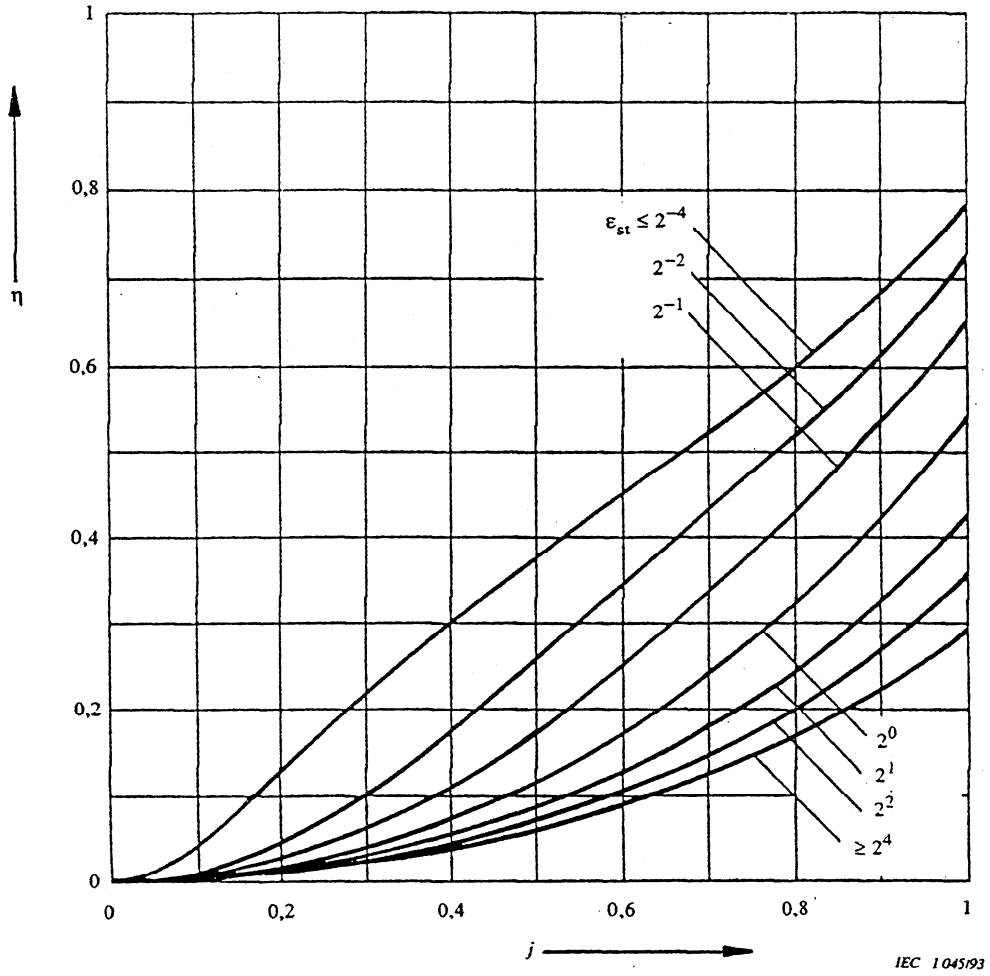

Figure 30—η as a function of *j* and ε_{st} for 10.0 < $a_s/d_s \leq$ 15.0[31]

11.3.5.8 Precision of simplified calculations for strain bus under short circuit

The simplified calculation method given in this subclause is based on extensive research and analytical representation of a complex phenomena that is nonlinear in nature. However, it yields representative results and compares well to experiments as detailed in IEC 60685-1 Ed. 2-1993 [B16] as well as CIGRE WG 02 [B36].

11.3.5.9 Calculation example

A calculation example is presented in Annex G along with a comparison with finite-element calculation for strain bus as described next.

[31]Copyright © 1993 IEC, Geneva, Switzerland, www.iec.ch.

Copyright © 2010 IEEE. All rights reserved.
Copyright The Institute of Electrical and Electronics Engineers, Inc.
Provided by IHS under license with IEEE
No reproduction or networking permitted without license from IHS
Order Number: 02120914
Sold to:EGAT [700166108393] - VARRIS.Y@EGAT.CO.TH,
Not for Resale,2016-09-15 03:57:47 UTC

11.3.6 Finite-element calculations for short circuit loads on strain bus

11.3.6.1 Description of the method

The use and advantages of the finite-element methodology for strain buses are similar in many ways to the application of this methodology for rigid buses. However, one major difference is that due to the flexibility of the flexible conductors composing strain buses, large displacement may be experienced during a short circuit. This implies that contrary to rigid buses, the electromagnetic loads on a strain bus vary not only with the variation of the current wave-form but also with the displacement of the conductors themselves; this is especially significant for the pinch effect when subconductors within a bundle are rapidly attracted to each other. This results in a nonlinear behavior because the changing loads between elements must be evaluated in a step-by-step fashion as they displace in space and time. Also, the large deflection that the conductors may experience themselves results in a geometrical nonlinearity as the stiffness of the conductors change as they deform. Nonlinearity may also arise due to the construction of the conductor in layers as these may slip over each other during motion, resulting in a varying bending stiffness. This latter nonlinearity might not, however, be significant with long spans but may have some effects near spacers and attachment points for short spans, which is typical of interconnection between substation equipment.

The use of a nonlinear finite-element software is mandatory for strain bus analysis, with step-by-step time integration. Such a method is reserved to experienced users as it requires considerable judgment in its use and interpretation, as well as sound knowledge in the inherent numerical methods for a proper use of them. However, when mastered, it provides representative results.

One important limitation of the finite-element method for strain bus is that it may be difficult to calculate forces from the pinch effect as this may lead to numerical instabilities (or unrealistic results) when the subconductors clash effectively (and the distance between them goes to zero).

11.3.6.2 Calculation example

A calculation example is presented in Annex G along with a comparison with a simplified calculation.

11.4 Thermal loads

The thermal expansion or contraction in length of the conductor as a result of a change in temperature can be computed using the following equation:

$$\Delta L = \alpha L_i (T_f - T_i) \tag{65}$$

where

ΔL is the change in span length, (m) [ft]
α is the coefficient of thermal expansion (1/ °C) [1/ °F], Table 17
T_i is the initial installation temperature (°C) [°F]
T_f is the final temperature (°C) [°F]
L_i is the conductor span length at the initial temperature, (m) [ft]

Copyright © 2010 IEEE. All rights reserved.

Copyright The Institute of Electrical and Electronics Engineers, Inc.
Provided by IHS under license with IEEE
No reproduction or networking permitted without license from IHS

Order Number: 02120914
Sold to:EGAT [700166108393] - VARRIS.Y@EGAT.CO.TH,
Not for Resale,2016-09-15 03:57:47 UTC

Table 17—Coefficient of thermal expansion for common materials

Material	α (1/ °C)	α (1/ °F)
Aluminum	23.1×10^{-6}	12.8×10^{-6}
Copper	16.8×10^{-6}	9.33×10^{-6}
Stainless steel	17.8×10^{-6}	9.89×10^{-6}
Steel	11.7×10^{-6}	6.50×10^{-6}

11.4.1 Rigid bus conductor thermal expansion effects without expansion fittings

Insulators, supporting the rigid bus conductors, restrain thermal expansion or contraction of the conductors, resulting in compression or tension of the conductors and bending of the insulators (and the mounting frame). Assuming the mounted frame supporting insulators is a rigid structure, the tension/compression force in the conductors and the bending moment of the insulators can be conservatively estimated using the following equations. If the flexibility of the mounting frame is considered in the design, then a complex analysis of the conductors, insulators, and mounting structure needs to be used; the finite-element method is appropriate for such calculations. Note that these equations only apply when no expansion fittings are present in the conductor assemblage between two insulators.

The tension or compression force generated in the conductor due to thermal expansion ΔL is conservatively given by:

$$F_{TE} = \frac{E_c A_c \Delta L}{L_i} = E_c A_c \alpha (T_f - T_i) \tag{66}$$

where

F_{TE} is the thermal force, (N) [lbf]
A_c is the conductor cross section area, (m^2) [in^2]
E_c is the conductor material Young's modulus, (N/m^2) [lbf/in^2]

It is observed that the thermal force F_{TE} is independent of the span length.

The bending moment experienced at the base of the insulator due to the tension or compression force generated from thermal expansion ΔL is conservatively given by:

$$M_{TE} = F_{TE} h_i \tag{67}$$

where

M_{TE} is the insulator bending moment as effect of conductor expansion/contraction, (N-m) [lbf-in]
h_i is the height of the insulator, (m) [in]

11.4.2 Expansion fittings

To avoid or minimize the thermal expansion effects described in the previous subclause, provisions should be made for expansion in any bus-conductor span. These provisions may be made with expansion fittings for long buses, or by considering deflection of a bus conductor, bus-conductor bends, insulators, or mounting structures for short buses.

Copyright © 2010 IEEE. All rights reserved.

Copyright The Institute of Electrical and Electronics Engineers, Inc.
Provided by IHS under license with IEEE
No reproduction or networking permitted without license from IHS

Order Number: 02120914
Sold to:EGAT [700166108393] - VARRIS.Y@EGAT.CO.TH,
Not for Resale,2016-09-15 03:57:47 UTC

11.4.3 Strain bus conductor sag under thermal load

Ambient temperature significantly impacts the sag and tension of the strain conductors. In general, conductors should have minimum sag. However, the associated tension needs to be balanced with economics considering the imposed temperature effect. Spring bolts can be used to maintain controlled tension within a span to limit changes in conductor sag. These spring bolts are typically available in the tension range of 0 to 25 kN (approximately 6000 lbs) with deflection rates of 25 kN/m to 50 kN/m (approximately 1500 lbs per inch to 3000 lbs per inch), depending on the length of the bolt and size of the tension spring.

The actual shape of the curve taken up by a conductor at a given tension can be described by a hyperbolic equation. When the sag-to-span ratio is smaller than 1/8, the parabola is accurate enough for most purposes. On this basis, the parabolic equation for anchor points at the same level is:

$$D_s = \frac{\overline{m}\, gL^2}{8H} \tag{68}$$

where

D_s is the conductor sag, (m) [ft]
$\overline{m}$ is the mass by unit length of the conductor, (kg/m) [lbm/ft]
g is the gravitational constant (9.82 m/s^2), [32.2 ft/s^2]
L is the conductor span length (m) [ft]
H is the tension in the conductor under a given temperature, (N) [lbf]

The final tension due to temperature change may be calculated from Equation (69) below by trial and error until both sides match; the final sag can then be calculated by Equation (68) using T_f and $\overline{m}_f$. For nonlevel anchors and special cases, such as concentrated loads, more sophisticated techniques are required.

$$E_c\, A_c\, \alpha (T_f - T_i) + H_f - H_i = \frac{g^2 L^2 E_c\, A_c}{24}\left(\frac{\overline{m}_f^2}{H_f^2} - \frac{\overline{m}_i^2}{H_i^2} \right) \tag{69}$$

where

H_i initial tension, (N) [lb]
H_f final tension, (N) [lb]
A_c is the cross section area of conductor, (m^2) [in^2]
E_c is the equivalent Young's modulus of all the layers of the conductor including the core (N/m^2) [lbf/in^2]
α is the equivalent coefficient of thermal expansion for the conductor (1/ °C) [1/ °F], Table 17
T_i initial temperature, (°C) [°F]
T_f final temperature, (°C) [°F]
$\overline{m}_i$ initial mass by unit length of the conductor, (kg/m) [lbm/ft]
$\overline{m}_f$ final mass by unit length, (kg/m) [lbm/ft], (may include ice loading or else is equal to $\overline{m}_i$)

Copyright © 2010 IEEE. All rights reserved.

Copyright The Institute of Electrical and Electronics Engineers, Inc.
Provided by IHS under license with IEEE
No reproduction or networking permitted without license from IHS

Order Number: 02120914
Sold to:EGAT [700166108393] - VARRIS.Y@EGAT.CO.TH,
Not for Resale,2016-09-15 03:57:47 UTC

NOTE—Use of Equation (69) by trial and error might be time consuming. It is recommended instead to use a sag-tension computer program.

12. Dimensional, strength, and other design considerations

Rigid bus conductors should not sag excessively under normal conditions. Any span of a rigid bus conductor and the supporting insulators must also have enough stiffness and strength to withstand the expected forces of gravity, wind, and short circuits while maintaining its mechanical and electrical integrity. The maximum allowable span length will therefore be primarily limited by acceptable vertical deflection, the fiber stress of the conductor, and the cantilever strength rating of the insulators supporting the rigid bus conductor. In addition, the maximum allowable span may be limited by induced vibrations from either wind or alternating current forces. Also, clearances should be considered for the spacing in between conductors. The following subclauses will discuss each of these design limiting factors in details.

12.1 Maximum allowable span based on vertical deflection limits

The allowable vertical deflection of a bus conductor is usually limited by appearance. Commonly used limits are based either on the ratio of conductor deflection to span length (such as 1/150 or 1/200) or the conductor diameter (0.5 to 1 times the diameter). These criteria should be applied with the dead weight of the rigid bus, with the damping material inside the conductor if any. In practice, because appearance is usually not considered during icing conditions, the ice weight is usually not considered for vertical deflection. However, if the vertical deflection during icing conditions is important, then ice weight should be considered.

The vertical deflection of rigid bus conductors is measured from the attachment point of the bus conductor at the insulators to the mid-span point. It can be calculated using structural design formulas for beams or more precisely using the finite-element method with modeling of the supporting structure.

The allowable span with respect to the vertical deflection limit will be denoted as L_V. To evaluate L_V, we present the next simplified equations for single-level, single-span bus conductors supported at both ends, and for continuous bus conductors supported at equal spans without concentrated loads.

Vertical deflection depends on the total gravitational force. The total gravitational force on a conductor is the sum of the weights of the conductor, damping material, and ice if the latter is of concern in the allowable deflection.

$$F_G = F_c + F_D + F_I \tag{70}$$

where

F_G is the total gravitational unit weight, N/m [lbf/in]
F_c is the conductor unit weight, N/m [lbf/in]
F_D is damping material unit weight, N/m [lbf/in]
F_I is the ice unit weight, N/m [lbf/in] [Equation (6)]

If the bus span is subjected to concentrated loads, the force distribution on that span should be analyzed more thoroughly through more advanced methods, such as structural analysis or the finite-element method.

Copyright © 2010 IEEE. All rights reserved.

Copyright The Institute of Electrical and Electronics Engineers, Inc.
Provided by IHS under license with IEEE
No reproduction or networking permitted without license from IHS

Order Number: 02120914
Sold to:EGAT [700166108393] - VARRIS.Y@EGAT.CO.TH,
Not for Resale,2016-09-15 03:57:47 UTC

The maximum allowable bus span length is determined with a given vertical deflection limit, end conditions, and total gravitational unit weight. The deflection may be based on either the conductor diameter or a fraction of the span length.

End conditions for a single span range between fixed and pinned. A fixed end is not free to rotate (moment resisting), whereas a pinned end is free to rotate (not moment resisting). In reality, because of supporting structure flexibility and connection friction, the end conditions are not truly fixed or pinned.

If the end conditions of the single bus span are unknown, then the case of two pinned ends should be selected, because it is the most conservative.

For a typical continuous bus, end conditions are assumed to be pinned and mid-supports are fixed; therefore, end spans should then be considered pinned-fixed while mid spans should be considered fixed-fixed. For such buses, one should then select the type of span individually (pinned-fixed or fixed-fixed) to determine the maximum allowable length. However, other arrangements may be present in a continuous bus.

12.1.1 Single-span bus, pinned-pinned end conditions

For a single span with two pinned ends, the allowable span length based on vertical deflection may be calculated by either of the following equations, depending how the vertical deflection limit is specified.

For the vertical deflection limit specified as a given quantity δ_{max}:

$$L_V = \left(\frac{384 E J \delta_{\max}}{5 F_G} \right)^{\frac{1}{4}} \tag{71}$$

where

L_V is the allowable span based on the vertical deflection limit, m [in]
E is the Young's modulus of the conductor material, N/m^2 [lbf/in^2]
J is the bending moment of inertia of the conductor cross section, m^4 [in^4] [Equation (73)]
$\delta_{\max}$ is the vertical deflection limit, m [in]
F_G is the gravitational weight by unit length, N/m [lbf/in]

For the vertical deflection limit specified as a fraction of the allowable span α:

$$L_V = \left(\frac{384 E J \eta}{5 F_G} \right)^{\frac{1}{3}} \tag{72}$$

where

η is the fraction of the allowable span limit (e.g., 1/150 = 0.0067)

Copyright © 2010 IEEE. All rights reserved.

Copyright The Institute of Electrical and Electronics Engineers, Inc.
Provided by IHS under license with IEEE
No reproduction or networking permitted without license from IHS

Order Number: 02120914
Sold to:EGAT [700166108393] - VARRIS.Y@EGAT.CO.TH,
Not for Resale,2016-09-15 03:57:47 UTC

The bending moment of inertia J of a circular cross section is given by:

$$J = \pi \frac{\left(D_o^4 - D_i^4\right)}{64} \tag{73}$$

where

D_o is the conductor outside diameter, m [in]
D_i is the conductor inside diameter, m [in]

For other cross-section shapes, the bending moment of inertia can be obtained from a handbook or manufacturer's data.

12.1.2 Single-span bus, fixed-fixed end conditions

For a single span with both ends fixed, the allowable span length based on vertical deflection may be calculated by either of the following equations, depending how the vertical deflection limit is specified.

For the vertical deflection limit specified as a given quantity δ_{max}:

$$L_V = \left(\frac{384\,E\,J\,\delta_{\max}}{F_G}\right)^{\frac{1}{4}} \tag{74}$$

$$L_V = \left(\frac{384\,E\,J\,\eta}{F_G}\right)^{\frac{1}{3}} \tag{75}$$

12.1.3 Single-span bus, pinned-fixed end conditions

For a single span with one end pinned and the other fixed, the allowable span length based on vertical deflection may be calculated by either of the following equations, depending how the vertical deflection limit is specified.

For the vertical deflection limit specified as a given quantity δ_{max}:

$$L_V = \left(\frac{185\,E\,J\,\delta_{\max}}{F_G}\right)^{\frac{1}{4}} \tag{76}$$

Copyright © 2010 IEEE. All rights reserved.

Copyright The Institute of Electrical and Electronics Engineers, Inc.
Provided by IHS under license with IEEE
No reproduction or networking permitted without license from IHS

Order Number: 02120914
Sold to:EGAT [700166108393] - VARRIS.Y@EGAT.CO.TH,
Not for Resale,2016-09-15 03:57:47 UTC

For the vertical deflection limit specified as a fraction of the allowable span η:

$$L_V = \left(\frac{185\, E\, J\, \eta}{F_G} \right)^{\frac{1}{3}} \tag{77}$$

where all parameters are the same as for the pinned-pinned case.

12.1.4 Continuous bus

For a continuous bus, the maximum allowable span length may be calculated using the previous cases, depending on the end conditions of the span considered. If spans of equal length must be used, then the maximum allowable length L_V will be determined by the span where conditions are pinned-fixed [Equation (76) or Equation (77)], because this case provides the maximum deflection under uniform load, assuming that mid-supports are fixed while end conditions are assumed to be pinned. If other end conditions are present in the continuous bus, then one should use the previous case above corresponding to the actual end conditions.

NOTE—The above equations are for two-span buses. For continuous bus of more than two spans, the maximum deflection occurs in the end spans and is slightly less than that of the two-span bus. The allowable span will then be slightly longer.

12.2 Maximum allowable span length based on conductor fiber stress

Span length may be limited by the fiber stress of the conductor material under loading. Usually, the allowable fiber stress corresponds to the yield stress of the material (or a fraction of the yield stress if a safety factor is considered), for no permanent deformation of the conductor to occur. The allowable span with respect to fiber stress will be denoted as L_S. To evaluate L_S, we consider next the cases where the forces acting on the conductor are uniform and constant, including the short circuit force determined using the simplified calculations. We also consider the common case where all conductors are in a horizontal configuration at the same level between phases for the short circuit force. For more precise and less conservative calculations (especially for the evaluation of the short circuit force), the finite-element method should be used.

Where welded fittings are used for bus, the allowable stress for the bus should be reduced to allow for annealing due to welding. Tests have shown that the reduction in allowable stress is approximately 50% for aluminum. The reduction in allowable stress for copper is dependent on the welding method (brazing, exothermic, etc.) and should be discussed with the manufacturers. Locating the weld in a region of moderate stress is a usual method of offsetting the effect of weld annealing. Where welded splices are used with a tubular bus, the reduction in allowable stress may not be required if a reinforcing insert is incorporated.

To calculate the maximum span length based on fiber stress, the maximum force by unit length on the conductor should first be determined. The forces that should be considered are as follows:

- The total gravitational weight F_G [as defined in the preceding subclause—Equation (70)]
- The wind force without or with ice: F_w or F_{WI} [(Equation (8) or Equation (9)]
- The short circuit force: F_{sc} [Equation (14), Equation (15), or Equation (16)]

Some of these forces occur in the vertical direction (such as F_G), whereas the others occur in the horizontal direction, perpendicular to the conductor direction (F_w or F_{WI} and F_{SC} in the case of a horizontal bus arrangement). Also for each direction, because the corresponding forces may not necessarily happen at the same time (for example, wind and short

Copyright © 2010 IEEE. All rights reserved.

Copyright The Institute of Electrical and Electronics Engineers, Inc.
Provided by IHS under license with IEEE
No reproduction or networking permitted without license from IHS

Order Number: 02120914
Sold to:EGAT [700166108393] - VARRIS.Y@EGAT.CO.TH,
Not for Resale,2016-09-15 03:57:47 UTC

circuit), they should be considered either separately or together, based on utility design standards. The combination of forces that leads to the smaller allowable length (the maximum fiber stress) should determine the design.

The maximum force acting on the conductor is therefore the vectorial resultant of the forces considered at the same time in both the vertical and horizontal direction, given by:

$$F_T = \sqrt{F_V^2 + F_H^2} \tag{78}$$

where

F_T is the total force acting on the conductor by unit length, N/m [lbf/in]
F_V is the total vertical force acting on the conductor by unit length, N/m [lbf/in]
F_H is the total horizontal force acting on the conductor by unit length, N/m [lbf/in] in the perpendicular direction of the conductor

For example, if we consider together F_G, F_W, and F_{SC}, the net resultant force will be given by:

$$F_T = \sqrt{(F_G)^2 + (F_W + F_{SC})^2} \ .$$

If the conductors are not at the same level or are in a vertical configuration, then F_V and F_H must be evaluated accordingly.

The maximum allowable span length for fiber stress L_S is determined for any given conductor by the total force F_T; allowable stress depends on the end conditions of the span considered, as was the case with the vertical deflection limit. If the conductor cross section is not symmetrical about the direction of the total force, then calculations should be made accordingly.

12.2.1 Single-span bus, pinned-pinned end conditions

For a single span with two pinned ends, the allowable span length based on fiber stress is given by:

$$L_S = \sqrt{\frac{16 J \sigma_{\text{allowable}}}{F_T D_o}} \tag{79}$$

where

L_S is the allowable span based on the maximum fiber stress, m [in]
$\sigma_{\text{allowable}}$ is the allowable stress of the conductor material, N/m^2 [lbf/in^2]
J is the bending moment of inertia of the conductor cross section, m^4 [in^4]
F_T is the total force acting on the conductor by unit length, N/m [lbf/in]
D_o is the conductor outside diameter, m [in]

Copyright © 2010 IEEE. All rights reserved.
Copyright The Institute of Electrical and Electronics Engineers, Inc.
Provided by IHS under license with IEEE
No reproduction or networking permitted without license from IHS
Order Number: 02120914
Sold to:EGAT [700166108393] - VARRIS.Y@EGAT.CO.TH,
Not for Resale,2016-09-15 03:57:47 UTC

12.2.2 Single-span bus, fixed-fixed end conditions

For a single span with both ends fixed, the allowable span length based on fiber stress is given by:

$$L_S = \sqrt{\frac{24\,J\,\sigma_{\text{allowable}}}{F_T\,D_o}} \tag{80}$$

12.2.3 Single-span bus, pinned-fixed end conditions

For a single span with one end pinned and the other fixed, the allowable span length based on fiber stress is given by:

$$L_S = \sqrt{\frac{16\,J\,\sigma_{\text{allowable}}}{F_T\,D_o}} \tag{81}$$

which is the same as the pinned-pinned base.

12.2.4 Continuous bus

For a continuous bus, the evaluation of allowable span length based on fiber stress is more complex and should be analyzed more thoroughly.

12.3 Simplified evaluation of insulator cantilever force

Because the loads on the bus conductors are transmitted to the insulators, the strength of the insulators must be considered. With various bus configurations, insulators may be required to withstand cantilever, compression, tensile, and torsional forces. Advanced analytical or numerical methods, such as the finite-element method, inherently takes account of all those forces. However, for the sake of simplicity and basic first-hand evaluations, this guide presents a simplified method of analysis where only the cantilever forces from the different loads are considered statically. The method presented under is for rigid buses in straight-line arrangements with identical phases. Note that other forces (compression, tension, and torsion) may sometimes be critical and/or contribute substantially to the resulting stresses in the insulator, thus requiring additional consideration in design.

Two bus arrangements are considered for the evaluation of the cantilever forces. The usual case is when the insulator-support system is vertical, that is, when the bus arrangement is mounted on the ground. The alternative case is when the insulator-support system is horizontal, that is, when the bus arrangement is either mounted on a wall or a section of the bus runs vertically. Hence, depending on whether the bus arrangement is vertical or horizontal, the forces to consider in the evaluation of the net cantilever force on an insulator may consist of the following:

- The total gravitational weight F_G on the bus conductor, when the bus arrangement is horizontal
- The additional gravitational weight from the insulator itself, from ice on it, and from any concentrated mass on top of it (fittings, etc.), when the bus arrangement is horizontal

Copyright © 2010 IEEE. All rights reserved.

Copyright The Institute of Electrical and Electronics Engineers, Inc.
Provided by IHS under license with IEEE
No reproduction or networking permitted without license from IHS

Order Number: 02120914
Sold to:EGAT [700166108393] - VARRIS.Y@EGAT.CO.TH,
Not for Resale,2016-09-15 03:57:47 UTC

— The wind force with or without ice on the bus conductor and on the insulator: F_w or F_{WI} for both vertical and horizontal arrangements

— The short circuit force F_{sc} for both vertical and horizontal arrangements

— The thermal expansion force from the bus F_{TE}, when no expansion fittings are used, for both vertical and horizontal arrangements

As in the determination of the maximum fiber stress in conductors, it is to be recognized that some of these forces may not necessarily happen at the same time (for example, wind and short circuit), and therefore, they should be considered either separately or together, based on utility design standards. The combination of forces that leads to the maximum cantilever force should determine the design. Also, some of these forces do not act in the same direction as will be discussed.

12.3.1 Cantilever forces from loads on conductors

The insulator cantilever force resulting from the combination of gravitational, wind and short circuit loads on the bus conductors can be given for some common bus arrangements as a function of the effective conductor span length L_E supported by the insulator. The effective conductor span length L_E depends on the span length and the bus-support conditions. For particular support conditions and number of spans, Table 18 gives the corresponding value of L_E.

Table 18 —Maximum effective bus span length L_E supported by insulator for common bus arrangements

Bus configuration	Support (boundary) conditions					Maximum span length L_E
	S1	S2	S3	S4	S5	
Single-span	P	P				L/2
Single-span	P	F				5 L/8 (Max at S2)
Single-span	F	F				L/2
Two Cont.-span	P	C	P			5 L/4 (Max at S2)
Two Cont.-span	P	F	F			9L/8 (Max at S2)
Two Cont.-span	F	F	F			L (Max at S2)
Three Cont.-span	P	C	C	P		11 L/10 (Max at S2)
Four Cont.-span	P	C	C	C	P	8 L/7 (Max at S2)

where

L is the bus span between supports (assumed equal between all supports)
P is for pinned-end condition at the support
F is for fixed-end condition at the support
C is for mid-support condition of continuous span

NOTE—This table is applicable only to equal-span bus arrangement. The mid-support of a continuous bus has only reaction force resistance but no moment resistance, although the continuous bus conductor connected to it has a moment. For continuous spans of more than the spans shown, use the value of L_E for the largest span shown for the same end conditions.

Copyright © 2010 IEEE. All rights reserved.

Copyright The Institute of Electrical and Electronics Engineers, Inc.
Provided by IHS under license with IEEE
No reproduction or networking permitted without license from IHS

Order Number: 02120914
Sold to:EGAT [700166108393] - VARRIS.Y@EGAT.CO.TH,
Not for Resale,2016-09-15 03:57:47 UTC

12.3.1.1 Cantilever force from gravitational load on bus

As presented ealier, the gravitational force on a conductor is the sum of the weights of the conductor, damping material (if any), and ice (if any). When the bus arrangement is horizontal, the resulting cantilever force transmitted from the bus to the bus-support fitting on top of the insulator is given by:

$$F_{GC} = F_G \; L_E \tag{82}$$

where

F_{GC} is the bus conductor gravitational cantilever force, N [lbf]
F_G is the total gravitational unit weight on the conductor, N/m [lbf/ft], given by Equation (70)
L_E is the effective conductor span length from Table 18, m [ft]

12.3.1.2 Cantilever force from wind on bus

The cantilever force from wind transmitted from the bus to the bus-support fitting on top of the insulator is given by:

$$F_{WC} = F_W \; L_E \tag{83}$$

where

F_{WC} is the wind cantilever force, N [lbf]
F_W is the wind load by unit length on the conductor with or without ice, N/m [lbf/ft], given by Equation (8) when no ice is considered and by Equation (9) when ice is considered
L_E is the effective conductor span length from Table 18, m [ft]

12.3.1.3 Cantilever force from short circuit on bus

The cantilever force from short circuit transmitted from the bus to the bus-support fitting on top of the insulator is given by:

$$F_{scC} = F_{sc} \; L_E \tag{84}$$

where

F_{scC} is the short circuit cantilever force, N [lbf]
F_{sc} is the short circuit force by unit length, N/m [lbf/ft]
L_E is the effective conductor span length from Table 18, m [ft]

Copyright © 2010 IEEE. All rights reserved.

Copyright The Institute of Electrical and Electronics Engineers, Inc.
Provided by IHS under license with IEEE
No reproduction or networking permitted without license from IHS

Order Number: 02120914
Sold to:EGAT [700166108393] - VARRIS.Y@EGAT.CO.TH,
Not for Resale,2016-09-15 03:57:47 UTC

12.3.1.4 Cantilever force from thermal expansion

When no expansion fittings are used, a cantilever force resulting from the thermal expansion of the bus is applied at the bus insulator-fitting on top of the insulator. This force F_{TE} is given by Equation (66) and acts axially in the conductor direction (as opposed to the other forces above which act perpendicular to the conductor direction).

12.3.2 Cantilever forces from loads on insulators

Cantilever loads also arise from forces acting directly on the insulator from the effect of wind and, when the bus arrangement is horizontal, from the insulator weight and the weight of ice on it. Contrary to the forces transmitted from the bus, the latter forces do not act at the bus-support fitting on top of the insulator but uniformly over its length. These uniform forces can however be replaced by concentrated forces at the center of the insulator when of constant section. The evaluation of these equivalent concentrated forces is now given.

12.3.2.1 Cantilever force from the insulator weight and ice on it

When the bus arrangement is horizontal, the weight of the insulator and the ice on it (if any) produce gravitational forces acting on the insulator and contribute to the cantilever loading. The weight of the insulator F_{gI} is given in the manufacturer's data and acts at the center of mass of the insulator (generally at the center of the insulator when of uniform section). The cantilever force from the insulator weight and ice on it is given by:

$$F_{GI} = F_{gI} + F_{II}\, H_T \tag{85}$$

where

F_{GI} is the cantilever force from the weight of the insulator and ice on it, N [lbf]
F_{gI} is the weight of the insulator
F_{II} is the ice unit weight on the insulator, N/m [lbf/ft], given by Equation (6) where the conductor diameter D_o in this latter equation must be replaced by the effective insulator diameter with ice D_{ice} as evaluated under
H_T is the total height of the insulator column (Figure 31), m [ft]

The ice on the insulator is considered to act uniformly over its length and around its skirts. Due to the insulator outside skirts, the effective insulator diameter with ice is approximated by the average diameter within the skirts, given by:

$$D_{ice} = \frac{D_{so} + D_{si}}{2} \tag{86}$$

where

D_{ice} is the effective insulator diameter with ice, m [in]
D_{so} is the outside diameter of the insulator, m [in]
D_{si} is the diameter of the insulator at the root of the skirts, m [in]

For tapered insulators, the cantilever force from the weight of ice must be calculated individually for each section and is considered to act at the midpoint of each section.

Copyright © 2010 IEEE. All rights reserved.

Copyright The Institute of Electrical and Electronics Engineers, Inc.
Provided by IHS under license with IEEE
No reproduction or networking permitted without license from IHS

Order Number: 02120914
Sold to:EGAT [700166108393] - VARRIS.Y@EGAT.CO.TH,
Not for Resale,2016-09-15 03:57:47 UTC

12.3.2.2 Cantilever force from the wind on the insulator

The wind force on the insulator is given by:

$$F_{WCI} = F_W \; H_T \tag{87}$$

where

F_{WCI} is the cantilever force from the wind on the insulator, N [lbf]
F_W is the wind load by unit length on the insulator with or without ice, N/m [lbf/ft], given by Equation (8) when no ice is considered and by Equation (9) when ice is considered, where the conductor diameter D_o in these two latter equations must be replaced by the effective insulator diameter D_i as evaluated under
H_T is the total height of the insulator column (Figure 31), m [ft]

The effective insulator diameter D_i is usually considered as the insulator diameter over the skirts. For tapered insulators, the effective diameter is the average diameter given by:

$$D_i = \frac{D_1 + D_2 + ... + D_n}{n} \tag{88}$$

where D_1, D_2, …. , D_n are the outside diameters of each subassembly for the 1st, 2nd, and nth sections of the insulator (Figure 31).

The total cantilever force from the wind F_{WCI} on a uniform-diameter insulator acts at the center of the insulator column $H_T/2$. For a tapered insulator, the total force is usually considered acting at the center also because the resulting error is of a small magnitude and is conservative.

12.3.2.3 Cantilever force from concentrated loads on insulators

Cantilever loads may also arise from concentrated loads such as the weight of fittings or other hardware on top of insulators. These concentrated loads will be denoted by F_{CCI} in the following discussion.

12.3.3 Evaluation of total cantilever force

12.3.3.1 Vertically mounted insulator

The loads that may act on a vertically mounted insulator are illustrated in Figure 31. In this figure, x is the horizontal direction perpendicular to the bus, y is the horizontal direction in the bus direction, and z is the vertical direction.

Copyright © 2010 IEEE. All rights reserved.

Copyright The Institute of Electrical and Electronics Engineers, Inc.
Provided by IHS under license with IEEE
No reproduction or networking permitted without license from IHS

Order Number: 02120914
Sold to:EGAT [700166108393] - VARRIS.Y@EGAT.CO.TH,
Not for Resale,2016-09-15 03:57:47 UTC

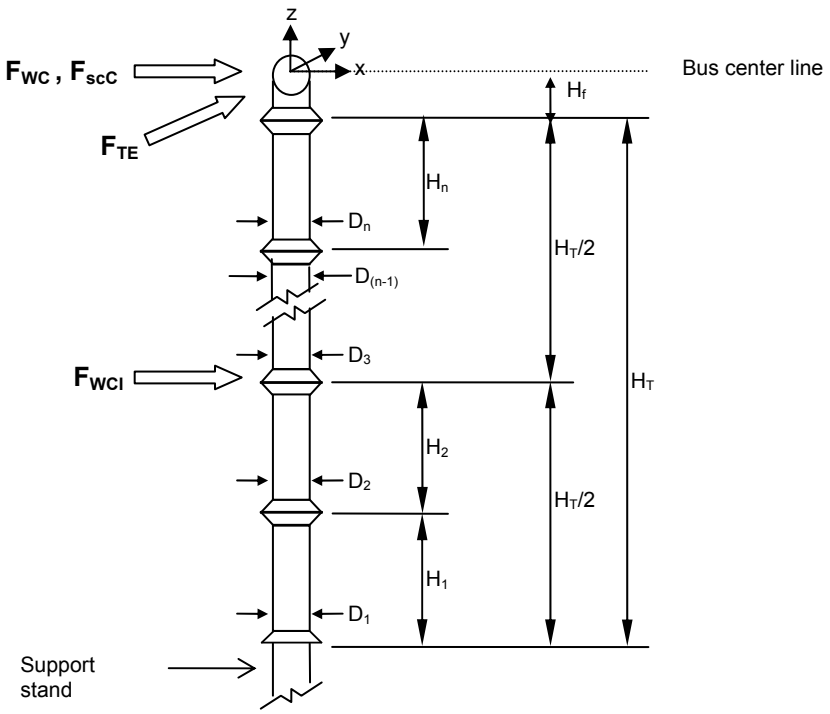

Figure 31—Cantilever forces on a vertically mounted insulator

It is observed in Figure 31 that F_{WC}, F_{scC}, and F_{WCI} act in the x direction while F_{TE} acts in the y direction. To obtain the net equivalent cantilever force, we must first obtain the equivalent cantilever force in each direction separately and then combine the resulting cantilever forces in both directions. As mentioned, these forces may not necessarily happen at the same time; therefore, they should be combined based on the utility design standard.

The equivalent cantilever force in a given direction *j* is the force applied at the top of the insulator that produces the same bending moment at the base of the insulator column as the one produced by the sum of the contribution of each considered force. For a set of forces F_{ij} (with *i* from 1 to *n*), each applied at a distance h_i from the base of the column, the equivalent cantilever force is given as follows:

$$F_{C\_j} = \frac{1}{H_T} \sum_{i=1}^{n} k_i F_{ij} h_i \tag{89}$$

where

F_{C_j} is the equivalent cantilever force in the *j* direction (x or y), N [lbf]
H_T is the total height of the insulator column (Figure 31), m [ft]
k_i is the load factor of force F_{ij} as discussed below
F_{ij} is the cantilever force *i* in the *j* direction, N [lbf]
h_i is the distance of the application point of force F_{ij} from the base of the insulator, m [ft]

Copyright © 2010 IEEE. All rights reserved.

Copyright The Institute of Electrical and Electronics Engineers, Inc.
Provided by IHS under license with IEEE
No reproduction or networking permitted without license from IHS

Order Number: 02120914
Sold to:EGAT [700166108393] - VARRIS.Y@EGAT.CO.TH,
Not for Resale,2016-09-15 03:57:47 UTC

For example, the equivalent cantilever force resulting from the simultaneous application of F_{WC}, F_{scC}, and F_{WCI} in the x direction, assuming a load factor of 1 for all forces for the sake of this example, is given by:

$$F_{C\_x} = \frac{F_{WCI}}{2} + \frac{(H_T + H_f)F_{WC}}{H_T} + \frac{(H_T + H_f)F_{scC}}{H_T}$$

The net cantilever force from the contribution of the x and y horizontal directions is given as the vectorial sum of each component direction as follows:

$$F_C = \sqrt{F_{C\_x}^2 + F_{C\_y}^2} \tag{90}$$

For example, the total cantilever load resulting from the simultaneous application of F_{WC}, F_{scC}, and F_{WCI} in the x direction and F_{TE} in the y direction (using k factors equal to 1) is given as follows:

$$F_C = \sqrt{\left(\frac{F_{WCI}}{2} + \frac{(H_T + H_f)F_{WC}}{H_T} + \frac{(H_T + H_f)F_{scC}}{H_T}\right)^2 + \left(F_{TE}\left(\frac{H_T + H_f}{H_T}\right)\right)^2}$$

12.3.3.2 Horizontally mounted insulator

The loads that may act on a horizontally mounted insulator are illustrated in Figure 32. In this figure, x is the horizontal direction perpendicular to the bus (in the insulator direction), y is the horizontal direction in the bus direction, and z is the vertical direction.

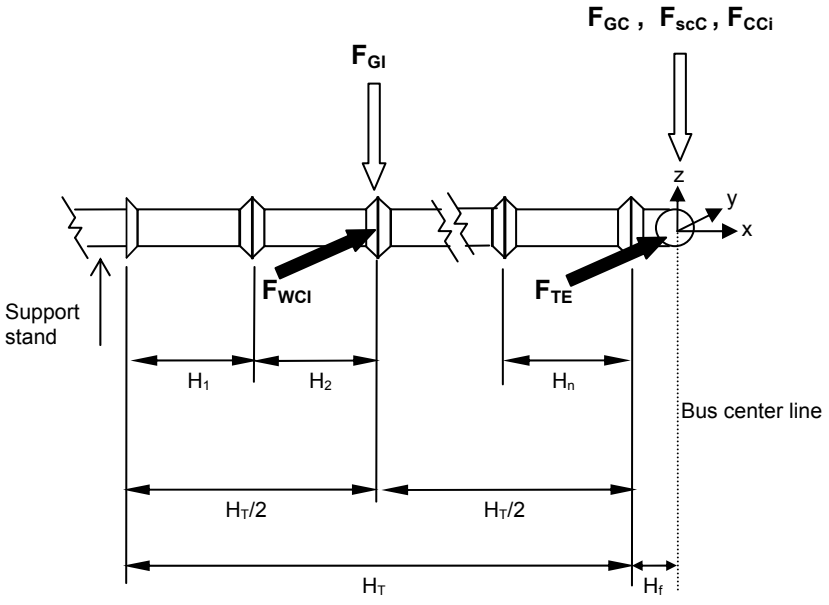

Figure 32—Cantilever forces on a horizontally mounted insulator

Copyright © 2010 IEEE. All rights reserved.

Copyright The Institute of Electrical and Electronics Engineers, Inc.
Provided by IHS under license with IEEE
No reproduction or networking permitted without license from IHS

Order Number: 02120914
Sold to:EGAT [700166108393] - VARRIS.Y@EGAT.CO.TH,
Not for Resale,2016-09-15 03:57:47 UTC

Note that F_{GI} may be replaced by individual forces at the midpoint of each insulator in the column if different diameters are used and ice is present. As for the case of the vertical arrangement, the equivalent cantilever force must first be obtained separately in each considered direction (here y and z) using Equation (89), and then the net cantilever force is obtained from the contribution of each direction here as the vectorial sum of each component direction as follows:

$$F_C = \sqrt{F_{C\_y}^2 + F_{C\_z}^2} \tag{91}$$

For example, the total cantilever load resulting from the simultaneous application of F_{WCI} and F_{TE} in the y direction and F_{scC}, F_{GC}, F_{CCi}, F_{GI} in the z direction (using k factors equal to 1) is given as follows:

$$F_C = \sqrt{\left(\frac{F_{GI}}{2} + \frac{(H_T + H_f)(F_{GC} + F_{scC} + F_{CCi})}{H_T}\right)^2 + \left(\frac{F_{WCI}}{2} + F_{TE}\left(\frac{H_T + H_f}{H_T}\right)\right)^2}$$

12.3.4 Load factors

The load factors k_i to use in obtaining the total cantilever force depend on the design methodology used (LRFD or ASD) and/or are based on utility design standards or published guidelines applicable to substation bus structures. The load factors are used to combine the different loads in a statistically coherent manner because they cannot generally all happen at the same time. The load factors should also be established by considering which strength resistance factor has been used in determining the strength capacity of the insulator, to which the net force will be compared against to determine the adequacy of the chosen insulator.

Another consideration in the case of the short circuit force is how the latter has been established. Since the simplified method presented earlier is usually very conservative by comparison with finite-element calculations, the load factor for the short circuit force can therefore vary accordingly. When the short circuit force has been established using the simplified method, the following conditions should be satisfied:

a) The natural frequency of vibration of the insulator together with the effective weight of the conductor span, denoted by f_1, should be less than one half the short-circuit-current-force frequency, that is:

$$f_1 < \frac{120}{2} Hz \quad \text{for a 60 Hz system (100/2 for a 50 Hz system)} \tag{92}$$

b) The first two natural frequencies of the insulator/mounting structure combination f_{s1} and f_{s2} and the natural frequency of the conductor span f_b (12.6) differ by a factor of at least two, that is:

$$\frac{f_{s1}}{f_b} < \frac{1}{2} \; or \; \frac{f_{s1}}{f_b} > 2 \tag{93}$$

and

Copyright © 2010 IEEE. All rights reserved.

Copyright The Institute of Electrical and Electronics Engineers, Inc.
Provided by IHS under license with IEEE
No reproduction or networking permitted without license from IHS

Order Number: 02120914
Sold to:EGAT [700166108393] - VARRIS.Y@EGAT.CO.TH,
Not for Resale,2016-09-15 03:57:47 UTC

$$\frac{f_{s2}}{f_b} < \frac{1}{2} \; or \; \frac{f_{s2}}{f_b} > 2 \tag{94}$$

where

f_{s1}	is the first natural frequency of insulator/mounting structure combination, Hz
f_{s2}	is the second natural frequency of insulator/mounting structure combination, Hz
f_b	is the natural frequency of the conductor span, Hz

The natural frequencies f_1, f_{s1}, and f_{s2} can be determined from a handbook on natural frequencies of mechanical systems, using the geometric and material properties of the insulator and mounting structure. Preferably, a civil, structural, or mechanical engineer should be consulted for such calculations.

If either of the previous conditions in item a) or item b) are not satisfied, then a dynamic study should be made to determine an appropriate load factor, according to the design methodology used as well as the strength resistance factor used in obtaining the insulator capacity in bending (see 12.4).

12.4 Strength of porcelain insulators

12.4.1 Verification of insulator capacity

Porcelain insulators are assembly generally consisting of end fittings, bonding medium, and a porcelain body. Although any of the components of the insulator can be sources of failure, the focus of most investigations is the porcelain body and bonding. Typically, porcelain insulators have relatively good tension and compression characteristics in contrast to the cantilever and torsional strengths.

In general, climatic loading such as wind will generate mostly cantilever (bending) loadings in insulators. However, dynamic loading such as short circuit may also generate high torsional loading due to the complex dynamic response of the structure (which can be obtained using the finite-element methodology). Both bending and torsional strengths should therefore be checked, based on all the loads acting on insulators.

Note that it is a current industry practice to consider that all types of loadings (bending, torsional, tension, etc.) act independently and should therefore be checked accordingly, even though in practice, the net resultant stress in an insulator is usually made from the combination of different types of loading.

For bending, an insulator is considered adequate if the net cantilever force F_C acting on it is equal or below its rated strength calibrated by a strength resistance factor according to the design methodology used (LRFD or ASD). Because the net effect of the cantilever force F_C is a bending moment at the bottom of the insulator, the cantilever force is translated as an equivalent moment M_C at the base of the insulator:

$$M_C = F_C H_T \tag{95}$$

An insulator is therefore considered adequate if:

$$M_C \leq M_b \tag{96}$$

Copyright © 2010 IEEE. All rights reserved.

Copyright The Institute of Electrical and Electronics Engineers, Inc.
Provided by IHS under license with IEEE
No reproduction or networking permitted without license from IHS

Order Number: 02120914
Sold to:EGAT [700166108393] - VARRIS.Y@EGAT.CO.TH,
Not for Resale,2016-09-15 03:57:47 UTC

where

M_b is the bending moment capacity at the base of the insulator as presented in 12.4.2

In the same way for torsion, an insulator is considered adequate if:

$$T_C \leq T_b \tag{97}$$

where

T_C is the net torsional moment acting on the insulator
T_b is the torsional moment capacity at the base of the insulator as presented in 12.4.2

12.4.2 Insulator capacity in bending and torsion

Porcelain insulators are generally manufactured 1 to 3 standard deviations above the rated strength, which for bending corresponds to the given cantilever rating. The cantilever rating is the maximum horizontal load that can be applied at the top of the insulator with its base fixed. Manufacturers typically recommend multiplying the cantilever rating by a strength resistance factor of 0.4 for working or allowable loads. However, it is also recommended that a strength resistance factor of 1.0 shall be used when evaluating strength to short duration forces such as from short circuit loading. *It is, however, important to emphasize that currently, there is no general agreement in the industry as how to define appropriately the cantilever strength of an insulator and the use of the appropriate strength resistance factors.* Indeed, depending on how many standard deviations are used in the definition of the rated strength, and on the value itself of the standard deviation, it is readily deduced that the appropriate strength resistance factor could vary greatly from manufacturer to manufacturer. Also, utility practices may differ based on their own experience and/or acceptable risk. Therefore, the strength resistance factors discussed in this subclause should be considered as indicative only. However, in most cases, the strength resistance factors presented in this subclause will lead to conservative design. Note that the strength resistance factor value under the same conditions will also vary according to the design methodology used (LRFD or ASD) as discussed below.

The bending moment capacity at the base of the insulator (generally the area of higher stress) is equal to:

$$M_b = S_{rf} \; C_s \; h_i \tag{98}$$

where

M_b is the bending moment capacity at the base of the insulator
S_{rf} is the strength resistance factor
Cs is the cantilever rated strength
h_i is the insulator height

The strength resistance factor S_{rf} of 0.4 should be increased to provide similar insulator selections between working strength (ASD methodology) and ultimate strength (LRFD methodology) designs. A value of 0.5 is recommended for S_{rf} using the LRFD methodology. As mentioned, a factor of 1.0 should be used when evaluating the strength to bending moments from short circuit forces.

For torsional strength, manufacturers specify a torsional moment rating, corresponding to the maximum torsional moment that can be applied at the top of the insulator with its base fixed. As for the bending moment, it is

--`,,,,,,`,```,,`,`,,`,-`-`,,```,,,`---
Copyright © 2010 IEEE. All rights reserved.
Copyright The Institute of Electrical and Electronics Engineers, Inc.
Provided by IHS under license with IEEE
No reproduction or networking permitted without license from IHS
Order Number: 02120914
Sold to:EGAT [700166108393] - VARRIS.Y@EGAT.CO.TH,
Not for Resale,2016-09-15 03:57:47 UTC

recommended to multiply this rating by a strength resistance factor, to obtain the torsional moment capacity of the insulator:

$$T_b = S_{rf}\ T_s \tag{99}$$

where

T_b is the torsional moment capacity of the insulator
S_{rf} is the strength resistance factor
T_s is the torsional rated strength

An S_{rf} factor of 0.5 is recommended for torsion using the ASD methodology and of 0.6 using the LRFD methodology; for short duration forces, such as from short circuit loading, a factor of 1.0 is recommended. Note also that the same factors are recommended for tension loading in the case of a strain bus insulator.

Note that when the equivalent bending moment M_C and/or the net torsional moment T_C are obtained by a combination of working loads (wind, ice, and weight) and short duration loads (short circuit), the question arises as to which strength resistance factor to use (e.g., 0.4 or 1.0). The way to evaluate the strength in such cases is to calibrate adequately the different loads before combining them. For example, in determining the net cantilever force according to Equation (90), the load factors k_i for the short circuit force should be divided by 2.5 *if* a strength resistance factor of 0.4 is used in determining the bending moment capacity of the insulator M_b.

12.5 Induced vibrations

For a laminar air flow around a conductor with wind speed less than 72 km/h (45 mph), eddies are shed from the boundaries of the conductor, alternating from edge to edge. The frequency of eddy shedding f_a is given by:

$$f_a = \frac{CV}{D_o} \tag{100}$$

where

C is the Strouhal number (a dimensionless number) and is approximately equal to 0.19 for a cylinder shape. It accounts for the oscillatory flow mechanism due to wind.
V is the wind velocity (m/s) [in/s].
D_o is the conductor outside diameter (m) [in].

When the frequency of eddy shedding f_a coincides with the natural frequency of the conductor, wind-induced vibration of the conductor may occur. It is recommended that an allowance for variations be allowed. This is accomplished by ensuring the ratio of the inducing frequency to the natural frequency is **outside** the range from 0.5 to $\sqrt{2}$.

$$\frac{1}{2} \le \frac{f_a}{f_b} \le \sqrt{2} \tag{101}$$

Copyright © 2010 IEEE. All rights reserved.
Copyright The Institute of Electrical and Electronics Engineers, Inc.
Provided by IHS under license with IEEE
No reproduction or networking permitted without license from IHS
Order Number: 02120914
Sold to:EGAT [700166108393] - VARRIS.Y@EGAT.CO.TH,
Not for Resale,2016-09-15 03:57:47 UTC

where

f_a is the frequency of eddy shedding, Hz
f_b is the natural frequency of the conductor, Hz (12.6)

For wind speeds in excess of 72 km/h (45 mph), the wind tends to be turbulent and steady exciting impulses are less probable. If the natural frequency of the conductor is such that it falls within the range describe by Equation (102), then attenuation measures should be taken as described below.

Another source of vibration for buses is related to alternating current. Current flowing through parallel conductors creates magnetic fields that interact and exert forces on the parallel conductors. This driving force oscillates at twice the power frequency (*2f*). If the calculated frequency of a bus span is found to be greater than half the current-force frequency, that is, greater than the power frequency:

$$f_b > f \tag{102}$$

then measures should be taken as described below or a dynamic analysis should be made to determine the stresses involved.

12.6 Natural frequency of rigid conductors

A span of rigid conductors has its own natural frequency of vibration. If the conductor is displaced from its equilibrium position and released, then it will begin to vibrate at this natural frequency. The magnitude of the oscillations will decay due to damping. If, however, the conductor is subjected to a periodic force whose frequency is near the natural frequency of the span, the bus may continue to vibrate and the amplitude will increase. Such vibration may cause damage to the bus conductor by fatigue or by excessive fiber stress.

The natural frequency of a conductor span is dependent on the manner in which the ends are supported and on the conductor's length, mass, and stiffness. The natural frequency of a conductor span can be calculated as follows:

$$f_b = \frac{\pi K^2}{2L^2}\sqrt{\frac{EJ}{m}} \tag{103}$$

where

f_b is the conductor natural frequency (Hz)
L is the span length (m) [in]
E is the modulus of elasticity of the conductor's material (N/m^2) [lbf/in^2]
J is the moment of inertia of the cross-sectional area (m^4) [in^4]
m is the mass per unit length of the conductor (kg/m) [lbm/in]
K is a dimensionless constant accounting for the boundary conditions at the conductor's ends:
K = 1.00 for two pinned ends
K = 1.25 for one pinned ends and one fixed (clamped) end
K = 1.51 for two fixed (clamped) ends.

Copyright © 2010 IEEE. All rights reserved.

Copyright The Institute of Electrical and Electronics Engineers, Inc.
Provided by IHS under license with IEEE
No reproduction or networking permitted without license from IHS

Order Number: 02120914
Sold to:EGAT [700166108393] - VARRIS.Y@EGAT.CO.TH,
Not for Resale,2016-09-15 03:57:47 UTC

NOTE—In Equation (103), the mass by unit length (m) is required, whereas in calculations, we often evaluate the weight by unit length (unit weight). To get mass by unit length in SI units from unit weight in N/m, divide the unit weight by 9.81. To get mass by unit length in British units from unit weight in lbf/in, divide the unit weight by 386.1.

End conditions can range between fixed and pinned. A fixed end is not free to rotate (moment resisting), whereas a pinned end is free to rotate (not moment resisting). Because of structure flexibility and connection friction, the end conditions are not truly fixed or pinned.

The finite-element method may also be used to calculate the natural frequency and corresponding mode shapes of a structure; it permits taking account directly of the effect of supports as well as the 3D behavior of structures.

12.7 Vibration attenuation

To prevent induced vibrations when the natural frequency of the conductor is in the vicinity of the excitation frequency from wind or from alternating current [Equation (102) or Equation (103)], it is preferred that the diameter of the conductor be increased to lower its natural frequencies, taking them out of the critical range. Another possible solution is to increase the bus span length, that is, to change the span between supports, which also has the effect of lowering the natural frequencies. Another solution is to provide damping elements. For tubular conductors, this can be accomplished by the following two methods: 1) installing stranded bare cable inside of the tubular bus conductor to dissipate vibration energy or 2) installing commercially available vibration dampers on the conductor.

Installing stranded bare cable inside the bus conductor requires that the weight of the stranded damping cable used must be between 10% and 33% of the bus conductor weight and that the damping cable be the same material as the bus conductor to prevent galvanic corrosion. The designer should also consider the audible noise that can be generated by the stranded damping cable inside of the bus conductor because this may not be acceptable in some locations. Note that the thermal expansion fittings could also act as energy dissipation devices.

Commercially available vibration dampers can also be used on both tubular and nontubular bus conductors and can be applied in both EHV and non-EHV locations. Spacing of the vibration dampers is based on 1/3 of the span length plus 0.6 m and can be located at either end of the span.

Vibration dampers should be applied when the maximum vibration-free span length is exceeded as listed in Table 19 through Table 21 for various bus conductor types.

Copyright © 2010 IEEE. All rights reserved.

Copyright The Institute of Electrical and Electronics Engineers, Inc.
Provided by IHS under license with IEEE
No reproduction or networking permitted without license from IHS

Order Number: 02120914
Sold to:EGAT [700166108393] - VARRIS.Y@EGAT.CO.TH,
Not for Resale,2016-09-15 03:57:47 UTC

Table 19—Maximum vibration-free span length for tubular bus

Nominal pipe size	Maximum safe span length
1”	1.5 m (5’-0”)
1 1/4”	1.9 m (6’-3”)
1 1/2”	2.1 m (7’-0”)
2”	2.7 m (9’-0”)
2 1/2”	3.3 m (10’-9”)
3”	4.0 m (13’-3”)
3 1/2”	4.6 m (15’-3”)
4”	5.2 m (17’-0”)
4 1/2”	5.8 m (19’-0”)
5”	6.5 m (21’-3”)
6”	7.7 m (25’-3”)
NOTE—These lengths are based on one cycle of vibration and apply to both the schedule 40 and the schedule 80 tubular bus. The lengths listed here can be increased approximately 20% with reasonable certainty that there will be no vibration.	

Table 20—Maximum vibration-free span length for universal angle bus conductor

Size	Maximum safe span length
3 ¼” × 3 ¼” × ¼”	3.7 m (12’-0”)
4” × 4” × ¼”	4.6 m (15’-0”)
4” × 4” × 3/8”	4.8 m (15’-9”)
4 ½” × 4 ½” × 3/8”	5.1 m (16’-9”)
5” × 5” × 3/8”	5.6 m (18’-6”)
NOTE—These lengths are based on one loop of vibration. The lengths listed here can be increased approximately 20% with reasonable certainty that there will be no vibration. However, this table does not apply for double back-to-back configurations.	

Table 21—Maximum vibration-free span length for integral web channel bus

Size	Maximum safe span length
4” × 4”	4.4 m (14’-6”)
6” × 4”	6.3 m (20’-9”)
6” × 5”	6.5 m (21’-3”)
6” × 6”	6.6 m (21’-9”)
7” × 7”	8.0 m (26’-3”)
8” × 5”	8.8 m (29’-0”)
NOTE—These lengths are based on one loop of vibration. The lengths listed here can be increased approximately 20% with reasonable certainty that there will be no vibration. However, this table does not apply for double back-to-back configurations.	

Copyright © 2010 IEEE. All rights reserved.

Copyright The Institute of Electrical and Electronics Engineers, Inc.
Provided by IHS under license with IEEE
No reproduction or networking permitted without license from IHS

Order Number: 02120914
Sold to:EGAT [700166108393] - VARRIS.Y@EGAT.CO.TH,
Not for Resale,2016-09-15 03:57:47 UTC

12.8 Clearances considerations

The fault current force on a bus conductor is inversely proportional to the center-to-center conductor spacing. The fault current force can be reduced by increasing the distance between the bus conductors. However, it is the usual substation design practice to reduce bus spacing rather than to increase the distance between conductors.

Increasing bus spacing increases the overall plan dimensions of the substation. The increase in substation area increases the cost of buswork, secondary circuit cable and raceway, real estate, and so on. As a result, it is usual to determine first the minimum required phase-to-phase spacing of the buses, rather than to increase the spacing to reduce fault current force.

The primary considerations in reducing the phase-to-phase spacing in the substation arrangement are electrical clearances and the space required for maintenance and repair activities. Bus layout and conductor-to-conductor spacing is dictated by the larger of the distance required for electrical clearance and the space required for maintenance and repair activities.

Spaces for maintenance and repair activities are specific to maintenance and the utilities requirements. The required space is determined from the land features within and outside of the substation, available equipment, staff training, and so on.

For a selected insulation level, phase-to-phase electrical clearance is determined from the required phase-to-ground clearance.

For high-voltage substations, minimum phase-to-phase spacing is based on the phase to-ground clearance required for the station BIL. Recommended clearances for standard BIL are given in IEEE Std 1427™-2006 [B24].

For EHV clearances, the consensus method for determining the minimum phase-to-ground clearance can be found in IEEE Std 1313.2-1999 [B22].

Calculations for minimum phase-to-ground clearance and phase-to-phase clearance have been made with the guidance available in IEEE Std 1313.2-1999 [B22], and they have been published in IEEE Std 1427-2006 [B24].

12.9 Rigid bus fittings

Rigid bus fittings are usually made from cast aluminum, which is a brittle material of moderate strength. Considerations must be given in design to their capacity to transfer the most critical combination of forces from the bus span to the supporting isolator.

Copyright © 2010 IEEE. All rights reserved.

Copyright The Institute of Electrical and Electronics Engineers, Inc.
Provided by IHS under license with IEEE
No reproduction or networking permitted without license from IHS

Order Number: 02120914
Sold to:EGAT [700166108393] - VARRIS.Y@EGAT.CO.TH,
Not for Resale,2016-09-15 03:57:47 UTC

Annex A

(informative)

Bibliography

[B1] Aluminum Electrical Conductor Handbook, Aluminum Company of America, 1989.[32]

[B2] American Society of Civil Engineers, "Wind forces on structures," Transaction Paper Number 3269-1961, vol. 126.[33]

[B3] ASTM B-1, 2007, Standard Specification for Hard-Drawn Copper Wire.

[B4] ASTM B-2, 2008, Standard Specification for Medium-Drawn Copper Wire.

[B5] ASTM B-3, 2007, Standard Specification for Soft or Annealed Copper Wire.

[B6] ASTM B-230, 2007, Standard Specification for Aluminum 1350-H19 Wire for Electrical Purposes.

[B7] ASTM B-317, 2007, Standard Specification for Aluminum-Alloy Extruded Bar, Rod, Tube, Pipe, Structural Profiles, and Profiles for Electrical Purposes (Bus Conductor).

[B8] ASTM B-398, 2007, Standard Specification for Aluminum-Alloy 6201-T81 Wire for Electrical Purposes.

[B9] Bates, A. C., "Basic concepts in the design of electric bus for short-circuit conditions," *AIEE Transactions*, vol. 77, no. 3, pp. 29–36, Apr. 1958.

[B10] Chaine, P. M., Verge, R. W., Castonguay, G., and Gariepy, J., Wind and Ice Loading in Canada, Industrial Meteorology-Study II, Toronto: Environment Canada, 1974.

[B11] *Chase Electrical Handbook*, Waterbury, CT: Chase Brass & Copper, Co., 1947.

[B12] CISPR 24, Information Technology Equipment - Immunity Characteristics - Limits and Methods of Measurements.

[B13] Hartzog, D., *Mechanical Vibrations*, New York: McGraw-Hill, 1956.

[B14] Hosemann, G., and Tsanakas, D., "Calculated and measured values of dynamic short-circuit stress in a high voltage test structure with and without reclosure," *Electra*, no. 63, Mar. 1979.

[B15] Hosemann, G., and Tsanakas, D., "Contraintes dynamiques dans les postes. Considérations des courants de court-circuits et des forces électromagnétiques dus aux défauts non simultanés," CIGRE, no. 23-04, Aug.-Sept. 1978.

[B16] IEC 60865-1, Ed. 2-1993, Short-Circuit Currents—Calculations of Effects. Part 1: Definition and Calculation Methods.[36]

[B17] IEC 61284, Overhead Lines—Requirements and Tests for Fitting.

[32]Aluminum Association publications are available from The Aluminum Association, 1525 Wilson Boulevard, Suite 600, Arlington, VA 22209, USA (www.aluminum.org).
[33]ASCE publications are available from the American Society of Civil Engineers, 1801 Alexander Bell Drive, Reston, VA 20191, USA (www.asce.org).
[36]IEC publications are available from the Sales Department of the International Electrotechnical Commission, Case Postale 131, 3 rue de Varembé, CH-1211, Genève 20, Switzerland/Suisse (http://www.iec.ch/). IEC publications are also available in the United States from the Sales Department, American National Standards Institute, 11 West 42nd Street, 13th Floor, New York, NY 10036, USA.

Copyright © 2010 IEEE. All rights reserved.
Copyright The Institute of Electrical and Electronics Engineers, Inc.
Provided by IHS under license with IEEE
No reproduction or networking permitted without license from IHS
Order Number: 02120914
Sold to:EGAT [700166108393] - VARRIS.Y@EGAT.CO.TH,
Not for Resale,2016-09-15 03:57:47 UTC

[B18] IEEE Committee Report, "Transmission system radio influence," *IEEE Transactions on Power Apparatus and Systems*, vol. 84, pp. 714, Aug. 1965.[34]

[B19] IEEE Std 80™-2000, IEEE Guide for Safety in AC Substation Grounding. [35]

[B20] IEEE Std 525™-2007, IEEE Guide for the Design and Installation of Cable Systems in Substations.

[B21] IEEE Std 738™-2006, IEEE Standard for Calculating the Current-Temperature of Bare Overhead Conductors.

[B22] IEEE Std 1313.2™-1999 (Reaff 2005), IEEE Guide for the Application of Insulation Coordination.

[B23] IEEE Std 1368™-2006, IEEE Guide for Aeolian Vibration Field Measurements of Overhead Conductors.

[B24] IEEE Std 1427™-2006, IEEE Guide for Recommended Electrical Clearances and Insulation Levels in Air-Insulated Electrical Power Substations.

[B25] Iordanescu, M., Hardy, C., and Nourry, J., "Structural analysis and testing of HV busbar assemblies with rigid conductors under short-circuit conditions," *IEEE Transactions on Power Delivery*, vol. 2, no. 4, pp. 1082–1089, Oct. 1987.

[B26] Jacobsen, L. S., and Ayre, R. S., *Engineering Vibrations*, New York: McGraw-Hill, 1958.

[B27] Juette, G. W., "Comparison of radio noise prediction methods with CIGRE/IEEE survey results," *IEEE Transactions on Power Apparatus and Systems*, vol. PAS-92, no. 3, pp. 1029–1042, May/June 1973.

[B28] Killian, C. D., "Forces due to short-circuit currents," *Delta-Star Magazine*, 1943.

[B29] Leslie, J. R., Bailey, B. M., Craine, L. B., Eteson, D. C., Grieves, R. E., Janischewskyj, W., Juette, G. W., and Taylor, E. R., "Radio noise design guide for high-voltage transmission lines," *IEEE Transactions on Power Apparatus and Systems*, vol. 90, no. 2, pp. 833–842, Mar./Apr. 1971.

[B30] Milton, R. M., and Chambers, F., "Behavior of high-voltage buses and insulators during short circuits," *AIEE Transactions*, Part 3, vol. 74, pp. 742–749, Aug. 1955.

[B31] Morse, P. M., *Vibration and Sound*, New York: McGraw-Hill, 1948.

[B32] Palante, G., "Study and conclusions from the results of the enquiry on the thermal and dynamic effects of heavy short-circuit currents in high-voltage substations," *Electra*, no. 12, pp. 51–89, Mar. 1970.

[B33] Pinkham, T. A., and Killeen, N. D., "Short-circuit forces on station post insulators," *IEEE Transactions on Power Apparatus and Systems*, vol. 90, no. 4, pp. 1688–1697, July 1971.

[B34] Schwartz, S. J., "Substation design shows need for bus damping," *Electrical World*, June 24, 1963.

[B35] Taylor, D. W., and Steuhler, C. M., "Short-circuit forces on 138 kV buses," *AIEE Transactions*, Part 3, vol. 75, pp. 739–747, Aug. 1956.

[B36] The Mechanical Effects of Short-Circuit Currents in Open Air Substations, CIGRE WG 02 of SC 23, 1987.

[B37] Tompkins, J. S., Merrill, L. L., and Jones, B. L., "Quantitative relationships in conductor vibration damping," *AIEE Transactions*, Part 3, vol. 75, pp. 879–896, Jan. 1956.

[B38] Wilson, W., *The Calculation and Design of Electrical Apparatus*, London: Chapman and Hill, Ltd., 1941.

[34]IEEE publications are available from the Institute of Electrical and Electronics Engineers, 445 Hoes Lane, Piscataway, NJ 08854, USA (http://standards.ieee.org/).

Copyright © 2010 IEEE. All rights reserved.

Copyright The Institute of Electrical and Electronics Engineers, Inc.
Provided by IHS under license with IEEE
No reproduction or networking permitted without license from IHS

Order Number: 02120914
Sold to:EGAT [700166108393] - VARRIS.Y@EGAT.CO.TH,
Not for Resale,2016-09-15 03:57:47 UTC

Annex B

(informative)

Rigid bus conductor ampacity

The rigid bus-ampacity data included in this annex have been taken from the following reference:

Prager, M., Pemberton, D. L., Craig, A. G., Jr., and Bleshman, N. A., "Thermal consideration for outdoor bus-conductor design ampacity tables," *IEEE Transactions on Power Apparatus and Systems*, vol. PAS-96, no. 4, July 1977.

The rigid bus ampacity values presented in this annex have been calculated using the formulas and methodology presented in this standard. A summary of the assumptions used in calculating rigid conductor ampacity is presented in Table B.1.

Table B.1 —Rigid conductor ampacity calculation assumption

Description	Value
Ambient temperature	40 °C
Latitude	40°N
Bus direction	East–west
Wind	0.6 m/s perpendicular to the conductor axis
Solar absorptivity	0.5

Copyright © 2010 IEEE. All rights reserved.

Copyright The Institute of Electrical and Electronics Engineers, Inc.
Provided by IHS under license with IEEE
No reproduction or networking permitted without license from IHS

Order Number: 02120914
Sold to:EGAT [700166108393] - VARRIS.Y@EGAT.CO.TH,
Not for Resale,2016-09-15 03:57:47 UTC

Table B.2 —Single aluminum rectangular bar ac ampacity, with sun (55.0% conductivity)

	Emissivity = 0.20 Temperature rise above 40 °C ambient							Emissivity = 0.50 Temperature rise above 40 °C ambient						
Size (in)	**30**	**40**	**50**	**60**	**70**	**90**	**110**	**30**	**40**	**50**	**60**	**70**	**90**	**110**
0.250 by 3.000	921	1059	1176	1278	1369	1527	1660	959	1118	1253	1371	1478	1665	1828
0.250 by 4.000	1130	1298	1441	1566	1678	1872	2039	1200	1394	1560	1707	1839	2073	2278
0.250 by 5.000	1320	1517	1685	1833	1965	2195	2393	1413	1644	1841	2016	2174	2455	2703
0.250 by 6.000	1497	1723	1915	2084	2235	2500	2729	1615	1881	2109	2311	2495	2821	3110
0.375 by 4.000	1385	1593	1769	1924	2063	2304	2510	1464	1704	1909	2091	2254	2544	2799
0.375 by 5.000	1608	1851	2057	2239	2401	2686	2931	1714	1998	2241	2456	2651	2997	3302
0.375 by 6.000	1815	2091	2326	2533	2718	3044	3326	1950	2275	2554	2801	3026	3426	3782
0.375 by 8.000	2202	2540	2829	3084	3313	3718	4070	2395	2800	3148	3458	3740	4247	4700
0.500 by 4.000	1589	1829	2034	2213	2374	2654	2895	1672	1951	2189	2399	2590	2926	3223
0.500 by 5.000	1835	2115	2353	2562	2750	3079	3364	1949	2276	2556	2805	3030	3430	3785
0.500 by 6.000	2071	2388	2659	2897	3111	3487	3814	2216	2590	2912	3197	3456	3918	4330
0.500 by 8.000	2511	2899	3231	3524	3788	4255	4662	2721	3186	3587	3943	4268	4851	5374
0.625 by 4.000	1776	2047	2277	2479	2660	2977	3249	1861	2177	2446	2683	2898	3278	3614
0.625 by 5.000	2034	2347	2613	2847	3058	3427	3747	2152	2519	2833	3111	3363	3812	4210
0.625 by 6.000	2286	2639	2940	3206	3445	3865	4231	2437	2855	3213	3531	3820	4337	4798
0.625 by 8.000	2760	3190	3558	3884	4177	4696	5151	2982	3498	3942	4337	4698	5347	5929
0.625 by 10.000	3190	3690	4120	4501	4845	5457	5996	3483	4091	4615	5084	5513	6238	6987
0.625 by 12.000	3560	4123	4608	5039	5430	6126	6744	3924	4615	5212	5748	6240	7131	7941
0.750 by 4.000	1935	2232	2486	2708	2907	3256	3557	2021	2368	2664	2926	3163	3582	3953
0.750 by 5.000	2216	2559	2851	3108	3340	3746	4098	2336	2740	3085	3391	3668	4162	4601
0.750 by 6.000	2472	2856	3184	3474	3735	4195	4597	2627	3083	3474	3821	4137	4702	5207
0.750 by 8.000	2984	3452	3852	4207	4527	5094	5592	3214	3776	4260	4691	5085	5793	6430
0.750 by 10.000	3518	4072	4548	4969	5350	6026	6622	3832	4505	5086	5605	6079	6935	7708
0.750 by 12.000	3875	4491	5021	5492	5919	6682	7359	4260	5015	5669	6255	6793	7768	8655

Copyright © 2010 IEEE. All rights reserved.

Copyright The Institute of Electrical and Electronics Engineers, Inc.
Provided by IHS under license with IEEE
No reproduction or networking permitted without license from IHS

Order Number: 02120914
Sold to:EGAT [700166108393] - VARRIS.Y@EGAT.CO.TH,
Not for Resale,2016-09-15 03:57:47 UTC

Table B.3 —Single aluminum rectangular bar ac ampacity, without sun (55.0% conductivity)

	Emissivity = 0.20 Temperature rise above 40 °C ambient							Emissivity = 0.50 Temperature rise above 40 °C ambient						
Size (in)	**30**	**40**	**50**	**60**	**70**	**90**	**110**	**30**	**40**	**50**	**60**	**70**	**90**	**110**
0.250 by 3.000	950	1084	1198	1298	1387	1542	1674	1027	1176	1303	1416	1518	1699	1857
0.250 by 4.000	1158	1322	1462	1585	1695	1887	2052	1265	1449	1608	1749	1877	2105	2306
0.250 by 5.000	1354	1546	1711	1856	1986	2213	2409	1492	1710	1899	2068	2221	2494	2737
0.250 by 6.000	1538	1757	1945	2111	2260	2521	2747	1708	1959	2177	2372	2549	2867	3150
0.375 by 4.000	1423	1625	1798	1950	2086	2324	2528	1553	1780	1975	2149	2308	2589	2838
0.375 by 5.000	1654	1890	2092	2270	2429	2710	2952	1821	2087	2319	2526	2714	3050	3349
0.375 by 6.000	1869	2136	2366	2569	2751	3072	3350	2073	2378	2644	2882	3099	3488	3835
0.375 by 8.000	2271	2598	2880	3130	3355	3753	4102	2552	2931	3262	3560	3833	4324	4767
0.500 by 4.000	1638	1871	2070	2246	2403	2679	2917	1786	2047	2273	2474	2657	2984	3273
0.500 by 5.000	1893	2164	2396	2601	2786	3109	3390	2082	2388	2654	2892	3109	3497	3843
0.500 by 6.000	2137	2444	2708	2941	3152	3522	3844	2369	2719	3024	3297	3546	3995	4396
0.500 by 8.000	2595	2970	3294	3580	3840	4298	4701	2912	3347	3726	4068	4381	4946	5457
0.625 by 4.000	1836	2098	2322	2520	2697	3008	3277	2002	2295	2549	2775	2981	3349	3675
0.625 by 5.000	2104	2406	2665	2894	3100	3463	3778	2313	2654	2951	3216	3458	3893	4281
0.625 by 6.000	2365	2706	2999	3259	3493	3906	4267	2620	3008	3346	3650	3928	4428	4877
0.625 by 8.000	2859	3274	3632	3949	4237	4747	5196	3206	3686	4106	4484	4831	5459	6027
0.625 by 10.000	3307	3790	4207	4579	4917	5518	6050	3748	4313	4809	5257	5669	6420	7102
0.625 by 12.000	3696	4239	4709	5129	5512	6196	6805	4227	4869	5434	5945	6418	7282	8072
0.750 by 4.000	2006	2293	2539	2756	2951	3293	3589	2188	2509	2787	3035	3262	3666	4026
0.750 by 5.000	2298	2628	2912	3163	3389	3788	4135	2526	2899	3224	3515	3780	4257	4684
0.750 by 6.000	2564	2934	3253	3535	3791	4243	4639	2838	3260	3628	3959	4262	4808	5299
0.750 by 8.000	3097	3548	3937	4283	4596	5153	5644	3472	3992	4448	4859	5237	5921	6542
0.750 by 10.000	3655	4188	4649	5060	5433	6097	6684	4140	4763	5311	5805	6260	7088	7841
0.750 by 12.000	4030	4622	5136	5595	6013	6762	7429	4605	5305	5921	6480	6996	7940	8804

Copyright © 2010 IEEE. All rights reserved.

Copyright The Institute of Electrical and Electronics Engineers, Inc.
Provided by IHS under license with IEEE
No reproduction or networking permitted without license from IHS

Order Number: 02120914
Sold to:EGAT [700166108393] - VARRIS.Y@EGAT.CO.TH,
Not for Resale,2016-09-15 03:57:47 UTC

Table B.4 — Aluminum tubular bus—schedule 40 ac ampacity (53.0% conductivity)

SPS[a] size	OD	Wall thickness	Emissivity = 0.20, with sun temperature rise above 40 °C ambient							Emissivity = 0.20, without sun temperature rise above 40 °C ambient						
(in)	(in)	(in)	30	40	50	60	70	90	110	30	40	50	60	70	90	110
1.0	1.315	0.133	591	688	770	840	903	1011	1102	638	728	804	871	931	1035	1123
1.5	1.900	0.145	837	978	1097	1199	1290	1447	1580	914	1043	1153	1250	1336	1486	1614
2.0	2.375	0.154	1035	1213	1362	1490	1605	1802	1969	1139	1300	1438	1558	1666	1854	2015
2.5	2.875	0.203	1377	1618	1818	1992	2147	2413	2640	1527	1743	1928	2090	2235	2488	2705
3.0	3.500	0.216	1666	1962	2208	2422	2612	2940	3220	1861	2126	2351	2550	2728	3038	3305
3.5	4.000	0.226	1897	2239	2523	2770	2989	3367	3690	2132	2435	2695	2923	3127	3484	3792
4.0	4.500	0.237	2134	2523	2847	3127	3376	3807	4175	2412	2755	3049	3307	3539	3945	4295
5.0	5.563	0.258	2636	3127	3536	3890	4204	4748	5213	3010	3439	3807	4131	4422	4933	5374
6.0	6.625	0.280	3153	3752	4250	4681	5063	5726	6294	3633	4152	4597	4990	5343	5963	6500
8.0	8.625	0.322	4142	4954	5629	6213	6731	7631	8404	4843	5538	6135	6662	7138	7975	8703
SPS size	OD	Wall thickness	Emissivity = 0.50, with sun temperature rise above 40 °C ambient							Emissivity = 0.50, without sun temperature rise above 40 °C ambient						
(in)	(in)	(in)	30	40	50	60	70	90	110	30	40	50	60	70	90	110
1.0	1.315	0.133	572	690	788	872	948	1078	1190	686	785	870	945	1013	1133	1238
1.5	1.900	0.145	805	981	1127	1252	1363	1556	1723	992	1136	1260	1370	1469	1645	1800
2.0	2.375	0.154	991	1217	1402	1561	1703	1949	2161	1244	1425	1581	1720	1845	2068	2264
2.5	2.875	0.203	1314	1623	1876	2094	2287	2623	2914	1677	1921	2132	2320	2490	2793	3060
3.0	3.500	0.216	1582	1969	2284	2555	2795	3214	3576	2056	2357	2617	2848	3059	3434	3766
3.5	4.000	0.226	1796	2248	2614	2929	3208	3694	4116	2366	2712	3012	3280	3523	3957	4342
4.0	4.500	0.237	2015	2534	2954	3315	3635	4192	4675	2686	3080	3421	3726	4004	4500	4940
5.0	5.563	0.258	2474	3142	3680	4141	4550	5262	5880	3375	3872	4304	4690	5041	5671	6232
6.0	6.625	0.280	2943	3771	4435	5003	5506	6382	7144	4098	4703	5230	5701	6131	6902	7591
8.0	8.625	0.322	3830	4982	5899	6681	7373	8581	9633	5515	6334	7048	7688	8274	9328	10 274

[a]SPS = standard pipe size.

Copyright © 2010 IEEE. All rights reserved.
Copyright The Institute of Electrical and Electronics Engineers, Inc.
Provided by IHS under license with IEEE
No reproduction or networking permitted without license from IHS
Order Number: 02120914
Sold to:EGAT [700166108393] - VARRIS.Y@EGAT.CO.TH,
Not for Resale,2016-09-15 03:57:47 UTC

Table B.5 —Aluminum tubular bus—schedule 80 ac ampacity (53.0% conductivity)

Size		Wall	Emissivity = 0.20, with sun temperature rise above 40 °C ambient							Emissivity = 0.20, without sun temperature rise above 40 °C ambient						
SPS	OD	thickness	30	40	50	60	70	90	110	30	40	50	60	70	90	110
(in)	(in)	(in)														
1.0	1.315	0.179	672	783	875	956	1027	1149	1253	726	828	915	991	1059	1177	1277
1.5	1.900	0.200	967	1131	1267	1385	1490	1671	1825	1056	1205	1332	1444	1543	1716	1864
2.0	2.375	0.218	1212	1420	1595	1745	1879	2110	2306	1334	1523	1684	1825	1952	2172	2360
2.5	2.875	0.276	1580	1855	2086	2285	2462	2768	3029	1751	1999	2211	2397	2564	2855	3104
3.0	3.500	0.300	1930	2273	2559	2807	3028	3408	3733	2157	2463	2725	2955	3161	3522	3832
3.5	4.000	0.318	2210	2608	2940	3228	3483	3925	4303	2484	2838	3140	3406	3645	4062	4422
4.0	4.500	0.337	2499	2954	3334	3663	3955	4460	4893	2824	3226	3570	3873	4146	4622	5034
5.0	5.563	0.375	3104	3683	4165	4583	4954	5598	6150	3544	4050	4484	4867	5212	5816	6340
6.0	6.625	0.432	3801	4525	5127	5649	6113	6919	7610	4379	5007	5546	6022	6450	7204	7859
8.0	8.625	0.500	4927	5898	6706	7407	8031	9118	10 056	5761	6592	7308	7943	8516	9528	10 413
Size		Wall	Emissivity = 0.50, with sun temperature rise above 40 °C ambient							Emissivity = 0.50, without sun temperature rise above 40 °C ambient						
SPS	OD	thickness	30	40	50	60	70	90	110	30	40	50	60	70	90	110
(in)	(in)	(in)														
1.0	1.315	0.179	650	785	896	992	1078	1226	1353	780	893	989	1075	1152	1289	1408
1.5	1.900	0.200	930	1134	1302	1446	1575	1798	1990	1146	1312	1455	1582	1697	1901	2079
2.0	2.375	0.218	1161	1425	1642	1829	1994	2282	2531	1457	1669	1851	2014	2161	2422	2652
2.5	2.875	0.276	1507	1862	2152	2402	2624	3009	3343	1923	2203	2445	2661	2856	3204	3512
3.0	3.500	0.300	1833	2282	2647	2961	3240	3725	4146	2382	2731	3032	3301	3545	3981	4366
3.5	4.000	0.318	2092	2619	3046	3413	3739	4307	4799	2756	3160	3510	3822	4106	4613	5063
4.0	4.500	0.337	2358	2967	3459	3882	4257	4911	5479	3144	3606	4006	4364	4690	5272	5789
5.0	5.563	0.375	2912	3700	4335	4879	5362	6204	6937	3974	4560	5069	5525	5941	6687	7352
6.0	6.625	0.432	3547	4548	5350	6037	6647	7711	8638	4940	5672	6309	6880	7401	8339	9178
8.0	8.625	0.500	4556	5931	7028	7965	8797	10 252	11 526	6561	7541	8396	9166	9871	11 145	12 293

Copyright © 2010 IEEE. All rights reserved.

Copyright The Institute of Electrical and Electronics Engineers, Inc.
Provided by IHS under license with IEEE
No reproduction or networking permitted without license from IHS

Order Number: 02120914
Sold to:EGAT [700166108393] - VARRIS.Y@EGAT.CO.TH,
Not for Resale,2016-09-15 03:57:47 UTC

Table B.6 —Single aluminum angle bus ac ampacity (55.0% conductivity)

	Emissivity = 0.20, with sun temperature rise above 40 °C ambient							Emissivity = 0.20, without sun temperature rise above 40 °C ambient						
Size (in)	**30**	**40**	**50**	**60**	**70**	**90**	**110**	**30**	**40**	**50**	**60**	**70**	**90**	**110**
3.250 by 3.250 by 0.250	1588	1857	2083	2279	2454	2757	3016	1734	1980	2191	2376	2542	2831	3081
4.000 by 4.000 by 0.250	1835	2153	2420	2652	2859	3217	3525	2022	2311	2557	2775	2970	3312	3608
4.000 by 4.000 by 0.375	2178	2557	2875	3153	3400	3831	4201	2401	2744	3039	3299	3533	3943	4300
4.500 by 4.500 by 0.375	2343	2757	3104	3408	3678	4150	4558	2597	2970	3291	3574	3829	4279	4670
5.000 by 5.000 by 0.375	2518	2969	3347	3677	3972	4488	4934	2806	3210	3557	3865	4143	4633	5061
	Emissivity = 0.50, with sun temperature rise above 40 °C ambient							**Emissivity = 0.50, without sun temperature rise above 40 °C ambient**						
Size (in)	**30**	**40**	**50**	**60**	**70**	**90**	**110**	**30**	**40**	**50**	**60**	**70**	**90**	**110**
3.250 by 3.250 by 0.250	1550	1889	2169	2412	2628	3007	3336	1902	2180	2420	2634	2828	3174	3481
4.000 by 4.000 by 0.250	1786	2194	2530	2821	3080	3535	3931	2236	2564	2848	3102	3334	3747	4114
4.000 by 4.000 by 0.375	2120	2606	3007	3354	3664	4208	4685	2654	3045	3385	3688	3965	4461	4904
4.500 by 4.500 by 0.375	2277	2813	3254	3637	3979	4580	5108	2885	3312	3683	4016	4320	4866	5356
5.000 by 5.000 by 0.375	2443	3032	3516	3936	4311	4973	5555	3130	3595	4000	4363	4696	5295	5833

Table B.7 —Double aluminium angle bus ac ampacity (55.0% conductivity)

	Emissivity = 0.20, with sun temperature rise above 40 °C ambient							Emissivity = 0.20, without sun temperature rise above 40 °C ambient						
Size (in)	**30**	**40**	**50**	**60**	**70**	**90**	**110**	**30**	**40**	**50**	**60**	**70**	**90**	**110**
3.250 by 3.250 by 0.250	2875	3370	3794	4166	4501	5086	5590	3045	3513	3917	4276	4600	5170	5663
4.000 by 4.000 by 0.250	3361	3949	4451	4892	5289	5984	6583	3579	4131	4608	5032	5415	6090	6675
4.000 by 4.000 by 0.375	3952	4646	5240	5764	6236	7065	7784	4208	4860	5426	5929	6385	7191	7893
4.500 by 4.500 by 0.375	4340	5109	5766	6346	6868	7786	8581	4636	5356	5980	6536	7040	7930	8707
5.000 by 5.000 by 0.375	4739	5585	6307	6945	7519	8528	9403	5077	5866	6552	7162	7715	8693	9546
	Emissivity = 0.50, with sun temperature rise above 40 °C ambient							**Emissivity = 0.50, without sun temperature rise above 40 °C ambient**						
Size (in)	**30**	**40**	**50**	**60**	**70**	**90**	**110**	**30**	**40**	**50**	**60**	**70**	**90**	**110**
3.250 by 3.250 by 0.250	2832	3407	3893	4318	4700	5370	5953	3247	3749	4187	4578	4933	5566	6122
4.000 by 4.000 by 0.250	3306	3996	4577	5086	5542	6345	7044	3835	4432	4952	5416	5839	6593	7258
4.000 by 4.000 by 0.375	3887	4702	5389	5992	6535	7492	8329	4510	5215	5830	6382	6885	7785	8582
4.500 by 4.500 by 0.375	4265	5173	5938	6609	7213	8277	9209	4983	5764	6446	7057	7615	8614	9499
5.000 by 5.000 by 0.375	4653	5658	6503	7245	7911	9087	10 117	5472	6331	7081	7755	8369	9470	10 447

Copyright © 2010 IEEE. All rights reserved.

Copyright The Institute of Electrical and Electronics Engineers, Inc.
Provided by IHS under license with IEEE
No reproduction or networking permitted without license from IHS

Order Number: 02120914
Sold to:EGAT [700166108393] - VARRIS.Y@EGAT.CO.TH,
Not for Resale,2016-09-15 03:57:47 UTC

Table B.8 —Aluminium integral web channel bus ac ampacity (55.0% conductivity)

	Emissivity = 0.20, with sun temperature rise above 40 °C ambient							Emissivity = 0.20, without sun temperature rise above 40 °C ambient						
Size	**30**	**40**	**50**	**60**	**70**	**90**	**110**	**30**	**40**	**50**	**60**	**70**	**90**	**110**
(in)														
4.000 by 4.000 by 0.250	2395	2948	3404	3799	4150	4761	5286	2949	3402	3795	4144	4461	5022	551
4.000 by 4.000 by 0.312	2603	3206	3703	4134	4517	5183	5757	3213	3706	4133	4514	4860	5472	600
6.000 by 4.000 by 0.375	3391	4168	4812	5370	5867	6734	7483	4161	4800	5356	5851	6301	7099	779
6.000 by 5.000 by 0.375	3558	4420	5129	5743	6289	7241	8062	4483	5175	5778	6316	6805	7674	843
6.000 by 6.000 by 0.550	4287	5335	6200	6950	7621	8795	9816	5412	6254	6990	7649	8250	9325	1027
8.000 by 5.000 by 0.500	4617	5695	6588	7365	8058	9272	10 326	5699	6582	7351	8039	8666	9783	1077
8.000 by 8.000 by 0.500	5849	7228	8375	9374	10 271	11 846	13 223	7212	8345	9335	10 224	11 036	12 491	1378
12.00 by 12.00 by 0.625	8610	10 614	12 296	13 774	15 108	17 477	19 574	10 466	12 138	13 608	14 936	16 156	18 361	2034
	Emissivity = 0.50, with sun temperature rise above 40 °C ambient							**Emissivity = 0.50, without sun temperature rise above 40 °C ambient**						
Size	**30**	**40**	**50**	**60**	**70**	**90**	**110**	**30**	**40**	**50**	**60**	**70**	**90**	**110**
(in)														
4.000 by 4.000 by 0.250	2463	3102	3627	4081	4486	5198	5819	3208	3707	4143	4535	4894	5538	611
4.000 by 4.000 by 0.312	2677	3376	3948	4444	4887	5665	6345	3497	4041	4517	4944	5336	6039	666
6.000 by 4.000 by 0.375	3572	4470	5211	5856	6434	7453	8349	4568	5280	5905	6467	6982	7911	874
6.000 by 5.000 by 0.375	3718	4722	5544	6256	6893	8014	8999	4929	5701	6379	6990	7551	8563	947
6.000 by 6.000 by 0.550	4403	5646	6661	7540	8329	9722	10 954	5963	6904	7733	8483	9174	10 428	1156
8.000 by 5.000 by 0.500	4886	6145	7185	8091	8906	10 347	11 622	6308	7300	8172	8960	9685	10 999	1218
8.000 by 8.000 by 0.500	5922	7594	8963	10 152	11 219	13 110	14 786	7990	9262	10 384	11 400	12 338	14 044	1559
12.00 by 12.00 by 0.625	8584	11 093	13 153	14 949	16 570	19 463	22 058	11 724	13 621	15 304	16 839	18 264	20 878	2327

Copyright © 2010 IEEE. All rights reserved.

Copyright The Institute of Electrical and Electronics Engineers, Inc.
Provided by IHS under license with IEEE
No reproduction or networking permitted without license from IHS

Order Number: 02120914
Sold to:EGAT [700166108393] - VARRIS.Y@EGAT.CO.TH,
Not for Resale,2016-09-15 03:57:47 UTC

Table B.9 —Single copper rectangular bar ac ampacity, with sun (99.0% conductivity)

	Emissivity = 0.35 temperature rise above 40 °C ambient							Emissivity = 0.85 temperature rise above 40 °C ambient						
Size (in)	**30**	**40**	**50**	**60**	**70**	**90**	**110**	**30**	**40**	**50**	**60**	**70**	**90**	**110**
0.250 by 4.000	1516	1751	1951	2127	2286	2564	2806	1661	1948	2194	2412	2611	2965	3281
0.250 by 5.000	1764	2040	2276	2484	2671	3002	3291	1955	2296	2589	2850	3088	3515	3898
0.250 by 6.000	2010	2327	2599	2838	3054	3437	3773	2250	2646	2987	3290	3568	4067	4517
0.375 by 4.000	1824	2112	2356	2572	2766	3107	3405	1985	2337	2638	2906	3149	3584	3973
0.375 by 5.000	2122	2458	2746	3000	3229	3633	3988	2337	2754	3112	3430	3721	4243	4712
0.375 by 6.000	2407	2792	3121	3412	3675	4141	4552	2679	3159	3573	3942	4279	4887	5436
0.375 by 8.000	2934	3409	3816	4178	4505	5089	5608	3319	3922	4442	4908	5335	6109	6813
0.500 by 4.000	2083	2415	2699	2948	3173	3569	3915	2253	2662	3011	3321	3603	4108	4560
0.500 by 5.000	2404	2790	3120	3412	3675	4141	4551	2633	3113	3524	3890	4224	4826	5367
0.500 by 6.000	2717	3156	3532	3865	4166	4701	5174	3007	3558	4031	4453	4839	5536	6167
0.500 by 8.000	3312	3853	4317	4730	5105	5774	6369	3729	4417	5011	5542	6030	6916	7723
0.625 by 4.000	2253	2617	2928	3203	3451	3889	4274	2423	2873	3258	3599	3911	4469	4971
0.625 by 5.000	2619	3045	3409	3731	4023	4540	4996	2854	3384	3840	4245	4615	5282	5885
0.625 by 6.000	2951	3433	3847	4213	4546	5137	5662	3251	3857	4378	4843	5269	6040	6739
0.625 by 8.000	3598	4192	4702	5156	5568	6306	6966	4034	4791	5443	6028	6565	7541	8433
0.625 by 10.000	4179	4875	5474	6009	6496	7372	8158	4752	5648	6424	7121	7763	8936	10 012
0.625 by 12.000	4758	5555	6244	6860	7422	8435	9348	5474	6511	7411	8222	8970	10 339	11 601
0.750 by 4.000	2455	2857	3199	3502	3775	4258	4683	2626	3125	3550	3928	4271	4888	5443
0.750 by 5.000	2834	3300	3699	4051	4370	4937	5438	3073	3656	4155	4599	5005	5737	6398
0.750 by 6.000	3204	3732	4185	4587	4951	5600	6177	3513	4179	4752	5262	5729	6575	7343
0.750 by 8.000	3881	4527	5082	5576	6026	6831	7551	4334	5159	5870	6507	7092	8157	9130
0.750 by 10.000	4509	5265	5917	6498	7029	7982	8840	5109	6085	6929	7687	8386	9662	10 835
0.750 by 12.000	5119	5983	6729	7396	8006	9107	10 100	5869	6995	7971	8850	9661	11 147	12 519

Copyright © 2010 IEEE. All rights reserved.

Copyright The Institute of Electrical and Electronics Engineers, Inc.
Provided by IHS under license with IEEE
No reproduction or networking permitted without license from IHS

Order Number: 02120914
Sold to:EGAT [700166108393] - VARRIS.Y@EGAT.CO.TH,
Not for Resale,2016-09-15 03:57:47 UTC

Table B.10—Single copper rectangular bar ac ampacity, without sun (99.0% conductivity)

	Emissivity = 0.35 temperature rise above 40 °C ambient							Emissivity = 0.85 temperature rise above 40 °C ambient						
Size (in)	**30**	**40**	**50**	**60**	**70**	**90**	**110**	**30**	**40**	**50**	**60**	**70**	**90**	**110**
0.250 by 4.000	1577	1802	1996	2168	2322	2595	2833	1793	2059	2290	2498	2688	3030	3337
0.250 by 5.000	1838	2102	2330	2533	2715	3039	3323	2114	2429	2705	2953	3180	3592	3965
0.250 by 6.000	2098	2401	2663	2896	3107	3481	3811	2436	2801	3121	3410	3675	4157	4595
0.375 by 4.000	1908	2182	2418	2627	2816	3150	3442	2167	2489	2770	3023	3254	3672	4049
0.375 by 5.000	2221	2542	2819	3065	3288	3683	4032	2550	2932	3266	3568	3844	4347	4802
0.375 by 6.000	2522	2889	3206	3488	3744	4199	4603	2924	3364	3751	4099	4421	5006	5539
0.375 by 8.000	3081	3532	3924	4274	4593	5164	5673	3628	4179	4665	5105	5513	6258	6941
0.500 by 4.000	2189	2505	2777	3018	3236	3623	3962	2485	2855	3179	3470	3737	4221	4658
0.500 by 5.000	2527	2894	3211	3493	3749	4204	4606	2900	3335	3717	4062	4379	4956	5480
0.500 by 6.000	2858	3275	3636	3958	4251	4773	5237	3310	3810	4250	4647	5014	5683	6294
0.500 by 8.000	3489	4002	4448	4847	5211	5863	6447	4103	4729	5281	5782	6246	7097	7879
0.625 by 4.000	2379	2724	3021	3286	3526	3953	4330	2700	3104	3458	3778	4071	4604	5088
0.625 by 5.000	2765	3168	3517	3828	4111	4615	5062	3171	3650	4069	4449	4799	5437	6019
0.625 by 6.000	3117	3573	3969	4323	4645	5222	5736	3607	4154	4636	5072	5475	6213	6889
0.625 by 8.000	3804	4365	4854	5291	5691	6411	7057	4469	5153	5757	6307	6816	7752	8615
0.625 by 10.000	4423	5081	5654	6169	6642	7496	8266	5262	6073	6792	7448	8057	9182	10 225
0.625 by 12.000	5042	5795	6454	7046	7591	8578	9473	6060	7000	7835	8597	9308	10 622	11 845
0.750 by 4.000	2605	2983	3310	3601	3865	4335	4750	2956	3400	3789	4139	4462	5049	5582
0.750 by 5.000	3006	3445	3825	4164	4473	5024	5515	3446	3967	4425	4839	5221	5918	6555
0.750 by 6.000	3397	3895	4328	4715	5067	5699	6263	3929	4526	5052	5529	5970	6778	7518
0.750 by 8.000	4117	4726	5256	5732	6167	6951	7655	4834	5575	6231	6827	7381	8399	9340
0.750 by 10.000	4787	5499	6122	6681	7195	8123	8963	5690	6569	7348	8059	8721	9944	11 078
0.750 by 12.000	5439	6253	6965	7607	8198	9269	10 242	6532	7547	8449	9273	10 043	11 468	12 795

Table B.11—Copper tubular bus—schedule 40 ac ampacity (99.0% conductivity)

Size		Wall	Emissivity = 0.35, with sun temperature rise above 40 °C ambient							Emissivity = 0.35, without sun temperature rise above 40°C ambient						
SPS	**OD**	**thickness**	**30**	**40**	**50**	**60**	**70**	**90**	**110**	**30**	**40**	**50**	**60**	**70**	**90**	**110**
(in)	**(in)**	**(in)**														
1.0	1.315	0.127	771	912	1029	1131	1220	1375	1506	878	1002	1107	1200	1283	1428	1552
1.5	1.900	0.150	1131	1347	1526	1681	1818	2054	2255	1313	1499	1658	1798	1923	2143	2332
2.0	2.375	0.157	1383	1656	1881	2075	2246	2543	2796	1628	1859	2056	2231	2387	2661	2899
2.5	2.875	0.188	1755	2111	2403	2655	2878	3264	3594	2091	2389	2644	2868	3071	3426	3734
3.0	3.500	0.219	2214	2675	3054	3380	3669	4169	4597	2673	3054	3381	3670	3930	4388	4787
4.0	4.500	0.250	2870	3492	4002	4441	4829	5502	6080	3530	4035	4470	4855	5202	5815	6350
6.0	6.625	0.250	3903	4807	5544	6177	6737	7708	8545	4955	5669	6285	6831	7324	8199	8968
8.0	8.625	0.313	5281	6570	7617	8514	9308	10 687	11 880	6871	7868	8728	9493	10 187	11 422	12 512
Size		**Wall**	**Emissivity = 0.85, with sun temperature rise above 40 °C ambient**							**Emissivity = 0.85, without sun temperature rise above 40 °C ambient**						
SPS	**OD**	**thickness**	**30**	**40**	**50**	**60**	**70**	**90**	**110**	**30**	**40**	**50**	**60**	**70**	**90**	**110**
(in)	**(in)**	**(in)**														
1.0	1.315	0.127	726	916	1069	1199	1315	1515	1688	978	1120	1243	1353	1452	1629	1786
1.5	1.900	0.150	1054	1354	1593	1797	1977	2289	2559	1482	1698	1886	2054	2206	2479	2722
2.0	2.375	0.157	1279	1665	1970	2230	2458	2855	3200	1851	2122	2358	2569	2762	3106	3414
2.5	2.875	0.188	1611	2123	2526	2867	3168	3689	4142	2394	2747	3054	3328	3579	4030	4433
3.0	3.500	0.219	2014	2692	3221	3668	4062	4745	5339	3083	3539	3936	4292	4618	5204	5729
4.0	4.500	0.250	2579	3517	4242	4852	5389	6321	7131	4112	4723	5256	5736	6175	6968	7682
6.0	6.625	0.250	3425	4848	5925	6827	7617	8988	10 182	5863	6741	7509	8201	8836	9988	11 031
8.0	8.625	0.313	4543	6632	8190	9488	10 624	12 596	14 315	8220	9459	10 545	11 527	12 431	14 075	15 569

--`,,,,,,`,```,,`,`,,`,-`-`,```,,,`---
Copyright © 2010 IEEE. All rights reserved.

Copyright The Institute of Electrical and Electronics Engineers, Inc.
Provided by IHS under license with IEEE
No reproduction or networking permitted without license from IHS

Order Number: 02120914
Sold to:EGAT [700166108393] - VARRIS.Y@EGAT.CO.TH,
Not for Resale,2016-09-15 03:57:47 UTC

Table B.12—Copper tubular bus—schedule 80 ac ampacity (99.0% conductivity)

Size		Wall	Emissivity = 0.35, with sun temperature rise above 40 °C ambient							Emissivity = 0.35, without sun temperature rise above 40 °C ambient						
SPS	OD	Thickness	30	40	50	60	70	90	110	30	40	50	60	70	90	110
(in)	(in)	(in)														
1.0	1.315	0.182	903	1069	1206	1325	1430	1611	1765	1029	1174	1297	1406	1503	1673	1818
1.5	1.900	0.203	1289	1536	1741	1917	2073	2343	2573	1498	1710	1891	2051	2194	2445	2661
2.0	2.375	0.221	1610	1928	2190	2416	2616	2962	3258	1895	2164	2395	2598	2780	3100	3377
2.5	2.875	0.280	2093	2517	2866	3168	3434	3896	4292	2493	2848	3153	3422	3664	4089	4459
3.0	3.500	0.304	2536	3065	3501	3876	4209	4785	5279	3062	3500	3876	4209	4508	5036	5497
4.0	4.500	0.341	3256	3963	4543	5043	5486	6255	6917	4004	4580	5075	5513	5910	6610	7224
6.0	6.625	0.437	4789	5906	6820	7606	8306	9525	10 584	6081	6965	7730	8411	9030	10 132	11 108
8.0	8.625	0.500	6076	7571	8790	9841	10 776	12 412	13 842	7906	9066	10 073	10 973	11 794	13 265	14 579
Size		Wall	Emissivity = 0.85, with sun temperature rise above 40 °C ambient							Emissivity = 0.85, without sun temperature rise above 40 °C ambient						
SPS	OD	Thickness	30	40	50	60	70	90	110	30	40	50	60	70	90	110
(in)	(in)	(in)														
1.0	1.315	0.182	851	1073	1252	1405	1540	1775	1978	1146	1313	1457	1585	1701	1909	2092
1.5	1.900	0.203	1202	1544	1817	2050	2255	2612	2920	1690	1937	2151	2343	2517	2829	3106
2.0	2.375	0.221	1489	1938	2294	2597	2863	3326	3728	2155	2471	2746	2992	3216	3619	3978
2.5	2.875	0.280	1921	2532	3013	3420	3780	4404	4946	2855	3276	3642	3971	4271	4810	5293
3.0	3.500	0.304	2308	3086	3693	4207	4659	5446	6130	3532	4056	4512	4922	5296	5972	6579
4.0	4.500	0.341	2926	3992	4816	5511	6122	7186	8113	4664	5360	5967	6513	7015	7921	8739
6.0	6.625	0.437	4203	5956	7288	8407	9391	11 107	12 612	7195	8282	9236	10 099	10 894	12 343	13 664
8.0	8.625	0.500	5277	7642	9452	10 967	12 300	14 629	16 679	9457	10 899	12 170	13 324	14 391	16 346	18 140

Table B.13—Double copper channel bus ac ampacity (99% conductivity)

	Emissivity = 0.35, with sun temperature rise above 40 °C ambient							Emissivity = 0.35, without sun temperature rise above 40 °C ambient						
Size (in)	30	40	50	60	70	90	110	30	40	50	60	70	90	110
3.000 by 1.313 by 0.216	2785	3347	3819	4232	4601	5246	5801	3178	3671	4098	4478	4822	5430	5961
4.000 by 1.750 by 0.240	3697	4470	5118	5684	6190	7075	7841	4283	4951	5531	6048	6517	7348	8076
4.000 by 1.750 by 0.338	4106	4969	5695	6331	6902	7906	8780	4757	5504	6155	6737	7267	8212	9044
5.000 by 2.188 by 0.338	4967	6040	6942	7731	8440	9686	10 772	5827	6746	7548	8266	8920	10 087	11 117
6.000 by 2.688 by 0.384	5932	7235	8332	9293	10 159	11 686	13 025	6995	8107	9079	9953	10 751	12 182	13 453
	Emissivity = 0.85, with sun temperature rise above 40 °C ambient							Emissivity = 0.85, without sun temperature rise above 40 °C ambient						
Size (in)	30	40	50	60	70	90	110	30	40	50	60	70	90	110
3.000 by 1.313 by 0.216	2733	3430	4003	4499	4941	5718	6395	3504	4053	4533	4963	5356	6061	6689
4.000 by 1.750 by 0.240	3619	4593	5390	6078	6693	7772	8714	4764	5514	6171	6762	7303	8276	9145
4.000 by 1.750 by 0.338	4019	5106	5998	6771	7464	8685	9759	5290	6129	6867	7532	8143	9248	10 241
5.000 by 2.188 by 0.338	4851	6222	7341	8310	9177	10 706	12 052	6526	7565	8480	9306	10 065	11 440	12 680
6.000 by 2.688 by 0.384	5770	7460	8836	10 029	11 099	12 990	14 663	7888	9154	10 271	11 283	12 217	13 915	15 455

Copyright © 2010 IEEE. All rights reserved.

Copyright The Institute of Electrical and Electronics Engineers, Inc.
Provided by IHS under license with IEEE
No reproduction or networking permitted without license from IHS

Order Number: 02120914
Sold to:EGAT [700166108393] - VARRIS.Y@EGAT.CO.TH,
Not for Resale,2016-09-15 03:57:47 UTC

Annex C

(informative)

Thermal considerations for outdoor bus-conductor design

C.1 Abstract

The current rating of both the outdoor rigid bus conductor and the strain bus conductor is based on several limiting criteria. This annex brings to a single source the thermal considerations of both the rigid bus and the strain conductor, namely, the heat transfer and properties of material. Historically, thermal designs have been conservative. This annex will allow the engineer to reexamine the factors involved in increased current loadings of the rigid bus and strain bus conductor and possibly to determine new thermal limits.

The material in this annex is mostly from the paper, "Thermal considerations for outdoor bus-conductor design," by the Substation Committee of the IEEE Power Engineering Society.[37] However, some equations have been corrected and/or updated, and relevant additional material has also been added.

NOTE—The English units used in the original paper have been converted to the SI system in this annex.

C.2 Introduction

Thermal considerations entering into the design of bus conductors for outdoor substations fall into two general categories, heat transfer and properties of materials. Each of these subjects will be considered in detail in this annex. The first, heat transfer to and from the conductor, is relatively independent of the material and is mainly a function of the geometry of the conductor, proximity to other surfaces or conductors, atmospheric conditions, and geographic location. The most important element in the computation is the estimate of forced convection arising from wind currents. A method is given here to compute heat losses due to forced and natural convection and radiation and heat gained from the sun. Using the formulas provided, it is possible to calculate the current-carrying capacity of any conductor corresponding to a given temperature rise. Examples are provided showing methods for calculating the ampacity of conventional types of bus conductors (e.g., bar, tube, channel, angle, and integral web).

The second subject, properties of materials, includes the effects of temperature and outdoor exposure on the mechanical strength, electrical resistivity, dimensional stability, and surface condition of the conductor. Aluminum alloys, copper, and copper alloys are included in the discussion and tabulations. No attempt has been made to consider the relative merits of the conductors. Instead, technical information is provided that must be coupled with economic factors when optimizing design and selecting materials.

[37]Published by *IEEE Transaction on Power Apparatus and Systems*, vol. PAS-95, no. 4, July/Aug. 1976. Paper F 76 205-5. Recommended and approved by the IEEE Substations Committee of the IEEE Power Engineering Society for presentation at the IEEE PES Winter Meeting & Tesla Symposium, New York, NY, January 25–30, 1976. Manuscript submitted October 31, 1975; made available for printing November 24, 1975.

Copyright © 2010 IEEE. All rights reserved.

Copyright The Institute of Electrical and Electronics Engineers, Inc.
Provided by IHS under license with IEEE
No reproduction or networking permitted without license from IHS

Order Number: 02120914
Sold to:EGAT [700166108393] - VARRIS.Y@EGAT.CO.TH,
Not for Resale,2016-09-15 03:57:47 UTC

C.3 Heat transfer

Usually more than half the heat generated by resistance losses in a bus conductor is removed from the surface by convection of the surrounding air. The remainder is given off by radiation from external surfaces. Unfortunately, it is not at all convenient to run controlled outdoor tests to determine the appropriate heat transfer coefficients. As a result, there is very little independent support for the formulas found in the literature.

A variety of formulas can be found for the sizes of conductors of interest. All show that convective heat transfer outdoors exceeds that in the indoors when it is assumed that the wind velocity is 0.6 m/s (2 ft/s). However, the difference between the indoor and outdoor rating is often not very great. If a slower wind velocity is assumed, then the outdoor heat losses may be calculated as lower than those indoors. This is not plausible. It is, therefore, concluded that assumption of a 0.6 m/s wind is a conservative, yet realistic, approach, and it will be used in the examples given herein.

The difference between indoor and outdoor convection losses are found to diminish with increasing conductor size and with increasing temperature rise. This is because an increase in the temperature rise leads to natural drafts, which can be as effective as a slight breeze in promoting heat transfer. Similarly, with large conductors, the assumed 0.6 m/s wind speed is so low as to add very little benefit over natural convection.

For the purpose of calculating ampacity, conditions that are the least advantageous for convection must be considered. Thus, it is assumed that there is only a 0.6 m/s wind. (See NOTE 1 following the references of this annex.) It is to be expected that when the flow is at an angle or normal to the surface, heat transfer will increase. Likewise, it is wise to stipulate that the emissivity is a low value when there is no solar heating. This will provide the most conservative ampacity rating. In contrast, when there can be considerable solar heating, a high value of emissivity essentially equal to solar absorptivity may give the most conservative ampacity rating.

In connection with this last point, it should be noted that solar heating of the conductor always diminishes ampacity and can result in outdoor current ratings that are lower than indoor ratings. This is less likely on smaller conductors for which forced (outdoor) convective heat transfer coefficients are relatively high. However, for large conductors with high absorptivity, the heat gain from solar radiation can exceed the improvement in convective heat transfer due to the wind effect, and ratings are reduced accordingly.

C.3.1 Assumptions

Some assumptions will be made about the properties of air in order to reduce the number of terms that should be carried through the computations. These approximations will have a negligible effect on the accuracy of the calculated ampacity. First, it is assumed that the properties of air are constant and may be evaluated at mid-range temperatures. This is reasonable because variations in heat capacity, conductivity, density, and viscosity of air tend to compensate for one another and have very little net effect on heat transfer over the temperature range of interest. For example, the Prandtl number of air:

$$\mathrm{Pr} = C_{pa}\frac{\mu_a}{k_a}$$

is commonly taken as 0.7 over a wide range of ordinary temperatures and pressures using the properties for air at 60 °C as follows:

$C_{\rho a}$ is the heat capacity of air = 1006 J/(kg °C)
μ_a is the dynamic viscosity of air = 2.04×10^{-5} kg/(m s)
k_a is the thermal conductivity of air = 0.0288 W/(m °C)

Copyright © 2010 IEEE. All rights reserved.

Copyright The Institute of Electrical and Electronics Engineers, Inc.
Provided by IHS under license with IEEE
No reproduction or networking permitted without license from IHS

Order Number: 02120914
Sold to:EGAT [700166108393] - VARRIS.Y@EGAT.CO.TH,
Not for Resale,2016-09-15 03:57:47 UTC

ρ_a is the density of air = 1.08 kg/m^3
$v_a = \mu_a/\rho_a$ is the kinematic viscosity of air = 18.9 × 10^{-6} m^2/s

As a result, only the temperature difference between the conductor and the surrounding air is important in calculating convective heat losses. For example, the convection losses calculated for a 40 °C temperature rise apply equally for a 70 °C conductor in 30 °C air or an 85 °C conductor in 45 °C air.

One might expect that the ampacities in the above instances would be different because the resistivities at 70 °C and 85 °C are different. However, it will be seen that the radiation losses that increase with the absolute temperature rather than the temperature difference tend to offset the rise in resistivities. As a result, ampacities based on the 40 °C ambient apply quite well to ambients from about 20 °C to 50 °C. Thus, for any temperature rise, there is a single ampacity (irrespective of the ambient), and it is usually not necessary to calculate a different ampacity for each ambient temperature and temperature rise.

C.3.2 Computation method

The general approach suggested for calculating the ampacity of any outdoor bus conductor is summarized below. A detailed explanation of each item follows.

Step by step, the procedure is as follows:

a) Identify all exterior surfaces that should be treated as flat planes subject to forced convection.

b) Identify any exterior surfaces that should be treated as cylindrical surfaces subject to forced convection.

c) Identify any surfaces that may be shielded from the wind and only lose heat via natural convection (the same as indoors).

d) Identify surfaces that will lose heat also by radiation.

e) Ascertain the orientation and location of the conductors in determining the projected area exposed to solar heat gain.

f) For each of the appropriate areas [items a), b), and c)], compute the total convective heat losses q_c.

g) For the appropriate values of emittance and area [item c)], compute the total heat lost through radiation, q_r.

h) Consider the projected area, latitude, altitude, seasonal factors, absorptivity, and so on, and compute the solar heat gain, q_s.

i) Sum the heat gain and loss terms, and for the appropriately temperature compensated values of resistance (R) and skin effect coefficient (F), compute ampacity using using Equation (C.1):

$$I = \sqrt{\frac{q_c + q_r - qs}{R\,F}} \tag{C.1}$$

where

I is the current for the allowable temperature rise, A
q_c is the convective heat loss, W/m
q_r is the radiation loss, W/m
q_s is the solar heat gain, W/m

Copyright © 2010 IEEE. All rights reserved.

Copyright The Institute of Electrical and Electronics Engineers, Inc.
Provided by IHS under license with IEEE
No reproduction or networking permitted without license from IHS

Order Number: 02120914
Sold to:EGAT [700166108393] - VARRIS.Y@EGAT.CO.TH,
Not for Resale,2016-09-15 03:57:47 UTC

R is the direct current resistance at the operating temperature, Ω/m
F is the skin effect coefficient for 60 H current

The following is an analysis of each operation. It will show that the basic equations can be reduced to easy-to-handle forms.

C.3.2.1 Forced convection over flat surfaces

When air flows parallel to and over a flat planar surface, Equation (C.2) may be used to calculate the heat transfer coefficient:

$$h = 0.664 \frac{k_a}{L} \mathrm{Re}^{1/2} \mathrm{Pr}^{1/3} \quad \text{(C.2)}$$

where

h is the heat transfer coefficient, W/(m^2 °C)
k_a is the thermal conductivity of air, W/(m^2 °C)
L is the length of flow path over conductor (normally the width or thickness), m
Re is the Reynolds number, equal to $\frac{L\,V}{\nu_a}$
V is the air velocity, m/s

The total heat lost (in W/m) from the surface due to forced convection is given by Equation (C.3):

$$q_c = h\ A\,\Delta T \quad \text{(C.3)}$$

where

q_c are the convection losses, W/m
A is the area of flat surfaces, m^2/linear m of conductor
ΔT is the temperature difference between the surface of the conductor (T_c) and the surrounding air (T_a), °C

At elevations above sea level multiply q_c by $P^{0.5}$ where P is the air pressure in atmospheres. This will reduce the convective coefficient for lower pressures.

For the properties of air noted earlier in C.3.1, q_c is given, using the variables defined above, by Equation (C.4):

$$q_c = 3.906 \times \sqrt{\frac{V}{L}}\ A\ \Delta T \quad \text{(C.4)}$$

Copyright © 2010 IEEE. All rights reserved.
Copyright The Institute of Electrical and Electronics Engineers, Inc.
Provided by IHS under license with IEEE
No reproduction or networking permitted without license from IHS
Order Number: 02120914
Sold to:EGAT [700166108393] - VARRIS.Y@EGAT.CO.TH,
Not for Resale,2016-09-15 03:57:47 UTC

For $V = 0.6$ m/s, q_c is given by Equation (C.5):

$$q_c = 3.05 \times \sqrt{\frac{1}{L}}\ A\ \Delta T \tag{C.5}$$

This simplified formula applies to air flow parallel to the surface. Outdoor air flow is seldom unidirectional and cannot always be parallel to the surface. However, it is assumed that air circulating around the conductor will be in more turbulent flow and provide a greater heat transfer on average than would be calculated using the above equation.

The convective loss formula above should be applied to each flat surface of the conductor.

Example

Consider a rectangular conductor 0.1524 m × 0.0127 m (6 in × ½ in) operating at 100 °C in a 40 °C ambient.

For the 0.1524 m faces, A = 2 × □0.1524 = 0.3048 m^2/m, $\Delta T = 100 - 40 = 60$ °C, $L = 0.1524$ m.

Then

$$q_{c6} = 3.05 \times \sqrt{\frac{1}{0.1524}} \times 0.3048 \times 60 = 142.9\ \text{W/m}$$

For the 0.0127 m edges, $A = 2 \times (0.0127) \times = 0.0254$ m^2/m.

Then

$$q_{c(1/2)} = 3.05 \times \sqrt{\frac{1}{0.0127}} \times 0.0254 \times 60 = 41.2\ \text{W/m}$$

Then the total convective losses are given by

$$q_C = q_{c6} + q_{c(1/2)} = 184.1\ \text{W/m}$$

Note that for a 0.1524 m square tube, the convective heat loss would have been twice q_{c6} calculated above or 285.8 W/m. The heat loss per unit area q_c/A is 285.8/0.6096 or 469 W/m^2. It will be interesting to compare this value with that calculated for a 0.1524 m cylindrical pipe by a different method in C.3.2.2.

C.3.2.2 Forced convection over cylindrical surfaces

From the McAdams [3] text or Perry's Handbook [2], heat transfer for a cylindrical shape at least 0.0254 m (1 in) in diameter may be estimated by Equation (C.6) when there is a 0.6 m/s wind and 1 atmosphere pressure:

$$q_c = 3.561 \times D^{-0.4} \times A\ \Delta T \tag{C.6}$$

Copyright © 2010 IEEE. All rights reserved.

Copyright The Institute of Electrical and Electronics Engineers, Inc.
Provided by IHS under license with IEEE
No reproduction or networking permitted without license from IHS

Order Number: 02120914
Sold to:EGAT [700166108393] - VARRIS.Y@EGAT.CO.TH,
Not for Resale,2016-09-15 03:57:47 UTC

where

D is the diameter of the cylinder, m
A is the surface area by unit length, m^2/m
ΔT is the temperature difference between the surface of the conductor (T_c) and surrounding air (T_a), °C

Example

For a hypothetical pipe with an OD of 0.1524 m and ΔT = 60 °C, we have $A = 0.1524 \cdot \pi = 0.4788$ m^2/m. Using Equation (C.6) we obtain:

$$q_c = 3.561 \times 0.1524^{-0.4} \times 0.4788 \times 60 = 217.1 \text{ W/m}$$

The heat transfer per unit area is q_c/A = 453 W/m^2. This value is virtually identical to that calculated for the square tube of the same major dimension and may be taken as an indication of the credibility of both methods.

It is of interest to make the comparison between square tubes and pipes for conductors of other sizes.

	q_c/A (W/m^2)	
Major dimension (d or L) M	**Square tube [Equation (C.5)]**	**Pipe [Equation (C.6)]**
0.0762 (3 in)	667	598
0.1524 (6 in)	469	453
0.2286 (9 in)	385	386

It is seen that for the larger bus conductors, the heat transfer efficiency of the pipe is about the same as that of the square tube. In fact they are identical at about 0.2286 m. Note that the heat transfer efficiency decreases with the increasing size of the conductor.

To evaluate the current rating of a conductor at a wind speed other than 0.6 m/s and to account for both air density and viscosity, Equation (C.7) should be used:

$$q_c = \frac{k_a}{L}\left[0.3 + \frac{0.62\,\mathrm{Re}^{1/2}\,\mathrm{Pr}^{1/3}}{\left[1+\left(\frac{0.4}{\mathrm{Pr}}\right)^{2/3}\right]^{1/4}}\left[1+\left(\frac{\mathrm{Re}}{282\,000}\right)^{5/8}\right]^{4/5}\right] A\,\Delta T \qquad \text{(C.7)}$$

where

k_a is the thermal conductivity of air, W/(m °C)
L is the length of the flow path over the conductor (normally the width or thickness), m
Re is the Reynolds number, equal to $\frac{L\,V}{\nu_a}$

Copyright © 2010 IEEE. All rights reserved.

Copyright The Institute of Electrical and Electronics Engineers, Inc.
Provided by IHS under license with IEEE
No reproduction or networking permitted without license from IHS

Order Number: 02120914
Sold to:EGAT [700166108393] - VARRIS.Y@EGAT.CO.TH,
Not for Resale,2016-09-15 03:57:47 UTC

Pr is the Prandtl number of air = 0.7
V is the air velocity, m/s
A is the surface area by unit length, m^2/m
ΔT is the temperature difference between the surface of the conductor (T_c) and the surrounding air (T_a), °C

ρ_a, μ_a, and k_a are given in Table C.1 extracted from IEEE Std 738-2006 at T_{film}, which is given by Equation (C.8):

$$T_{film} = \frac{T_c + T_a}{2} \quad (C.8)$$

where

T_c is the surface temperature of the conductor, °C
T_a is the ambient air temperature, °C

Table C.1—Viscosity, density, and thermal conductivity of air

T_{film} (°C)	Dynamic viscosity of air [kg/(m s)]	Air density ρ_a (kg/m^3)				Thermal conductivity of air [W/(m °C)]
	μ_a	Sea level	1524 m (5000 ft)	3048 m (10 000 ft)	4572 m (15 000 ft)	k_a
0	17.19	1.2954	1.0771	0.8893	0.7304	0.0242
5	17.44	1.2729	1.0594	0.8748	0.7175	0.0246
10	17.69	1.2505	1.0402	0.8588	0.7047	0.0250
15	17.94	1.2280	1.0209	0.8443	0.6918	0.0254
20	18.19	1.2071	1.0049	0.8299	0.6806	0.0257
25	18.39	1.1879	0.9888	0.8154	0.6694	0.0261
30	18.64	1.1686	0.9728	0.8026	0.6597	0.0265
35	18.89	1.1493	0.9567	0.7898	0.6485	0.0268
40	19.10	1.1301	0.9407	0.7769	0.6373	0.0272
45	19.35	1.1124	0.9262	0.7641	0.6276	0.0276
50	19.59	1.0964	0.9118	0.7528	0.6180	0.0280
55	19.80	1.0787	0.8973	0.7416	0.6084	0.0283
60	20.05	1.0610	0.8829	0.7288	0.5987	0.0287
65	20.26	1.0466	0.8700	0.7191	0.5891	0.0291
70	20.46	1.0322	0.8588	0.7095	0.5827	0.0295
75	20.71	1.0177	0.8459	0.6999	0.5747	0.0298
80	20.92	1.0065	0.8379	0.6918	0.5682	0.0302
85	21.13	0.9888	0.8235	0.6790	0.5570	0.0306
90	21.33	0.9760	0.8122	0.6710	0.5506	0.0309
95	21.58	0.9615	0.7994	0.6613	0.5426	0.0312
100	21.79	0.9487	0.7898	0.6517	0.5345	0.0317

C.3.2.3 Natural convection for flat and cylindrical surfaces

Some surfaces on conductors or in arrays of conductors may be shielded from direct exposure to wind. Assuming that there is nevertheless sufficient space for natural convection to occur, such surfaces may be treated as though convective losses outdoors would be the same as natural convective losses indoors. For such shielded surfaces, heat losses are calculated using generally accepted equations for natural convection.

Copyright © 2010 IEEE. All rights reserved.
Copyright The Institute of Electrical and Electronics Engineers, Inc.
Provided by IHS under license with IEEE
No reproduction or networking permitted without license from IHS
Order Number: 02120914
Sold to:EGAT [700166108393] - VARRIS.Y@EGAT.CO.TH,
Not for Resale,2016-09-15 03:57:47 UTC

Examples of areas requiring such treatment are the spaces between double angles, double channels, or parallel rectangular conductors. The use of the natural convection equations is probably justified when the space between conductors is greater than 20% of the major dimension of the conductor or 0.0254 m (1 in), whichever is smaller. This estimate of the permissible spacing is based on the fact that the boundary layer for mass transfer is, very roughly, 10% of the length of the flow path. When the spacing between conductors is greater than the major dimension of the conductor, then the forced convection formulas given above may apply.

Because of the restricted flow away from the interior surfaces of integral web conductors, it is suggested that the natural convection loss formulas given here for surfaces facing down be applied to all interior surfaces.

The appropriate natural convection formulas are as follows:

Vertical surfaces, vertical cylinders, and upward facing horizontal surfaces—Equation (C.9):

$$q_c = 1.38\ \Delta T^{1.25}\ L^{-0.25}\ A \tag{C.9}$$

Downward facing horizontal surfaces—Equation (C.10):

$$q_c = 0.69\ \Delta T^{1.25}\ L^{-0.25}\ A \tag{C.10}$$

where

ΔT is the temperature difference between the surface of the conductor (T_c) and the surrounding air (T_a), °C
L is the length of conductor surface (width or thickness), m
A is the conductor surface area by unit length of conductor, m^2/m
q_c is the conductive heat loss, W/linear m

Example

For 0.0762 m (3 in), 0.1524 m (6 in), and 0.2286 m (9 in) wide vertical surfaces at a 60 °C temperature difference:

For 0.0762 m:

$$q_C / A = \frac{1.38 \times (60)^{1.25}}{0.0762^{0.25}} = 439\ \text{W/m}^2$$

For 0.1524 m:

$$q_C / A = 370\ \text{W/m}^2$$

For 0.02286 m:

$$q_c / A = 334\ \text{W/m}^2$$

Copyright © 2010 IEEE. All rights reserved.
Copyright The Institute of Electrical and Electronics Engineers, Inc.
Provided by IHS under license with IEEE
No reproduction or networking permitted without license from IHS
Order Number: 02120914
Sold to:EGAT [700166108393] - VARRIS.Y@EGAT.CO.TH,
Not for Resale,2016-09-15 03:57:47 UTC

When surfaces face downward, the heat transfer per unit area is only half the value calculated in the above example.

Example

Considering some other temperature differences, we get the following comparison between forced convection and natural convection.

For a 0.1524 m flat conductor:

	q_c/A (W/m^2)		
	ΔT = 80 °C	**ΔT = 60 °C**	**ΔT = 40 °C**
Forced convection (outdoor)	629	472	315
Natural convection (indoor or confined spaces)	530	370	223
Indoor/outdoor	0.843	0.784	0.708

Thus, for large conductors and large temperature rises, the calculated benefit of the 0.6 m/s wind of heat transfer outdoors over natural convection on favorably oriented surfaces indoors is only 10% to 20%. The effect on ampacity will be even less and may be as low as only 2% or 3% for large conductors and high temperatures.

With zero wind speed, IEEE Std 738-2006 gives Equation (C.11) for calculating natural convection for a **horizontal cylinder**:

$$q_c = 4.0\ \rho_a^{0.5}\ D^{0.75}\ \Delta T^{1.25} \tag{C.11}$$

where

ρ_a is the density of air, kg/m^3
D is the conductor diameter, m
ΔT is the temperature difference between the surface of the conductor (T_c) and the surrounding air (T_a), °C

C.3.2.4 Determinig maximum heat convection

The heat convection is calculated using Equation (C.9) through Equation (C.11), according to the shape and geometry. The maximum value of these three values should be used to calculate the conductor rating. The maximum heat convection should be multiplied by the wind direction factor K_{angle}, which is calculated by Equation (C.12):

$$K_{\text{angle}} = 1.194 - \cos(\Phi) + 0.194\cos(2\Phi) + 0.368\sin(2\Phi) \tag{C.12}$$

where

Φ is the angle of wind direction and the conductor axis

Copyright © 2010 IEEE. All rights reserved.
Copyright The Institute of Electrical and Electronics Engineers, Inc.
Provided by IHS under license with IEEE
No reproduction or networking permitted without license from IHS
Order Number: 02120914
Sold to:EGAT [700166108393] - VARRIS.Y@EGAT.CO.TH,
Not for Resale,2016-09-15 03:57:47 UTC

C.3.2.5 Radiation loss

The basic Stefan-Boltzmann equation for radiation from a surface (or narrow slits, which are treated as black bodies) is given by Equation (C.13):

$$q_r = 5.6697 \times 10^{-8} \times \varepsilon A \left[(T_c + 273)^4 - (T_a + 273)^4 \right] \quad \text{(C.13)}$$

where

q_r is the radiation loss, W/linear m
ε is the emissivity corresponding to the temperatures of interest. Here it is assumed emissivity at T_c equals absorptivity of energy spectrum at T_a. This is usually a good approximation.
T_c is the temperature of conductor, °C
T_a is the temperature of surrounding bodies, °C
A is the conductor surface area by unit length of conductor, m^2/m

For cylinders Equation (C.13) becomes Equation (C.14):

$$q_r = 5.6697 \times 10^{-8} \times \varepsilon \pi D \left[(T_c + 273)^4 - (T_a + 273)^4 \right] \quad \text{(C.14)}$$

where

D is the conductor diameter, m

The typical values of ε for bus conductors are in the range of 0.3 to 0.9. A value of 0.5 would apply to heavily weathered aluminum, whereas 0.8 to 0.85 is appropriate for copper, which has achieved a dense green or black- brown patina (see Table C.11 for values of ε for copper and aluminum). High values of emittance may also be achieved with special paints, coatings, or wrappings on the conductor. Although high emittance improves heat dissipation via radiation, it would also increase heat gain via solar absorption.

Example

Consider the conductor of emittance equal to 0.5 operating at 100 °C in an environment of 40 °C; then from Equation (C.14):

$$q_r/A = (5.6697 \times 10^{-8}) \times (0.5) \times (373^4 - 313^4) = 276.7 \text{ W/m}^2$$

By comparing this figure with the forced convective losses calculated earlier, it can be seen that radiation losses may make up 30% to 40% of the total heat losses. For large conductors with high emissivity, losses by radiation may exceed those due to convection.

Copyright © 2010 IEEE. All rights reserved.

Copyright The Institute of Electrical and Electronics Engineers, Inc.
Provided by IHS under license with IEEE
No reproduction or networking permitted without license from IHS

Order Number: 02120914
Sold to:EGAT [700166108393] - VARRIS.Y@EGAT.CO.TH,
Not for Resale,2016-09-15 03:57:47 UTC

C.3.2.6 Solar heat gain

The heat gained from incident solar radiation is estimated by Equation (C.15):

$$q_S = \varepsilon' Q_S A' K \sin(\theta) \quad \text{(C.15)}$$

where

q_s is the solar heat gain by conductor length in W/ m
ε' is the coefficient of solar absorption, usually somewhat higher than emmitance but generally taken as equal to that used for radiation loss
θ is the effective angle of incidence of sun, $\cos^{-1}$ [(cos (H_c) cos ($Z_c - Z_l$)]
H_c is the altitude of sun, degrees (Table C.2)
Z_c is the azimuth of sun, degrees (Table C.2)
Z_l is the azimuth of conductor line, degrees
= 0 or 180 for N-S
= 90 or 270 for E-W
A' is the projected area of conductor by unit length of conductor, m^2/m (area casting shadow)
Q_s is the total solar and sky radiated heat on a surface normal to sun's rays, W/m^2 (Table C.3)
K is the heat multiplying factors for high altitudes

In cases where solar heat input is high, it is important to consider whether solar heating will peak during the time the maximum current load is on the circuit. If not, the estimate of the solar load should be reduced accordingly in order to arrive at the most cost-effective conductor size.

The projected area of a flat surface is the area of its shadow on a plane normal to the direction of the sun's rays, e.g., per conductor length. It is given by Equation (C.16):

$$A' = \sin \zeta \times A \quad \text{(C.16)}$$

where

ζ is the angle between the plane of the conductor surface and the sun's altitude. For a vertical surface: $\zeta = 90 - H_c$. For a horizontal surface: $\zeta = H_c$
H_c is the altitude of the sun in degrees
A is the conductor surface area by unit length of conductor, m^2/m. For cylinders $A = D$ (diameter) and $\sin \zeta = 1$

Copyright © 2010 IEEE. All rights reserved.

Copyright The Institute of Electrical and Electronics Engineers, Inc.
Provided by IHS under license with IEEE
No reproduction or networking permitted without license from IHS

Order Number: 02120914
Sold to:EGAT [700166108393] - VARRIS.Y@EGAT.CO.TH,
Not for Resale,2016-09-15 03:57:47 UTC

Table C.2 —Altitudes and azimuth of the sun in degrees at various latitudes

Declination 23.0° Northern Hemisphere June 10 and July 3						
Degrees north latitude	10:00 AM		12:00 NOON		2:00 PM	
	H_c	Z_c	H_c	Z_c	H_c	Z_c
20	62	78	87	0	62	282
25	62	88	88	180	62	272
30	62	98	83	180	62	262
35	61	107	78	180	61	253
40	60	115	73	180	60	245
45	57	122	68	180	57	238
50	54	128	63	180	54	232
60	47	137	53	180	47	223
70	40	143	43	180	40	217

Table C.3 —Total heat received by a surface normal to the sun at sea level[a]

Q_s (W/m^2)		
Solar altitude degrees H_C	Clear atmosphere	Industrial atmosphere
5	233.5	135.6
10	432.5	239.9
15	583.1	328.1
20	692.8	421.7
25	769.2	501.3
30	828.4	570.2
35	876.8	618.6
40	912.3	661.6
45	940.3	693.9
50	968.3	726.2
60	999.5	770.3
70	1022.0	809.0
80	1030.7	832.7
90	1037.1	848.8

[a] See Yellot [7] at the end of this annex.[38]

Table C.4 —Solar heat multiplying factor for high altitudes

Solar heat multiplying factors (K) for high altitudes[a]	
Elevation above sea level (m)	Multiplier for Q_s
0	1.00
1500 (5000')	1.15
3000 (10 000')	1.25
4500 (15 000')	1.30

[a] See Yellot [7] at the end of this annex.

[38]The numbers in brackets correspond to the references in C.6.

Copyright © 2010 IEEE. All rights reserved.

Copyright The Institute of Electrical and Electronics Engineers, Inc.
Provided by IHS under license with IEEE
No reproduction or networking permitted without license from IHS

Order Number: 02120914
Sold to:EGAT [700166108393] - VARRIS.Y@EGAT.CO.TH,
Not for Resale,2016-09-15 03:57:47 UTC

Examples of solar heating

Example 1

Assume conductors are in an industrial area on an E-W line at 30°N latitude at 1524 m (5000 ft) elevation. If maximum current is required, at 10:00 AM, we obtain from Table C.2 through Table C.4:

$Z_c = 98°$, $H_c = 62°$
$Q_{s\ \text{industrial}} = 777.8\ \text{W/m}^2$
$K = 1.15$ at 1524 m

Then

$\theta = \cos^{-1}[\cos(62)\cos(98 - 90)]$
$\theta = 62.3°$, $\sin\theta = 0.885$

For a cylinder $\sin\zeta = 1$, the projected area is D (m^2/m). Then for a 0.1524 m (6 in) cylinder with $\varepsilon = 0.8$:

$$q_s = 0.8 \times 777.8 \times (0.1524) \times 1.15 \times 0.885 = 96.5\ \text{W/m}^2$$

Example 2

Compute typical 10:00 AM summertime solar radiation incident on a 0.1524 × 0.0127 m (6 × ½ in) rectangular bus conductor ($\varepsilon = 0.5$) running N-S at 45°N latitude in a clear atmosphere at 1524 m (5000 ft).

From Table C.2 through Table C.4, $H_c = 57°$, $Z_c = 122°$, $Q_s = 989.8\ \text{W/m}^2$, $\zeta = 33°$ (horizontal), and $\zeta = 57°$ (vertical), and we have:

$A' = [0.1524 \sin 33° + 0.0127 \sin 57°] = 0.09365\ \text{m}^2/\text{m}$
$\theta = \cos^{-1}[(\cos 57)[\cos(122 - 180)]] = \cos^{-1}[(0.545)(0.53)] = 73.2°$
$\sin\theta = 0.957$

Therefore

$$q_s = 0.5 \times 989.8 \times 1.15 \times 0.09365 \times 0.957 = 51.0\ \text{W/m}$$

For comparison, consider the radiation loss for the same conductor at 80 °C with 40° ambient.

$$q_r = 5.6697 \times 10^{-8} \times 0.5 \times 2(0.0127 + 0.1524) \times (353^4 - 312^4) = 56.6\ \text{W/m}$$

This is a case where emissivity (absorptivity) is of minor importance in the rating of a bus conductor. In contrast, at a lower altitude and for a greater temperature rise, high emissivity would provide for improved ampacity. It should be noted that except during periods of peak solar loads, high emissivity provides the lowest operating temperatures and therefore the least power loss.

C.3.2.7 Summation of convective losses

For each of the conventional types of bus conductor, the convective loss areas for which the formulas given in C.3.2.1 through C.3.2.3 apply are given in Table C.5.

Copyright © 2010 IEEE. All rights reserved.

Copyright The Institute of Electrical and Electronics Engineers, Inc.
Provided by IHS under license with IEEE
No reproduction or networking permitted without license from IHS

Order Number: 02120914
Sold to:EGAT [700166108393] - VARRIS.Y@EGAT.CO.TH,
Not for Resale,2016-09-15 03:57:47 UTC

Table C.5—Convective loss areas

Shape	Area for forced convection	Area for natural convection	Summation of convection losses
Single rectangle	$2\,(l + t)$	0	$6.1\ \Delta T(l^{1/2} + t^{1/2})$
Multiple (N) rectangles	$2(l + Nt)$	$2l(N–1)$	$6.1\ \Delta T(l^{1/2} + Nt^{1/2}) +$ $2.76\ \Delta T^{1.25}\ l^{0.75}\ (N–1)$
Round tube	πd	0	$11.19\ \Delta T\ d^{0.6}$
Square tube	$4l$	0	$12.2\ \Delta T l^{1/2}$
Rectangular tube ($l \cdot w$)	$2(l + w)$	0	$6.1\ \Delta T(l^{1/2} + w^{1/2})$
Universal angle ($l \cdot w$)(ignoring thickness)	$2(l + w)$	0	$6.1\ \Delta T(l^{1/2} + w^{1/2})$
Double angles (for two angles)	$2(l + w)$	$2(l + w)$[a]	$6.1\ \Delta T(l^{1/2} + w^{1/2}) +$ $2.415\ \Delta T^{1.25}\ (l^{0.75} + w^{0.25})$
Single channel	$2(l + 2w)$	0	$6.1\ \Delta T(l^{1/2} + 2w^{1/2})$
Double channel	$24(l + 2w)$	$2(l + 2w)$[a]	$6.1\ \Delta T(l^{1/2} + 2w^{1/2}) +$ $2.415\ \Delta T^{1.25}\ (l^{0.75} + 2w^{0.75})$
Integral web 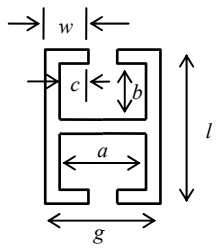	$2(l + 2w)$	$2(a + 2b + 2c)$[b]	$6.1\ \Delta T(l^{1/2} + 2w^{1/2}) +$ $1.38\ T^{1.25}\ (a^{0.75} + 2b^{0.75} + 2c^{0.25})$

[a]Average over all surfaces on interior assuming the equivalent of three favorably oriented surfaces and one unfavorable:

$$\left[\frac{3(1.38) + (0.69)}{4}\right] \times 2 = 2.415$$

[b]Due to overhang, count all interior surfaces as unfavorably oriented for natural convection.

C.3.2.8 Summation of radiation losses

For each of the conventional bus conductors the areas which radiate energy are given in Table C.6.

Copyright © 2010 IEEE. All rights reserved.

Copyright The Institute of Electrical and Electronics Engineers, Inc.
Provided by IHS under license with IEEE
No reproduction or networking permitted without license from IHS

Order Number: 02120914
Sold to:EGAT [700166108393] - VARRIS.Y@EGAT.CO.TH,
Not for Resale,2016-09-15 03:57:47 UTC

Table C.6—Loss areas for radiation

Shape	Surface area of material	Areas that behave as black body slit or hole (ε′= 1)	Summation of radiation: Loss / $[(T_c + 273)^4 - (T_a + 273)^4]10^{-8}$
Single rectangle	$2(l + t)$	0	$11.34\varepsilon(l + t)$
Multiple (N) rectangles (spacing = S)	$2(l + Nt)$	(N–1)2S	$11.34\ \varepsilon\ (l + Nt) + 11.34\ (N-1)\ S$
Round tube or bar square Tube	πd $4l$	0 0	$17.812\varepsilon\ d$ $22.68\varepsilon\ l$
Rectangular tube ($l \times w$)	$2(l + w)$	0	$11.34\varepsilon\ (l + w)$
Universal angle	$2(l + w)$	0	$11.34\varepsilon\ (l + w)$
Double angle (two angles) (spacing = S)	$2(l + w)$	2S	$11.34\varepsilon\ (l + w + S/\varepsilon)$
Channel	$2(l + 2w)$	0	$11.34\varepsilon\ (l + 2w)$
Double channel (two channels) (spacing = S)	$2(l + 2w)$	0	$11.34\varepsilon\ (l + 2w + S/\varepsilon)$
Integral web (overall dimensions $l \times g$)	$2(l + g)$	0	$11.34\varepsilon\ (l + g)$

C.3.2.9 Summation of solar radiation gains

The effective projected area for each of the conventional shapes is given in Table C.7. Only direct solar radiation has been considered. A smaller amount of energy is radiated from the sky. However, it has been ignored here. If data are available for the particular location, sky radiation impinging on other surfaces may be added to the overall energy balance.

Table C.7—Effective projected areas

Shape	Effective projected area
Single rectangle	$[l \sin(90-H_c) + t \sin H_c]$
Multiple (N) rectangles	$[l \sin(90-H_c) + (Nt + (N-1)S/\varepsilon) \sin H_c]$
Round tube or bar	d
Square tube	$l\ [\sin(90-H_c) + \sin H_c]$
Rectangular tube ($l \cdot w$)	$[l\sin(90-H_c) + w \sin H_c]$
Universal angle	$[l\sin(90-H_c) + w \sin H_c]$
Double angle	$[l\sin(90-H_c) + w \sin H_c]$
Channel	$[l\sin(90-H_c) + w \sin H_c]$
Double channel	$[l\sin(90-H_c) + (2w + S/\varepsilon) \sin H_c]$
Integral web	$[l\sin(90-H_c) + 2w \sin H_c + [(g-2w)/\varepsilon)] \sin H_c]$

C.3.2.10 Computation of ampacity

The ampacity computation requires dividing the sum of the heat losses by the product of the resistance (R) and the skin effect factor (F).

Resistance increases with increasing temperature, and this should be accounted for in the calculation. Skin effect factors are a function of resistance, frequency, and geometry. The factors are readily available for simple shapes. Calculating skin effect factors for complex shapes is beyond the scope of this annex, and no guidance will be offered except that the factors can be significant and should be included when calculations are performed. The skin effect factors decrease slightly with increasing temperature and should be adjusted accordingly. This subject is discussed in C.4 on properties of materials.

Copyright © 2010 IEEE. All rights reserved.

Copyright The Institute of Electrical and Electronics Engineers, Inc.
Provided by IHS under license with IEEE
No reproduction or networking permitted without license from IHS

Order Number: 02120914
Sold to:EGAT [700166108393] - VARRIS.Y@EGAT.CO.TH,
Not for Resale,2016-09-15 03:57:47 UTC

As demonstrated in Clause 4, the resistance at any temperature may be calculated as follows:

For copper and copper alloys, the resistance R is given by Equation (C.17):

$$R = \frac{1.724\times10^{-6}}{C' A_c}\left[1+\frac{0.00393\times C'}{100}\times(T_2-20)\right] \quad \text{(C.17)}$$

For aluminum alloys, the resistance R is given by Equation (C.18):

$$R = \frac{1.724\times10^{-6}}{C' A_c}\left[1+\frac{0.00403\times C'}{61}\times(T_2-20)\right] \quad \text{(C.18)}$$

where

R is the DC resistance (Ω/m)
C' is the conductivity as % IACS
A_c is the cross-sectional area, m^2
T_2 is the conductor temperature, °C

Example

Compute the 60 Hz outdoor ampacity of a 0.3048 m × 0.00635 m (12 in × ¼ in) copper conductor operating with a temperature rise of 65 °C above a 40 °C ambient. Assume $\varepsilon = 0.5$, no solar heating, $C' = 98\%$ IACS and $F = 1.28$.

$q_c = 6.1\times 65 \times [0.3048^{½} + 0.00635^{½}]$
$q_c = 250.5$ W/m
$q_r = 11.34 \times 0.5 \times (0.3048 + 0.00635) \times 10^{-8} \times (378^4 - 313^4)$
$q_r = 190.9$ W/m
$q_c + q_r = 441.4$ W/m

$$R = \frac{1.724\times10^{-6}}{98\times(0.3048\times0.00635)}\times\left[1+\frac{0.00393\times98}{100}\times(105-20)\right] = 12.065\times10^{-6} \ (\Omega/\text{m})$$

$RF = 12.065\times10^{-6} \times 1.28 = 15.444 \times 10^{-6}$ Ω/m
$I = [(q_c + q_r) / RF]^{½} = (441.4 / 15.444 \times 10^{-6})^{½} = 5346$ A

C.3.2.11 Electrical resistance of other materials

The above equations calculate the resistance for copper and aluminum materials. Per IEEE Std 738-2006, the use of resistance data for temperatures of 25 °C and 75 °C, given in the Aluminum Electrical Conductor Handbook [B1], is adequate for rough calculations of steady-state and transient thermal ratings for conductor temperatures up to 175 °C, and these data may be used for approximate fault calculations up to the melting point of typical conductor materials.

Copyright © 2010 IEEE. All rights reserved.

Copyright The Institute of Electrical and Electronics Engineers, Inc.
Provided by IHS under license with IEEE
No reproduction or networking permitted without license from IHS

Order Number: 02120914
Sold to:EGAT [700166108393] - VARRIS.Y@EGAT.CO.TH,
Not for Resale,2016-09-15 03:57:47 UTC

The resistance at conductor temperature, R_{Tc}, is calculated by Equation (C.19):

$$R_{T_c} = \left[\frac{R_{T_{\text{High}}} - R_{T_{\text{Low}}}}{T_{\text{High}} - T_{\text{Low}}}\right](T_c - T_{\text{Low}}) + R_{T_{\text{Low}}} \quad \text{(C.19)}$$

where

R_{T_c} is the 60 Hz ac resistance per linear m of conductor at T_c (Ω/m)
$R_{T_{\text{High}}}$ is the 60 Hz ac resistance per linear m of conductor at 75 °C (Ω/m)
$R_{T_{\text{Low}}}$ is the 60 Hz ac resistance per linear m of conductor at 25 °C (Ω/m)

C.3.2.12 Heat balance equation

Per IEEE Std 738-2006, a linear non-steady-state heat balance equation is given by Equation (C.20):

$$T_c(t) = T_i + (T_f - T_i) \times (1 - e^{-t/\tau}) \quad \text{(C.20)}$$

with τ given by Equation (C.21):

$$\tau = \frac{(T_f - T_i)mC_p}{R_{T_c}(I_f^{\,2} - I_i^{\,2})} \quad \text{(C.21)}$$

where

T_i is the conductor temperature prior to step increase (°C)
T_f is the conductor temperature attained many time constants after step increase (°C)
τ is the thermal time constant in seconds
I_i is the initial current before step change (A at 60 Hz)
I_f is the final current after step change (A at 60 Hz)
t is the time to reach temperature T_f
R_{Tc} is the conductor resistance at temperature $(T_f + T_i)/2$
mC_p is the specific heat of the conductor material (J/(m °C)) and is given by Equation (C.22):

$$mC_p = \sum m_i C_{pi} \quad \text{(C.22)}$$

where

m_i is the mass by unit length (linear mass) of the ith conductor, kg/m
C_{pi} is the specific heat of the ith conductor material, (J/(kg °C)) given in Table C.8

Copyright © 2010 IEEE. All rights reserved.

Copyright The Institute of Electrical and Electronics Engineers, Inc.
Provided by IHS under license with IEEE
No reproduction or networking permitted without license from IHS

Order Number: 02120914
Sold to:EGAT [700166108393] - VARRIS.Y@EGAT.CO.TH,
Not for Resale,2016-09-15 03:57:47 UTC

Table C.8 —Specific heat of common material

Material	C_p J/(kg °C)
Aluminum	954.6
Copper	423.3
Steel	476.2
Alumoweld	934.8

Example

To calculate mC_p for an ACSR conductor, the m_iC_{pi} values of the aluminum and steel components are calculated individually and then added. For the Cardinal (954 ACSR) conductor, the aluminum part has a linear mass of 0.605 kg/m (0.9 lb/ft) and the steel part has a linear mass of 0.221 kg/m (0.329 lb/ft). From Table C.8, the mC_p for the conductor can be calculated as follows:

For aluminum m_iC_{pi} = 0.605× 954.6 = 577.5 J/kg °C
For steel m_iC_{pi} = 0.221 × 476.2 = 105.2 J/kg °C

Therefore, for the Cardinal conductor, the total value mC_p = 577.5 + 105.2 = 682.7 J/(kg °C).

From these equations, by trial and error, the time required to reach maximum allowed temperature can be calculated. This time can be compared with the fault clearing time.

C.4 Properties of materials

C.4.1 Thermal expansion

When at least one end is unconstrained, bus conductors expand as their temperatures rise. The amount of expansion may be calculated by multiplying the thermal expansion coefficients listed below, by the increase in temperature and the conductor span length at the initial temperature. The base temperature corresponding to zero expansion is the installation temperature, not the ambient temperature. The net elongation under thermal expansion is given by Equation (C.23):

$$\Delta L = \alpha L_i (T_f - T_i) \tag{C.23}$$

where

ΔL is the change in span length, m
α is the coefficient of thermal expansion, (1/°C), Table C.9
T_i is the initial installation temperature, °C
T_f is the final temperature, °C
L_i is the conductor span length at the initial temperature, m, or the length of the restrained conductor when both ends are fixed

The corresponding strain under thermal expansion, using the variables defined above, is given by Equation (C.24):

$$\varepsilon = \frac{\Delta L}{L_i} \tag{C.24}$$

Copyright © 2010 IEEE. All rights reserved.
Copyright The Institute of Electrical and Electronics Engineers, Inc.
Provided by IHS under license with IEEE
No reproduction or networking permitted without license from IHS
Order Number: 02120914
Sold to:EGAT [700166108393] - VARRIS.Y@EGAT.CO.TH,
Not for Resale,2016-09-15 03:57:47 UTC

Table C.9—Thermal expansion coefficient α

Material	α 1/°C	α 1/°F
Aluminum	23.1×10^{-6}	12.8×10^{-6}
Copper	16.8×10^{-6}	9.33×10^{-6}
Stainless steel	17.8×10^{-6}	9.89×10^{-6}
Steel	11.7×10^{-6}	6.50×10^{-6}
Concrete	6.3 to 14.4×10^{-6}	3.5 to 8×10^{-6}

Example

What is the total thermal expansion ΔL of a 457.2 cm (4.572 m) (15 ft) run of copper bus conductor installed on a concrete pad at 20 °C and operating at 50 °C over a 40 °C ambient (i.e., at 90 °C)?

For the bus conductor:

$$\Delta L_{copper} = \text{total expansion} = 457.2 \times 16.8 \times \square 10^{-6} \times (90 - 20) = 0.538 \text{ cm}$$

For the concrete pad (assume the expansion coefficient $\alpha = 10 \times 10^{-6}$):

$$\Delta L_{concrete} = 457.2 \times 10 \times 10^{-6} \times (40 - 20) = 0.091 \text{ cm}$$

The net amount of restraint on the bus conductor is the difference between the expansion of the bus and the concrete pad:

$$\Delta L_{net} = 0.538 - 0.091 = 0.447 \text{ cm}$$

The strain in the copper conductor (assuming massive rigid pad) is as follows:

$$\varepsilon = \frac{\Delta L_{net}}{L_i} = \frac{0.447}{457.2} = 9.78 \times 10^{-4}$$

C.4.2 Stresses and forces due to thermal expansion

When a material is totally restrained from expanding or contracting normally as temperature changes, normal stresses are induced to account for the effective change in length that would otherwise takes place.

The stress, *S*, is given by Equation (C.25):

$$S = E\varepsilon \tag{C.25}$$

where

Copyright © 2010 IEEE. All rights reserved.

Copyright The Institute of Electrical and Electronics Engineers, Inc.
Provided by IHS under license with IEEE
No reproduction or networking permitted without license from IHS

Order Number: 02120914
Sold to:EGAT [700166108393] - VARRIS.Y@EGAT.CO.TH,
Not for Resale,2016-09-15 03:57:47 UTC

E is the modulus of elasticity, N/m^2 or Pa (see Table 1 in the main portion of the guide for common values)
ε is the strain under thermal expansion [Equation (C.24)]

The associated thermal expansion force at the conductor's ends, assuming complete restraint, is given by Equation (C.26):

$$F_{\mathrm{TE}} = S\,A_c \tag{C.26}$$

where

F_{TE} is the thermal expansion force at the conductor's ends assuming complete restraint, N
S is the thermal stress, N/m^2 or Pa
A_{c} is the cross-sectional area of the conductor, m^2

Example

For the example above, the stress in the copper conductor (modulus of elasticity of 110 GPa) is given by

$$S = 110 \times 10^{9} \times 9.78 \times 10^{-4} = 1.08 \times 10^{8} = 108 \text{ MPa}$$

For the 15.24 cm × 1.27 cm (6 in × ½ in) bus conductor, the cross-sectional area is 1.936×10^{-3} m^2 and the associated force on the bus supports is therefore:

$$F_{TE} = S\,A_c = 108 \times 10^{6} \times 1.936 \times 10^{-3} = 2.090 \times 10^{5} \text{ N} = 209 \text{ kN}$$

In practice, this high load would not be generated. Complete restraint is unlikely due to bending, sliding, or plastic deformation of the conductors. However, to be sure loads are not excessive, it is suggested that expansion joints be provided to minimize thermally generated stresses.

C.4.3 Maximum operating stresses

Metals may deform plastically to accommodate thermal stresses and strains and to reduce other applied loads. Although bus conductor alloys can deform appreciably, it is suggested that stresses be maintained below levels at which plastic deformation is expected. If the loads will be applied occasionally and for only a short time the maximum stress should be below the yield strength. It should be remembered that, at the yield stress of a material, a small amount of deformation (less than 0.5%) occurs. For extended operation or negligible deformation, lower stresses should be employed to avoid creep, relaxation, or fatigue damage. To provide a margin of safety, designers may limit stresses to 2/3 the values given in Table C.10.

Copyright © 2010 IEEE. All rights reserved.

Copyright The Institute of Electrical and Electronics Engineers, Inc.
Provided by IHS under license with IEEE
No reproduction or networking permitted without license from IHS

Order Number: 02120914
Sold to:EGAT [700166108393] - VARRIS.Y@EGAT.CO.TH,
Not for Resale,2016-09-15 03:57:47 UTC

Table C.10—Operating stresses

Representative yield strength levels MPa (ksi)			
	20 °C	**100 °C**	**150 °C**
Aluminum alloys			
6101-T6	172 (25)	154 (22.3)	116 (16.9)
6063-T6	172 (25)	156 (22.7)	112 (16.2)
Copper (hard)	172 (25)	152 (22)	138 (20)
Copper (soft)	62 (9)	62 (9)	62 (9)
Maximum stresses for continuous operation MPa (ksi)			
	20 °C	**100 °C**	**150 °C**
Aluminum alloys			
6101-T6	103 (15)	92 (13.4)	70 (10.1)
6063-T6	103 (15)	94 (13.6)	67 (9.7)
Copper (hard)	62 (9)	62 (9)	60 (8.7)
Copper (soft)	35 (5.1)	33 (4.8)	32 (4.7)

The above strength levels apply to the usual conductor materials. Special alloys of aluminum or copper and coppers with small additions of silver may be used where higher strength or resistance to relaxation or softening are required.

C.4.4 Resistance

Resistance of bus conductors increases with increasing temperature. For aluminum and copper alloys, resistance at an elevated temperature (T_2) may be expressed in terms of resistance at 20 °C by Equation (C.27):

$$R_{T2} = R_{20}\ \left[1 + \alpha_R (T_2 - 20)\right] \tag{C.27}$$

where

R_{T2} is the resistance of bus conductor at elevated temperature T_2, Ω
T_2 is the elevated temperature, °C
α_R is the temperature coefficient of resistance at a base temperature of 20 °C, (Ω /(Ω °C))
R_{20} is the resistance at 20 °C per unit length in Ω /m = ρ/A_c
ρ is the resistivity, Ω m^2/m
A_c is the cross-sectional area of conductor at 20 °C, m^2

The temperature coefficient of resistance for copper of conductivity equal to 100% of the International Annealed Copper Standard (IACS) is 0.00393/°C, and for aluminum of conductivity equal to 61% IACS, it is 0.00403/°C. For copper and aluminum conductors of other conductivities, Equation (C.28) for copper and Equation (C.29) for aluminum may be written as:

$$\alpha_{R\_\text{copper}} = \frac{0.00393 \times C'}{100} \tag{C.28}$$

Copyright © 2010 IEEE. All rights reserved.
Copyright The Institute of Electrical and Electronics Engineers, Inc.
Provided by IHS under license with IEEE
No reproduction or networking permitted without license from IHS
Order Number: 02120914
Sold to:EGAT [700166108393] - VARRIS.Y@EGAT.CO.TH,
Not for Resale,2016-09-15 03:57:47 UTC

$$\alpha_{R\_alu} = \frac{0.00403 \times C'}{61} \tag{C.29}$$

where

C' is the % conductivity (as % IACS)

Using Equation (C.27) and Equation (C.28), R_{T2} for copper is given by Equation (C.30):

$$R_{T2} = \frac{\rho}{A_c} \times \left[1 + \frac{0.00393 \times C'}{100} \times (T_2 - 20) \right] \tag{C.30}$$

Using Equation (C.27) and Equation (C.29), R_{T2} for aluminum is given by Equation (C.31):

$$R_{T2} = \frac{\rho}{A_c} \times \left[1 + \frac{0.00403 \times C'}{61} \times (T_2 - 20) \right] \tag{C.31}$$

For copper of 100% IACS conductivity, the resistivity, ρ, is 1.724×10^{-8} Ω m^2/m. Using this value in Equation (C.30), we obtain Equation (C.17) for copper as presented earlier. In the same way, we obtain Equation (C.18) for aluminum as presented earlier.

C.4.5 Emissivity and absorptivity

For ordinary calculations, the emissivity and absorptivity of a bus conductor are taken as equal. Strictly speaking, since they apply to different energy spectra, they are not equal, but for practical purposes, the error is small. Values for aluminum and copper are given in Table C.11.

Copyright © 2010 IEEE. All rights reserved.

Copyright The Institute of Electrical and Electronics Engineers, Inc.
Provided by IHS under license with IEEE
No reproduction or networking permitted without license from IHS

Order Number: 02120914
Sold to:EGAT [700166108393] - VARRIS.Y@EGAT.CO.TH,
Not for Resale,2016-09-15 03:57:47 UTC

Table C.11—Values of emissivity and absorptivity for copper and aluminum

ε = Emissivity, absorptivity		
	Copper	**Aluminum**
Clean mill finish	0.1	0.1
Light tarnish (recent outdoor installation or indoor)	0.3–0.4	0.2
After extended outdoor exposure	0.7–0.85	0.3–0.5
Painted black	0.9–0.95	0.9–0.95

C.4.6 Skin effect

For a common conductor, shapes plots are available that provide skin effect coefficients as a function of current frequency and resistivity. When such plots are available, the variation in skin effect with temperature may be determined by computing the resistivity of the shape at various temperatures and by determining the associated skin effect coefficients. When only a single value of the skin effect coefficient is suitable or when a convenient equation is needed for computer calculations, the following procedure may be used to obtain a conservative (slightly) high estimate of the skin effect coefficient at a higher temperature.

The skin effect coefficient F_2 at temperature T_2 is given as a function of the skin effect F_1 at temperature T_1 by Equation (C.32):

$$F_2 = F_1 + \frac{\Delta F}{\Delta T}(T_2 - T_1) \tag{C.32}$$

where

F_1 is the skin effect at temperature T_1
F_2 is the skin effect at temperature $T2_1$
$\Delta F/\Delta T$ is the slope of the variation of the skin coefficient with the temperature

It can be shown that Equation (C.33) provides an approximation for $\Delta F/\Delta T$:

$$\frac{\Delta F}{\Delta T} \approx -\frac{(F_1 - 1)}{2}\alpha_R \tag{C.33}$$

where

α_R is the temperature coefficient of resistance at T_1 (Ω /(Ω –°C))

Using Equation (C.33) in Equation (C.32), we obtain Equation (C.34) for F_2:

$$F_2 = F_1 - \frac{1}{2}(T_2 - T_1)(F_1 - 1)\alpha_R \tag{C.34}$$

Copyright © 2010 IEEE. All rights reserved.

Copyright The Institute of Electrical and Electronics Engineers, Inc.
Provided by IHS under license with IEEE
No reproduction or networking permitted without license from IHS

Order Number: 02120914
Sold to:EGAT [700166108393] - VARRIS.Y@EGAT.CO.TH,
Not for Resale,2016-09-15 03:57:47 UTC

C.5 Ampacity tabulations

The procedures described herein have been used to calculate ampacity tables—see [4].

C.6 References

[1] American Society of Heating and Air-Conditioning Engineers, *Heating, Ventilating and Air-Conditioning Guide 1956*. New York: American Society of Heating and Air-Conditioning Engineers, 1956.

[2] McAdams, W. H., "Heat transmission," in Perry, J. H., ed., *Chemical Engineer's Handbook*, New York: McGraw-Hill Book Company, 1950.

[3] McAdams, W. H., *Heat Transmission,* New York: McGraw-Hill Book Co., 1954.

[4] Prager, M., Pemberton, D .L., Craig, A. G., Jr., Bleshman, N. A. "Thermal considerations for outdoor bus design ampacity tables," *IEEE Transactions on Power Apparatus and Systems,* vol. 96, no. 4, pp. 1341–1345, July 1977.

[5] *Sight Reduction Tables for Air Navigation,* U. S. Navy Hydrographic Office, H. O. Publication No. 249, vols. II and III.

[6] *The American Nautical Almanac,* Washington, D.C.: U.S. Naval Observatory, 1957.

[7] Yellot, J. I., "Power from solar energy," *ASME Transactions,* vol. 79, no. 6, pp. 1349–1357, Aug. 1957.

NOTE 1—The wind is considered a forced draft with the air circulating parallel to each surface of the conductor and perpendicular to the length.

Copyright © 2010 IEEE. All rights reserved.

Copyright The Institute of Electrical and Electronics Engineers, Inc.
Provided by IHS under license with IEEE
No reproduction or networking permitted without license from IHS

Order Number: 02120914
Sold to:EGAT [700166108393] - VARRIS.Y@EGAT.CO.TH,
Not for Resale,2016-09-15 03:57:47 UTC

Annex D

(informative)

Corona and substation bus design

D.1 Corona and gap discharge

Corona and gap discharges have effects that should be considered in the design of substation air insulated bus. These effects include:

a) Corona losses
b) EMI
c) Insulation degradation
d) Audible noise
e) Ozone production
f) Light emissions

Corona losses are a significant concern in the engineering of transmission lines, and information is given in Chapter 11 of the EPRI Redbook [13].[39] For the relatively short spans of station buses compared with transmission lines, it is not likely that corona losses need to be considered in switchyard bus design.

Corona caused audible noise, ozone production, and light emissions may be community acceptance issues. These issues are addressed in the EPRI Redbook [13]. The Redbook addresses transmission lines, and the issues affect a wider area and may have a greater impact than substation buses.

The EMI and insulation degradation should be considerations in station bus design.

D.1.1 Corona physical process

Corona discharges occur on air-insulated conductors when the electric field intensity at the conductor surface causes ionization in air. The field intensity at the initiation of the discharges is known as "corona onset gradient."

There have been laboratory correlations to determine the conductor corona onset gradient. The laboratory experiments include tests using single, small, smooth, concentric, and cylindrical conductors.

In work published in 1929, Peek [29] included an empirical formula for calculation of the corona onset gradient that has been widely used. Using data from laboratory measurements at alternating voltages on small, smooth cylindrical conductors, Peek developed the following formula that has been widely used:

[39]The numbers in brackets correspond to the references in D.7.

Copyright © 2010 IEEE. All rights reserved.

Copyright The Institute of Electrical and Electronics Engineers, Inc.
Provided by IHS under license with IEEE
No reproduction or networking permitted without license from IHS

Order Number: 02120914
Sold to:EGAT [700166108393] - VARRIS.Y@EGAT.CO.TH,
Not for Resale,2016-09-15 03:57:47 UTC

$$E_c = m E_0 D_a \left(1 + \frac{C}{\sqrt{D_a r_c}}\right) \quad \text{(D.1)}$$

where

E_c is the corona onset gradient, kV/cm
E_0 is an empirical constant
C is an empirical constant
m is the conductor irregularity factor
D_a is the relative air density
r_c is the conductor outside radius, cm

Peek found E_0 = 30 kV/cm (peak value) or 21.1 kV/cm (rms value) and C = 0.301 cm^{-1}.

The conductor irregularity factor m is the factor that takes the surface condition of the conductor into account. Experimental results have shown that the irregularity factor may vary from 0.3 to 0.85 depending on the conductor surface condition. Stranding, nick, cut, abrasions, animal debris, and water droplets all can have an effect on the conductor irregularity. In some cases of extreme deposition of foreign material, the value of m may be as low as 0.2. For stranded bus conductors with little deposition of foreign material, the range of m = 0.6 to 0.85 seems reasonable.

The relative air density D_a density is a function of altitude and temperature:

$$D_a = \left(\frac{273 + T_0}{273 + T}\right)\frac{P}{P_0} \quad \text{(D.2)}$$

where

T is the temperature of the ambient air, °C
P is the ambient air pressure, kPa
P_0 and T_0 are pressure and temperature use in the determination of the empirical constants E_0 and C, and the factor m

Although it is not certain what values of P_0 and T_0 were used by Peek to develop the empirical constants and m factor, it is usual to adjust experimental results to a common basis of T_0 = 25 °C. It is also usual to adjust experimental results to a common basis of air pressure at sea level where P_0 = 100 kPa (approximately).

Additional research by Mercure [26] shows that

$$\frac{P}{P_0} = 1 - \frac{A}{10} \quad \text{(D.3)}$$

where A is the altitude in kilometers.

Over the decades, corona studies have continued. Although the electric field intensity is an important variable, the corona onset gradient is affected by many other variables. The relationship between the onset of corona and these other variables is difficult to determine, and the occurrence of these variables is difficult to predict. In Juette [24] test data

Copyright © 2010 IEEE. All rights reserved.
Copyright The Institute of Electrical and Electronics Engineers, Inc.
Provided by IHS under license with IEEE
No reproduction or networking permitted without license from IHS
Order Number: 02120914
Sold to:EGAT [700166108393] - VARRIS.Y@EGAT.CO.TH,
Not for Resale,2016-09-15 03:57:47 UTC

show a 16-to-1 variation in EMI from "very clean conductors" to "very polluted conductors," as well as a 16-to-1 variation from dry weather to heavy rain EMI. Research has shown that corona and EMI will occur at voltage gradients from 10 kV/cm to more than 30 kV/cm.

In the previous edition of this guide, it was stated that the corona onset gradient was 15 kV/cm. From the time of Peek's empirical equation to today's research, it is clear that there is no physical law to support a single value of corona onset voltage. It is not possible to determine a field gradient below which corona will never occur. Current practice is a statistical presentation of probabilities of corona and "exceedence" levels with a probability of occurrence.

The previous edition of the guide also stated that "In practice, corona has not been a factor in rigid-bus design at 115 kV and below." Although most of the research in EMI from transmission lines has been in the range of 230 kV to 800 kV, there has been research on transmission lines with nominal voltages as low as 69 kV.

D.1.2 Gap discharge

Gap discharge is the breakdown of air insulation between two electrodes separated by a gap of a few millimeters. Most gap discharges occur between metallic electrodes that occur because of loose fittings or between a metallic electrode and the surface of an insulator.

For overhead lines, the great majority of reported EMI is due to gap discharge, although gaps appear to be more likely on distribution lines. Gaps are not likely to result with properly designed and constructed substation buses. Gaps do develop in substation operation, but the source of EMI is usually easily located. An EPRI Report [14] provides guidance in locating EMI sources in substations.

D.2 Corona effects

D.2.1 Electromagnetic interference

A principal concern with corona and gap discharge is the generation of electromagnetic interference. There has been considerable research over the last several decades in the area of corona-generated radiated EMI and the effect on AM radio broadcast signals (535 kHz to 1605 kHz) and television signals in the lower TV broadcast range (88 MHz to 108 MHz).

D.2.2 Insulation damage

There have been instances of damage to transmission line insulators due to corona. Corona with water droplets can create nitric acid. Any damage to the insulator polymer sheath of a composite insulator could allow the ingress of the nitric acid and damage the insulator fiberglass rod core. Rod damage may result in premature mechanical failure of the insulator.

D.2.3 Audible noise

Substation bus audible noise results from corona and gap discharge. The audible noise caused by corona may include a sound power that has a dominant second harmonic component. Because of this low-frequency "hiss," it is difficult to correlate EMI with corona sound power.

Copyright © 2010 IEEE. All rights reserved.

Copyright The Institute of Electrical and Electronics Engineers, Inc.
Provided by IHS under license with IEEE
No reproduction or networking permitted without license from IHS

Order Number: 02120914
Sold to:EGAT [700166108393] - VARRIS.Y@EGAT.CO.TH,
Not for Resale,2016-09-15 03:57:47 UTC

The sound power of audible noise at any location in a substation can be calculated if the strength of the point sources is known. For most substations, the audible noise from transformers will likely be the strongest sound power source in the substation, and audible noise from corona is not likely to be a dominant consideration in bus design.

D.2.4 Light emission

The spectrum of corona light emission falls within the spectrum of sunlight.

D.3 Electromagnetic interference

EMI is any electric field disturbance that adversely affects the operation of electrical equipment. Corona and gap-generated EMI in substations are broadband in the range of 100 kHz to 1 GHz and measured as electric field strength in kV per meter (or kV per centimeter).

The EMI electric field strength and frequency characteristics are a function of the corona and gap sources, the configuration of the source(s) with respect to ground planes, and the distance from the source.

D.3.1 Effects of EMI

The focus on the effects of EMI has been on radiated fields from overhead transmission lines and the effect on radiated signal reception from commercial broadcasters. Theoretically, EMI can be an issue in any frequency spectra. However, most of the research has been in the AM radio band (535 kHz to 1605 kHz) and the commercial TV range (channels 2 to 6, audio 54 MHz to 88 MHz). The primary concern has been degradation of the signal-to-noise ratio for AM and television receivers.

In substations, radiated EMI may affect the operation of devices that are located in the switchyard or located such that there is no ground plane to shield the device from radiated EMI.

EMI radiation may be coupled to switchyard metal conductor cables that are located, or have a cable construction, to reduce interference through shielding by a ground plane (e.g., metal conduit or cable sheath). Depending on the effectiveness of the shielding, the coupled EMI may then cause conducted EMI interference with analog signals to equipment that are necessary for control, protection, and data acquisition (e.g., relays and remote terminal units). The level of interference is a function of the EMI field strength at the cable surface, the receiver impedance, and so on. Carrier communications located in the switchyard are the most likely equipment to be affected by radiated EMI.

D.3.2 Determination of substation bus corona and EMI performance

The onset of corona can only be treated statistically. The corona and EMI performance of a substation bus design could be evaluated to determine the “excedence level” (the probability that EMI will exceed a reference level) and the EMI magnitude and frequency spectrum.

The previous edition of this guide included a Figure D.1 that was represented as a relationship between conductor diameter and “allowable voltage gradient”. It was inferred that the “allowable voltage gradient” given in Figure D.1 could be compared with calculated electric field strength for a conductor diameter. The inference is that a calculated field strength that is less than the “allowable field gradient” will not result in corona. Figure D.1 appears to be an adaptation of a figure (reproduced below) that was first published by the IEEE Radio Noise Committee [16], and again published in 1971 by Leslie et al. [25].

Copyright © 2010 IEEE. All rights reserved.

Copyright The Institute of Electrical and Electronics Engineers, Inc.
Provided by IHS under license with IEEE
No reproduction or networking permitted without license from IHS

Order Number: 02120914
Sold to:EGAT [700166108393] - VARRIS.Y@EGAT.CO.TH,
Not for Resale,2016-09-15 03:57:47 UTC

Although the previous edition of this guide used the phrase “for equal radio-influence (RI) generation,” the importance of that phrase appears to have been overlooked.

The upper curve given in the new Figure D.1 is the curve of allowable voltage gradient versus conductor diameter to:

— Maintain an EMI level of 600 μV (due to conductor corona) per meter
— During fair weather
— Measured at a distance of 15 m (50 ft) from the outer conductor of three phase conductors
— In a horizontal configuration
— At approximately 12 m (40 ft) above grade
— Using an ANSI 62.3 m (at 1 MHz, using a quasi-peak filter)

The publications from the IEEE Radio Noise Committee [16] and Leslie et al. [25] have been superseded by more recent research.

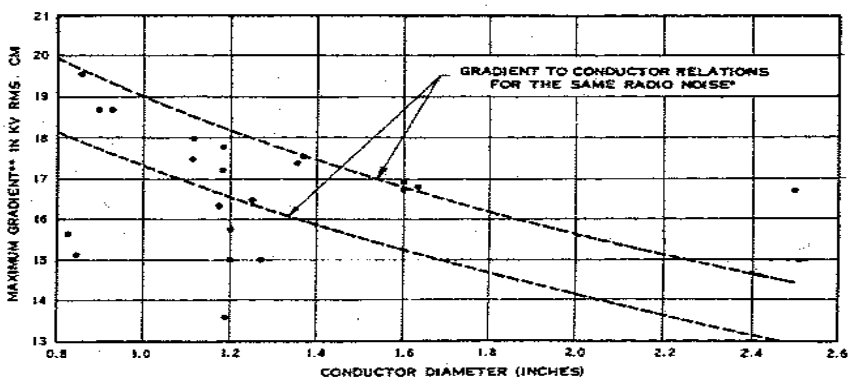

* Fair weather level below 100 μV/m (optional QP) at 100 ft lateral distance from outside conductor.

** Maximum gradient around the periphery of a subconductor on any phase.

• Lines in operation in 1971.

Figure 9.3-5 Range of operating gradient and conductor size for single or bundle conductors for comparable noise levels (IEEE Working Group on Line Design 1971).

Figure D.1—Gradient to conductor relations for the same radio noise [25]

The definitive work in comparison of the acceptable calculation of transmission line EMI is the IEEE Radio Noise Subcommittee Report [25]. However, there appears to be no research that specifically addresses the calculation of substation bus EMI.

The previous edition of this guide provided the formulas for calculation of the maximum electric fields in various substation bus configurations. And the simple relation given in Peek’s equation [29] could be used to give some

Copyright © 2010 IEEE. All rights reserved.

Copyright The Institute of Electrical and Electronics Engineers, Inc.
Provided by IHS under license with IEEE
No reproduction or networking permitted without license from IHS

Order Number: 02120914
Sold to:EGAT [700166108393] - VARRIS.Y@EGAT.CO.TH,
Not for Resale,2016-09-15 03:57:47 UTC

indication of the corona onset gradient. However, Peek's equation does not, by any modern research, assure that there will be no corona if the calculated corona onset voltage is less than 15 kV/cm.

Peek's equation has no mechanism to calculate the probability of corona below the calculated voltage. Also, Peek's equation has no mechanism to calculate the magnitude and frequency spectrum of radiated EMI due to the design of the substation bus.

The Electronic Power Researh Institute's Redbook [13] does explicitly address EMI in stations. But stations are considered from the point of view of longitudinal injection of EMI from the station into connected transmission lines and the conclusion is that the contribution of station-generated noise is negligible when compared with the transmission lin-generated EMI. The conclusion is based on the theoretical calculation of the relative magnitude of the surge impedances.

The inference from the statement about relative magnitude of the surge impedance is that a significant amount of transmission-line EMI will be injected into the station. Because there may be several lines connected to a station, similar conductor configurations in both the station and the transmission lines may result in more EMI injection from the transmission lines than is generated in the station itself.

Typical measured values of transmission lines are given in Juette [24]. The transmission line conductor EMI levels are in the range of 10 μV to 100 μV/m at 1 MHz. There is no similar research for EMI levels generated in the station, but it is interesting to compare these results with allowable EMI from station apparatus such as disconnect switches and transformers.

For comparison, ANSI C37.32-1996 establishes a limit of 500 μV/m for switches that are rated 123 kV and above. Station power transformers no longer have EMI emission limits set by national standards. However, NEMA TR 1 establishes a limit of 100 μV/m for distribution transformers.

Because EMI is generated by all equipment within the station, it is likely that the EMI contribution from the station apparatus will be significantly greater than EMI from substation buses.

Juette [24] presents 10 different methods for calculation of EMI for transmission-line conductors. Any of these methods could be applied to the calculation of EMI from the substation bus. The eight methods that are labeled "comparative" appear to be more practical in application. But there are some critical differences between the configuration of substation buses and the configuration of transmission-line conductors.

Transmission-line EMI research has been directed almost exclusively at transmission lines with the bottom-line conductor 10 m or more above grade. Because the electric field and associated EMI increases as height decreases, the transmission-line research will give calculated substation EMI levels that are greater than the expected levels.

Some of the research in analog signal interference has included consideration of conductive coupling of the radiated field into metal structures that are typical of air-insulated substation and reradiation of EMI. However, there appears to be little research in the magnitude and frequency spectrum of the reradiated noise.

It is noteworthy that the electric field calculation in the previous edition of the guide includes the effect of bundled conductors. Most of the comparative methods in Juette [24] include the diameter of the conductor (or subconductor) in the calculation. Some of the comparative methods include the number of subconductors. However, the paper states the following:

"Some empirical equations … have a term for the change in RN (editorial comment: EMI) with the number of subconductors in the bundle. Laboratory tests on bundle and single conductors subjected to heavy rain have shown the RN generation to be independent of the number of conductors in the bundle."

Copyright © 2010 IEEE. All rights reserved.

Copyright The Institute of Electrical and Electronics Engineers, Inc.
Provided by IHS under license with IEEE
No reproduction or networking permitted without license from IHS

Order Number: 02120914
Sold to:EGAT [700166108393] - VARRIS.Y@EGAT.CO.TH,
Not for Resale,2016-09-15 03:57:47 UTC

D.3.3 EMI tolerance of substation control, protection, and communications equipment

In the United States, no regulations exist on a local or federal level that expressly set the probability of the occurrence of corona, or limit the level of EMI that a transmission line, or substation bus, may produce.

While concentrating in the AM (535 kHz to 1605 kHz) and TVI (88 MHz to 108 MHz) bandwidths, the effects of corona generated EMI on analog signals has been the subject of considerable research.

There appears to be little research in the effects of corona-generated EMI on digital signals, although one of the objectives in the movement to digital signaling has been noise immunity. And there appears to be little research to support EMI tolerance levels for substation signaling equipment.

The principal concern for EMI in substations is interference with station relaying, control, and communications equipment. Protection equipment is a particular concern. Five IEEE standards, which include IEEE Std C37.90™-2005 [17], IEEE Std C37.90.1™-2002 [18], IEEE Std C37.90.2™-2004 [19], IEEE Std C37.90.3™-2001 [20], and IEEE Std 1613™-2003 [22], do include some treatment of radiated EMI and conducted signal interference.

IEEE Std C37.90-2005 [17] states that “excessive electrical noise” and “electromagnetic radiation” are “other conditions” that require special treatment.

The tests that are specified in IEEE Std C37.90.1-2002 [18] require connection of the test generator to “external connections” and appear to be intended to test the tolerance level of conducted signal interference. The test signal interference includes one test with a single frequency (1 MHz) decaying oscillatory waveform. The second test is a fast rise time, bipolarity repeating surge that would include high-frequency components. However, the standard is intended to provide surge tolerance limits, and neither the frequency spectrum nor the bandwidth are the focus of the signal noise.

IEEE Std C37.90.2-2004 [19] addresses radiated EMI. The focus of the standard is immunity to mobile communications devices. The test does include an amplitude modulated radiated frequency with a specified sweep frequency and provides evidence of some level of tolerance to corona EMI.

IEEE Std C37.90.3-2001 [20] addresses electrical interference that is applied to the enclosure through electrostatic discharge. The test wave form is a pulse that would include high-frequency components, and like IEEE Std C37.90.2-2004 [19] it would provide evidence of some level of tolerance to corona EMI.

There are three other IEEE standards that address signal interference, which include IEEE Std 1613-2003 [22], IEEE Std C37.90.2-2004 [19], and IEEE Std 1615-2007 [23].

CISPR 24 am 1-2001 [12] provides tolerance limits for equipment that bears some resemblance to the type of equipment that is used in substations.

D.3.4 Reducing corona generated radiated and conducted signal interference

Enclose switchyard and control house protection control and communications equipment in grounded metal enclosures to reduce the corona radiated EMI exposure of the equipment.

Proven methods to reduce conducted corona generated signal interference are given in the recommendations given in IEEE Std 525™-2007 [21].

Copyright © 2010 IEEE. All rights reserved.

Copyright The Institute of Electrical and Electronics Engineers, Inc.
Provided by IHS under license with IEEE
No reproduction or networking permitted without license from IHS

Order Number: 02120914
Sold to:EGAT [700166108393] - VARRIS.Y@EGAT.CO.TH,
Not for Resale,2016-09-15 03:57:47 UTC

D.4 Methods of reducing the probability of substation corona

Substation bus corona will probably occur. There is no physical law that supports any specific onset voltage. The probability that corona will occur depends on many factors, such as bus contamination, weather, and surface nicks, as well as on field voltage gradient.

Although substantial guidance is available from transmission-line research, past design practice is the best guidance for achieving acceptable audible noise and light-emission levels for substation buses.

Reducing the probability of insulator damage from corona is an area that is still evolving. Continued research is needed to develop design practices that will lead to determination of a corona probability that leads to an acceptable level of insulator tolerance for damage.

There is some probability that corona-generated interference will occur. Following good practices in design and specification of substation bus hardware assemblies, and proper installation of the hardware, will reduce the probability.

The specification of industry standard equipment EMI performance levels in some equipment standards will also reduce the probability of corona. For connectors, NEMA CC 1-2005 [27] provides an EMI performance level. Although not specifically a bus design component, ANSI C37.32-2002 [1] provides EMI performance requirements for air disconnect switches.

Although the scope of CISPR 18-3 Ed. 1.0-1996 [11] is transmission lines, the guidance available can be extended to the substation bus design practices. In addition, the focus of IEC 61284 Ed. 2.0-1998 [15] is transmission lines, but the testing guidance may be used in the specification of substation bus hardware. However, corona EMI levels are not included in that standard.

If there is a desire to calculate a level of corona onset voltage gradient, without any indication of the probability of occurrence, the simplistic approach in the variation of Peek's equation (see equations under) may be used. The calculation result can be compared with the maximum field gradient using the theoretical equations also given in this guide.

However, any design change made to the bus diameter is not soundly made with this approach. Any change in bus conductor size will be made without any knowledge of the change in corona probability.

D.4.1 Measurement of substation EMI

Instrumentation to be used in the measurement of EMI is covered in ANSI C63.2-1996 [2] as well as in CISPR 16-1-1 Ed. 2.2-2007 [3] through CISPR 16-1-5 Ed. 1.0-2003 [7].

Methods for measurement are covered in NEMA 107 [28], CISPR 16-2-1 Ed. 2.0-2008 [8], CISPR 16-2-2 Ed. 1.2-2005 [9], and 16-2-3 Ed. 2.0-2006 [10].

Inspection of operational substation for corona is addressed in an EPRI Report #1001792 [14].

D.5 Calculations of maximum voltage gradient

The maximum voltage gradient on the surface of the conductor can be calculated for different conductor configurations as follows.

Copyright © 2010 IEEE. All rights reserved.

Copyright The Institute of Electrical and Electronics Engineers, Inc.
Provided by IHS under license with IEEE
No reproduction or networking permitted without license from IHS

Order Number: 02120914
Sold to:EGAT [700166108393] - VARRIS.Y@EGAT.CO.TH,
Not for Resale,2016-09-15 03:57:47 UTC

D.5.1 Single conductors

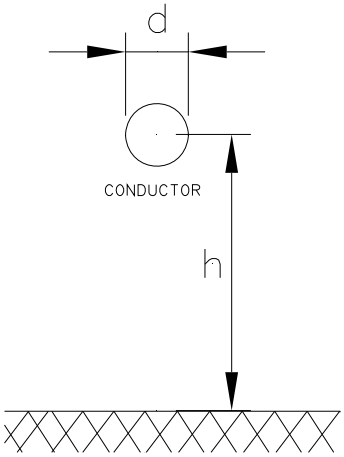

Figure D.2—Single conductor

$$E_a = \frac{V_1}{\frac{d}{2} \times \ln\left(\frac{4h}{d}\right)} \quad \text{(D.4)}$$

$$E_m = \frac{h}{h - d/2} E_a \quad \text{(D.5)}$$

where

E_a is the average voltage gradient at the surface of the conductor, kV/cm [kV/in]
E_m is the maximum voltage gradient at the surface of the conductor, kV/cm [kV/in]
V_1 is the line-to-ground test voltage, kV
d is the conductor diameter (Figure D.2)
h is the conductor center distance from ground, cm [in]

Copyright © 2010 IEEE. All rights reserved.

Copyright The Institute of Electrical and Electronics Engineers, Inc.
Provided by IHS under license with IEEE
No reproduction or networking permitted without license from IHS

Order Number: 02120914
Sold to:EGAT [700166108393] - VARRIS.Y@EGAT.CO.TH,
Not for Resale,2016-09-15 03:57:47 UTC

D.5.2 Three-phase conductor

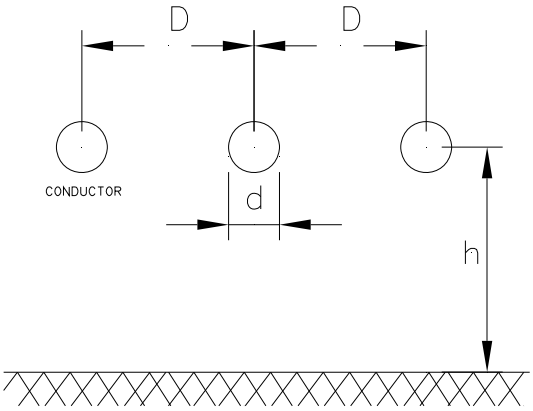

Figure D.3—Three-phase conductor

$$E_a = \frac{V_1}{\frac{d}{2} \times \ln\left(\frac{4h_e}{d}\right)} \tag{D.6}$$

$$E_m = \frac{h_e}{h_e - d/2} E_a \tag{D.7}$$

$$h_e = \frac{h\,D}{\sqrt{4h^2 + D^2}} \tag{D.8}$$

where in addition to the previous variable definitions:

h_e is the equivalent distance from center of conductor to ground plane for three phases, cm [in]
D is the phase-to-phase spacing for three phases, cm [in] (Figure D.3)

NOTE—V_1 is 110% of nominal operating line-to-ground voltage.

For the three-phase configuration, the center conductor has a gradient approximately 5% higher than the outside conductors. For bundled circular conductors, formulas for calculating the surface voltage gradient may be obtained from NEMA CC 1-2005 [27].

For satisfactory operation, E_m must be less than E_o.

Copyright © 2010 IEEE. All rights reserved.

Copyright The Institute of Electrical and Electronics Engineers, Inc.
Provided by IHS under license with IEEE
No reproduction or networking permitted without license from IHS

Order Number: 02120914
Sold to:EGAT [700166108393] - VARRIS.Y@EGAT.CO.TH,
Not for Resale,2016-09-15 03:57:47 UTC

D.5.3 Bundle conductor—single phase

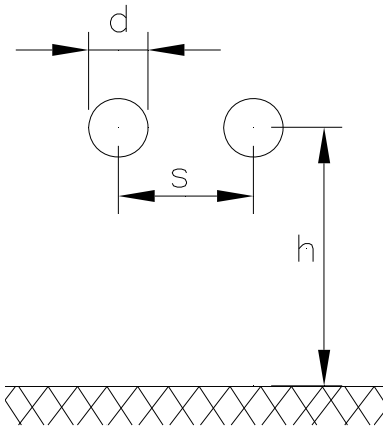

Figure D.4—Bundle conductor—single phase

$$E_a = \frac{V_1}{nr \ln\left(\frac{2h}{r_e}\right)} \tag{D.9}$$

$$E_m = \frac{h}{h - r_e} \cdot E_a \tag{D.10}$$

where E_a is defined in Equation (D.5) and where in addition to the previous variable definitions:

n is the number of subconductors in bundle
g is equal to 1 for bundle of 1, 2, or 3 subconductors and is equal to 1.12 for bundle of 4 subconductors
d is the conductor diameter, cm [in]
s is the distance between conductors, cm [in] (Figure D.4)
r is the conductor radius, cm [in] and is given by $d/2$
r_e is the equivalent single-conductor radius of bundle subconductors, cm [in], is given by:

$$r_e = r\left(g \times \frac{s}{r}\right)^{\frac{n-1}{n}} \tag{D.11}$$

For satisfactory operation, E_m must be less an E_o.

Copyright © 2010 IEEE. All rights reserved.

Copyright The Institute of Electrical and Electronics Engineers, Inc.
Provided by IHS under license with IEEE
No reproduction or networking permitted without license from IHS

Order Number: 02120914
Sold to:EGAT [700166108393] - VARRIS.Y@EGAT.CO.TH,
Not for Resale,2016-09-15 03:57:47 UTC

D.5.4 Bundle conductor—three phase

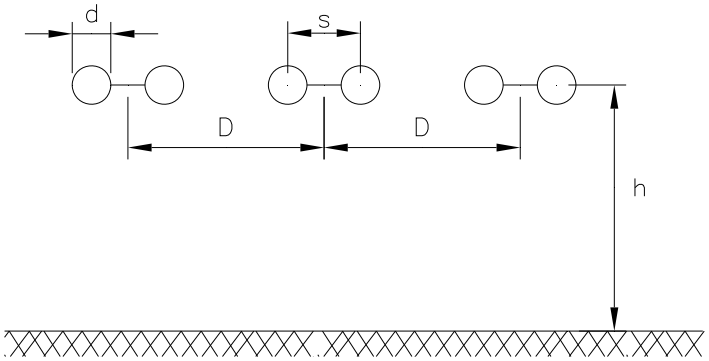

Figure D.5—Bundle conductor—three phase

$$E_a = \frac{V_1}{nr \ln\left(\frac{2h_e}{r_e}\right)} \tag{D.12}$$

$$E_m = \frac{h_e}{h_e - r_e} E_a \tag{D.13}$$

where h_e is defined in Equation (D.8) and r_e is defined by Equation (D.11). All other variables are defined in D.5.3.

D.6 Glossary

***corona*:** A chain of ionization events in the air surrounding an electrode. When the electric field intensity at the conductor surface is above a certain critical value, sometimes referred to as a "corona onset gradient," there is a partial breakdown of the air near the highly stressed electrode and the formation of corona discharges.

***gap discharge*:** Complete breakdown of air insulation between two electrodes separated by a short gap is known as a gap discharge.

***electromagnetic interference (EMI)*:** Degradation of the performance of a device, a piece of equipment, or a system caused by an electromagnetic disturbance. Note: The English words "interference" and "disturbance" are often used interchangeably.

Copyright © 2010 IEEE. All rights reserved.

Copyright The Institute of Electrical and Electronics Engineers, Inc.
Provided by IHS under license with IEEE
No reproduction or networking permitted without license from IHS

Order Number: 02120914
Sold to:EGAT [700166108393] - VARRIS.Y@EGAT.CO.TH,
Not for Resale,2016-09-15 03:57:47 UTC

D.7 References

[1] ANSI C37.32-2002, American National Standard for High Voltage Switches, Bus Supports, and Accessories Schedules of Preferred Ratings, Construction Guidelines, and Specifications.[40]

[2] ANSI C63.2-1996, American National Standard for Electromagnetic Noise and Field Strength Instrumentation, 10 Hz to 40 GHz—Specifications—Description.

[3] CISPR 16-1-1 Ed. 2.2-2007, Specification for Radio Disturbance and Iimmunity Measuring Apparatus and Methods—Part 1-1: Radio Disturbance and Immunity Measuring Apparatus—Measuring Apparatus.[41]

[4] CISPR 16-1-2 Ed. 1.2-2009, Specification for Radio Disturbance and Immunity Measuring Apparatus and Methods—Part 1-2: Radio Disturbance and Immunity Measuring Apparatus—Ancillary Equipment—Conducted Disturbances.

[5] CISPR 16-1-3 Ed. 2.0-2006, Specification for Radio Disturbance and Immunity Measuring Apparatus and Methods—Part 1-3: Radio Disturbance and Immunity Measuring Apparatus—Ancillary Equipment—Disturbance Power.

[6] CISPR 16-1-4 Ed. 2.1-2008, Specification for Radio Disturbance and Immunity Measuring Apparatus and Methods—Part 1-4: Radio Disturbance and Immunity Measuring Apparatus—Ancillary Equipment—Radiated Disturbances.

[7] CISPR 16-1-5 Ed. 1.0-2003, Specification for Radio Disturbance and Immunity Measuring Apparatus and Methods—Part 1-5: Radio Disturbance and Immunity Measuring Apparatus—Antenna Calibration Test Sites for 30 MHz to 1 000 MHz.

[8] CISPR 16-2-1 Ed. 2.0-2008, Specification for Radio Disturbance and Immunity Measuring Apparatus and Methods—Part 2-1: Methods of Measurement of Disturbances and Immunity—Conducted Disturbance Measurements.

[9] CISPR 16-2-2 Ed. 1.2-2005, Specification for Radio Disturbance and Immunity Measuring Apparatus and Methods—Part 2-2: Methods of Measurement of Disturbances and Immunity—Measurement of Disturbance Power.

[10] CSIPR 16-2-3 Ed. 2.0-2006, Specification for Radio Disturbance and Immunity Measuring Apparatus and Methods—Part 2-3: Methods of Measurement of Disturbances and Immunity—Radiated Disturbance Measurements.

[11] CISPR 18-3 Ed. 1.0-1996, Radio Interference Characteristics of Overhead Power Lines and High-Voltage Equipment—Part 3: Code of Practice for Minimizing the Generation of Radio Noise.

[12] CISPR 24 am 1-2001, Information Technology Equipment—Immunity Characteristics—Limits and Methods of Measurement.

[13] Electronic Power Research Institute, *EPRI Transmission Line Reference Book-200 kV and Above, Third Edition: The "Red Book.*" Palo Alto, CA: EPRI, 2008.[42]

[14] EPRI Report # 1001792, Guide to Corona and Arcing Inspection of Substations, 2002.

[15] IEC 61284 Ed. 2.0-1998, Overhead Lines—Requirements and Tests for Fittings.[43]

[40] ANSI publications are available from the Sales Department, American National Standards Institute, 25 West 43rd Street, 4th Floor, New York, NY 10036, USA (http://www.ansi.org/).

[41] CISPR documents are available from the International Electrotechnical Commission, 3, rue de Varembé, Case Postale 131, CH 1211, Genève 20, Switzerland/Suisse (http://www.iec.ch/). They are also available in the United States from the Sales Department, American National Standards Institute, 11 West 42nd Street, 13th Floor, New York, NY 10036, USA.

[42] EPRI publications are available from the Electric Research and Power Institute, 3420 Hillview Avenue, Palo Alto, CA 94304 (www.epri.com).

Copyright © 2010 IEEE. All rights reserved.

Copyright The Institute of Electrical and Electronics Engineers, Inc.
Provided by IHS under license with IEEE
No reproduction or networking permitted without license from IHS

Order Number: 02120914
Sold to:EGAT [700166108393] - VARRIS.Y@EGAT.CO.TH,
Not for Resale,2016-09-15 03:57:47 UTC

[16] IEEE Committee Report, "Transmission system radio influence," *IEEE Transactions on Power Apparatus and Systems*, vol. 84, pp. 714, Aug. 1965.[44]

[17] IEEE Std C37.90™-2005, IEEE Standard for Relays and Relay Systems Associated with Electric Power Apparatus.[45]

[18] IEEE Std C37.90.1™-2002, IEEE Standard for Surge Withstand Capability (SWC) Tests for Relays and Relay Systems Associated with Electric Power Apparatus.

[19] IEEE Std C37.90.2™-2004, IEEE Standard for Surge Withstand Capability of Relay Systems to Radiated Electromagnetic Interference from Transceivers.

[20] IEEE Std C37.90.3™-2001 (Reaff 2006), IEEE Standard Electrostatic Discharge Tests for Protective Relays.

[21] IEEE Std 525™-2007, IEEE Guide for the Design and Installation of Cable Systems in Substations.

[22] IEEE Std 1613™-2003, IEEE Standard Environmental and Testing Requirements for Communications Networking Devices in Electric Power Substations.

[23] IEEE Std 1615™-2007, IEEE Recommended Practice for Network Communication in Electric Power Substations.

[24] Juette, G. W., "Comparison of radio noise prediction methods with CIGRE/IEEE survey results," *IEEE Transactions on Power Apparatus and Systems*, vol. PAS-92, no. 3, pp. 1029–1042, May/June 1973.

[25] Leslie, J. R., Bailey, B. M., Craine, L. B., Eteson, D. C., Grieves, R. E., Janischewskyj, W., Juette, G. W., and Taylor, E. R., "Radio noise design guide for high-voltage transmission lines," *IEEE Transactions on Power Apparatus and Systems*, vol. 90, no. 2, pp. 833–842, Mar./Apr. 1971.

[26] Mercure, H. P., "Insulator pollution performance at high altitudes: major trends," *IEEE Transactions Power Delivery*, vol. 4, no. 2, pp. 1461–1468, April 1989.

[27] NEMA CC 1-2005, Electric Power Connection for Substations.[46]

[28] NEMA 107, Methods of Measurement of Radio Influence Voltage (RIV) of High Voltage Apparatus.

[29] Peek, F. W., *Dielectric Phenomena in High-Voltage Engineering*. New York: McGraw-Hill, 1929.

[43]IEC publications are available from the Sales Department of the International Electrotechnical Commission, Case Postale 131, 3 rue de Varembé, CH-1211, Genève 20, Switzerland/Suisse (http://www.iec.ch/). IEC publications are also available in the United States from the Sales Department, American National Standards Institute, 11 West 42nd Street, 13th Floor, New York, NY 10036, USA.

[44]IEEE publications are available from the Institute of Electrical and Electronics Engineers, 445 Hoes Lane, Piscataway, NJ 08854, USA (http://standards.ieee.org/).

[45]The IEEE standards or products referred to in this clause are trademarks owned by the Institute of Electrical and Electronics Engineers, Incorporated.

[46]NEMA publications are available from Global Engineering Documents, 15 Inverness Way East, Englewood, Colorado 80112, USA (http://global.ihs.com/).

Copyright © 2010 IEEE. All rights reserved.

Copyright The Institute of Electrical and Electronics Engineers, Inc.
Provided by IHS under license with IEEE
No reproduction or networking permitted without license from IHS

Order Number: 02120914
Sold to:EGAT [700166108393] - VARRIS.Y@EGAT.CO.TH,
Not for Resale,2016-09-15 03:57:47 UTC

Annex E

(informative)

Physical properties of common bus conductors

Table descriptions:

E.1 All-Aluminum Conductor (AAC), Aluminum Alloy 1350, Concentric-Lay Stranded Per ASTM B231

E.2 All-Aluminum Conductor (AAC), Aluminum Alloy 6201-T81, Concentric-Lay Stranded Per ASTM B399

E.3 Aluminum Conductor, Coated-Steel Reinforced (ACSR), Concentric-Lay Stranded Per ASTM B232

E.4 Aluminum Conductor, Coated-Steel Reinforced (ACSR), Standard Metric Conductor Sizes Per ASTM B232

E.5 Aluminum Conductor, Aluminum-Clad Steel Reinforced (ACSR/AW), Concentric-Lay Stranded Per ASTM B549

E.6 Aluminum Conductor, Aluminum-Alloy Reinforced (ACAR, 1350/6201), Concentric-Lay Stranded Per ASTM B524

E.7 Aluminum Conductor, Aluminum-Alloy Reinforced (ACAR, 1350/6201), Standard Metric Conductor Sizes per ASTM B524

E.8 Aluminum Conductor, Coated Steel Supported (ACSS), Concentric-Lay Stranded Per ASTM B856

E.9 Copper Conductor, Hard-Drawn, Concentric-Lay Stranded Per ASTM B1 and ASTM B8

E.10 Copper Conductor, Medium-Hard-Drawn, Concentric-Lay Stranded Per ASTM B2 and ASTM B8

E.11 Tubular Aluminum Conductor Per ANSI H35.2

E.12 Tubular Copper Conductor Per ASTM B-188

Copyright © 2010 IEEE. All rights reserved.

Copyright The Institute of Electrical and Electronics Engineers, Inc.
Provided by IHS under license with IEEE
No reproduction or networking permitted without license from IHS

Order Number: 02120914
Sold to:EGAT [700166108393] - VARRIS.Y@EGAT.CO.TH,
Not for Resale,2016-09-15 03:57:47 UTC

Table E.1—Physical properties of common bus conductors
AAC aluminum alloy 1350, concentric-lay stranded per ASTM B231

Conductor size		Code word per aluminum association publication 50	ASTM stranding class (NOTE 1)	Number of strands	Overall conductor diameter		Mass		Rated strength	
mm^2	AWG or cmils				mm	in	kg per km	lbs per 1000 ft	kN	kips
1773	3 500 000	Bluebonnet	A	127	54.81	2.158	4977	3345	261	58.7
1520	3 000 000	Trillium	A	127	50.70	1.996	4226	2840	223	50.3
1393	2 750 000	Bitterroot	A	91	48.59	1.913	3872	2602	205	46.1
1267	2 500 000	Lupine	A	91	46.30	1.823	3519	2365	186	41.9
1140	2 250 000	Sagebrush	A	91	43.92	1.729	3166	2128	167	37.7
1013	2 000 000	Cowslip	A	91	41.40	1.630	2787	1873	153	34.2
886.7	1 750 000	Jessamine	AA	61	38.74	1.525	2442	1641	132	29.7
805.7	1 590 000	Coreopsis	AA	61	36.93	1.454	2216	1489	120	27.0
765.4	1 510 000	Gladiolus	AA,A	61	35.99	1.417	2108	1417	114	25.6
725.1	1 431 000	Carnation	AA,A	61	35.03	1.379	1997	1342	108	24.3
694.8	1 351 000	Columbine	AA,A	61	34.04	1.340	1884	1266	104	23.4
644.5	1 272 000	Narcissus	AA,A	61	33.02	1.300	1774	1192	98.1	22.0
604.2	1 192 500	Hawthorn	AA,A	61	31.95	1.258	1662	1117	93.5	21.1
564.0	1 113 000	Marigold	AA,A	61	30.89	1.216	1553	1044	87.3	19.7
523.7	1 033 500	Bluebell	AA	37	29.72	1.170	1441	968.4	78.8	17.7
523.7	1 033 500	Larkspur	A	61	29.77	1.172	1442	969.2	81.3	18.3
506.7	1 000 000	Hawkweed	AA	37	29.21	1.150	1395	937.3	76.2	17.2
506.7	1 000 000	Camellia	A	61	29.26	1.152	1394	936.8	78.3	17.7
483.4	954 000	Magnolia	AA	37	28.55	1.124	1331	894.5	72.6	16.4
483.4	954 000	Goldenrod	A	61	28.60	1.126	1331	894.8	75.0	16.9
456.0	900 000	Cockscomb	AA	37	27.74	1.092	1256	844.0	68.4	16.4
456.0	900 000	Snapdragon	A	61	27.79	1.094	1256	844.0	70.8	15.9
402.8	795 000	Arbutus	AA	37	26.06	1.026	1109	745.3	61.8	13.9
402.8	795 000	Lilac	A	61	26.11	1.028	1110	745.7	63.8	14.3
380.0	750 000	Petunia	AA	37	25.32	0.997	1046	703.2	58.6	13.1
380.0	750 000	Cattail	A	61	25.35	0.998	1046	703.2	60.3	13.5
362.6	715 500	Violet	AA	37	24.74	0.974	998.5	671	56.7	12.8
362.6	715 500	Nasturtium	A	61	24.77	0.975	998.5	671	58.4	13.1
354.7	700 000	Verbena	AA	37	24.46	0.963	975.7	655.7	55.4	12.5
354.7	700 000	Flag	A	61	24.49	0.964	975.8	655.8	57.1	12.9
329.4	650 000	Heuchera	AA	37	23.57	0.928	907.4	609.8	51.7	11.6
322.3	636 000	Orchid	AA,A	37	23.32	0.918	886.9	596.0	50.4	11.4
304.0	600 000	Meadowsweet	AA,A	37	22.63	0.891	836.3	562.0	47.5	10.7
282.0	556 500	Dahlia	AA	19	21.74	0.856	775.8	521.4	43.3	9.75
282.0	556 500	Mistletoe	A	37	21.79	0.858	775.7	521.3	44.3	9.94
253.3	500 000	Zinnia	AA	19	20.60	0.811	697.1	486.5	38.9	8.76
253.3	500 000	Hyacinth	A	37	20.65	0.813	696.8	486.3	40.5	9.11
241.7	477 000	Cosmos	AA	19	20.14	0.793	664.8	446.8	37.0	8.36
241.7	477 000	Syringa	A	37	20.19	0.795	664.8	446.8	38.6	8.69
228.0	450 000	Goldentuff	AA	19	19.53	0.769	627.6	421.8	35.0	7.89
201.4	397 500	Canna	AA,A	19	18.39	0.724	554.9	372.9	31.6	7.11
177.3	350 000	Daffodil	A	19	17.25	0.679	487.9	327.9	28.4	6.39
170.5	336 400	Tulip	A	19	16.92	0.666	469.5	315.5	27.3	6.15
152.0	300 000	Peony	A	19	15.98	0.629	418.3	281.4	24.3	5.48
135.2	266 800	Daisy	AA	7	14.88	0.586	372.3	250.2	21.4	4.83
135.2	266 800	Laurel	A	19	15.06	0.593	372.2	250.1	22.1	4.97

Copyright © 2010 IEEE. All rights reserved.

Copyright The Institute of Electrical and Electronics Engineers, Inc.
Provided by IHS under license with IEEE
No reproduction or networking permitted without license from IHS

Order Number: 02120914
Sold to:EGAT [700166108393] - VARRIS.Y@EGAT.CO.TH,
Not for Resale,2016-09-15 03:57:47 UTC

Table E.1—Physical properties of common bus conductors
AAC aluminum alloy 1350, concentric-lay stranded per ASTM B231

Conductor size		Code word per aluminum association publication 50	ASTM stranding class (NOTE 1)	Number of strands	Overall conductor diameter		Mass		Rated strength	
mm^2	AWG or cmils				mm	in	kg per km	lbs per 1000 ft	kN	kips
126.7	250 000	Sneezewort	AA	7	14.40	0.567	348.8	234.4	20.1	4.52
126.7	250 000	Valerian	A	19	14.58	0.574	348.6	234.3	20.7	4.66
107.2	4/0	Oxlip	AA,A	7	13.26	0.522	295.2	198.4	17.0	3.83
85.0	3/0	Phlox	AA,A	7	11.79	0.464	233.9	157.2	13.5	3.04
67.4	2/0	Aster	AA,A	7	10.52	0.414	185.7	124.8	11.1	2.51

NOTE 1—See 6.4.1 for ASTM stranding description.

NOTE 2—The metric values listed above represent a soft conversion and as such may not be the same as metric masses calculated from basic metric density.

NOTE 3—See Table 1 for common properties of aluminum and copper.

NOTE 4—Conversion factors:

1 in = 25.4 mm
1 cmil = 0.0005067 mm^2
1 lb/1000 ft = 1.488 kg/km
1 lb = 0.4536 kg
1 lbf = 0.004448 kN
1 kip = 1000 lbf

Copyright © 2010 IEEE. All rights reserved.

Copyright The Institute of Electrical and Electronics Engineers, Inc.
Provided by IHS under license with IEEE
No reproduction or networking permitted without license from IHS

Order Number: 02120914
Sold to:EGAT [700166108393] - VARRIS.Y@EGAT.CO.TH,
Not for Resale,2016-09-15 03:57:47 UTC

Table E.2—Physical properties of common bus conductors
AAC, aluminum alloy 6201-T81, concentric-lay stranded per ASTM B399

Conductor size		ASTM stranding class	Number of strands	Overall conductor diameter		Mass		Rated strength	
mm^2	AWG or cmils			mm	in	kg per km	lbs per 1000 ft	kN	kips
886	1 750 000	AA	61	38.74	1.525	2431	1632	251	56.9
759	1 500 000	AA	61	35.84	1.411	2082	1399	215	48.8
631	1 250 000	AA	61	32.72	1.288	1732	1165	179	40.6
508	1 000 000	AA	37	29.24	1.151	1393	932.5	146	32.9
456	900 000	AA	37	27.74	1.092	1250	839.7	131	29.6
404	800 000	AA	37	26.14	1.029	1109	745.6	116	26.3
381	750 000	AA	37	25.32	0.997	1045	699.6	109	24.7
354	700 000	AA	37	24.46	0.963	971.2	652.3	101	23.0
330	650 000	AA	37	23.57	0.928	905.5	605.7	94.9	21.4
303	600 000	AA,A	37	22.63	0.891	831.9	559.1	91.0	20.6
279	550 000	AA,A	37	21.67	0.853	766.2	512.7	83.9	18.9
253	500 000	AA	19	20.60	0.811	695.0	466.1	74.2	16.8
228	450 000	AA	19	19.56	0.770	626.0	419.6	66.8	15.1
203	400 000	AA,A	19	18.44	0.726	557.5	373.0	59.5	13.4
178	350 000	A	19	17.25	0.679	487.3	326.3	52.0	11.8
152	300 000	A	19	15.98	0.629	416.7	280.0	46.6	10.5
126	250 000	A	19	14.58	0.574	346.7	233.1	38.8	8.76
107	4/0	AA,A	7	13.26	0.522	294.7	197.4	32.5	7.34
84.9	3/0	AA,A	7	11.79	0.464	233.0	156.4	25.7	5.82
67.3	2/0	AA,A	7	10.52	0.414	184.8	124.1	20.4	4.62
53.5	1/0	AA,A	7	9.35	0.368	146.8	98.43	17.0	3.82
33.5	2	AA,A	7	7.42	0.292	92.00	61.92	10.6	2.40
21.1	4	A	7	5.89	0.232	57.90	38.90	6.69	1.51
13.2	6	A	7	4.67	0.184	36.20	24.49	4.18	0.949

NOTE 1—See Table E.1 for general notes.

Copyright © 2010 IEEE. All rights reserved.

Copyright The Institute of Electrical and Electronics Engineers, Inc.
Provided by IHS under license with IEEE
No reproduction or networking permitted without license from IHS

Order Number: 02120914
Sold to:EGAT [700166108393] - VARRIS.Y@EGAT.CO.TH,
Not for Resale,2016-09-15 03:57:47 UTC

Copyright The Institute of Electrical and Electronics Engineers, Inc.
Provided by IHS under license with IEEE
No reproduction or networking permitted without license from IHS

Table E.3—Physical properties of common bus conductors
ACSR, concentric-lay stranded per ASTM B232

Conductor size AWG or cmils	Code word per aluminum association publication 50	ASTM stranding class	Stranding design Alum/steel	Nominal OD In	Mass lbs/1000 ft	Rated strength by type of steel core wire (NOTE 2)				
						ACSR/GA ACSR/MA kips	ACSR/GB ACSR/MB kips	ACSR/GC ACSR/MC kips	ACSR/HS ACSR/MS kips	ACSR/AZ kips
2 312 000	Thrasher	AA	76/19	1.802	2523	56.7	55.8	54.8	58.5	54.8
2 167 000	Kiwi	AA	72/7	1.735	2301	49.8	49.1	48.4	51.3	48.1
2 156 000	Bluebird	AA	84/19	1.762	2508	60.3	59.0	57.7	62.8	57.1
1 780 000	Chukar	AA	84/19	1.602	2072	51.0	49.9	48.9	53.1	48.9
1 590 000	Falcon	AA	54/19	1.545	2042	54.5	53.0	51.6	57.5	50.8
1 590 000	Lapwing	AA	45/7	1.504	1790	42.2	41.4	40.5	43.9	39.7
1 510 500	Parrot	AA	54/19	1.505	1938	51.7	50.3	48.9	54.5	48.2
1 510 500	Nuthatch	AA	45/7	1.466	1700	40.1	39.3	38.5	41.6	37.7
1 431 000	Plover	AA	54/19	1.465	1838	49.1	47.7	46.4	51.7	45.7
1 431 000	Bobolink	AA	45/7	1.427	1611	38.3	37.6	36.9	39.8	36.5
1 351 500	Martin	AA	54/19	1.424	1735	46.3	45.1	43.8	48.8	43.2
1 351 500	Dipper	AA	45/7	1.386	1521	36.2	35.5	34.8	37.6	34.4
1 272 000	Pheasant	AA	54/19	1.382	1634	43.6	42.4	41.2	46.0	40.7
1 272 000	Bittern	AA	45/7	1.345	1432	34.1	33.4	32.8	35.4	32.4
1 272 000	Skylark	AA	36/1	1.316	1286	26.4	26.1	26.0	27.0	25.4
1 192 500	Grackle	AA	54/19	1.338	1531	41.9	40.8	39.7	44.1	39.7
1 192 500	Bunting	AA	45/7	1.302	1342	32.0	31.3	30.7	33.2	30.4
1 113 000	Finch	AA	54/19	1.293	1430	39.1	38.1	37.0	41.2	37.0
1 113 000	Bluejay	AA	45/7	1.259	1254	29.8	29.3	28.7	31.0	28.4
1 033 500	Curlew	AA	54/7	1.245	1329	36.6	35.6	34.6	38.6	33.6
1 033 500	Ortolan	AA	45/7	1.212	1163	27.7	27.1	26.6	28.8	26.3
1 033 500	Tanager	AA	36/1	1.186	1044	21.4	21.2	21.1	21.9	20.6
954 000	Cardinal	AA	54/7	1.196	1227.1	33.8	32.9	32.0	35.7	31.0
954 000	Rail	AA	45/7	1.165	1074	25.9	25.4	24.9	26.9	24.7
954 000	Catbird	AA	36/1	1.140	964	19.8	19.6	19.5	20.3	19.1
900 000	Canary	AA	54/7	1.162	1158	31.9	31.0	30.2	33.7	29.3
900 000	Ruddy	AA	45/7	1.131	1013	24.4	24.0	23.5	25.4	23.3
795 000	Mallard	AA	30/19	1.140	1233.9	38.4	37.1	35.8	41.1	35.1
795 000	Condor	AA	54/7	1.092	1022	28.2	27.4	26.6	29.7	25.8
795 000	Tern	AA	45/7	1.063	895	22.1	21.7	21.2	22.9	21.2
795 000	Drake	AA	26/7	1.108	1093	31.5	30.5	29.6	33.5	28.6
795 000	Cuckoo	AA	24/7	1.092	1023	27.9	27.1	26.4	29.5	25.6
795 000	Coot	AA	36/1	1.040	803.6	16.8	16.6	16.5	17.2	16.3
715 500	Redwing	AA	30/19	1.081	1109.3	34.6	33.4	32.2	36.9	31.6
715 500	Starling	AA	26/7	1.051	983.7	28.4	27.5	26.6	30.1	25.7
715 500	Stilt	AA	24/7	1.036	921	25.5	24.8	24.1	26.9	23.7

Order Number: 02120914
Sold to:EGAT,[7001661083931] - VARRIS.Y@EGAT.CO.TH,
Not for Resale,2016-09-15 03:57:47 UTC

Copyright © 2010 IEEE. All rights reserved.

Copyright The Institute of Electrical and Electronics Engineers, Inc.
Provided by IHS under license with IEEE
No reproduction or networking permitted without license from IHS

Table E.3—Physical properties of common bus conductors
ACSR, concentric-lay stranded per ASTM B232

Conductor size AWG or cmils	Code word per aluminum association publication 50	ASTM stranding class	Stranding design Alum/steel	Nominal OD In	Mass lbs/1000 ft	Rated strength by type of steel core wire (NOTE 2)				
						ACSR/GA ACSR/MA kips	ACSR/GB ACSR/MB kips	ACSR/GC ACSR/MC kips	ACSR/HS ACSR/MS kips	ACSR/AZ kips
666 600	Gannet	AA	26/7	1.014	916.2	26.4	25.6	24.8	28.0	24.0
666 600	Flamingo	AA	24/7	1.000	857.9	23.7	23.1	22.4	25.0	22.1
636 000	Egret	AA	30/19	1.019	987.2	31.5	30.5	29.4	33.6	29.4
636 000	Scoter	AA	30/7	1.019	995.1	30.4	29.3	28.7	33.2	27.6
636 000	Grosbeak	AA	26/7	0.990	874.2	25.2	24.4	23.6	26.8	22.9
636 000	Rook	AA	24/7	0.977	818.2	22.6	22.0	21.4	23.9	21.1
636 000	Swift	AA	36/1	0.930	642.8	13.8	13.6	13.5	14.0	13.4
636 000	Kingbird	AA	18/1	0.940	689.9	15.7	15.4	15.3	16.3	14.8
605 000	Teal	AA	30/19	0.994	938.6	30.0	29.0	28.0	32.0	28.0
605 000	Wood Duck	AA	30/7	0.994	946.5	28.9	27.9	27.3	31.6	26.3
605 000	Squab	AA	26/7	0.966	831.3	24.3	23.6	22.8	25.8	22.5
605 000	Peacock	AA	24/7	0.953	778.8	21.6	21.0	20.4	22.7	20.1
556 500	Eagle	AA	30/7	0.953	870.7	27.8	26.8	25.8	29.7	24.8
556 500	Dove	AA	26/7	0.927	765.2	22.6	21.9	21.2	24.0	20.9
556 500	Parakeet	AA	24/7	0.914	716.1	19.8	19.3	18.7	20.9	18.5
556 500	Osprey	AA	18/1	0.879	603.3	13.7	13.5	13.4	14.3	12.9
477 000	Hen	AA	30/7	0.883	746.4	23.8	23.0	22.1	25.5	21.3
477 000	Hawk	AA	26/7	0.858	655.3	19.5	18.9	18.4	20.7	18.1
477 000	Flicker	AA	24/7	0.846	613.9	17.2	16.7	16.2	18.1	16.0
477 000	Pelican	AA	18/1	0.814	517.3	11.8	11.6	11.5	12.3	11.1
397 500	Lark	AA	30/7	0.806	621.8	20.3	19.6	18.9	21.7	18.6
397 500	Ibis	AA	26/7	0.783	546.0	16.3	15.8	15.3	17.2	15.1
397 500	Brant	AA	24/7	0.772	511.4	14.6	14.3	13.9	15.4	13.9
397 500	Chickadee	AA	18/1	0.743	431.0	9.9	9.8	9.7	10.4	9.5
336 400	Oriole	AA	30/7	0.741	526.4	17.3	16.7	16.2	18.5	15.9
336 400	Linnet	AA	26/7	0.720	462.0	14.1	13.7	13.3	14.9	13.3
336 400	Merlin	AA	18/1	0.684	364.8	8.7	8.5	8.4	9.0	8.3
300 000	Ostrich	AA	26/7	0.680	412.2	12.7	12.3	12.0	13.4	12.0
266 800	Partridge	AA	26/7	0.642	366.9	11.3	11.0	10.6	11.9	10.6
266 800	Waxwing	AA	18/1	0.609	289.1	6.9	6.8	6.7	7.1	6.5
211 600	Penguin	AA	6/1	0.563	290.8	8.35	8.08	7.95	9.01	7.42
211 300	Cochin	AA(HS)	12/7	0.664	526.8	20.7	19.8	18.9	22.6	17.9
203 200	Brahma	AA(HS)	16/9	0.714	674.6	28.4	27.1	25.8	31.1	25.1
190 800	Dorking	AA(HS)	12/7	0.631	475.7	18.7	17.9	17.0	20.4	16.2
176 900	Dotterel	AA(HS)	12/7	0.607	440.9	17.3	16.6	15.8	18.9	15.0
167 800	Pigeon	AA,A	6/1	0.502	230.5	6.62	6.41	6.30	7.15	5.88

Order Number: 02120914
Sold to:EGAT,[7001661083931] - VARRIS.Y@EGAT.CO.TH,
Not for Resale,2016-09-15 03:57:47 UTC

Copyright © 2010 IEEE. All rights reserved.

Copyright The Institute of Electrical and Electronics Engineers, Inc.
Provided by IHS under license with IEEE
No reproduction or networking permitted without license from IHS

Table E.3—Physical properties of common bus conductors
ACSR, concentric-lay stranded per ASTM B232

Conductor size AWG or cmils	Code word per aluminum association publication 50	ASTM stranding class	Stranding design Alum/steel	Nominal OD In	Mass lbs/1000 ft	Rated strength by type of steel core wire (NOTE 2)				
						ACSR/GA ACSR/MA kips	ACSR/GB ACSR/MB kips	ACSR/GC ACSR/MC kips	ACSR/HS ACSR/MS kips	ACSR/AZ kips
159 000	Guinea	AA(HS)	12/7	0.576	396.3	16.0	15.3	14.6	17.4	14.2
134 600	Leghorn	AA(HS)	12/7	0.530	335.5	13.6	13.0	12.4	14.8	12.1
133 100	Quail	AA,A	6/1	0.447	182.8	5.30	5.13	5.05	5.72	4.88
110 800	Minorca	AA(HS)	12/7	0.481	276.3	11.3	10.8	10.3	12.2	10.1
105 600	Raven	AA,A	6/1	0.398	145.2	4.38	4.25	4.12	4.65	3.98

NOTE 1—See Table E.1 for general notes.

NOTE 2—Steel core abbreviations:

GA = Galvanized steel core wire, coating class A in accordance with ASTM B498.

GB = Galvanized steel core wire, coating class B in accordance with ASTM B498.

GC = Galvanized steel core wire, coating class C in accordance with ASTM B498.

HS = High strength galvanized steel core wire in accordance with ASTM B606.

MA = Zn-5A1-MM coated steel core wire, coating class A in accordance with ASTM B802.

MB = Zn-5A1-MM coated steel core wire, coating class B in accordance with ASTM B802.

MC = Zn-5A1-MM coated steel core wire, coating class C in accordance with ASTM B802.

MS = High strength Zn-5A1-MM coated steel core wire in accordance with ASTM B803.

AZ = Aluminized steel core wire in accordance with ASTM B341.

Order Number: 0212094
Sold to:EGAT,[700166108393] - VARRIS.Y@EGAT.CO.TH,
Not for Resale,2016-09-15 03:57:47 UTC

Copyright © 2010 IEEE. All rights reserved.

Copyright The Institute of Electrical and Electronics Engineers, Inc.
Provided by IHS under license with IEEE
No reproduction or networking permitted without license from IHS

Table E.4—Physical properties of common bus conductors
ACSR, standard metric conductor sizes per ASTM B232

Conductor size mm^2	ASTM stranding class	Stranding design Alum/steel	Nominal OD mm	Mass kg/km	Rated strength by type of steel core wire (NOTE 2)				
					ACSR/GA ACSR/MA kN	ACSR/GB ACSR/MB kN	ACSR/GC ACSR/MC kN	ACSR/HS ACSR/MS kN	ACSR/AZ kN
1250	AA	84/19	47.85	4274	306	300	293	319	289
1250	AA	76/19	47.34	4023	269	265	260	278	260
1250	AA	72/7	46.99	3901	250	246	242	257	239
1120	AA	84/19	45.31	3833	275	269	263	286	259
1120	AA	76/19	44.74	3595	240	236	232	248	232
1120	AA	72/7	44.51	3499	226	223	219	232	218
1000	AA	84/19	42.77	3416	245	239	234	254	231
1000	AA	72/7	42.11	3132	202	199	196	208	195
900	AA	84/19	40.57	3073	226	221	217	236	217
900	AA	72/7	39.9	2812	181	179	176	186	175
800	AA	54/19	39.04	3015	240	233	227	252	223
800	AA	45/7	38.07	2652	186	182	179	193	175
710	AA	54/19	36.79	2678	213	207	201	224	198
710	AA	45/7	35.85	2351	167	164	160	173	158
630	AA	54/19	34.65	2375	189	184	179	199	176
630	AA	45/7	33.75	2084	148	145	142	153	140
560	AA	54/19	32.68	2112	173	168	164	182	164
560	AA	45/7	31.83	1854	132	129	126	136	125
500	AA	54/7	30.87	1889	154	150	145	163	141
500	AA	45/7	30.09	1656	118	115	113	122	112
450	AA	54/7	29.34	1706	139	135	131	147	128
450	AA	45/7	28.56	1492	108	106	104	112	103
400	AA	30/19	28.83	1824	170	164	158	181	155
400	AA	26/7	28.07	1622	139	135	131	148	126
400	AA	24/7	27.65	1515	123	120	116	130	113
355	AA	30/19	27.17	1620	151	146	140	161	137
355	AA	26/7	26.4	1435	123	119	115	131	112
355	AA	24/7	26.03	1343	111	108	105	117	103
315	AA	30/19	25.64	1443	138	133	128	147	128
315	AA	26/7	24.9	1277	110	106	103	117	99.3
315	AA	24/7	24.55	1194	98.7	96.0	93.2	104	91.7
315	AA	18/1	23.6	1014	68.0	66.8	66.3	70.8	64.0
280	AA	30/7	24.15	1291	122	118	113	131	109
280	AA	26/7	23.44	1131	100	97.2	94.1	106	92.4
280	AA	24/7	23.11	1058	87.5	85.1	82.6	92.0	81.2
280	AA	18/1	22.25	901	60.4	59.4	58.9	63.0	56.8

Order Number: 02120914
Sold to:EGAT,[7001661083931] - VARRIS.Y@EGAT.CO.TH,
Not for Resale,2016-09-15 03:57:47 UTC

Copyright © 2010 IEEE. All rights reserved.

Copyright The Institute of Electrical and Electronics Engineers, Inc.
Provided by IHS under license with IEEE
No reproduction or networking permitted without license from IHS

Table E.4—Physical properties of common bus conductors
ACSR, standard metric conductor sizes per ASTM B232

Conductor size mm^2	ASTM stranding class	Stranding design Alum/steel	Nominal OD mm	Mass kg/km	Rated strength by type of steel core wire (NOTE 2)				
					ACSR/GA ACSR/MA kN	ACSR/GB ACSR/MB kN	ACSR/GC ACSR/MC kN	ACSR/HS ACSR/MS kN	ACSR/AZ kN
250	AA	30/7	22.82	1152	109	105	101	117	97.4
250	AA	26/7	22.16	1011	89.5	86.8	84.1	94.6	82.5
250	AA	24/7	21.85	946	79.4	77.2	75.0	83.4	73.8
250	AA	18/1	21.05	806.4	54.1	53.1	52.7	56.4	50.9
200	AA	30/7	20.37	918.2	89.7	86.6	83.4	95.5	81.6
200	AA	26/7	19.81	808.3	71.5	69.3	67.2	75.6	65.9
200	AA	24/7	19.55	757.6	64.2	62.5	60.7	67.7	60.7
200	AA	18/1	18.8	643.2	43.1	42.4	42.1	45.0	41.3
180	AA	30/7	19.32	826.0	80.7	77.9	75.0	85.9	73.4
180	AA	26/7	18.81	728.6	65.4	63.4	61.4	69.0	60.3
180	AA	24/7	18.54	681.2	57.8	56.2	54.7	60.9	54.7
180	AA	18/1	17.85	579.9	40.4	39.7	39.1	41.4	38.1
160	AA	30/7	18.27	738.6	72.9	70.4	67.9	77.6	66.4
160	AA	26/7	17.74	648.0	58.9	57.2	55.4	62.4	55.4
160	AA	24/7	17.46	604.2	52.0	50.6	49.2	54.8	49.2
160	AA	18/1	16.8	513.7	35.8	35.2	34.6	37.0	34.0
140	AA	26/7	16.6	567.4	52.2	50.7	49.2	55.3	49.2
140	AA	24/7	16.38	531.8	46.4	45.2	44.0	48.9	44.0
140	AA	18/1	15.75	451.5	31.5	30.9	30.4	32.5	29.9
125	AA	26/7	15.64	503.7	46.9	45.6	44.2	49.6	44.2
125	AA	24/7	15.48	474.9	41.5	40.4	39.3	43.6	39.3
125	AA	18/1	14.85	401.3	28.8	28.3	27.9	29.7	27.6
100	AA(HS)	16/19	17.84	972.4	123	117	111	133	106
100	AA(HS)	12/7	16.3	734.1	85.9	82.0	78.0	93.8	74.1
100	AA,A	6/1	13.83	404.8	34.6	33.5	33.0	37.3	30.8
90	AA(HS)	12/7	15.45	659.5	77.2	73.6	70.1	84.2	66.6
80	AA(HS)	12/7	14.55	584.9	70.6	67.5	64.4	76.4	62.6
80	AA,A	6/1	12.36	323.3	27.6	26.7	26.4	29.8	24.6
71	AA(HS)	12/7	13.7	518.6	62.9	60.2	57.4	68.1	55.8
63	AA(HS)	12/7	12.95	463.4	56.2	53.8	51.3	60.8	49.9
63	AA,A	6/1	10.98	255.2	22.1	21.4	21.1	23.8	20.4
56	AA(HS)	12/7	12.2	411.2	50.2	48.0	45.8	54.3	44.5

Order Number: 02120914
Sold to:EGAT,[700166108393] - VARRIS.Y@EGAT.CO.TH,
Not for Resale,2016-09-15 03:57:47 UTC

Copyright © 2010 IEEE. All rights reserved.

Copyright The Institute of Electrical and Electronics Engineers, Inc.
Provided by IHS under license with IEEE
No reproduction or networking permitted without license from IHS

Table E.4—Physical properties of common bus conductors
ACSR, standard metric conductor sizes per ASTM B232

Conductor size mm^2	ASTM stranding class	Stranding design Alum/steel	Nominal OD mm	Mass kg/km	Rated strength by type of steel core wire (NOTE 2)				
					ACSR/GA ACSR/MA kN	ACSR/GB ACSR/MB kN	ACSR/GC ACSR/MC kN	ACSR/HS ACSR/MS kN	ACSR/AZ kN

NOTE 1—See Table E.1 for general notes.

NOTE 2—Steel core abbreviations:

GA = Galvanized steel core wire, coating class A in accordance with ASTM B498.

GB = Galvanized steel core wire, coating class B in accordance with ASTM B498.

GC = Galvanized steel core wire, coating class C in accordance with ASTM B498.

HS = High strength galvanized steel core wire in accordance with ASTM B606.

MA = Zn-5A1-MM coated steel core wire, coating class A in accordance with ASTM B802.

MB = Zn-5A1-MM coated steel core wire, coating class B in accordance with ASTM B802.

MC = Zn-5A1-MM coated steel core wire, coating class C in accordance with ASTM B802.

MS = High strength Zn-5A1-MM coated steel core wire in accordance with ASTM B803.

AZ = Aluminized steel core wire in accordance with ASTM B341.

Order Number: 0212094
Sold to:EGAT [7001661083931 - VARRIS.Y@EGAT.CO.TH,
Not for Resale,2016-09-15 03:57:47 UTC

Copyright © 2010 IEEE. All rights reserved.

Copyright The Institute of Electrical and Electronics Engineers, Inc.
Provided by IHS under license with IEEE
No reproduction or networking permitted without license from IHS

Table E.5—Physical properties of common bus conductors ACSR/AW, concentric-lay stranded per ASTM B549

Conductor size		Code word per aluminum association publication 50	ASTM stranding class	Stranding design	Nominal OD		Mass		Rated strength	
mm^2	cmils			Alum/ alum-clad steel	mm	in	kg/km	lbs/1000 ft	kN	kips
1,171	2 312 000	Thrasher/AW	AA	76/19	45.85	1.802	3,679	2472	246	55.3
1,098	2 167 000	Kiwi/AW	AA	72/7	44.07	1.735	3,366	2262	218	49.1
1,092	2 156 000	Bluebird/AW	AA	84/19	44.75	1.762	3,627	2437	262	59.0
902	1 780 000	Chukar/AW	AA	84/19	40.69	1.602	2,996	2013	220	49.4
806	1 590 000	Falcon/AW	AA	54/19	39.24	1.545	2,917	1960	236	53.0
806	1 590 000	Lapwing/AW	AA	45/7	38.20	1.504	2,598	1746	186	41.8
765	1 510 500	Parrot/AW	AA	54/19	38.23	1.505	2,768	1860	224	50.3
765	1 510 500	Nuthatch/AW	AA	45/7	37.24	1.466	2,467	1658	177	39.7
725	1 431 000	Plover/AW	AA	54/19	37.21	1.465	2,625	1764	212	47.7
725	1 431 000	Bobolink/AW	AA	45/7	36.24	1.427	2,336	1570	167	37.6
685	1 351 500	Martin/AW	AA	54/19	36.17	1.424	2,478	1665	201	45.1
685	1 351 500	Dipper/AW	AA	45/7	35.20	1.386	2,207	1483	158	35.5
645	1 272 000	Pheasant/AW	AA	54/19	35.10	1.382	2,333	1568	189	42.4
645	1 272 000	Bittern/AW	AA	45/7	34.16	1.345	2,078	1396	149	33.4
645	1 272 000	Skylark/AW	AA	36/1	33.43	1.316	1,893	1272	114	25.7
604	1 192 500	Grackle/AW	AA	54/19	33.99	1.338	2,188	1470	179	40.2
604	1 192 500	Bunting/AW	AA	45/7	33.07	1.302	1,948	1,309	139	31.3
564	1 113 000	Finch/AW	AA	54/19	32.84	1.293	2,043	1373	167	37.5
564	1 113 000	Bluejay/AW	AA	45/7	31.98	1.259	1,819	1222	130	29.3
524	1 033 500	Curlew/AW	AA	54/7	31.62	1.245	1,896	1274	158	35.6
524	1 033 500	Ortolan/AW	AA	45/7	30.78	1.212	1,688	1134	121	27.1
524	1 033 500	Tanager/AW	AA	36/1	30.12	1.186	1,537	1033	94	21.1
483	954 000	Cardinal/AW	AA	54/7	30.38	1.196	1,752	1177	146	32.9
483	954 000	Rail/AW	AA	45/7	29.59	1.165	1,558	1047	113	25.4
483	954 000	Catbird/AW	AA	36/1	28.96	1.140	1,420	954	87	19.5
456	900 000	Canary/AW	AA	54/7	29.51	1.162	1,653	1111	138	31.0
456	900 000	Ruddy/AW	AA	45/7	28.73	1.131	1,470	988	107	24.0
403	795 000	Mallard/AW	AA	30/19	28.96	1.140	1,726	1160	165	37.1
403	795 000	Condor/AW	AA	54/7	27.74	1.092	1,458	980	124	27.8
403	795 000	Tern/AW	AA	45/7	27.00	1.063	1,298	872	96	21.5
403	795 000	Drake/AW	AA	26/7	28.14	1.108	1,549	1041	136	30.5
403	795 000	Cuckoo/AW	AA	24/7	27.74	1.092	1,460	981	122	27.5
403	795 000	Coot/AW	AA	36/1	26.42	1.040	1,183	795	74	16.6
363	715 500	Redwing/AW	AA	30/19	27.46	1.081	1,552	1043	149	33.4
363	715 500	Starling/AW	AA	26/7	26.70	1.051	1,393	936	122	27.5
363	715 500	Stilt/AW	AA	24/7	26.31	1.036	1,314	883	110	24.8
338	666 600	Gannet/AW	AA	26/7	25.76	1.014	1,298	872	116	26.0

Order Number: 02120914
Sold to:EGAT,[700166108393] - VARRIS.Y@EGAT.CO.TH,
Not for Resale,2016-09-15 03:57:47 UTC

Copyright © 2010 IEEE. All rights reserved.

Copyright The Institute of Electrical and Electronics Engineers, Inc.
Provided by IHS under license with IEEE
No reproduction or networking permitted without license from IHS

Table E.5—Physical properties of common bus conductors ACSR/AW, concentric-lay stranded per ASTM B549

Conductor size		Code word per aluminum association publication 50	ASTM stranding class	Stranding design	Nominal OD		Mass		Rated strength	
mm^2	cmils			Alum/ alum-clad steel	mm	in	kg/km	lbs/1000 ft	kN	kips
338	666 600	Flamingo/AW	AA	24/7	25.40	1.000	1,225	823	103	23.1
322	636 000	Egret/AW	AA	30/19	25.88	1.019	1,381	928	133	29.9
322	636 000	Scoter/AW	AA	30/7	25.88	1.019	1,391	935	130	29.3
322	636 000	Grosbeak/AW	AA	26/7	25.15	0.990	1,238	832	110	24.8
322	636 000	Rook/AW	AA	24/7	24.82	0.977	1,168	785	98	22.0
322	636 000	Swift/AW	AA	36/1	23.62	0.930	946	636	61	13.6
322	636 000	Kingbird/AW	AA	18/1	23.88	0.940	1,006	676	67	15.0
307	605 000	Teal/AW	AA	30/19	25.25	0.994	1,314	883	127	28.5
307	605 000	Wood Duck/AW	AA	30/7	25.25	0.994	1,323	889	126	28.4
307	605 000	Squab/AW	AA	26/7	24.54	0.966	1,177	791	105	23.6
307	605 000	Peacock/AW	AA	24/7	24.21	0.953	1,112	747	93	21.0
282	556 500	Eagle/AW	AA	30/7	24.21	0.953	1,217	818	119	26.8
282	556 500	Dove/AW	AA	26/7	23.55	0.927	1,083	728	97	21.9
282	556 500	Parakeet/AW	AA	24/7	23.22	0.914	1,022	687	86	19.3
282	556 500	Osprey/AW	AA	18/1	22.33	0.879	880	591	59	13.2
242	477 000	Hen/AW	AA	30/7	22.43	0.883	1,043	701	104	23.4
242	477 000	Hawk/AW	AA	26/7	21.79	0.858	929	624	84	18.9
242	477 000	Flicker/AW	AA	24/7	21.49	0.846	877	589	74	16.7
242	477 000	Pelican/AW	AA	18/1	20.68	0.814	765	507	51	11.5
202	397 500	Lark/AW	AA	30/7	20.47	0.806	869	584	87	19.6
201	397 500	Ibis/AW	AA	26/7	19.89	0.783	774	520	70	15.8
201	397 500	Brant/AW	AA	24/7	19.61	0.772	731	491	63	14.1
201	397 500	Chickadee/AW	AA	18/1	18.87	0.743	628	422	44	9.8
170	336 400	Oriole/AW	AA	30/7	18.82	0.741	737	495	74	16.7
170	336 400	Linnet/AW	AA	26/7	18.29	0.720	655	440	60	13.5
170	336 400	Merlin/AW	AA	18/1	17.37	0.684	531	357	38	8.5
152	300 000	Ostrich/AW	AA	26/7	17.27	0.680	583	392	54	12.1
135	266 800	Partridge/AW	AA	26/7	16.31	0.642	519	349	48	10.8
135	266 800	Waxwing/AW	AA	18/1	15.47	0.609	421	283	30	6.8
107	211 600	Penguin/AW	AA	6/1	14.30	0.563	412	277	34	7.7
107	211 300	Cochin/AW	AA(HS)	12/7	16.86	0.664	710	477	88	19.8
103	203 200	Brahma/AW	AA(HS)	16/9	18.14	0.714	894	601	121	27.1
96.7	190 800	Dorking/AW	AA(HS)	12/7	16.03	0.631	641	431	81	18.3
89.6	176 900	Dotterel/AW	AA(HS)	12/7	15.42	0.607	594	399	75	16.9
85	167 800	Pigeon/AW	AA,A	6/1	12.75	0.502	326	219	28	6.3
80.6	159 000	Guinea/AW	AA(HS)	12/7	14.63	0.576	534	359	68	15.3
68.2	134 600	Leghorn/AW	AA(HS)	12/7	13.46	0.530	452	304	58	13.0

Order Number: 0212094
Sold to:EGAT [700166108393] - VARRIS.Y@EGAT.CO.TH,
Not for Resale,2016-09-15 03:57:47 UTC

Copyright © 2010 IEEE. All rights reserved.

Copyright The Institute of Electrical and Electronics Engineers, Inc.
Provided by IHS under license with IEEE
No reproduction or networking permitted without license from IHS

Table E.5—Physical properties of common bus conductors ACSR/AW, concentric-lay stranded per ASTM B549

Conductor size		Code word per aluminum association publication 50	ASTM stranding class	Stranding design	Nominal OD		Mass		Rated strength	
mm^2	cmils			Alum/ alum-clad steel	mm	in	kg/km	lbs/1000 ft	kN	kips
67.4	133 100	Quail/AW	AA,A	6/1	11.35	0.447	259	174	23	5.1
56.1	110 800	Minorca/AW	AA(HS)	12/7	12.22	0.481	372	250	48	10.8
53.5	105 600	Raven/AW	AA,A	6/1	10.11	0.398	205	138	19	4.3

NOTE 1—See Table E.1 for general notes.

Order Number: 0212094
Sold to:EGAT [700166108393] - VARRIS.Y@EGAT.CO.TH,
Not for Resale,2016-09-15 03:57:47 UTC

Copyright © 2010 IEEE. All rights reserved.

Copyright The Institute of Electrical and Electronics Engineers, Inc.
Provided by IHS under license with IEEE
No reproduction or networking permitted without license from IHS

Table E.6—Physical properties of common bus conductors
ACAR, 1350/6201, concentric-lay stranded per ASTM B524

Conductor size		Number of strands	Overall conductor diameter		Mass		Rated strength	
mm^2	AWG or cmils	Alum alloy 1350/6201	mm	in	kg per km	lbs per 1000 ft	kN	kips
1520	3 000 000	72/19	50.74	1.998	4221	2837	270	60.7
1520	3 000 000	63/28	50.74	1.998	4216	2835	287	64.5
1520	3 000 000	54/37	50.74	1.998	4218	2836	308	69.3
1393	2 750 000	72/19	48.56	1.912	3871	2601	247	55.6
1393	2 750 000	63/28	48.56	1.912	3860	2597	263	59.1
1393	2 750 000	54/37	48.56	1.912	3867	2594	282	63.5
1267	2 500 000	72/19	46.30	1.823	3515	2362	225	50.6
1267	2 500 000	63/28	46.30	1.823	3516	2361	239	53.7
1267	2 500 000	54/37	46.30	1.823	3508	2360	257	57.7
1140	2 250 000	72/19	43.92	1.729	3164	2126	202	45.5
1140	2 250 000	63/28	43.92	1.729	3163	2126	215	48.3
1140	2 250 000	54/37	43.92	1.729	3159	2124	231	52.0
1013	2 000 000	72/19	41.40	1.630	2785	1871	182	41.0
1013	2 000 000	63/28	41.40	1.630	2783	1870	193	43.4
1013	2 000 000	54/37	41.40	1.630	2784	1870	207	46.6
1013	2 000 000	54/7	41.40	1.630	2788	1874	169	37.9
887	1 750 000	54/7	38.73	1.525	2439	1639	148	33.2
887	1 750 000	48/13	38.73	1.525	2437	1638	158	35.5
887	1 750 000	42/19	38.73	1.525	2438	1638	171	38.5
887	1 750 000	33/28	38.73	1.525	2436	1637	186	41.7
760	1 500 000	54/7	35.85	1.411	2090	1405	127	28.4
760	1 500 000	48/13	35.85	1.411	2089	1404	135	30.4
760	1 500 000	42/19	35.85	1.411	2089	1404	147	33.0
760	1 500 000	33/28	35.85	1.411	2086	1402	159	35.7
633	1.250 000	54/7	32.72	1.288	1741	1170	107	24.1
633	1.250 000	48/13	32.72	1.288	1740	1169	114	25.7
633	1.250 000	33/28	32.72	1.288	1738	1168	133	30.0
633	1.250 000	30/7	32.70	1.287	1741	1770	114	25.6
507	1 000 000	54/7	29.26	1.152	1393	936	87.9	19.8
507	1 000 000	48/13	29.26	1.152	1393	936	94.1	21.1
507	1 000 000	42/19	29.26	1.152	1391	935	102	22.9
507	1 000 000	33/28	29.26	1.152	1391	935	110	24.8
507	1 000 000	33/4	29.23	1.151	1394	937	83.9	18.9
507	1 000 000	30/7	29.23	1.151	1393	936	91.0	20.4
507	1 000 000	24/13	29.23	1.151	1393	936	101	22.6
507	1 000 000	18/19	29.23	1.151	1391	935	112	25.2
380	750 000	33/4	25.32	0.997	1045	703	64.0	14.5

Order Number: 0212091 4
Sold to:EGAT [7001661083 93] - VARRIS.Y@EGAT.CO.TH,
Not for Resale,2016-09-15 03:57:47 UTC

Copyright © 2010 IEEE. All rights reserved.

Copyright The Institute of Electrical and Electronics Engineers, Inc.
Provided by IHS under license with IEEE
No reproduction or networking permitted without license from IHS

Table E.6—Physical properties of common bus conductors
ACAR, 1350/6201, concentric-lay stranded per ASTM B524

Conductor size		Number of strands	Overall conductor diameter		Mass		Rated strength	
mm^2	AWG or cmils	Alum alloy 1350/6201	mm	in	kg per km	lbs per 1000 ft	kN	kips
380	750 000	30/7	25.32	0.997	1045	702	69.2	15.6
380	750 000	24/13	25.32	0.997	1045	702	76.2	17.1
380	750 000	18/19	25.32	0.997	1043	701	84.7	19.0
253	500 000	33/4	20.66	0.813	696	468	44.4	10.0
253	500 000	30/7	20.66	0.813	696	468	48.0	10.8
253	500 000	24/13	20.66	0.813	696	468	52.9	11.7
253	500 000	18/19	20.66	0.813	695	467	58.8	13.2
253	500 000	15/4	20.60	0.811	696	468	46.2	10.4
253	500 000	12/7	20.60	0.811	696	468	52.4	11.8
177	350 000	15/4	20.60	0.811	487	328	33.2	7.47
177	350 000	12/7	20.60	0.811	487	327	37.4	8.41
107	4/0	4/3	13.25	0.522	294	198	23.0	5.18
85.0	3/0	4/3	11.80	0.464	234	157	18.3	4.11
67.4	2/0	4/3	10.52	0.414	185	124	14.7	3.31
53.5	1/0	4/3	9.35	0.368	147	98.7	12.0	2.69

NOTE 1—See Table E.1 for general notes.

Order Number: 0212094
Sold to:EGAT [700166108393] - VARRIS.Y@EGAT.CO.TH,
Not for Resale,2016-09-15 03:57:47 UTC

Copyright © 2010 IEEE. All rights reserved.

Copyright The Institute of Electrical and Electronics Engineers, Inc.
Provided by IHS under license with IEEE
No reproduction or networking permitted without license from IHS

Table E.7—Physical properties of common bus conductors
ACAR, 1350/6201, standard metric conductor sizes per ASTM B524

Conductor size		Number of strands	Overall conductor diameter		Mass		Rated strength	
mm^2	AWG or cmils	alum alloy 1350/6201	mm	in	kg per km	lbs per 1,000 ft	kN	kips
1600	3 157 687	72/19	52.03	2.048	4,493	3019	283	63.6
1600	3 157 687	63/28	52.03	2.048	4,491	3018	300	67.4
1600	3 157 687	54/37	52.03	2.048	4,488	3016	323	72.6
1250	2 466 943	72/19	45.98	1.810	3,476	2336	221	49.7
1250	2 466 943	63/28	45.98	1.810	3,474	2335	234	52.6
1250	2 466 943	54/37	45.98	1.810	3,472	2333	253	56.9
1000	1 973 554	72/19	41.14	1.620	2,782	1870	180	40.5
1000	1 973 554	63/28	41.14	1.620	2,780	1868	190	42.7
1000	1 973 554	54/37	41.14	1.620	2,779	1868	204	45.9
1000	1 973 554	54/7	41.13	1.619	2,786	1872	166	37.3
1000	1 973 554	48/13	41.13	1.619	2,786	1872	178	40.0
1000	1 973 554	42/19	41.13	1.619	2,783	1870	192	43.2
1000	1 973 554	33/28	41.13	1.619	2,781	1869	206	46.3
800	1 578 843	54/7	36.81	1.449	2,209	1485	133	29.9
800	1 578 843	48/13	36.81	1.449	2,209	1485	142	31.9
800	1 578 843	42/19	36.81	1.449	2,207	1483	154	34.6
800	1 578 843	33/28	36.81	1.449	2,205	1482	167	37.5
630	1 243 339	54/7	32.67	1.286	1,741	1170	107	24.1
630	1 243 339	48/13	32.67	1.286	1,740	1169	114	25.6
630	1 243 339	42/19	32.67	1.286	1,739	1169	123	27.7
630	1 243 339	33/28	32.67	1.286	1,737	1167	133	29.9
630	1 243 339	33/4	32.62	1.284	1,740	1169	104	23.4
630	1 243 339	30/7	32.62	1.284	1,740	1169	113	25.4
630	1 243 339	24/13	32.62	1.284	1,737	1167	125	28.1
630	1 243 339	18/19	32.62	1.284	1,736	1167	139	31.3
500	986 777	54/7	29.07	1.445	1,378	926.1	86.5	19.44
500	986 777	48/13	29.07	1.445	1,377	925.4	93.6	21.04
500	986 777	42/19	29.07	1.445	1,377	925.4	100	22.48
500	986 777	33/28	29.07	1.445	1,376	924.7	109	24.51
500	986 777	33/4	29.05	1.444	1,380	927.4	82.6	18.57
500	986 777	30/7	29.05	1.444	1,379	926.7	89.5	20.12
500	986 777	24/13	29.05	1.444	1,379	926.7	98.8	22.21
500	986 777	18/19	29.05	1.444	1,377	925.4	110	24.73
400	789 422	33/4	25.97	1.022	1,103	741.3	67.3	15.13
400	789 422	30/7	25.97	1.022	1,103	741.3	72.7	16.34
400	789 422	24/13	25.97	1.022	1,102	740.6	79.9	17.96
400	789 422	18/19	25.97	1.022	1,100	739.2	88.7	19.94

Order Number: 02120914
Sold to:EGAT [700166108393] - VARRIS.Y@EGAT.CO.TH,
Not for Resale,2016-09-15 03:57:47 UTC

Copyright © 2010 IEEE. All rights reserved.

Copyright The Institute of Electrical and Electronics Engineers, Inc.
Provided by IHS under license with IEEE
No reproduction or networking permitted without license from IHS

Table E.7—Physical properties of common bus conductors
ACAR, 1350/6201, standard metric conductor sizes per ASTM B524

Conductor size		Number of strands	Overall conductor diameter		Mass		Rated strength	
mm^2	AWG or cmils	alum alloy 1350/6201	mm	in	kg per km	lbs per 1,000 ft	kN	kips
315	621 670	33/4	23.03	0.907	867	582.7	53.7	12.07
315	621 670	30/7	23.03	0.907	867	582.7	57.9	13.02
315	621 670	24/13	23.03	0.907	866	582.0	63.4	14.25
315	621 670	18/19	23.03	0.907	865	581.3	70.2	15.78
250	493 389	33/4	20.51	0.807	688	462.4	42.9	9.64
250	493 389	30/7	20.51	0.807	688	462.4	46.6	10.48
250	493 389	24/13	20.51	0.807	686	461.0	51.4	11.56
250	493 389	18/19	20.51	0.807	687	461.7	57.4	12.90
250	493 389	12/7	20.45	0.805	687	461.7	51.4	11.56
250	493 389	15/4	20.45	0.805	688	462.4	45.3	10.18
200	394 711	12/7	18.30	0.720	550	369.6	41.6	9.35
200	394 711	15/4	18.30	0.720	550	369.6	36.9	8.30
160	315 769	12/7	16.35	0.644	439	295.0	33.5	7.53
160	315 769	15/4	16.35	0.644	440	295.7	29.8	6.70
125	246 694	4/3	14.31	0.563	344.3	231.4	26.7	6.00
100	197 355	4/3	12.78	0.503	274.6	184.5	17.2	3.87
63	124 334	4/3	10.17	0.400	173.9	116.9	13.7	3.08
40	78 942	4/3	8.10	0.319	110.3	74.1	8.95	2.01
25	49 339	4/3	6.39	0.252	68.6	46.1	5.57	1.25
16	31 577	4/3	5.13	0.202	44.2	29.7	3.59	0.81

NOTE 1—See Table E.1 for general notes.

Order Number: 0212091-4
Sold to:EGAT [7001661083931] - VARRIS.Y@EGAT.CO.TH,
Not for Resale,2016-09-15 03:57:47 UTC

Copyright © 2010 IEEE. All rights reserved.

Copyright The Institute of Electrical and Electronics Engineers, Inc.
Provided by IHS under license with IEEE
No reproduction or networking permitted without license from IHS

Table E.8—Physical properties of common bus conductors
ACSS, concentric-lay stranded per ASTM B856

Conductor size AWG or cmils	Code word per aluminum association publication 50	ASTM stranding class	Stranding design alum/steel	Nominal OD In	Mass lbs/1000 ft	Rated strength by type of steel core wire (NOTE 2)		
						ACSS/HS ACSS/MS kips	ACSS/GA ACSS/MA kips	ACSS/AW kips
2 312 000	Thrasher/ACSS	AA	76/19	1.802	2523	38.1	35.6	34.1
2 167 000	Kiwi/ACSS	AA	72/7	1.735	2301	30.8	29.0	28.2
2 156 000	Bluebird/ACSS	AA	84/19	1.762	2508	45.5	42.1	40.7
1 780 000	Chukar/ACSS	AA	84/19	1.602	2,072	38.2	35.4	33.6
1 590 000	Falcon/ACSS	AA	54/19	1.545	2042	46.6	42.6	41.1
1 590 000	Lapwing/ACSS	AA	45/7	1.504	1790	29.6	27.9	27.0
1 510 500	Parrot/ACSS	AA	54/19	1.505	1938	44.2	40.4	38.9
1 510 500	Nuthatch/ACSS	AA	45/7	1.466	1700	28.1	26.5	25.7
1 431 000	Plover/ACSS	AA	54/19	1.465	1838	41.9	38.4	36.9
1 431 000	Bobolink/ACSS	AA	45/7	1.427	1611	27.0	25.1	24.3
1 351 500	Martin/ACSS	AA	54/19	1.424	1735	39.6	36.2	34.9
1 351 500	Dipper/ACSS	AA	45/7	1.386	1521	25.5	23.7	23.0
1 272 000	Pheasant/ACSS	AA	54/19	1.382	1634	37.3	34.1	32.8
1 272 000	Bittern/ACSS	AA	45/7	1.345	1432	24.0	22.3	21.6
1 192 500	Grackle/ACSS	AA	54/19	1.338	1531	35.5	32.6	30.8
1 192 500	Bunting/ACSS	AA	45/7	1.302	1342	23.5	21.4	20.8
1 113 000	Finch/ACSS	AA	54/19	1.293	1430	33.2	30.4	28.8
1 113 000	Bluejay/ACSS	AA	45/7	1.259	1254	21.1	19.5	18.9
1 033 500	Curlew/ACSS	AA	54/7	1.245	1329	30.3	28.2	26.1
1 033 500	Ortolan/ACSS	AA	45/7	1.212	1163	19.5	18.1	17.6
954 000	Cardinal/ACSS	AA	54/7	1.196	1227.1	28.0	26.0	24.6
954 000	Rail/ACSS	AA	45/7	1.165	1074	18.0	16.7	16.2
900 000	Canary/ACSS	AA	54/7	1.162	1158	26.4	24.6	23.2
900 000	Ruddy/ACSS	AA	45/7	1.131	1013	17.0	15.8	15.3
795 000	Mallard/ACSS	AA	30/19	1.140	1233.9	37.9	34.3	32.9
795 000	Condor/ACSS	AA	54/7	1.092	1022	23.3	21.7	20.9
795 000	Tern/ACSS	AA	45/7	1.063	895	15.2	14.2	13.5
795 000	Drake/ACSS	AA	26/7	1.108	1093	28.0	25.9	24.4
795 000	Cuckoo/ACSS	AA	24/7	1.092	1023	23.3	21.7	20.9
715 500	Redwing/ACSS	AA	30/19	1.081	1109.3	34.0	30.8	29.5
715 500	Starling/ACSS	AA	26/7	1.051	983.7	25.2	23.3	22.0
715 500	Stilt/ACSS	AA	24/7	1.036	921	21.3	19.5	18.8
666 600	Gannet/ACSS	AA	26/7	1.014	916.2	23.4	21.7	20.9
666 600	Flamingo/ACSS	AA	24/7	1.000	857.9	19.9	18.2	17.5
636 000	Egret/ACSS	AA	30/19	1.019	987.2	30.9	28.0	26.3
636 000	Scoter/ACSS	AA	30/7	1.019	995.1	29.7	27.4	25.1
636 000	Grosbeak/ACSS	AA	26/7	0.990	874.2	22.4	20.7	19.9
636 000	Rook/ACSS	AA	24/7	0.977	818.2	19.0	17.3	16.7

Order Number: 0212091 4
Sold to:EGAT [700166108393] - VARRIS.Y@EGAT.CO.TH,
Not for Resale,2016-09-15 03:57:47 UTC

Copyright © 2010 IEEE. All rights reserved.

Copyright The Institute of Electrical and Electronics Engineers, Inc.
Provided by IHS under license with IEEE
No reproduction or networking permitted without license from IHS

Table E.8—Physical properties of common bus conductors
ACSS, concentric-lay stranded per ASTM B856

Conductor size AWG or cmils	Code word per aluminum association publication 50	ASTM stranding class	Stranding design alum/steel	Nominal OD In	Mass lbs/1000 ft	Rated strength by type of steel core wire (NOTE 2)		
						ACSS/HS ACSS/MS kips	ACSS/GA ACSS/MA kips	ACSS/AW kips
605 000	Teal/ACSS	AA	30/19	0.994	938.6	29.3	26.6	25.0
605 000	Wood Duck/ACSS	AA	30/7	0.994	946.5	28.3	26.0	24.4
605 000	Squab/ACSS	AA	26/7	0.966	831.3	21.3	19.7	19.0
605 000	Peacock/ACSS	AA	24/7	0.953	778.8	18.1	16.5	15.9
556 500	Eagle/ACSS	AA	30/7	0.953	870.7	26.5	24.5	22.9
556 500	Dove/ACSS	AA	26/7	0.927	765.2	19.9	18.2	17.5
556 500	Parakeet/ACSS	AA	24/7	0.914	716.1	16.6	15.2	14.6
477 000	Hen/ACSS	AA	30/7	0.883	746.4	22.7	21.0	20.1
477 000	Hawk/ACSS	AA	26/7	0.858	655.3	17.1	15.6	14.9
477 000	Flicker/ACSS	AA	24/7	0.846	613.9	14.2	13.0	12.5
397 500	Lark/ACSS	AA	30/7	0.806	621.8	19.3	17.5	16.7
397 500	Ibis/ACSS	AA	26/7	0.783	546.0	14.2	13.0	12.4
397 500	Brant/ACSS	AA	24/7	0.772	511.4	12.1	11.0	10.4
336 400	Oriole/ACSS	AA	30/7	0.741	526.4	16.3	14.8	14.2
336 400	Linnet/ACSS	AA	26/7	0.720	462.0	12.3	11.2	10.5
300 000	Ostrich/ACSS	AA	26/7	0.680	412.2	10.9	10.0	9.40
266 800	Partridge/ACSS	AA	26/7	0.642	366.9	9.73	8.88	8.37
211 300	Cochin/ACSS	AA(HS)	12/7	0.664	526.8	23.1	21.2	19.7
203 200	Brahma/ACSS	AA(HS)	16/9	0.714	674.6	34.1	30.5	29.1
190 800	Dorking/ACSS	AA(HS)	12/7	0.631	475.7	20.9	19.1	18.3
176 900	Dotterel/ACSS	AA(HS)	12/7	0.607	440.9	19.4	17.7	16.9
159 000	Guinea/ACSS	AA(HS)	12/7	0.576	396.3	17.8	15.9	15.2
134 600	Leghorn/ACSS	AA(HS)	12/7	0.530	335.5	15.0	13.5	12.9
110 800	Minorca	AA(HS)	12/7	0.481	276.3	12.4	11.1	10.6

NOTE 1—See Table E.1 for notes.
NOTE 2—Steel core abbreviations:
ACSS/AW = Supported with aluminum-clad core wire per ASTM B502.
ACSS/GA =Supported with galvanized steel core wire, coating Class A per ASTM B498.
ACSS/HS = Supported with high-strength galvanized steel core wire per ASTM B606.
ACSS/MA = Supported with Zn-5A1-MM coated steel core, coating Class A per ASTM B802.
ACSS/MS = Supported with high-strength Zn-5A1-MM coated steel core per ASTM B803.

Order Number: 0212091 4
Sold to:EGAT [7001661083 93] - VARRIS.Y@EGAT.CO.TH,
Not for Resale,2016-09-15 03:57:47 UTC

Copyright © 2010 IEEE. All rights reserved.

Copyright The Institute of Electrical and Electronics Engineers, Inc.
Provided by IHS under license with IEEE
No reproduction or networking permitted without license from IHS

Table E.9—Physical properties of common bus conductors copper conductor, hard-drawn, concentric-lay-stranded per ASTM B1 and ASTM B8

Conductor size		ASTM stranding class	Number of strands	Overall conductor diameter		Mass		Minimum ultimate strength (NOTE 2)	
mm^2	AWG or cmils			mm	in	kg per km	lbs per 1000 ft	kN	kips
507	1 000 000	AA	37	29.24	1.151	4596	3088	194.8	43.8
456	900 000	AA	37	27.74	1.092	4136	2779	175.7	39.5
405	800 000	AA	37	26.14	1.029	3676	2470	156.1	35.1
380	750 000	AA	37	25.32	0.997	3447	2316	148.6	33.4
355	700 000	AA	37	24.46	0.963	3216	2161	138.8	31.2
304	600 000	AA,A	37	22.63	0.891	2758	1883	120.1	27.0
253	500 000	AA	19	20.60	0.811	2298	1544	97.4	21.9
228	450 000	AA	19	19.56	0.770	2067	1389	88.1	19.8
203	400 000	AA,A	19	18.44	0.726	1838	1235	79.2	17.8
177	350 000	A	19	17.25	0.679	1609	1081	69.4	15.6
152	300 000	A	19	15.98	0.629	1378.6	926.3	60.0	13.5
127	250 000	A	19	14.58	0.574	1148.8	771.9	50.7	11.4
107	4/0	AA,A	7	13.26	0.522	972.0	653.1	40.74	9.16
85.0	3/0	AA,A	7	11.79	0.464	771.1	518.1	32.74	7.36
67.4	2/0	AA,A	7	10.52	0.414	611.5	410.9	26.38	5.93
53.5	1/0	AA,A	7	9.35	0.368	484.9	325.8	21.13	4.75

NOTE 1—See Table E.1 for general notes.
NOTE 2—The minimum breaking strength of the overall conductor is computed as 90% of the specified minimum breaking strength of the component wires in accordance with ASTM B8.

Order Number: 0212091-4
Sold to:EGAT [7001661083931 - VARRIS.Y@EGAT.CO.TH,
Not for Resale,2016-09-15 03:57:47 UTC

Copyright © 2010 IEEE. All rights reserved.

Copyright The Institute of Electrical and Electronics Engineers, Inc.
Provided by IHS under license with IEEE
No reproduction or networking permitted without license from IHS

Table E.10—Physical properties of common bus conductors copper conductor, medium-hard-drawn, concentric-lay-stranded per ASTM B2 AND ASTM B8

Conductor size		ASTM stranding class	Number of strands	Overall Conductor Diameter		Mass		Minimum tensile strength (See NOTE 2)		Maximum tensile strength	
mm^2	AWG or cmils			mm	in	kg per km	lbs per 1000 ft	kN	kips	kN	kips
507	1 000 000	AA	37	29.24	1.151	4596	3088	153.0	34.4	194.4	43.7
456	900 000	AA	37	27.74	1.092	4136	2779	138.8	31.2	176.1	39.6
405	800 000	AA	37	26.14	1.029	3676	2470	123.2	27.7	156.6	35.2
380	750 000	AA	37	25.32	0.997	3447	2316	116.5	26.2	147.7	33.2
355	700 000	AA	37	24.46	0.963	3216	2161	108.5	24.4	137.4	30.9
304	600 000	AA,A	37	22.63	0.891	2758	1883	93.4	21.0	118.8	26.7
253	500 000	AA	19	20.60	0.811	2298	1544	76.9	17.3	97.9	22.0
228	450 000	AA	19	19.56	0.770	2067	1389	69.4	15.6	88.1	19.8
203	400 000	AA,A	19	18.44	0.726	1838	1235	61.8	13.9	78.3	17.6
177	350 000	A	19	17.25	0.679	1609	1081	54.3	12.2	68.9	15.5
152	300 000	A	19	15.98	0.629	1378.6	926.3	46.7	10.5	59.6	13.4
127	250 000	A	19	14.58	0.574	1148.8	771.9	39.3	8.83	49.8	11.2
107	4/0	AA,A	7	13.26	0.522	972.0	653.1	32.4	7.28	41.2	9.26
85.0	3/0	AA,A	7	11.79	0.464	771.1	518.1	25.8	5.81	32.8	7.38
67.4	2/0	AA,A	7	10.52	0.414	611.5	410.9	20.6	4.64	26.2	5.89
53.5	1/0	AA,A	7	9.35	0.368	484.9	325.8	16.5	3.71	20.9	4.7

NOTE 1—See Table E.1 for general notes.
NOTE 2—The minimum breaking strength of the overall conductor is computed as 90% of the specified minimum breaking strength of the component wires in accordance with ASTM B8.

Order Number: 0212091-4
Sold to:EGAT [7001661083931 - VARRIS.Y@EGAT.CO.TH,
Not for Resale,2016-09-15 03:57:47 UTC

Copyright © 2010 IEEE. All rights reserved.

Copyright The Institute of Electrical and Electronics Engineers, Inc.
Provided by IHS under license with IEEE
No reproduction or networking permitted without license from IHS

Table E.11—Physical properties of common bus conductors tubular aluminum conductor per ANSI H35.2

Nominal pipe size (NOTE 1)		Schedule number	Nominal outside diameter		Nominal inside diameter		Nominal wall thickness		Mass		Moment of inertia		Section modulus	
mm	in		mm	in	mm	in	mm	in	kg/m	lbs/ft	mm^4	in^4	mm^3	in^3
19	0.75	40	26.70	1.050	20.96	0.824	2.87	0.113	0.58	0.391	15 401	0.0370	1155	0.0705
		80	26.70	1.050	18.88	0.742	3.91	0.154	0.76	0.510	18 647	0.0448	1398	0.0853
25	1.0	40	33.40	1.315	26.64	1.049	3.38	0.133	0.86	0.581	36 337	0.0873	2176	0.1328
		80	33.40	1.315	24.30	0.957	4.55	0.179	1.11	0.751	43 954	0.1056	2632	0.1606
32	1.25	40	42.20	1.660	35.08	1.380	3.56	0.140	1.17	0.786	81 040	0.1947	3844	0.2346
		80	42.20	1.660	32.50	1.278	4.85	0.191	1.54	1.037	100 645	0.2418	4774	0.2913
38	1.5	40	48.30	1.900	40.94	1.610	3.68	0.145	1.39	0.940	128 990	0.3099	5345	0.3262
		80	48.30	1.900	38.14	1.500	5.08	0.200	1.86	1.256	162 830	0.3912	6748	0.4118
51	2.0	40	60.30	2.375	52.48	2.067	3.91	0.154	1.87	1.264	277 085	0.6657	9187	0.5606
		80	60.30	2.375	49.22	1.939	5.54	0.218	2.57	1.737	361 247	0.8679	11 977	0.7309
64	2.5	40	73.00	2.875	62.68	2.469	5.16	0.203	2.97	2.004	636 834	1.5300	17 436	1.0640
		80	73.00	2.875	58.98	2.323	7.01	0.276	3.92	2.650	800 829	1.9240	21 942	1.3390
76	3.0	40	88.90	3.500	77.92	3.068	5.49	0.216	3.88	2.621	1 255 770	3.0170	28 251	1.7240
		80	88.90	3.500	73.66	2.900	7.62	0.300	5.25	3.547	1 620 805	3.8940	36 461	2.2250
89	3.5	40	101.60	4.000	90.12	3.548	5.74	0.226	4.67	3.151	1 992 916	4.7880	39 231	2.3940
		80	101.60	4.000	85.44	3.364	8.08	0.318	6.41	4.326	2 614 350	6.2810	51 455	3.1400
102	4.0	40	114.30	4.500	102.26	4.026	6.02	0.237	5.53	3.733	3 010 186	7.2320	52 668	3.2140
		80	114.30	4.500	97.18	3.826	8.56	0.337	7.68	5.183	4 000 400	9.6110	70 006	4.2720
127	5.0	40	141.30	5.563	128.20	5.047	6.55	0.258	7.49	5.057	6 310 069	15.1600	89 326	5.4510
		80	141.30	5.563	122.24	4.813	9.53	0.375	10.65	7.188	8 603 504	20.6700	121 789	7.4320
152	6.0	40	168.30	6.625	154.08	6.065	7.11	0.280	9.72	6.564	11 712 752	28.1400	139 225	8.4960
		80	168.30	6.625	146.36	5.761	10.97	0.432	14.64	9.884	16 853 211	40.4900	200 250	12.2200
203	8.0	40	219.10	8.625	202.74	7.981	8.18	0.322	14.63	9.878	30 172 616	72.4900	275 467	16.8100
		80	219.10	8.625	193.70	7.625	12.70	0.500	22.23	15.010	44 003 986	105.7200	401 647	24.5100

NOTE 1—See Table E.1 for general notes.
NOTE 2—For manufacturing tolerances, see ANSI H35.2.
NOTE 3—Mass, moment of inertia and section modulus are computed based on nominal values.
NOTE 4—For aluminum alloy properties such as tensile strength, conductivity and the modulus of elasticity, see Table 1.

Order Number: 0212091-4
Sold to:EGAT [7001661083931 - VARRIS.Y@EGAT.CO.TH,
Not for Resale,2016-09-15 03:57:47 UTC

Copyright © 2010 IEEE. All rights reserved.

Copyright The Institute of Electrical and Electronics Engineers, Inc.
Provided by IHS under license with IEEE
No reproduction or networking permitted without license from IHS

Table E.12—Physical properties of common bus conductors tubular copper conductor per ASTM B-188

Nominal pipe size (NOTE 1)		Schedule	Nominal outside diameter		Nominal inside diameter		Nominal wall thickness		Mass		Moment of inertia		Section modulus	
mm	in		mm	in	mm	in	mm	in	kg/m	lbs/ft	mm^4	in^4	mm^3	in^3
19	0.75	Regular	26.7	1.050	20.9	0.822	2.90	0.114	1.93	1.30	15 525	0.0373	1163	0.0710
		Extra strong	26.7	1.050	18.7	0.736	3.99	0.157	2.54	1.71	18 855	0.0453	1413	0.0862
25	1.0	Regular	33.4	1.315	27.0	1.063	3.20	0.126	2.71	1.82	35 005	0.0841	2096	0.1279
		Extra strong	33.4	1.315	24.2	0.951	4.62	0.182	3.73	2.51	44 370	0.1066	2658	0.1622
32	1.25	Regular	42.2	1.660	34.7	1.368	3.71	0.146	2.69	4.00	83 579	0.2008	3966	0.2420
		Extra strong	42.2	1.660	32.3	1.272	4.93	0.194	5.15	3.46	101 644	0.2442	4823	0.2943
38	1.5	Regular	48.3	1.900	40.6	1.600	3.81	0.150	4.76	3.20	132 362	0.318	5486	0.3348
		Extra strong	48.3	1.900	37.9	1.494	5.16	0.203	6.23	4.19	164 495	0.3952	6817	0.4160
51	2.0	Regular	60.3	2.375	52.4	2.063	3.96	0.156	6.28	4.22	279 999	0.6727	9283	0.5665
		Extra strong	60.3	2.375	49.1	1.933	5.61	0.221	8.63	5.80	364 827	0.8765	12 095	0.7381
64	2.5	Regular	73.0	2.875	63.5	2.501	4.75	0.187	9.11	6.12	596 460	1.4330	16 338	0.9970
		Extra strong	73.0	2.875	58.8	2.315	7.11	0.280	13.2	8.85	809 154	1.9440	22 155	1.3520
76	3.0	Regular	88.9	3.500	77.8	3.062	5.56	0.219	13.0	8.75	1 269 922	3.0510	28 563	1.7430
		Extra strong	88.9	3.500	73.6	2.892	7.72	0.304	17.6	11.80	1 636 622	3.9320	36 822	2.2470
89	3.5	Regular	102.0	4.000	88.9	3.500	6.35	0.250	17.0	11.40	2 164 403	5.2000	42 606	2.6000
		Extra strong	102.0	4.000	85.3	3.358	8.15	0.321	21.4	14.40	2 632 664	6.3250	51 816	3.1620
102	4.0	Regular	114.0	4.500	102.0	4.000	6.35	0.250	19.2	12.90	3 147 958	7.5630	55 077	3.3610
		Extra strong	114.0	4.500	97.0	3.818	8.66	0.341	25.7	17.30	4 036 612	9.6980	70 628	4.3100
127	5.0	Regular	141.0	5.562	129.0	5.062	6.35	0.250	24.1	16.20	6 139 414	14.7500	86 901	5.3030
		Extra strong	141.0	5.562	122.0	4.812	9.52	0.375	35.3	23.70	8 599 341	20.6600	121 739	7.4290
152	6.0	Regular	168.0	6.625	156.0	6.125	6.35	0.250	28.9	19.40	10 601 414	25.4700	126 017	7.6900
		Extra strong	168.0	6.625	146.0	5.751	11.1	0.437	49.0	32.90	17 011 378	40.8700	202 216	12.3400
203	8.0	Regular	219.0	8.625	203.0	8.001	7.92	0.312	47.0	31.60	29 340 153	70.4900	267 765	16.3400
		Extra strong	219.0	8.625	194.0	7.625	12.70	0.500	73.7	49.50	44 003 986	105.7200	401 647	24.5100

NOTE 1—See Table E.1 for general notes.
NOTE 2—For manufacturing tolerances, see ASTM B-188.
NOTE 3—Mass, moment of inertia and section modulus are computed based on nominal values.
NOTE 4—For copper properties such as tensile strength, conductivity and the modulus of elasticity, see Table 1.

Order Number: 02120914
Sold to:EGAT [7001661083931 - VARRIS.Y@EGAT.CO.TH,
Not for Resale,2016-09-15 03:57:47 UTC

Copyright © 2010 IEEE. All rights reserved.

Annex F

(informative)

Calculation example of short circuit analysis on rigid bus systems

To illustrate the main features of short circuit force calculations, this annex presents a simple calculation example for rigid bus under short circuit. It presents both simplified calculations according to 11.3.3 and with finite-element calculations according to 11.3.4, which illustrates the differences between both methods. The example used is based on an actual structure that was tested and thus provides a quantitative assessment of the precision of the calculation methods in this guide.

F.1 CIGRE structure D

This example consists of a 220 kV simple bus structure with two spans that was submitted to testing under controlled short circuit conditions, with and without reclosure on fault. The complete description of tests and results can be found in Hosemann and Tsanakas [B14].

F.1.1 Description

The structure under consideration is presented in Figure F.1 along with main dimensions in millimeters (unless otherwise noted in meters). It is submitted to a phase-to-phase fault, with and without reclosure, with a 1 m distance between the two phases. The measurement points on the structure that we will consider in this example are also illustrated and denoted by m_{Ii} for moment at base of insulator of column i. In Figure F.1, columns are numbered 1, 2, and 3 from left to right.

Copyright © 2010 IEEE. All rights reserved.

Copyright The Institute of Electrical and Electronics Engineers, Inc.
Provided by IHS under license with IEEE
No reproduction or networking permitted without license from IHS

Order Number: 02120914
Sold to:EGAT [700166108393] - VARRIS.Y@EGAT.CO.TH,
Not for Resale,2016-09-15 03:57:47 UTC

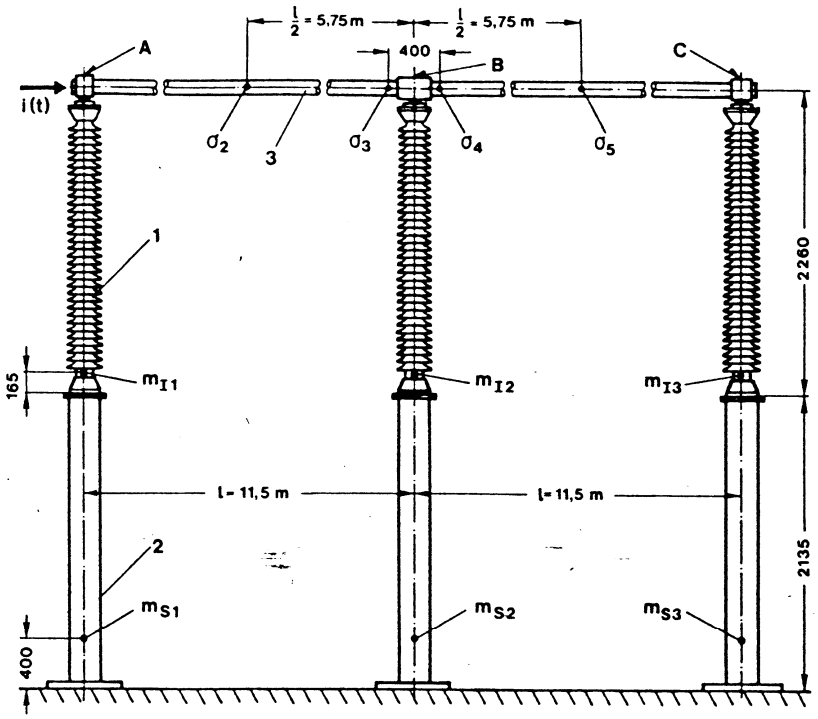

Figure F.1—CIGRE structure D (from Hosemann and Tsanakas [B14])

The structural data used in calculations is presented in Table F.1. The fault parameters are presented in Table F.2.

Table F.1—Structural data

Characteristic	Conductor	Insulator	Support
Length *L*	span of 11.5 m (including portion in conductor clamps)	2.10 m	2.135 m
Material	Aluminum	Porcelain	Steel
Young's modulus *E*	70 GPa	30.6 GPa	206 GPa
Area *A*	2.238E-3 m^2	36.14E-3 m^2	4.714E-3 m^2
Moment of inertia *I*	3.704E-6 m^4	76.08E-6 m^4	26.83E-6 m^4
Mass	6.04 kg/m	180 kg	36.8 kg/m

NOTE 1—In the finite-element model, the insulator length was extended to 2.26 m in order to reach the midconductor position.

NOTE 2—For the insulator and support, the moment of inertia used was obtained from measurements on equivalent spring stiffness (3EI/L3) as provided in Hosemann and Tsanakas [B14]; this is why in Table F.1 the values given do not necessarily correspond to the actual dimensions.

NOTE 3—The bending stiffness for the insulator is assumed constant along its length to correspond to an equivalent beam of constant section although its shape is conical.

NOTE 4—In the finite-element model, lumped masses of 13.8 kg, 18.2 kg, and 13.8 kg have been added at the top of columns 1, 2, and 3, respectively, to account for actual clamp masses. Lumped masses of 36.8 kg have been added to the top of each steel support to account for mass of top plate.

NOTE 5—Conductor is assumed to be pinned at top of columns 1 and 3 and fixed a top of column 2.

Copyright © 2010 IEEE. All rights reserved.

Copyright The Institute of Electrical and Electronics Engineers, Inc.
Provided by IHS under license with IEEE
No reproduction or networking permitted without license from IHS

Order Number: 02120914
Sold to:EGAT [700166108393] - VARRIS.Y@EGAT.CO.TH,
Not for Resale,2016-09-15 03:57:47 UTC

Table F.2—Fault data

Characteristic	Value
RMS current I_{sc}	15.6 kA
Frequency f	50 Hz
X/R	20
Voltage angle at fault initiation	0°
First fault duration	0.135 s
Delay before reclosure	0.445 s
Second fault duration	0.305 s
Phase-to-phase distance D	1 m

F.2 Simplified calculations

The first step consists of calculating the force by unit length generated by the fault on the conductor. This force acts in the horizontal direction perpendicular to the conductor [Figure F.2(a)]. We will calculate here by accounting for the momentary peak force factor effect as well as the mounting structure flexibility effect. Note that simplified calculations cannot account for fault reclosure effect so the calculated value here is only valid for the first fault duration here.

According to Equation (16), the force by unit length is given here by:

$$F_{sc\_\text{corrected}} = D_f^2 \times K_f \times \frac{16 \times \Gamma \times I_{sc}^2}{10^7 \times D} = 1.0 \times 0.86 \times \frac{16 \times 1 \times (15.6 \times 10^3)^2}{10^7 \times 1.0} = 335\ \text{N/m}$$

where

K_f is equal to 1 according to Figure 20 for a bus height of 4.395 m (14.4 ft) for a structure of type B-Tubular and wide flange steel and wood pole.
D_f^2 is equal to 0.86 for an X/R value of 20 according to Table 14
Γ is equal to 1 for a phase-to-phase fault according to Table 13

According to the boundary conditions at the conductor clamps and beam theory, this force by unit length corresponds to the equivalent forces presented in Figure F.2(b) at the top of each column.

Copyright © 2010 IEEE. All rights reserved.
Copyright The Institute of Electrical and Electronics Engineers, Inc.
Provided by IHS under license with IEEE
No reproduction or networking permitted without license from IHS
Order Number: 02120914
Sold to:EGAT [700166108393] - VARRIS.Y@EGAT.CO.TH,
Not for Resale,2016-09-15 03:57:47 UTC

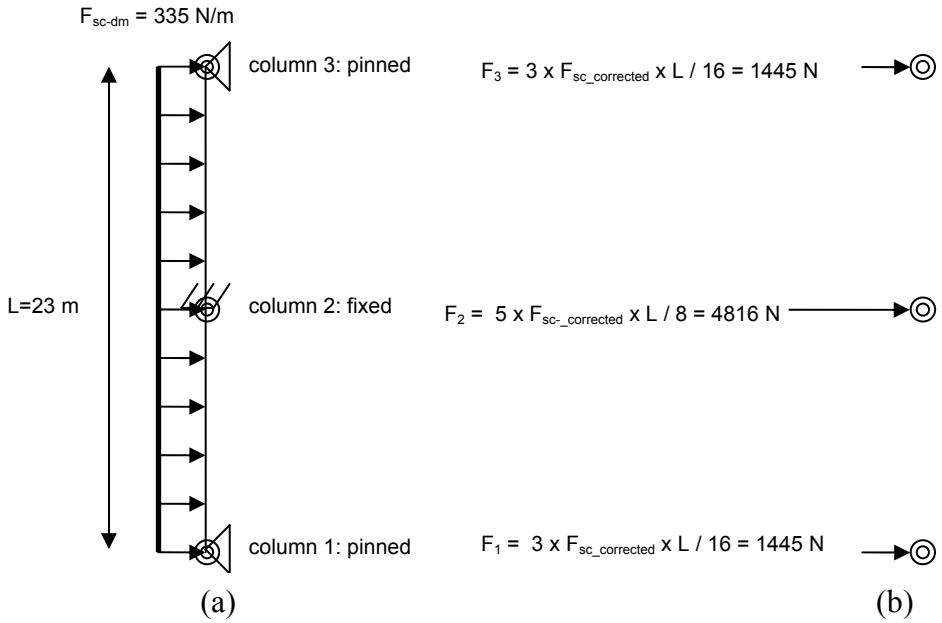

Figure F.2—(a) Short circuit force representation and (b) equivalent forces at top of columns

Using the equivalent forces from Figure F.2, we now calculate the bending moments M_{I1}, M_{I2} at the points m_{I1} and $m_{I2.}$ The bending moments at these points are the product of the force at the top of columns times the cantilever length l from midconductor to the measurement point, which is here equal to 2.095 m.

At point m_{I1} we obtain:

$$M_{I1} = F_1 \; l = 1445 \times 2.095 = 3027 \text{ N-m}$$

At point m_{I2} we obtain:

$$M_{I2} = F_2 \; l = 4816 \times 2.095 = 10090 \text{ N-m}$$

These moments will be compared with the results of experiments as well as finite-element calculations.

F.3 Finite-element calculations

In finite-element analysis, the structure is meshed into a given number of elements and analyzed. The representation of the mesh used here is presented in Figure F.3 along with all points at the boundary of elements (called nodes). Data from Table F.1 and Table F.2 were used, and the first fault as well as the reclosure on the fault was simulated.

Copyright © 2010 IEEE. All rights reserved.
--`,,,,,,`-`-`,,`,,`,`,,`-`-`,,`,,`,`,,`---
Copyright The Institute of Electrical and Electronics Engineers, Inc.
Provided by IHS under license with IEEE
No reproduction or networking permitted without license from IHS
Order Number: 02120914
Sold to:EGAT [700166108393] - VARRIS.Y@EGAT.CO.TH,
Not for Resale,2016-09-15 03:57:47 UTC

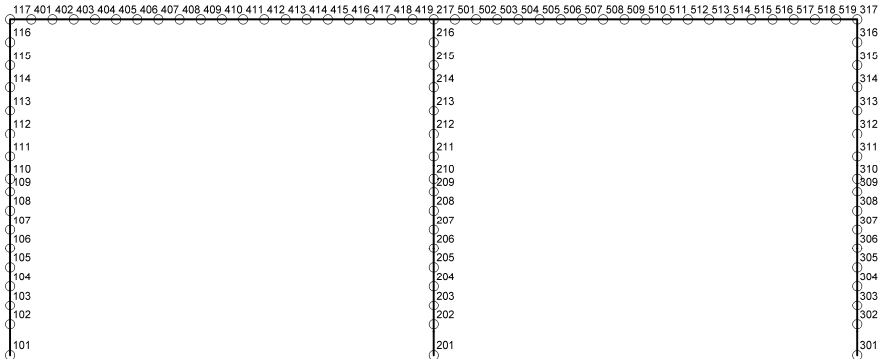

Figure F.3—Finite-element mesh of *CIGRE structure D*

Some details about the numerical parameters used in calculations are presented in Table F.3.

Table F.3—Numerical parameters used in finite-element calculations

Characteristic	Value
Numerical method	Modal superposition
Number of modes used	32
Modal damping[a]	2%
Time step	5e-4 s
Calculated frequency mode-1	3.36 Hz
Calculated frequency mode-32	68.7 Hz

[a]The damping value used of 2% is typical of substation structures.

F.3.1.1 Results for first fault (without reclosure)

One significant advantage of the finite-element method is that it provides not only the maximum values required for design but also their time variation. For example, we present in Figure F.4 the variation of transversal displacement at the middle of the first conductor span (node 410 on model—Figure F.3) as well as the bending moment at the measurement point mI2 (node 210 on model—Figure F.3).

Copyright © 2010 IEEE. All rights reserved.

Copyright The Institute of Electrical and Electronics Engineers, Inc.
Provided by IHS under license with IEEE
No reproduction or networking permitted without license from IHS

Order Number: 02120914
Sold to:EGAT [700166108393] - VARRIS.Y@EGAT.CO.TH,
Not for Resale,2016-09-15 03:57:47 UTC

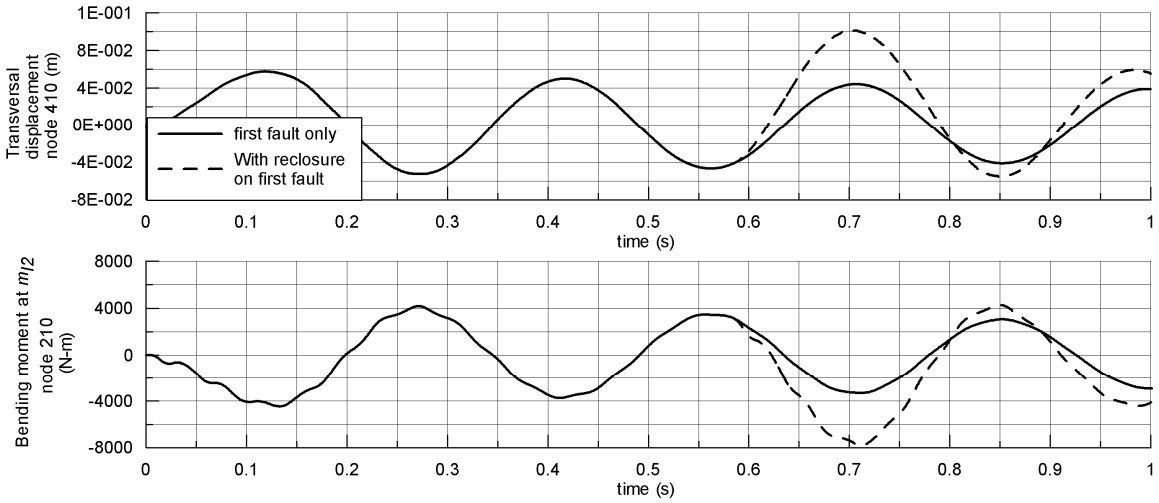

Figure F.4—Time variation of some results from finite-element calculations

The maximum bending moments M_{I1} and M_{I2} at the points m_{I1} and m_{I2} from finite-element calculations are as follows:

At point m_{I1} we obtain:

$M_{I1} = 1335$ N-m

At point m_{i2} we obtain:

$M_{I2} = 4467$ N-m

It is observed that these values are considerably lower than the ones obtained from simplified calculations.

F.3.1.2 Results for second fault (after reclosure)

Another significant advantage of the finite-element method is that it permits calculation of the effects of reclosure on the first fault, which is impossible with simplified calculations. Depending on the delay between the end of the first fault and the reclosure, this effect can sometimes be very significant. We have performed here the simulation with reclosure using data from Table F.2. The time variation of the same results as before is also illustrated as dotted lines in Figure F.4. It is observed here that the reclosure effect is here significant.

The maximum bending moments M_{I1} and M_{I2} at the points m_{I1} and $m_{I2.}$ from finite-element calculations after reclosure are as follows:

At point m_{I1} we obtain:

$M_{I1} = 2327$ N-m

At point m_{i2} we obtain:

$M_{I2} = 7777$ N-m

Copyright © 2010 IEEE. All rights reserved.
Copyright The Institute of Electrical and Electronics Engineers, Inc.
Provided by IHS under license with IEEE
No reproduction or networking permitted without license from IHS
Order Number: 02120914
Sold to:EGAT [700166108393] - VARRIS.Y@EGAT.CO.TH,
Not for Resale,2016-09-15 03:57:47 UTC

By comparison with the results from the simulation with the first fault only, it is observed that the maximum bending moments have been significantly increased.

F.4 Comparisons of calculations with experimental results

A comparison of calculations with experimental results from Hosemann and Tsanakas [B14] are presented in Table F.4 for the first fault.

Table F.4—Comparison of calculation results with experimental results

Result		Experimental	Simplified calculation	Finite element
M_{I1}	Value (N-m)	1600	3027	1335
	% error/exp.	—	89%	17%
M_{I2}	Value (N-m)	5080	10 090	4467
	% error/exp.	—	99%	12%

It is observed here that the simplified calculations overestimate significantly the experimental response as opposed to finite-element calculations that slightly underestimate them.

F.5 Final notes

This example showed that the finite-element method is much more precise than simplified calculations and that it permits to investigate the time variation of quantities of interest, as well as the effect of reclosure on fault. In general, it has been observed that simplified calculations can overestimate finite-element results by factors from 2 to 6. The finite-element method can therefore lead in many situations to significant optimization in design. However, as with any calculation method, proper care must be taken in its use as well as in the collection of data required as input.

Copyright © 2010 IEEE. All rights reserved.

Copyright The Institute of Electrical and Electronics Engineers, Inc.
Provided by IHS under license with IEEE
No reproduction or networking permitted without license from IHS

Order Number: 02120914
Sold to:EGAT [700166108393] - VARRIS.Y@EGAT.CO.TH,
Not for Resale,2016-09-15 03:57:47 UTC

Annex G

(informative)

Calculation example of short circuit analysis on strain bus systems

To illustrate the main features of short circuit force calculations, this annex presents a simple calculation example for strain bus under short circuit. It presents both simplified calculations according to 11.3.5 and with finite-element calculations according to 11.3.6, thus illustrating the differences between both methods. As mentioned in 11.3.5, the simplified calculation method provides here relatively representative results as opposed to the simplified calculations for rigid bus as seen in Annex F.

G.1 Example 4.2.4 from CIGRE brochure [B36]

We repeat here the example provided in 4.2.4 in CIGRE brochure [B36]. This example consists of a 245 kV three-phase system with bundles of two subconductors. Note that the simplified calculation method provided in this guide is similar to the IEC method in IEC 60865-1 Ed. 2-1993 [B16] and is slightly different than the CIGRE one, so similar although not exact results to the ones in CIGRE brochure [B36] are obtained here.

G.1.1 Description

The structure is similar to the one in Figure 21 with the exception that two subconductors are used per bundle in each phase and that the conductors are supported by vertical insulators on a steel structure. The data input for the problem is summarized in Table G.1 with the variables used in this guide.

Table G.1—Data input for strain bus calculation example

Data	Description	Value	Note
l	Span	11.5 m	
n	Number of sub conductors in bundle	2	
a	Phase-to-phase distance	3 m	
a_s	Distance between subconductors in a bundle	0.07 m	
l_s	Distance between spacers	5.75 m	One spacer at midspan
d	Sag	0.43 m	At –20 °C
l_i	Strain insulator length	0	No strain insulators; vertical insulators
A_{s1}	Steel cross-sectional area	50 mm^2	ASCR conductor by subconductor
A_{s2}	Aluminum cross-sectional area	560 mm^2	ASCR conductor by subconductor
E_{s1}	Steel Young's modulus	200 GPa	
E_{s2}	Aluminum Young's modulus	50 GPa	
$\overline{m}$	Subconductor linear mass	1.955 kg/m	Equal to 3.91 kg/m for bundle
I_{k3}	RMS fault current	40 kA	
T_{kl}	Fault duration	0.16 s	
X/R		13.33	Only used for finite-element calculations
f	Current frequency	50 Hz	
S	Equivalent support stiffness	1×10^5 N/m	Common value
voltage angle	Voltage angle at initiation of fault	0	Only used for finite-element calculations

Copyright © 2010 IEEE. All rights reserved.

Copyright The Institute of Electrical and Electronics Engineers, Inc.
Provided by IHS under license with IEEE
No reproduction or networking permitted without license from IHS

Order Number: 02120914
Sold to:EGAT [700166108393] - VARRIS.Y@EGAT.CO.TH,
Not for Resale,2016-09-15 03:57:47 UTC

G.2 Simplified calculations

There are several equations to solve simplified calculations, and it is best to program them in a spreadsheet, although some steps cannot be automated since they refer to one of the figures in 11.3.5. Once programmed, the simplified calculation method in this guide will yield results with minimum effort. We present below the calculation steps in order. We use below all of the equations from 11.3.5.

Preliminary calculations

a) Characteristic electromagnetic load

$$F' = \frac{\mu_0}{2\pi} \times 0.75 \times \frac{I_{k3}^2}{\mathrm{a}} \frac{l_c}{l} = \frac{1.257 \times 10^{-6}}{2\pi} \times 0.75 \times \frac{(40 \times 10^3)^2}{3} \times \frac{11.5}{11.5} = 80\ \mathrm{N/m}$$

b) Ratio of electromagnetic force to gravitational force

$$r = \frac{F'}{F_g} = \frac{F'}{n\bar{m}g} = \frac{80}{2 \times 1.955 \times 9.81} = 2.09$$

c) Direction of resulting force exerted on conductor

$$\delta_1 = \arctan(\mathrm{r}) = \arctan(2.09) = 64.4°$$

d) Static tensile force

$$F_{st} = \frac{n\bar{m}gl^2}{8d} = \frac{2 \times 1.955 \times 9.81 \times 11.5^2}{8 \times 0.433} = 1464\ \mathrm{N}$$

e) Natural period of conductor oscillation T

$$T = 2\pi\sqrt{0.8\frac{d}{g}} = 2\pi\sqrt{0.8\frac{0.433}{9.81}} == 1.18\ \mathrm{s}$$

f) Period of oscillation during short circuit

$$T_{\mathrm{res}} = \frac{T}{\sqrt[4]{1+r^2}\left[1-\frac{\pi^2}{64}\left(\frac{\delta_1}{90^o}\right)^2\right]} = \frac{1.18}{\sqrt[4]{1+2.09^2 \times \left[1-\frac{\pi^2}{64}\left(\frac{64.4}{90}\right)^2\right]}} = 0.842\ \mathrm{s}$$

g) Maximum swing-out angle

$$\frac{T_{k1}}{T_{\mathrm{res}}} = \frac{0.16}{0.842} = 0.19 \le 0.5$$

Copyright © 2010 IEEE. All rights reserved.

Copyright The Institute of Electrical and Electronics Engineers, Inc.
Provided by IHS under license with IEEE
No reproduction or networking permitted without license from IHS

Order Number: 02120914
Sold to:EGAT [700166108393] - VARRIS.Y@EGAT.CO.TH,
Not for Resale,2016-09-15 03:57:47 UTC

Therefore,

$$\delta_k = \delta_1 \left[1 - \cos\left(360^o \frac{T_{k1}}{T_{res}} \right) \right] = 64.4 \times \left[1 - \cos\left(360^o \times 0.19 \right) \right] = 40.7^o$$

now because $\delta_k < 90°$:

$$\chi = 1 - \mathrm{r} \sin(\delta_\mathrm{k}) = 1 - 2.09 \times \sin(40.7) = -0.36$$

Therefore, the maximum swing-out angle is obtained as follows:

$$\delta_\mathrm{m} = 10^\mathrm{o} + \arccos(\chi) = 10 + \arccos(-0.36) = 121^\mathrm{o}$$

h) Flexibility norm of conductor-insulator system

The first step is to calculate the equivalent stiffness of the system. We first calculate the equivalent conductor stiffness. Because we have a bundle of two conductors we use:

$$k_c = n \left(\frac{\mathrm{E_{s1}\,A_{s1} + E_{s2}\,A_{s2}}}{\mathrm{l_c}} \right) = 2 \left(\frac{2 \times 10^{11} \times 50 \times 10^{-6} + 5 \times 10^{10} \times 560 \times 10^{-6}}{11.5} \right) = 6.6 \times 10^6 \text{ N/m}$$

Next we calculate the equivalent stiffness of the conductor-insulator system. Because we have a strained conductor attached to vertical support insulators we use:

$$\frac{1}{k_\mathrm{eq}} = \frac{1}{k_\mathrm{c}} + \frac{1}{S} = \frac{1}{6.6 \times 10^6} + \frac{1}{1 \times 10^5} = 1.02 \times 10^{-5} \text{ m/N}$$

so that $k_{eq} = 9.85 \times 10^4 \text{ N/m}$.

The flexibility norm of the system is then given by:

$$N = \frac{1}{k_\mathrm{eq}\, l} = \frac{1}{9.85 \times 10^4 \times 11.5} = 8.83 \times 10^{-7} \text{ N}^{-1}$$

Copyright © 2010 IEEE. All rights reserved.

Copyright The Institute of Electrical and Electronics Engineers, Inc.
Provided by IHS under license with IEEE
No reproduction or networking permitted without license from IHS

Order Number: 02120914
Sold to:EGAT [700166108393] - VARRIS.Y@EGAT.CO.TH,
Not for Resale,2016-09-15 03:57:47 UTC

i) Stress factor

$$\zeta = \frac{(n g \overline{m} l)^2}{24 F_{st}^3 N} = \frac{(2 \times 9.81 \times 1.955 \times 11.5)^2}{24 \times 1464^3 \times 8.83 \times 10^{-7}} = 2.92$$

Maximum tensile force during the short circuit

j) load parameter φ

Since $T_{k1} < \frac{T_{\text{res}}}{4} : 0.16 < \frac{0.842}{4}$ we use:

$$\varphi = 3(r \sin \delta_k + \cos \delta_k - 1) = 3(2.09 \times \sin(40.7) + \cos(40.7) - 1) = 3.36$$

k) Factor ψ with φ =3.36 and the stress factor ζ = 2.92

$$\psi = 0.67$$

l) Maximum tensile force during short circuit

Because n ≥ 2:

$$F_t = 1.1 \times F_{st} \times (1 + \varphi \psi) = 1.1 \times 1464 \times (1 + 3.36 \times 0.67) = 5240 \text{ N}$$

Maximum tensile force after short circuit when conductor drops back

$$F_f = 1.2 \times F_{st} \times \sqrt{1 + 8 \zeta \frac{\delta_m}{180^o}} = 1.2 \times 1464 \times \sqrt{1 + 8 \times 2.92 \times \frac{121}{180}} = 7180 \text{ N}$$

Maximum horizontal displacement and minimum air clearance

m) Elastic deformation to the change in tension

$$\varepsilon_{\text{elas}} = N (F_t - F_{st}) = 8.83 \times 10^{-7} \times (5240 - 1464) = 3.33 \times 10^{-3}$$

Copyright © 2010 IEEE. All rights reserved.

Copyright The Institute of Electrical and Electronics Engineers, Inc.
Provided by IHS under license with IEEE
No reproduction or networking permitted without license from IHS

Order Number: 02120914
Sold to:EGAT [700166108393] - VARRIS.Y@EGAT.CO.TH,
Not for Resale,2016-09-15 03:57:47 UTC

n) Elastic deformation to thermal expansion

Because $T_{k1} < \frac{T_{\text{res}}}{4} : 0.16 < \frac{0.842}{4}$:

$$\varepsilon_{th} = c_{th}\left[\frac{I_{k3}}{n\,A_s}\right]^2 T_{k1} = 0.27\times10^{-18}\times\left[\frac{40\times10^3}{2\times(560+50)\times10^{-6}}\right]^2\times0.16 = 4.64\times10^{-5}$$

where c_{th} has been obtained with the ratio of aluminum to steel cross section = 560/50 = 11.2 > 6.

o) Maximum horizontal displacement

Because the system is strained conductors with vertical insulators we use:

$$C_D = \sqrt{1+\frac{3}{8}\left[\frac{l}{d}\right]^2\left(\varepsilon_{\text{elas}}+\varepsilon_{th}\right)} = \sqrt{1+\frac{3}{8}\left[\frac{11.5}{0.433}\right]^2\left(3.33\times10^{-3}+4.64\times10^{-5}\right)} = 1.38$$

Because $r = 2.09 > 1.8$ we have:

$$C_F = 1.15$$

Because the maximum swing-out angle $\delta_m = 121° > 90°$ we obtain:

$$b_h = C_F\,C_D\,d = 1.15\times1.38\times0.433 = 0.69\,\text{m}$$

p) Minimum air clearance

$$a_{\min} = a - 2\,b_h = 3 - 2\times0.69 = 1.62\,\text{m}$$

G.3 Finite-element calculations

In finite-element analysis, the structure is meshed into a given number of elements and analyzed. The representation of the mesh used here is presented in Figure G.1 along with all points at the boundary of elements (called nodes). Input data from Table G.1 was used. Note that in the finite-element representation, a bundle of two subconductors have been replaced by one equivalent conductor of equivalent cross-sectional area (twice the subconductor cross section). This is to avoid the numerical instabilities related to conductor clashing due to the pinch effect. Also, the equivalent support stiffness has been modeled here with the addition of a nodal spring element at each end of the conductor.

Copyright © 2010 IEEE. All rights reserved.

Copyright The Institute of Electrical and Electronics Engineers, Inc.
Provided by IHS under license with IEEE
No reproduction or networking permitted without license from IHS

Order Number: 02120914
Sold to:EGAT [700166108393] - VARRIS.Y@EGAT.CO.TH,
Not for Resale,2016-09-15 03:57:47 UTC

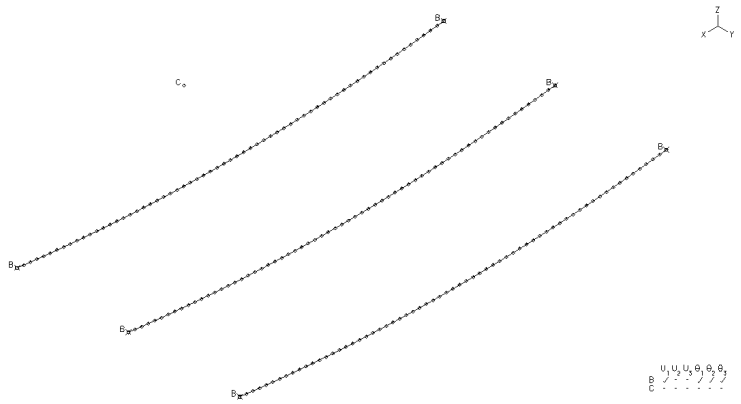

Figure G.1—Finite-element mesh of strain bus example

Some details about the numerical parameters used in calculations are presented in Table G.2.

Table G.2—Numerical parameters used in finite-element calculations

Characteristic	Value
Numerical method	Step-by-step time integration using Wilson-Theta method
Iteration method to obtain convergence	Full Newton-Rapshon with energy tolerance = 1e-6
Kinematics	Large displacement / Small deformation
Time step	5e-4 s

One significant advantage of the finite-element method is that it provides not only the maximum values required for design but also their time variation. For example, we present in Figure G.2 the variation of transversal displacement at the middle of conductor span as well as the variation of the tensile force at the end of conductor.

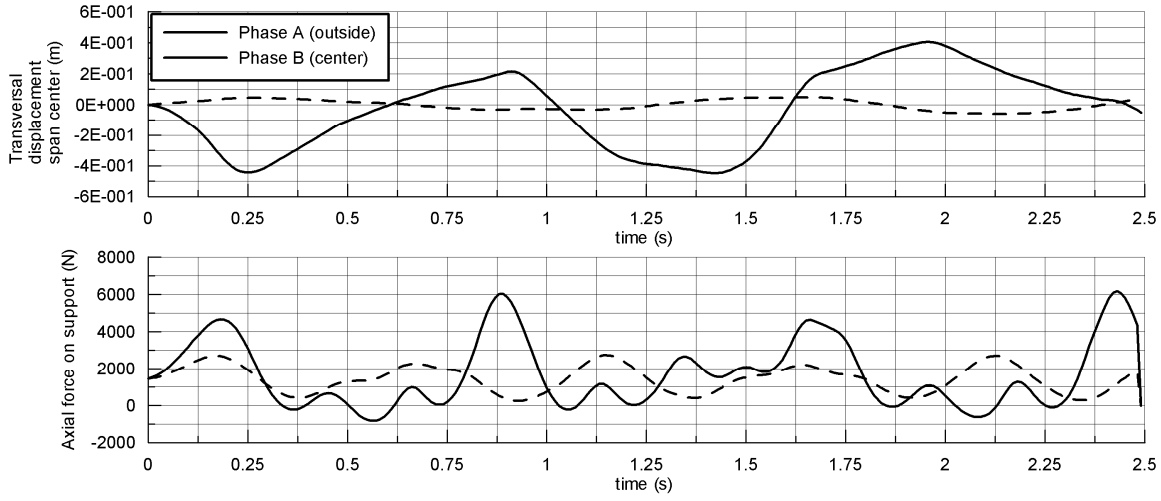

Figure G.2—Finite-element results of strain bus example

Copyright © 2010 IEEE. All rights reserved.

Copyright The Institute of Electrical and Electronics Engineers, Inc.
Provided by IHS under license with IEEE
No reproduction or networking permitted without license from IHS

Order Number: 02120914
Sold to:EGAT [700166108393] - VARRIS.Y@EGAT.CO.TH,
Not for Resale,2016-09-15 03:57:47 UTC

G.4 Comparisons of simplified calculations with finite-element results

A comparison of both methods for the results calculated here are presented in Table G.3. We also present the results from the *CIGRE* methodology in Taylor and Steuhler [B35]. It it observed that all methods lead to results of the same order, although there are some non-negligible variations, particularly for a_{min}. This is explained as the finite-element method calculates the "real" displacement of both adjacent spans while simplified calculations assume that both spans have the same opposite behavior; as observed on Figure G.2, it is observed that finite element predicts that the middle span does not move by much and has definitively not the same behavior as the outside phase.

Table G.3—Comparison of simplified calculations with finite-element method

Result	Simplified calculation	CIGREWG 02 [B36]	Finite element
F_t (N)	5240	6790	4280
F_f (N)	7180	8440	6185
b_h (m)	0.69	0.74	0.46
a_{min} (m)	1.62	1.52	2.55

G.5 Final notes

The CIGRE WG 02 published a document [B36] that contains comparisons of finite-element results with experiments. A close agreement is observed, whereas the simplified calculations seem to overpredict the experimental results. However, finite-element simulation precision is very dependent on the accuracy of data required as input, especially the equivalent stiffness at the conductor attachment points. The better the structural properties are known, the better the results will be. In general, the results obtained by any method here should be understood as giving a good order of the expected forces; if those seem to be problematic, then a more thorough study should be undertaken to gauge more precisely the results obtained.

Copyright © 2010 IEEE. All rights reserved.

Copyright The Institute of Electrical and Electronics Engineers, Inc.
Provided by IHS under license with IEEE
No reproduction or networking permitted without license from IHS

Order Number: 02120914
Sold to:EGAT [700166108393] - VARRIS.Y@EGAT.CO.TH,
Not for Resale,2016-09-15 03:57:47 UTC

Annex H

(informative)

Example rigid bus design

H.1 Description

This example illustrates the process of designing rigid bus using the information and equations presented in this guide. It considers the single bus, single breaker bus arrangement shown in Figure H.1 and discussed in Clause 4 of the guide. In addition, calculations typically performed to select flexible bus for interconnections will be included. The information required for the rigid bus design is shown in Table H.1.

Table H.1—Design parameters

Parameter	Value
Maximum load	180 MVA, 1506 A
Maximum fault current	20 kA
Maximum operating voltage	69 kV
Fault clearing time	0.25 s (15 cycles)
Phase spacing	2.44 m (8 ft)
Operating bus temperature	90 °C (194°F)
Maximum allowable temperature	250 °C (482°F)
Minimum/maximum ambient temperature	0 °C/ 40 °C (32 °F/ 104 °F)
Maximum wind speed	144 km/h (90 mph)
High wind speed with ice	64 km/h (40 mph)
Maximum anticipated icing condition	6.35 mm (0.25 in)
Latitude/longtitude	30°N, 112°W
Elevation	366 m (1200 ft)
Seismic activity	Insignificant
Atmospheric condition	Clear

NOTE—The parameters used for this example are for illustration purposes only. The users should determine appropriate values for their own design.

Copyright © 2010 IEEE. All rights reserved.

Copyright The Institute of Electrical and Electronics Engineers, Inc.
Provided by IHS under license with IEEE
No reproduction or networking permitted without license from IHS

Order Number: 02120914
Sold to:EGAT [700166108393] - VARRIS.Y@EGAT.CO.TH,
Not for Resale,2016-09-15 03:57:47 UTC

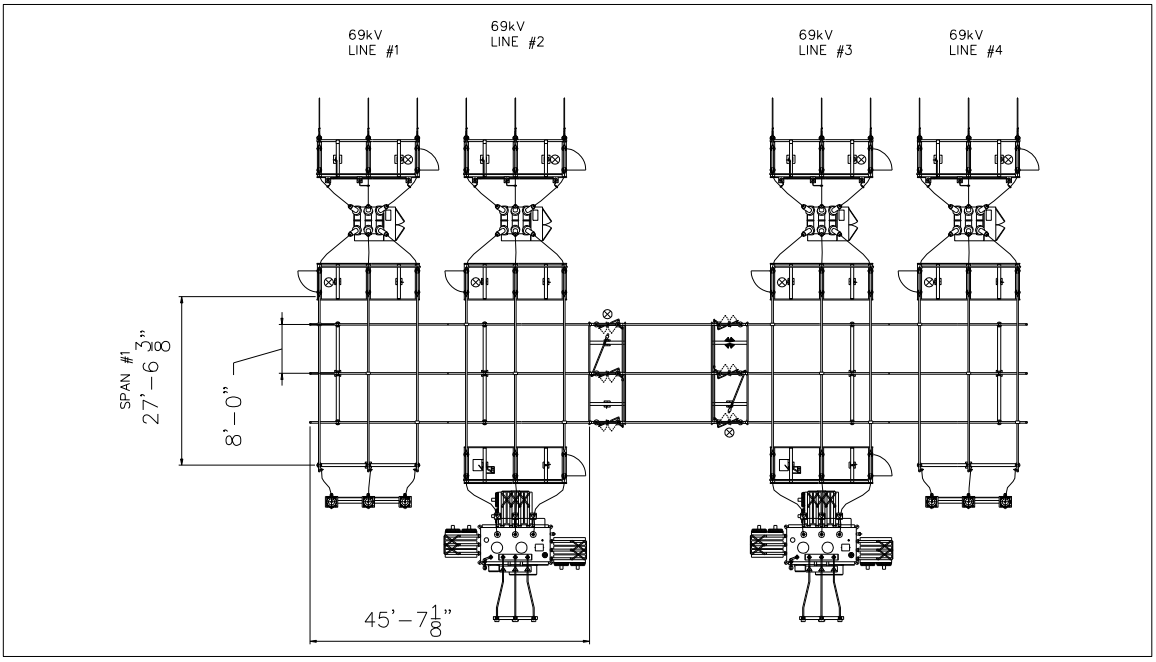

Figure H.1—General bus layout

Using the data from Table H.1 and information from the guide, the following design parameters can be determined:

a) Determine bus conductor size required for both maximum normal load and short circuit current (Clause 8 and Annex C).

b) Determine maximum corona on the bus and equipment (Clause 9 and Annex D).

c) Determine maximum forces on the structures (Clause 11).

d) Determine maximum span length of the bus based on vertical deflection limit and fiber stress (12.1 and 12.2).

e) Determine maximum required insulator rating (12.3 and 12.4).

f) Determine thermal expansion requirements (11.4).

g) Determine bus vibration and damping requirements (12.5, 12.6, and 12.7).

H.2 General

Conductors will be 6106-T6 (55% IACS) aluminum tube for rigid bus work and 1350-H19 (61% IACS) all aluminum conductor (AAC) for equipment connections. The size for each will be selected for both normal and short-circuit conditions.

The full load current is 1506 A. A 20% allowance will be made for future growth and overloading. The design load current then becomes 1807 A.

Copyright © 2010 IEEE. All rights reserved.

Copyright The Institute of Electrical and Electronics Engineers, Inc.
Provided by IHS under license with IEEE
No reproduction or networking permitted without license from IHS

Order Number: 02120914
Sold to:EGAT [700166108393] - VARRIS.Y@EGAT.CO.TH,
Not for Resale,2016-09-15 03:57:47 UTC

H.3 Ampacity

H.3.1.1 Minimum size for load current

Refer to 8.1 and Annex C.

The conductors will be sized for a load current of 1807 A. The maximum continuous conductor temperature will be 90 °C as recommended in 8.2.1. The designer needs to verify that the maximum temperature is appropriate for the equipment being used in the substation.

Ampacity tables may be used to select the conductor size. However, tables may not be available to match the design parameters. Initial sizes will be selected from tables, and then values for the design parameters will be calculated.

H.3.2 Rigid bus

From Table B.4, with sun, 0.5 emissivity, and a temperature rise of 50 °C, a 64 mm (2.5 in) SPS schedule 40 aluminum tube provides an ampacity of 1876 A. This conductor will be selected as a trial size, and the ampacity will be confirmed for the design parameters using Equation (C.1).

H.3.2.1.1 DC resistance

Refer to Equation (C.18). The DC resistance is given by:

$$R = \frac{1.724\times10^{-6}}{C' A_c}\left(1+\frac{0.00403C'}{61}(T_2-20)\right)$$

To calculate the cross-sectional area of 64 mm (2.5 in) SPS, schedule 40 bus, refer to Table B.4 to obtain outside diameter (D) and wall thickness (t):

$$A_c = \frac{\pi}{4}\times\left[(D)^2-(D-2\times t)^2\right] = \frac{\pi}{4}\times\left[(0.0730)^2-(0.0730-2\times0.00516)^2\right] = 1.099\times10^{-3}\ \text{m}^2$$

Using the other parameters in Table H.2, the DC resistance is given by:

$$R = \frac{1.724\times10^{-6}}{C' A_2}\left(1+\frac{0.00403C'}{61}(T_2-20)\right) = \frac{1.724\times10^{-6}}{55\times1.099\times10^{-3}}\left(1+\frac{0.00403\times55}{61}(90-20)\right) = 35.8\ \mu\Omega/\text{m}$$

Table H.2—Variables for DC resistance calculations

Variable	Description	Value
C'	Conductivity, % IACS. For 6101-T6 alloy per Table 2.	55
T_2	Conductor temperature	90 °C

Copyright © 2010 IEEE. All rights reserved.

Copyright The Institute of Electrical and Electronics Engineers, Inc.
Provided by IHS under license with IEEE
No reproduction or networking permitted without license from IHS

Order Number: 02120914
Sold to:EGAT [700166108393] - VARRIS.Y@EGAT.CO.TH,
Not for Resale,2016-09-15 03:57:47 UTC

H.3.2.2 Forced convection loss

Refer to Equation (C.6). The heat transfer of a cylindrical shape at least 25 mm (1 in) in diameter and with 0.6 m/s (2 ft/s) wind and 1 atmosphere pressure is given by:

$$q_c = 3.561\ D^{-0.4}\ A\ \Delta T$$

The surface area by unit length of a 64 mm (2.5 in) SPS, schedule 40 bus, 1 m long is:

$$A = \pi D l = A = \pi \times 0.073 \times 1 = 0.229\ \text{m}^2/\text{m}$$

Table H.3—Variables for forced convection loss calculations

Variable	Description	Value
A	Surface area by unit length	0.229 m^2/m
D	Cylinder diameter, see Table B.4	0.073 m
ΔT	Temperature difference between ambient and conductor surface	50 °C

Using the values in Table H.3, the forced convection heat loss is:

$$q_c = 3.561\ D^{-0.4}\ A\ \Delta T = 3.561 \times 0.073^{-0.4} \times 0.229 \times 50 = 116.2 \quad \text{W/m}$$

H.3.2.3 Radiation loss

Refer to Equation (C.13). The emissivity of aluminum is dependent on its age and environmental conditions. Typical values are 0.2 for new aluminum and 0.5 for weathered aluminum. The value for weathered aluminum will be used. The radiation loss from a surface is given by:

$$q_r = 5.6697 \times 10^{-8}\ \varepsilon\ A \left[(T_c + 273)^4 - (T_a + 273)^4 \right]$$

Table H.4—Variables for radiation loss calculations

Variable	Description	Value
A	Surface area by unit length	0.229 m^2/m
ε	Emissivity (weathered aluminum)	0.5
T_a	Ambient temperature	40 °C
T_c	Conductor temperature	90 °C

Using the values in Table H.4, the radiation heat loss is:

$$q_r = 5.6697 \times 10^{-8} \times 0.5 \times 0.229 \times \left[(90 + 273)^4 - (40 + 273)^4 \right] = 50.4 \quad \text{W/m}$$

Copyright © 2010 IEEE. All rights reserved.

Copyright The Institute of Electrical and Electronics Engineers, Inc.
Provided by IHS under license with IEEE
No reproduction or networking permitted without license from IHS

Order Number: 02120914
Sold to:EGAT [700166108393] - VARRIS.Y@EGAT.CO.TH,
Not for Resale,2016-09-15 03:57:47 UTC

H.3.2.4 Solar heat gain

Refer to Equation (C.15). The effective angle of incidence of sun for conductors in a north – south direction is, using the data in Table H.5:

$$\theta = \cos^{-1}\left[\cos H_c \cos(Z_c - Z_1)\right] = \cos^{-1}\left[\cos(83)\cos(180-0)\right] = 97°$$

Table H.5—Variables for angle of incidence of sun

Variable	Description	Value
H_c	Altitude of sun for latitude of 30°N at noon time. See Annex C, Table C.2.	83°
Z_c	Azimuth of sun for latitude of 30°N at noon time. See Annex C, Table C.2.	180°
Z_1	Azimuth of conductor line for a north–south orientation. See Annex C, C.3.2.6.	0°

For solar heat gain calculation, the projected area for a cylinder is equal to its diameter:

$$A' = D = 0.073 \text{ m}^2/\text{m}$$

From Table C.3, the total radiated heat flux, Q_s, for a clear atmosphere is 1032.6 W/m (interpolated value for $H_c = 83^o$ between $H_c = 80^o$ and $H_c = 90^o$).

The heat gained from incident solar radiation is therefore given, using the parameters summarized in Table H.6, by:

$$q_s = \varepsilon' Q_s A' K \sin(\theta) = 0.5 \times 1032.6 \times 0.073 \times 1.036 \times \sin(97) = 38.8 \text{ W/m}$$

Table H.6—Variables for solar heat gain calculations

Variable	Description	Value
ε'	Solar absorption.	0.5
Q_s	For latitude of 30°N at noon, $H_c = 83$ and Z_c=180. See Annex C, Table C.3.	1032.6 W/m
A'	Projected area of conductor by unit length.	0.073 m^2/m
K	Heat multiplying factor based on elevation of 336 m, interpolated between 0 m and 1500 m from Table C.4.	1.036
θ	Angle of incidence of sun (calculated above).	97°

Copyright © 2010 IEEE. All rights reserved.

Copyright The Institute of Electrical and Electronics Engineers, Inc.
Provided by IHS under license with IEEE
No reproduction or networking permitted without license from IHS

Order Number: 02120914
Sold to:EGAT [700166108393] - VARRIS.Y@EGAT.CO.TH,
Not for Resale,2016-09-15 03:57:47 UTC

H.3.2.5 Ampacity calculation

Refer to Equation (C.1). The allowable current, using the results from the previous calculations summarized in Table H.7, is given by:

$$I = \sqrt{\frac{q_c + q_r - q_s}{RF}} = \sqrt{\frac{116.2 + 50.4 - 38.8}{35.8 \times 10^{-6}}} = 1889 \text{ A}$$

Table H.7—Variables for ampacity calculations

Variable	Description	Value
q_C	Convective heat loss	116.2 W/m
q_r	Radiation heat loss	50.4 W/m
q_S	Solar heat gain	38.8 W/m
R	DC resistance at operating temperature	35.8 μΩ/m
F	Skin effect coefficient. Normally included in the conductor resistance as published by the Aluminum Electrical Conductor Handbook [B1]. For tubular bus conductor at 60 Hz, the skin effect can be assumed to equal to 1.	1

Therefore, the 64 mm (2.5 in) SPS, schedule 40 aluminum tubular bus having an ampacity of 1889 A is suitable to carry the maximum load current of 1807 A.

H.3.3 Flexible bus

Two conductors will be used to carry the 1807 A load. From published tables, the Magnolia type conductor (954 kcmil) has a rating of 960 A based on 40 °C ambient and an emissivity of 0.5. This conductor will be selected as a trial size, and the ampacity will be confirmed for the design parameters using Equation (C.1). The required variables for the calculations are given in Table H.8.

Copyright © 2010 IEEE. All rights reserved.

Copyright The Institute of Electrical and Electronics Engineers, Inc.
Provided by IHS under license with IEEE
No reproduction or networking permitted without license from IHS

Order Number: 02120914
Sold to:EGAT [700166108393] - VARRIS.Y@EGAT.CO.TH,
Not for Resale,2016-09-15 03:57:47 UTC

Table H.8—Variables for ampacity calculations for flexible conductor

Variable		Value
Wind speed		0.6 m/s
Emissivity		0.5
Absorptivity		0.5
Ambient temperature (T_a)		40 °C
Maximum conductor temperature (T_c)		90 °C
T_{film} ($T_c - T_a$)/2		65 °C
Density of air (ρ_a) from Table C.1 for 366 m elevation for T_{film} = 65 °C		1.004 kg/m^3
Thermal conductivity of air (k_a), from Table C.1 for T_{film} = 65 °C		0.0291 W/m°°C
Dynamic viscosity of air (μ_a) for T_{film} = 65 °C		20.26 kg/m-s
Conductor outside diameter (D)		28.6 mm
Conductor resistance	R_{25C}	62.76 μΩ/km
	R_{75C}	75.46 μΩ/km
Conductor direction		north–south
Latitude		30°N
Atmospheric conditions		Clear
Time at which current is calculated		12 Noon
Conductivity, % IACS		61
Cross-sectional area		483.4 mm^2

H.3.3.1 DC resistance

Refer to Equation (C.18). The dc resistance is given, using the parameters in Table H.9, by:

$$R = \frac{1.724\times10^{-6}}{C' A_c}\left(1+\frac{0.00403C'}{61}(T_2-20)\right)=\frac{1.724\times10^{-6}}{61\times483.4\times10^{-6}}\left(1+\frac{0.00403\times61}{61}(90-20)\right)=74.96\ \mu\Omega/\text{m}$$

Table H.9—Variables for dc resistance calculations

Variable	Description	Value
A_c	Cross-sectional area	483.4 × 10^{-6} m^2
C'	Conductivity, % IACS. For 1350-H19 alloy per Table 2.	61
T_2	Conductor temperature	90 °°C

H.3.3.2 Forced convection loss

Refer to Equation (C.6). The heat transfer of a cylindrical shape at least 25 mm (1 in) in diameter and with 0.6 m/s (2 ft/s) wind and 1 atmosphere pressure, is given by:

$$q_c = 3.561\ D^{-0.4}\ A\ \Delta T$$

Copyright © 2010 IEEE. All rights reserved.

Copyright The Institute of Electrical and Electronics Engineers, Inc.
Provided by IHS under license with IEEE
No reproduction or networking permitted without license from IHS

Order Number: 02120914
Sold to:EGAT [700166108393] - VARRIS.Y@EGAT.CO.TH,
Not for Resale,2016-09-15 03:57:47 UTC

The surface area by unit length of a 28.6 mm diameter conductor, 1 m long, is:

$$A = \pi d\, l = \pi \times 0.0286 \times 1 = 0.0897 \text{ m}^2/\text{m}$$

Table H.10—Variables for forced convection loss calculations

Variable	Description	Value
A	Surface area	0.0897 m^2/m (see calculation above)
D	Cylinder diameter	0.0286 m
ΔT	Temperature difference between ambient and conductor surface	50 °C

Using the values in Table H.10, the forced convection heat loss is:

$$q_c = 3.561 \times D^{-0.4}\, A \times \Delta T = 3.561 \times 0.0286^{-0.4} \times 0.0897 \times 50 = 66.2 \text{ W/m}$$

H.3.3.3 Radiation loss

Refer to Equation (C.13). The radiation loss from a surface is given by:

$$q_r = 5.6697 \times 10^{-8}\, \varepsilon\, A \left[(T_c + 273)^4 - (T_a + 273)^4 \right]$$

Table H.11—Variables for flexible bus radiation loss calculation

Variable	Description	Value
A	Surface area by unit length	0.0897 m^2/m
ε	Emissivity (weathered aluminum)	0.5
T_a	Ambient temperature	40 °C
T_c	Conductor temperature	90 °C

Using the values in Table H.11, the radiation heat loss is:

$$q_r = 5.6697 \times 10^{-8}\, \varepsilon\, A \left[(T_c + 273)^4 - (T_a + 273)^4 \right]$$
$$= 5.6697 \times 10^{-8} \times 0.5 \times 0.0897 \left[(90 + 273)^4 - (40 + 273)^4 \right] = 19.8 \text{ W/m}$$

H.3.3.4 Solar heat gain

Refer to Equation (C.15).

The projected area for a cylinder is equal to its diameter:

$$A' = D = 0.0286 \text{ m}^2/\text{m}$$

Copyright © 2010 IEEE. All rights reserved.

Copyright The Institute of Electrical and Electronics Engineers, Inc.
Provided by IHS under license with IEEE
No reproduction or networking permitted without license from IHS

Order Number: 02120914
Sold to:EGAT [700166108393] - VARRIS.Y@EGAT.CO.TH,
Not for Resale,2016-09-15 03:57:47 UTC

The heat gained from incident solar radiation is therefore given, using the parameters summarized in Table H.12, by:

$$q_s = \varepsilon' Q_s A' K \sin(\theta) = 0.5 \times 1032.6 \times 0.0286 \times 1.036 \times \sin(97) = 15.2 \text{ W/m}$$

Table H.12—Variables for solar heat gain calculations

Variable	Description	Value
ε'	Solar absorption	0.5
Q_s	From Table H.6	1032.6 W/m
A'	Projected area of conductor	0.0286 m^2/m
K	From Table H.6	1.036
θ	From Table H.6	97°

H.3.3.5 Ampacity calculation

Refer to Equation (C.1). The allowable current, using the results from the previous calculations summarized in Table H.13, is given by:

$$I = \sqrt{\frac{q_c + q_r - q_s}{RF}} = \sqrt{\frac{66.2 + 19.8 - 15.2}{74.96 \times 10^{-6}}} = 972 \text{ A}$$

Table H.13—Variables for ampacity calculations for flexible bus

Variable	Description	Value
q_C	Convective heat loss	66.2 W/m
q_r	Radiation heat loss	19.8 W/m
q_S	Solar heat gain	15.2 W/m
R	DC resistance at operating temperature	74.96 μΩ/m
F	Skin effect coefficient	1

The rating of two conductors is equal to 972 × 2=**1944 A**.

Therefore, two 954 kcmil AAC conductors having an ampacity of 1944 A are suitable to carry the maximum load current of 1807 A.

H.4 Minimum size for short circuit current

The short circuit current rating of these conductors should be verified to ensure that they are capable of carrying the available short circuit current (20 kA) for the time specified (0.25 s).

Equation (3) in the guide, along with the variables in Table H.14, will be used to determine the maximum current that the conductors can carry for 0.25 s and a maximum conductor temperature of 250 °C:

$$I = C \times 10^6 \times A_c \sqrt{\frac{1}{t} \log_{10}\left(\frac{T_f - 20\ ^\circ\text{C} + (15\,150/G)}{T_i - 20\ ^\circ\text{C} + (15\,150/G)}\right)}$$

Copyright © 2010 IEEE. All rights reserved.
Copyright The Institute of Electrical and Electronics Engineers, Inc.
Provided by IHS under license with IEEE
No reproduction or networking permitted without license from IHS
Order Number: 02120914
Sold to:EGAT [700166108393] - VARRIS.Y@EGAT.CO.TH,
Not for Resale,2016-09-15 03:57:47 UTC

Table H.14—Variables for conductor short circuit current calculations

Variable	Description	Value
C	Constant	2.232×10^{-4} for metric units with A in mm^2
I_{sc}	Short-circuit current	20 kA
G	Conductivity, per Table 2	55% for 6101 T61 aluminum (rigid bus) 61% for 1350-H19 (flexible conductor)
t	Fault clearing time	0.25 s
T_f	Maximum conductor temperature	250 °C
T_i	Initial conductor temperature	90 °C
A_c (rigid)	Conductor area, tube	1099 mm^2
A_c (flexible)	Conductor area, flexible bus	483.4 mm^2

Allowable short circuit current for rigid bus:

$$I = C \times 10^6 \, A_c \sqrt{\frac{1}{t} \log_{10}\left(\frac{T_f - 20\ ^\circ\text{C} + (15\,150/G)}{T_i - 20\ ^\circ\text{C} + (15\,150/G)}\right)}$$

$$= 2.232 \times 10^{-4} \times 10^6 \times 1099 \sqrt{\frac{1}{0.25} \log_{10}\left(\frac{250 - 20\ ^\circ\text{C} + (15\,150/55)}{90 - 20\ ^\circ\text{C} + (15\,150/55)}\right)} = 199\,277 \text{ A} \cong 200 \text{ kA}$$

Allowable short circuit current for one flexible conductor:

$$I = C \times 10^6 \, A_c \sqrt{\frac{1}{t} \log_{10}\left(\frac{T_f - 20\ ^\circ\text{C} + (15\,150/G)}{T_i - 20\ ^\circ\text{C} + (15\,150/G)}\right)}$$

$$= 2.232 \times 10^{-4} \times 10^6 \times 483.4 \sqrt{\frac{1}{0.25} \log_{10}\left(\frac{250 - 20\ ^\circ\text{C} + (15\,150/61)}{90 - 20\ ^\circ\text{C} + (15\,150/61)}\right)} = 90\,662 \text{ A} \cong 91$$

For two flexible conductors, the allowable short circuit current will be twice the value above = 182 kA.

Based on the above calculations, both the rigid bus and flexible conductors are adequately rated for the short circuit current of 20 kA.

H.5 Voltage gradient

Corona cannot be eliminated, but it can be controlled to acceptable levels. The goal is that the corona is below the allowable voltage gradient. Refer to Clause 9 and Annex D.

First we need to evaluate the corona onset gradient given by Equation (D.1):

$$E_c = mE_0 D_a \left(1 + \frac{C}{\sqrt{D_a r_c}}\right)$$

Copyright © 2010 IEEE. All rights reserved.
Copyright The Institute of Electrical and Electronics Engineers, Inc.
Provided by IHS under license with IEEE
No reproduction or networking permitted without license from IHS
Order Number: 02120914
Sold to:EGAT [700166108393] - VARRIS.Y@EGAT.CO.TH,
Not for Resale,2016-09-15 03:57:47 UTC

Table H.15—Variables for corona onset gradient E_c calculation

Variable	Description	Value
m	Air density factor, use worst case of 0.6–0.85 range suggested in D.1.1	0.85
E_o	Empirical constant per D.1.1	21.1 kV/cm
D_a	Relative air density per Equation (D.2), Equation (D.3) and calculated below	0.917
C	Empirical constant	0.301 cm^{-1}
r_c	Conductor outside radius (equivalent radius for a bundle of n subconductors)	3.65 cm for rigid bus 3.81 cm for flexible conductor as calculated below
T	Ambient air temperature	40 °C
T_o	Air temperature used in determining constants E_o and C and factor m	25 °C
A	Altitude	0.366 km

$$D_a = \left(\frac{273+T_0}{273+T}\right)\left(1-\frac{A}{10}\right) = \left(\frac{273+25}{273+40}\right)\left(1-\frac{0.366}{10}\right) = 0.917$$

For rigid bus, E_c is given by:

$$E_c = mE_0D_a\left(1+\frac{C}{\sqrt{D_a r_c}}\right) = 0.85\times 21.1\times 0.917\times\left(1+\frac{0.301}{\sqrt{0.917\times 3.65}}\right) = 19.2 \text{ kV/cm}$$

For flexible conductor, we first need to calculate the equivalent single-conductor radius of bundle subconductors, using Equation (D.11) with $n = 2$ (2 flexible conductors):

$$r_e = r\times\left(g\times\frac{s}{r}\right)^{\frac{n-1}{n}} = 1.43\times\left(1\times\frac{10.16}{1.43}\right)^{\frac{2-1}{2}} = 3.812 \text{ cm}$$

Therefore

$$E_c = mE_0D_a\left(1+\frac{C}{\sqrt{D_a r_c}}\right) = 0.85\times 21.1\times 0.917\times\left(1+\frac{0.301}{\sqrt{0.917\times 3.812}}\right) = 19.1 \text{ kV/cm}$$

--`,,,,,,`,```,,`,`,,`,`,,`,-`-`,,`,,,`---
Copyright © 2010 IEEE. All rights reserved.
Copyright The Institute of Electrical and Electronics Engineers, Inc.
Provided by IHS under license with IEEE
No reproduction or networking permitted without license from IHS
Order Number: 02120914
Sold to:EGAT [700166108393] - VARRIS.Y@EGAT.CO.TH,
Not for Resale,2016-09-15 03:57:47 UTC

H.5.1 Rigid bus conductor voltage gradient

The maximum voltage gradient is evaluated using Equation (D.6), Equation (D.7), and Equation (D.8) using the data given in Table H.16.

Table H.16—Variables for voltage gradient calculations for rigid bus

Variable	Description	Value
h	Conductor height above ground	366 cm
d	Bus conductor diameter	7.30 cm
D	Phase-to-phase spacing	244 cm
V_1	Phase-to-ground voltage multiplied by 1.1	43.82 kV

Equivalent distance from center of conductor to ground per Equation (D.8):

$$h_e = \frac{hD}{\sqrt{4h^2 + D^2}} = \frac{366 \times 244}{\sqrt{4 \cdot 366^2 + 244^2}} = 115.74 \text{ cm}$$

Average voltage gradient per Equation (D.6):

$$E_a = \frac{V_1}{\frac{d}{2} \times \ln\left(\frac{4h_e}{d}\right)} = \frac{43.82}{\frac{7.3}{2} \times \ln\left(\frac{4 \times 115.74}{7.3}\right)} = 2.89 \text{ kV /cm}$$

Maximum voltage gradient per Equation (D.7):

$$E_m = \frac{h_e}{h_e - \frac{d}{2}} E_a = \frac{115.74}{115.74 - \frac{7.3}{2}} \times 2.89 = 2.98 \text{ kV /cm}$$

For satisfactory operation, $E_m < E_c$. The 64 mm (2.5 in) SPS, schedule 40 aluminum tube meets this criteria and is **acceptable.**

H.5.2 Flexible bus conductor voltage gradient

The maximum voltage gradient is evaluated using Equation (D.12) and Equation (D.13), and the data given in Table H.17.

Copyright © 2010 IEEE. All rights reserved.

Copyright The Institute of Electrical and Electronics Engineers, Inc.
Provided by IHS under license with IEEE
No reproduction or networking permitted without license from IHS

Order Number: 02120914
Sold to:EGAT [700166108393] - VARRIS.Y@EGAT.CO.TH,
Not for Resale,2016-09-15 03:57:47 UTC

Table H.17—Variables for voltage gradient calculations for flexible conductor bundle

Variable	Description	Value
h_e	Equivalent height to ground (calculated above)	115.74 cm
d	Bus conductor diameter	2.86 cm
r	Bus conductor radius	1.43 cm
D	Phase-to-phase spacing	244 cm
V_1	Phase-to-ground voltage multiplied by 1.1	43.82 kV
r_e	Equivalent single-conductor radius of bundle sub conductors (calculated above)	3.812 cm

Average voltage E_a gradient per Equation (D.12):

$$E_a = \frac{V_1}{nr\ln\frac{2h_e}{r_e}} = \frac{43.82}{2\times 1.43\times \ln\left(\frac{2\times 115.74}{3.81}\right)} = 3.73 \text{ kV/cm, rms}$$

Maximum voltage gradient per Equation (D.13):

$$E_m = \frac{h_e}{h_e - r_e} E_a = \frac{115.74}{115.74 - 3.81}\times 3.73 = 3.86 \text{ kV /cm, rms}$$

For satisfactory operation, $E_m < E_c$. The 954 kcmil AAC meets this criteria and is **acceptable.**

H.6 Rigid bus loads

H.6.1 Conductor weight

Based on Equation (5) and the data in Table H.18, the unit weight of the rigid bus is given by:

$$F_c = \pi w_c t_c (D_o - t_c) = \pi \times 26\,500 \times 0.0052 \times (0.073 - 0.0052) = 29.4 \text{ N/m}$$

Table H.18—Variables for rigid bus conductor force

Variable	Description	Value
w_c	Specific weight of aluminum, see Equation (5) description	26 500 N/m^3
t_c	Conductor wall thickness, see Table B.4	0.0052 m
D_o	Conductor outside diameter, see Table B.4	0.073 m

H.6.2 Ice load

Using Equation (6) and the data in Table H.19, the ice unit weight is given by:

$$F_i = \pi w_i r_i (D_o + r_i) = \pi \times 8820 \times 0.00635 \times (0.073 + 0.00635) = 14.0 \text{ N/m}$$

Copyright © 2010 IEEE. All rights reserved.

Copyright The Institute of Electrical and Electronics Engineers, Inc.
Provided by IHS under license with IEEE
No reproduction or networking permitted without license from IHS

Order Number: 02120914
Sold to:EGAT [700166108393] - VARRIS.Y@EGAT.CO.TH,
Not for Resale,2016-09-15 03:57:47 UTC

Table H.19—Variables for ice force on rigid bus

Variable	Description	Value
w_i	Ice weight, see Equation (6) description	8820 N/m^3
r_i	Equivalent uniform radial ice thickness	0.00635 m
D_o	Conductor outside diameter, see Table B.4	0.073 m

H.6.3 Wind loads

Extreme wind generally results in higher loads than high wind with ice. Both will be calculated to determine which is larger.

Here the extreme wind loading without ice will be calculated using Equation (8) and the data in Table H.20:

$$F_w = CV^2 D_o C_f K_Z G_f I = 0.613 \times 40^2 \times 0.073 \times 1.0 \times 0.7 \times 0.85 \times 1.15 = 49.0 \text{ N/m}$$

Table H.20—Variables for extreme wind load (without ice)

Variable	Description	Value
C	Constant, for metric units	0.613
V	Extreme wind velocity, from Figure 14	40 m/s (144 km/h)
D_o	Conductor outside diameter	0.073 m
C_f	Force coefficient for rigid tubular bus per 11.2.3	1.0
K_Z	Height and exposure factor, Exposure B from Table 7	0.57
G_f	Gust response factor, per 11.2.5	0.85
I	Importance factor, per 11.2.6	1.15

Here the high wind loading with ice will be calculated using Equation (9) and the data in Table H.21:

$$F_{WI} = CV_I^2 (D_o + 2 \times r_I) C_f K_Z G_f I = 0.613 \times 17.8^2 \times (0.073 + 2 \times 0.00635) \times 1.0 \times 0.7 \times 0.85 \times 1.15 = 11.4 \text{ N/m}$$

Table H.21—Variables for high wind with ice

Variable	Description	Value
C	Constant, for metric units	0.613
V_I	High wind velocity, from Figure 8	17.8 m/s (64 km/h)
D_o	Conductor outside diameter	0.073 m
r_i	Equivalent uniform radial thickness of ice	0.00635 m
C_f	Force coefficient for rigid tubular bus per 11.2.3	1.0
K_Z	Height and exposure factor, Exposure B from Table 7	0.7
G_f	Gust response factor, per 11.2.5	0.85
I	Importance factor, per 11.2.6	1.15

Copyright © 2010 IEEE. All rights reserved.

Copyright The Institute of Electrical and Electronics Engineers, Inc.
Provided by IHS under license with IEEE
No reproduction or networking permitted without license from IHS

Order Number: 02120914
Sold to:EGAT [700166108393] - VARRIS.Y@EGAT.CO.TH,
Not for Resale,2016-09-15 03:57:47 UTC

H.6.4 Short circuit load

The short circuit force for infinitely long parallel conductors is calculated using Equation (14) and Equation (16), which provides corrections to account for the momentary peak factor effect and mounting structure flexibility, using the data in Table H.22:

$$F_{sc\_\text{corrected}} = D_f^2 \, K_f \, F_{sc} = D_f^2 \, K_f \left(\frac{16 \, \Gamma \, I_{sc}^2}{10^7 \, D} \right) = 0.927^2 \times 1 \times \left(\frac{16 \times 0.866 \times 20{,}000^2}{10^7 \times 2.44} \right) = 195.2 \quad \text{N/m}$$

Table H.22—Variables for short-circuit calculations

Variable	Description	Value
I_{SC}	Short-circuit current	20 kA
D	Phase spacing	2.44 m
D_f	Half cycle decrement factor from Equation (18) and Equation (19) with X/R = 20	0.927
K_f	Mounting structure flexibility factor, from Figure 20 for a bus height of 4.27 m (14 ft) and steel structures (Type B)	1
Γ	Constant based on type of fault and conductor location, from Table 13 for a flat three phase configuration with the highest force (centre conductor)	0.866

H.6.5 Total gravitational force

The gravitational force to evaluate the maximum allowable span under the specified deflection limit will be evaluated without ice. It will be assumed that no damping material is used with the conductor. The gravitational force is therefore equal to the conductor weight:

$$F_G = F_c = 29.4 \quad \text{N/m}$$

H.6.6 Total force

The total force is given by the vector sum of the vertical and horizontal forces, as per Equation (78).

We will consider here that short circuit is concurrent with wind and will evaluate the cases without and with ice.

The total force for extreme wind with no ice, short circuit, and conductor weight is given by:

$$F_{T1} = \sqrt{F_H^2 + F_V^2} = \sqrt{\left(F_w + F_{sc}\right)^2 + F_c^{\,2}} = \sqrt{\left(49.0 + 195.2\right)^2 + 29.4^2} = 246.0 \quad \text{N/m}$$

Copyright © 2010 IEEE. All rights reserved.

Copyright The Institute of Electrical and Electronics Engineers, Inc.
Provided by IHS under license with IEEE
No reproduction or networking permitted without license from IHS

Order Number: 02120914
Sold to:EGAT [700166108393] - VARRIS.Y@EGAT.CO.TH,
Not for Resale,2016-09-15 03:57:47 UTC

The total force for high wind with ice, short circuit, and conductor weight is given by:

$$F_{T2} = \sqrt{F_H^2 + F_V^2} = \sqrt{(F_{WI} + F_{sc})^2 + (F_c + F_i)^2} = \sqrt{(11.4 + 195.2)^2 + (29.4 + 14.0)^2} = 211.1 \text{ N/m}$$

The higher loading occurs for extreme wind with no ice, F_{TI}.

H.7 Allowable span

H.7.1 Allowable span based on deflection limit

The deflection of a span with pinned-pinned end conditions will be calculated without any damping material. The recommended allowable deflection of 1:150 (0.67 %) will be used.

The allowable span is given by Equation (72), using the data in Table H.23:

$$L_V = \left(\frac{384 E J \eta}{5 F_G} \right)^{\frac{1}{3}} = \left(\frac{384 \times 68.9 \times 10^9 \times 6.40 \times 10^{-7} \times 0.0067}{5 \times 29.4} \right)^{1/3} = 9.17 \text{ m}$$

Table H.23—Variables for allowable span calculations based on deflection limit

Variable	Description	Value
η	Allowable deflection as a fraction of span length	0.0067 (1/150)
E	Modulus of elasticity for aluminium	68.9×10^9 N/m^2
J	Bending moment of inertia, per Equation (73), see calculation below	6.40×10^{-7} m^4
F_G	Gravitational force	33.7 N/m

$$J = \pi \frac{\left(D_o^4 - D_i^4\right)}{64} = \pi \frac{\left(0.073^4 - (0.073 - 2 \times 0.0052)^4\right)}{64} = 6.40 \times 10^{-7} \text{ m}^4$$

H.7.2 Allowable span based on fiber stress

Fiber stress will be based on a single span with pinned-pinned end conditions that provide a worst-case result.

The yield stress of 6061-T6 aluminium is 240 MPa (35 ksi) according to AWS D1.2-2003 (see Clause 2). Welded couplers and connectors will be used. Welding reduces the allowable stress to approximately 50% according to the Aluminum Design manual (see Clause 2). The allowable yield stress is therefore 120 MPa. Using Equation (79) and the data in Table H.24, the allowable span is given by:

$$L_S = \sqrt{\frac{16 J \sigma_{\text{allowable}}}{F_T D_o}} = \sqrt{\frac{16 \times 6.40 \times 10^{-7} \times 120 \times 10^6}{246.0 \times 0.073}} = 8.27 \text{ m}$$

Copyright © 2010 IEEE. All rights reserved.

Copyright The Institute of Electrical and Electronics Engineers, Inc.
Provided by IHS under license with IEEE
No reproduction or networking permitted without license from IHS

Order Number: 02120914
Sold to:EGAT [700166108393] - VARRIS.Y@EGAT.CO.TH,
Not for Resale,2016-09-15 03:57:47 UTC

Table H.24—Variables for allowable span calculations based on fiber stress

Variable	Description	Value
J	Bending moment of inertia (as calculate above)	6.42×10^{-7} m^4
$\sigma_{allowable}$	Allowable stress of material accounting for welds	120 MPa
F_T	Total force, per H.6.6	246.0 N/m
D_o	Conductor outside diameter	0.073 m

H.7.3 Maximum allowable span

The maximum span will be the lesser of the lengths based on deflection and fiber stress. For this example, the two values are 9.17 m and 8.27 m. The maximum span is therefore 8.27 m, and we will round up this value to 8.3 m in the following discussion.

H.8 Vibration

H.8.1 Natural frequencies of rigid bus spans

Since the end connections are never perfectly pinned-pinned or fixed-fixed, we will evaluate the natural frequency based on these two sets of end conditions to get the range of possible fundamental frequencies of a span. We will use the allowable span calculated above of 8.3 m.

The natural frequency is calculated using Equation (103) and the data in Table H.25.

For pinned-pinned conditions we have:

$$f_b = \frac{\pi K^2}{2L^2}\sqrt{\frac{EJ}{m}} = \frac{\pi \times 1.0^2}{2 \times 8.3^2}\sqrt{\frac{68.9 \times 10^9 \times 6.40 \times 10^{-7}}{3.00}} = 2.76 \text{ Hz}$$

For fixed-fixed conditions we have:

$$f_b = \frac{\pi K^2}{2L^2}\sqrt{\frac{EJ}{m}} = \frac{\pi \times 1.51^2}{2 \times 8.3^2}\sqrt{\frac{68.9 \times 10^9 \times 6.40 \times 10^{-7}}{3.00}} = 6.30 \text{ Hz}$$

Table H.25—Variables for natural frequency calculations

Variable	Description	Value
K	Constant based on bus end conditions	1.0 for pinned-pinned and 1.51 for fixed-fixed
L	Span length	8.3 m
E	Modulus of elasticity	68.9 N/m^2
J	Bending moment of inertia (as calculated above)	6.40×10^{-7} m^4
m	Mass per unit length, see calculation below	3.00 kg/m

$$m = \frac{F_c}{9.81\,m/s^2} = \frac{29.4\,N/m}{9.81\,m/s^2} = 3.00 \text{ kg/m}$$

Copyright © 2010 IEEE. All rights reserved.

Copyright The Institute of Electrical and Electronics Engineers, Inc.
Provided by IHS under license with IEEE
No reproduction or networking permitted without license from IHS

Order Number: 02120914
Sold to:EGAT [700166108393] - VARRIS.Y@EGAT.CO.TH,
Not for Resale,2016-09-15 03:57:47 UTC

H.8.2 Wind-induced vibration

Wind induced excitation frequency is calculated using Equation (100) and the data in Table H.26. *V* here is not the maximum wind speed expected at the site, but the speed expected under normal operation conditions. Since wind speeds below 8 km/h or above 72 km/h do not induce vibrations (based on the fact that outside the range spanned by these values, the flow around an average sized conductor does not induce vortex shedding leading to aeolian vibrations), these will be used as lower and upper boundaries of the speed expected at the site.

The upper frequency with the upper wind speed is given by:

$$f_a = \frac{C \times V}{D_o} = \frac{0.19 \times 20.0}{0.073} = 52.1 \text{ Hz}$$

The lower frequency with the lower wind speed is given by:

$$f_a = \frac{C \times V}{D_o} = \frac{0.19 \times 2.220}{0.073} = 5.78 \text{ Hz}$$

Table H.26—Variables for wind-induced vibration calculations

Variable	Value
C	0.19 for a cylinder per Equation (100) description
V	wind speed in m/s: Upper: 72 km/h = 20.00 m/s; Lower: 8 km/h = 2.22 m/s
D_o	0.073 m

A conductor will vibrate if its natural frequency is in the vicinity of either the wind frequency or that of the alternating current (*2f*). It is recommended that an allowance for variations be allowed. This is accomplished by ensuring the ratio of the natural frequency to the inducing frequency is not in the range 0.5 to $\sqrt{2}$, as given by Equation (101):

$$\frac{1}{2} \le \frac{f_a}{f_b} \le \sqrt{2}$$

Based on the excitation frequencies calculated above as well as the span natural frequencies for both pinned-pinned and fixed-fixed conditions, we can evaluate the worst combinations that could fall within the range to avoid:

Pinned-pinned

$$\frac{f_{a(\text{lower})}}{f_b} = \frac{5.78}{2.76} = 2.09$$

$$\frac{f_{a(\text{upper})}}{f_b} = \frac{52.1}{2.76} = 18.9$$

It is observed for the pinned-pinned conditions that the ratios are outside the range to avoid, so wind-induced vibration is *unlikely* to occur.

Copyright © 2010 IEEE. All rights reserved.

Copyright The Institute of Electrical and Electronics Engineers, Inc.
Provided by IHS under license with IEEE
No reproduction or networking permitted without license from IHS

Order Number: 02120914
Sold to:EGAT [700166108393] - VARRIS.Y@EGAT.CO.TH,
Not for Resale,2016-09-15 03:57:47 UTC

Fixed-fixed

$$\frac{f_{a(\text{lower})}}{f_b} = \frac{5.78}{6.30} = 0.92$$

$$\frac{f_{a(\text{upper})}}{f_b} = \frac{52.1}{6.30} = 8.27$$

It is observed for the fixed-fixed conditions that the ratio using the lower frequency of wind excitation is within the range to avoid, so wind-induced vibration is likely to occur.

H.8.3 Induced vibration from alternating current

Vibration due to alternating current excitation will occur when $f_b > f$ per Equation (102). Using the maximum possible value of f_b for fixed-fixed conditions, and the power frequency of 60 Hz, we have:

$$6.30 < 60$$

So the bus should not be affected by vibrations from alternating current excitation.

H.8.4 Vibration attenuation requirements

Based on this analysis, vibration dampers will be required due to wind-induced vibration. As discussed in 12.7, the use of either a damping cable or dampers is recommended. Therefore, the calculations for allowable span may have to be reviewed if a damping cable is used since this adds mass and therefore increases the weight by unit length in the vertical direction.

H.9 Thermal expansion

The expansion of this section of bus will be calculated for an installation temperature of 0 °C and the operating temperature of 90 °C, using the data in Table H.27. A length of 16.6 m will be used, which is the largest length for this example (two continuous spans of 8.3 m). Using Equation (65):

$$\Delta L = \alpha \times L_i \left(T_f - T_i\right) = 23.1 \times 10^{-6} \times 16.6 \times (90 - 0) = 0.0345 \text{ m or } 34.5 \text{ mm}$$

Table H.27—Variables for thermal expansion calculations

Variable	Value
α	23.1×10^{-6} 1/°C for aluminum per Table 17
T_i	0 °C, minimum normal temperature
T_f	90 °C, maximum normal temperature
L_i	16.6 m, length of bus

Copyright © 2010 IEEE. All rights reserved.

Copyright The Institute of Electrical and Electronics Engineers, Inc.
Provided by IHS under license with IEEE
No reproduction or networking permitted without license from IHS

Order Number: 02120914
Sold to:EGAT [700166108393] - VARRIS.Y@EGAT.CO.TH,
Not for Resale,2016-09-15 03:57:47 UTC

A 16.6 m section of bus will therefore have 34.5 mm of expansion over the minimum-to-maximum temperature range. Supports need to be selected to accommodate this movement, or a thermal expansion fitting at one support is recommended; the 16.6 m bus section in this example has two supports with a third at a disconnect switch terminal. One solution would be to fix the two outer supports and make the middle one an expansion support.

H.10 Insulator selection

A sample calculation will be done for a two-supports bus span. The designers will be required to carry out the same calculations for all spans and to select insulators for the entire substation based on the maximum force from them.

H.10.1 Trial insulator selection

Refer to insulator tables from a manufacturer. Most insulators are assigned a Technical Reference number, which all manufacturers can supply. Insulators with a BIL of 350 kV are typically used for this voltage level. The standard strength 350 kV BIL insulator is a TR-216 insulator with a rated cantilever strength of 6.67 kN (1500 lbf).

H.10.2 Span force calculations

Calculations will be done considering two continuous spans of 8.3 m with support boundary conditions P-C-P as per Table 18.

The sample bus uses vertically mounted insulators to support horizontal rigid bus. The total cantilever force on the mid insulator is calculated using Equation (89). In this example, only forces in the *x* direction (see Figure 31) will create cantilever forces because provision is made for bus expansion so that no force will be generated due to thermal effects. The formula to calculate the cantilever force, using extreme wind with no ice gives:

$$F_C = k_W\left[\frac{F_{WCI}}{2} + \frac{(H_T + H_f)F_{WC}}{H_T}\right] + k_{SC}\frac{(H_T + H_f)F_{scC}}{H_T}$$

The wind force on the insulator is calculated per Equation (8) and constants determined earlier in H.6.3:

$$F_{W1} = CV^2 D_i C_f K_Z G_f I = 0.613 \times 40^2 \times 0.28 \times 1.0 \times 0.7 \times 0.85 \times 1.15 = 187.9 \text{ N/m}$$

Incorporating Equation (83), Equation (84), and Equation (87), and the data in Table H.28, gives:

$$\begin{aligned} F_C = F_{C\_x} &= k_W\left[\frac{F_{W1}H_T}{2} + \frac{(H_T + H_f)F_{W2}L_E}{H_T}\right] + k_{sc}\frac{(H_T + H_f)F_{sc}L_E}{H_T} \\ &= 2.5\left[\frac{187.9 \times 0.762}{2} + \frac{(0.762 + 0.08) \times 49.0 \times 10.4}{0.762}\right] + 1.0\left[\frac{(0.762 + 0.08) \times 195.2 \times 10.4}{0.762}\right] \\ &= 3830 \text{ N} = 3.83 \text{ kN} \end{aligned}$$

Copyright © 2010 IEEE. All rights reserved.

Copyright The Institute of Electrical and Electronics Engineers, Inc.
Provided by IHS under license with IEEE
No reproduction or networking permitted without license from IHS

Order Number: 02120914
Sold to:EGAT [700166108393] - VARRIS.Y@EGAT.CO.TH,
Not for Resale,2016-09-15 03:57:47 UTC

Table H.28—Variables for cantilever force calculations

Variable	Description	Value
F_{W1}	Wind force on insulator calculated per calculation below	187.9 N/m
V	Extreme wind velocity, from Figure 14	40 m/s (144 km/h)
D_i	Effective insulator diameter	0.28 m
F_{W2}	Wind force on the conductor per H.6.3 (F_w)	49.0 N/m
F_{SC}	Short-circuit force on the conductor per H.6.4	195.2 N/m
L_E	Effective length of conductor span for two 8.3 m continuous spans with P-C-P conditions as per Table 18 (5 L/4)	10.4 m
H_T	Total height of the insulator column	0.762 m
H_f	Height from the insulator top to the bus center line, refer to bus support manufacturer for value	0.08 m
k_W	Load factor for wind forces	2.5
k_{SC}	Load factor for short-circuit current (the requirements of 12.3.4 have been met).	1.0

H.10.3 Insulator selection

The required rated cantilever strength is 3.83 kN. The selected TR-216 insulator has a rated cantilever strength of 6.67 kN. This selected insulator has acceptable cantilever strength.

H.11 Summary

The trial sizes for both the rigid and the flexible bus satisfy the electrical and structural requirements.

Copyright © 2010 IEEE. All rights reserved.

Copyright The Institute of Electrical and Electronics Engineers, Inc.
Provided by IHS under license with IEEE
No reproduction or networking permitted without license from IHS

Order Number: 02120914
Sold to:EGAT [700166108393] - VARRIS.Y@EGAT.CO.TH,
Not for Resale,2016-09-15 03:57:47 UTC

Annex I

(informative)

Example strain bus design

I.1 Introduction

The purpose of this example is to illustrate the process of strain bus design calculations using the information and equations presented in this guide. This example considers a simple 230kV bus (Figure I.1). The weight and effect of drops to the disconnect switches have been considered negligible in this example. Basic information required for the strain bus design is shown in Table I.1. Other information will be given once the conductor is selected.

Table I.1—Example data

Data		Description	Value
Load data MVA	I_{LOAD}	Maximum load current	4800 A
Fault current data	I_{k3}	rms fault current	63 kA
	T_{kl}	Fault duration	0.1 s
	F	System frequency	60 Hz
Span and structure data	L	Distance between the two supports including insulators	48.8 m
	l_i	Insulator length	2.00 m
	d_i	Insulator diameter	0.075 m
	E_i	Insulator Young's modulus	30 GPa
	l_c	Length of the conductor span carrying current	44.7 m
	l_s	Distance between spacers	22.37 m
	a	Phase-to-phase distance	4.12 m
	a_s	Distance between sub conductors	0.457 m
	S	Equivalent support stiffness	10^5 N/m
		Substation elevation	400 m
Wind		Surface roughness	D
		Exposure type	D
	V	Extreme wind speed	112 km/h
	V_I	Wind speed with ice	48 km/h
Ice	r_I	Uniform radial ice thickness	0.0127 m
Temperature		Summer ambient temperature	40 °C
		Winter ambient temperature	–10 °C

Copyright © 2010 IEEE. All rights reserved.

Copyright The Institute of Electrical and Electronics Engineers, Inc.
Provided by IHS under license with IEEE
No reproduction or networking permitted without license from IHS

Order Number: 02120914
Sold to:EGAT [700166108393] - VARRIS.Y@EGAT.CO.TH,
Not for Resale,2016-09-15 03:57:47 UTC

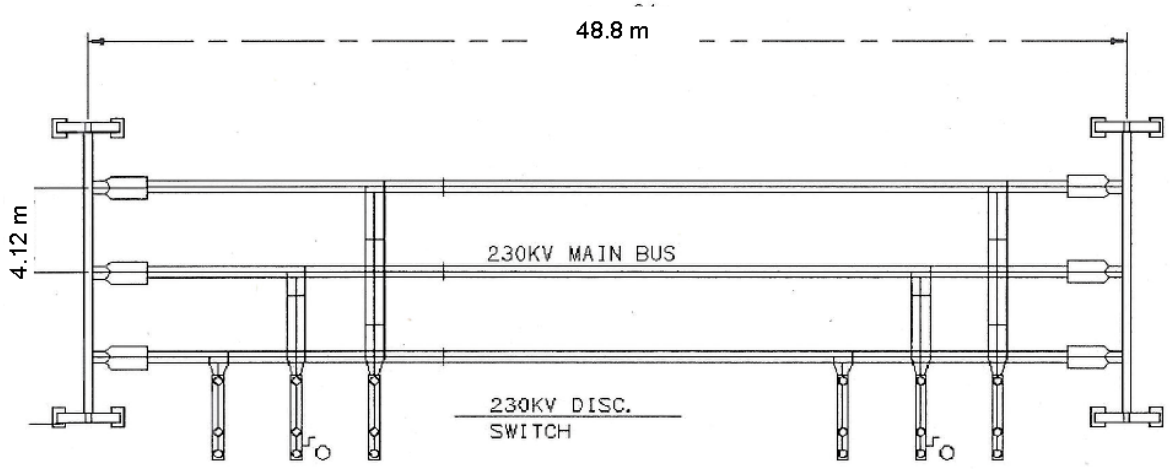

Figure I.1—Strain bus layout

Based on the above data, it is required to use the information and the equations given in the main body of this guide to calculate the following design parameters:

a) Determine the conductor requirements, which consist of:

1) Conductor type and size

2) Number of subconductors required

b) Calculate conductor sag at both winter temperature and maximum operating temperature

c) Determine maximum surface voltage gradient and determine if acceptable “corona”

d) Determine the following loads on the structure

1) Short circuit effects:

i) Short circuit force during short circuit current

ii) Short circuit force after short circuit current

iii) Pinch-effect forces due to short circuit current

iv) Calculate minimum phase-to-phase clearance as a result of conductor swing due to short circuit current

2) Ice load

3) Wind load

4) Combine load on the structure

e) Select the required hardware and insulator strength

I.2 Calculations

I.2.1 Conductor requirements

The bus design process starts by selecting the conductor type, size, and number of conductors required to carry the maximum continuous current, and to able to withstand the short circuit current for a time equal to the backup relay fault clearing time.

Copyright © 2010 IEEE. All rights reserved.

Copyright The Institute of Electrical and Electronics Engineers, Inc.
Provided by IHS under license with IEEE
No reproduction or networking permitted without license from IHS

Order Number: 02120914
Sold to:EGAT [700166108393] - VARRIS.Y@EGAT.CO.TH,
Not for Resale,2016-09-15 03:57:47 UTC

Annex C describes the process of calculating the conductor rating. The substation engineer must be aware of the factors that affect the current rating of the conductor. These factors are as follows:

Ambient temperature: A summer and a winter ambient temperature should be selected based on weather data collected for a particular area; the ambient temperatures used in this example are given in Table I.1. The ambient temperature has an important effect on the conductor rating since for a lower ambient temperature, a higher temperature rise is allowed that results in a higher conductor rating. The summer ambient temperature will be used in the calculations of the conductor rating since it is the highest.

Maximum temperature rise: The temperature rise for the conductor is normally dependent on the equipment connected to the conductor. This is normally 105 °C, which means a 65 °C temperature rise is allowed.

Wind speed: Wind speed is an important factor that affects the conductor rating. The higher the wind speed, the higher the conductor rating. A 0.6 m/s (2 ft/s) is used in this guide for the calculations of the bus conductor ampacity rating, which is a conservative but realistic number. Higher wind speed can be used for higher unconstrained buses. For the overhead line, a 1.0 m/s (3.4 ft/s) has been used. For this example, 0.6 m/s will be used.

Wind angle: This is the angle between the wind direction and the conductor axis (an angle of 0° corresponds to wind parallel to the conductor and 90° corresponds to wind perpendicular to the conductor). Figure I.2 gives the wind direction angle factor for angles from 0° to 90°. As shown in this figure, smaller angles result in a smaller angle factor, which results in a lower conductor ampacity. In this example, 90° will be used.

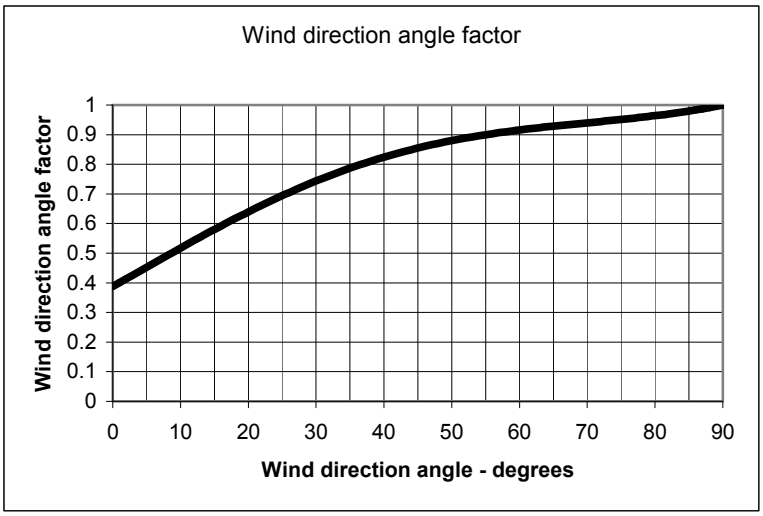

Figure I.2—Wind direction angle factor

Emissivity: The conductor ability to radiate heat is known as the emissivity factor. The emissivity factor is equal to zero for a conductor that retains all the heat —a perfect conductor–and equal to one for a conductor that radiates all the heat. Depending on the conductor degree of oxidation, discoloration of surface, its roughness, and stranding, the emissivity value ranges between 0.23 for newly installed conductor and up to 0.90 for a conductor after many years of service. The emissivity factor is used in the calculation of the radiated heat loss.

Solar absorptivity: The ability of the conductor to absorb heat is known as the absorptivity factor. Similar to the emissivity factor, the absorptivity factor increases with conductor age. A value of 0.5 for the emissivity and absorptivity factors provides a safety factor for the majority of exposed conductors and is used to calculate the ampacity of conductors.

Copyright © 2010 IEEE. All rights reserved.

Copyright The Institute of Electrical and Electronics Engineers, Inc.
Provided by IHS under license with IEEE
No reproduction or networking permitted without license from IHS

Order Number: 02120914
Sold to:EGAT [700166108393] - VARRIS.Y@EGAT.CO.TH,
Not for Resale,2016-09-15 03:57:47 UTC

Skin effect: The skin effect is the tendency of ac to distribute itself within a conductor so that the current density near the surface of the conductor is greater than that at its core. That is, the electric current tends to flow at the "skin" of the conductor. The skin effect causes the effective resistance of the conductor to increase with the frequency of the current. The skin effect is normally included in the conductor resistance as published by the Aluminum Electrical Conductor Handbook [B1]. For a tubular bus conductor, the skin effect can be assumed to be equal to 1.

Other factors: Bus direction, time of the day, substation latitude, atmosphere conditions (clear or industrial), and substation elevation are all factors that affect the solar heat gain and somehow affect the conductor ampacity rating.

Clause 6 discusses the conductor material. From this discussion, aluminum alloy 1350 EC grade aluminum (AAC) material will be used for the bus conductor in this example.

The information required to calculate the conductor current rating is shown in Table I.2.

Table I.2—Conductor current rating data

Data	Description	Value
T_a	Ambient temperature (summer)	40 °C
ΔT	Temperature rise	65 °C
T_c	Maximum conductor temperature	105 °C
	Wind speed	0.6 m/s
Φ	Wind direction angle	90°
	Latitude	30°N
ε	Emissivity	0.5
	Absorptivity (taken equal to emissity)	0.5
C'	Conductivity % of IASC	53 %
	Atmospheric conditions	Clear
	Time at which to calculate the current	10 AM
	Conductor direction	E-W

Due to high current requirements (4800 A) for the bus under consideration, more than one conductor must be used for this application. Using Annex C, the conductor ratings of the following all aluminum conductors have been calculated and are shown in Table I.3.

Table I.3—Conductor selection

Conductor code name	Conductor size KCM	Single conductor rating (A)	Bundle of three conductors rating (A)
CARNATION	1431	1436	4308
COREOPSIS	1590	1526	4578
JESSAMINE	1750	1612	4836
SAGEBRUSH	2250	1881	5643

From the calculated values in Table I.3, two conductor types can be used for this example: *Jessamine* and *Sagebrush*. Since the *Sagebrush* conductor has a higher rating, it will be retained for this example. The physical data for the Sagebrush shown in Table I.4 will be used for calculating the forces on the structure and the hardware due to short circuit current and other loads.

Copyright © 2010 IEEE. All rights reserved.
Copyright The Institute of Electrical and Electronics Engineers, Inc.
Provided by IHS under license with IEEE
No reproduction or networking permitted without license from IHS
Order Number: 02120914
Sold to:EGAT [700166108393] - VARRIS.Y@EGAT.CO.TH,
Not for Resale,2016-09-15 03:57:47 UTC

Table I.4—Physical data *Sagebrush* conductor

Data	Description	Value
D_o	Outside diameter	43.8 mm
A_C	Cross-sectionnal area	1140 mm^2
$\overline{m}_i$	Initial linear mass (winter)	3.712 kg/m
$\overline{m}_f$	Final linear mass (summer)	3.173 kg/m
E_C	Young's modulus	68.9 GPa
α	Coefficient of thermal expansion (1/°C)	2.31×10^{-5}

I.2.2 Sag requirements

Bus conductor sag is required for the calculations of the short circuit forces. As recommended in this guide, the short circuit forces must be calculated for sag calculated at both the summer and winter temperature. The maximum calculated forces will be used in the structure design calculations.

Several factors affect the sag as follows.

The clearance requirements should be determined based on the National Electrical Safety Code® (NESC®) (Accredited Standards Committee C-2) for both vehicles and foot clearances. The NESC code gives the required clearances a safety factor that is recommended. For this example, the clearance will meet both the traffic and foot clearances. From the NESC, the required clearances for 230 900 kV BIL is as follows:

a) Traffic clearances = 6.9 m (22.64 ft) with 10% safety factor; the required clearance is equal to 7.59 m (24.9 ft).

b) Foot clearances = 6.4 m (21 ft) with 10% safety factor; the required clearance is equal to 7.04 m (23.1 ft).

The required clearances will be verified for both foot and traffic clearances. The sag and tension calculation can be calculated using the simplified equations in 11.4.3.

Using Equation (68) with given wire physical data and assuming initial tension H_i = 11 120 N at winter temperature of –10 °C, we obtain:

$$D_s = \frac{\overline{m}\, g L^2}{8H} = \frac{3.712 \times 9.81 \times 48.8^2}{8 \times 11\,120} = 0.975\ \text{m}$$

This is the minimum sag at the ambient winter temperature when no current is flowing in the conductor. The maximum sag will be obtained at the summer ambient temperature when current is flowing in the conductor and its temperature has risen to 105 °C as discussed above.

To calculate the maximum sag, we first evaluate the tension at the summer operating temperature using Equation (69) to find the final tension H_f, which results in the following expression:

$$E_c\, A_c\, \alpha (T_f - T_i) + H_f - H_i = \frac{g^2 L^2 E_c\, A_c}{24} \left(\frac{\overline{m}_f^2}{H_f^2} - \frac{\overline{m}_i^2}{H_i^2} \right)$$

Copyright © 2010 IEEE. All rights reserved.
Copyright The Institute of Electrical and Electronics Engineers, Inc.
Provided by IHS under license with IEEE
No reproduction or networking permitted without license from IHS
Order Number: 02120914
Sold to:EGAT [700166108393] - VARRIS.Y@EGAT.CO.TH,
Not for Resale,2016-09-15 03:57:47 UTC

$$6.89\times10^{10}\times1.14\times10^{-3}\times2.31\times10^{-5}\times[105+10]+(H_f-11\,120)=\frac{9.81^2\times48.8^2\times6.89\times10^{10}\times1.14\times10^{-3}}{24}\times\left[\frac{3.173^2}{H_f{}^2}-\frac{3.712^2}{11\,120^2}\right]$$

By trial and error we find H_f = 5136 N, which balances both sides of the above equation.

Using Equation (68) with H_f, we obtain the maximum sag:

$$D_s=\frac{\overline{m}\,gL^2}{8H}=\frac{3.173\times9.81\times48.8^2}{8\times5136}=1.80\text{ m}$$

Based on the above calculations, the calculated sag is as follows:

- Minimum sag at winter temperature = **0.975 m**
- Maximum sag at summer temperature = **1.80 m**

Figure I.3 is used to verify that the maximum sag meets the vehicle and foot clearances as described above. Using a 9.75 m (32 ft) structure, this sag results in a ground clearance of over 7.95 m, which is greater than the minimum required clearance of 7.59 m.

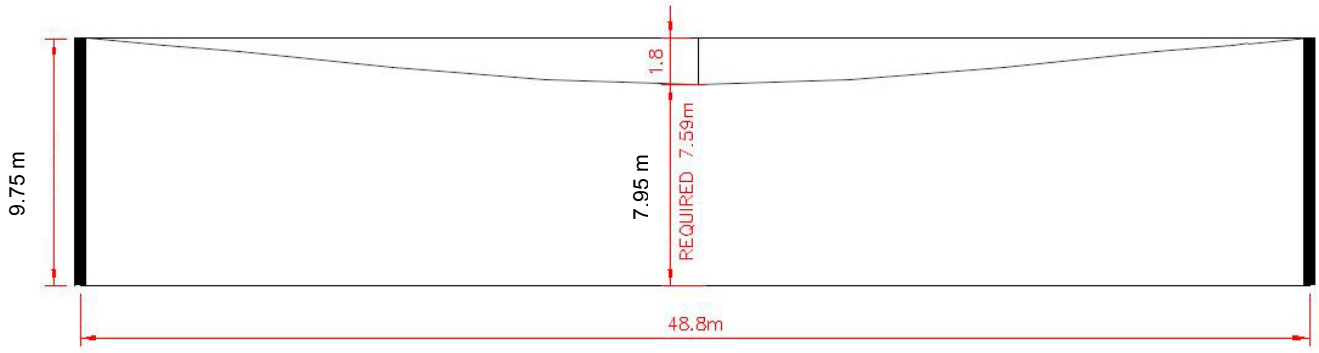

Figure I.3—Sag verification

I.2.3 Maximum surface voltage gradient “corona”

The calculation of corona is required to protect substation equipment and the associated hardware. Annex D provides the information required to evaluate the resulting corona at the bus. The following factors affect the magnitude of corona:

a) Bus voltage; a higher voltage results in higher corona.

b) Bus height above ground; the higher the bus, the less the corona.

c) Conductor diameter; larger conductor sizes result in less corona.

d) Number of conductor per phase; corona decreases with an increase in number of conductors per phase.

Copyright © 2010 IEEE. All rights reserved.
Copyright The Institute of Electrical and Electronics Engineers, Inc.
Provided by IHS under license with IEEE
No reproduction or networking permitted without license from IHS
Order Number: 02120914
Sold to:EGAT [700166108393] - VARRIS.Y@EGAT.CO.TH,
Not for Resale,2016-09-15 03:57:47 UTC

e) Atmospheric conditions and substation elevation.

The evaluation of corona consists of calculating the allowable voltage gradient and the actual voltage gradient. The allowable voltage should be greater than the actual resulting gradient voltage. The additional data required for corona calculation are given in Table I.5.

Table I.5—Corona calculation data

Data	Data description	Value
h	Conductor height above ground	7.95 m
r_f	Conductor roughness	1.0
D	Phase-to-phase clearance	4.12 m
n	Number of conductors/phase	3
s	Space between bundle conductors	0.457 m

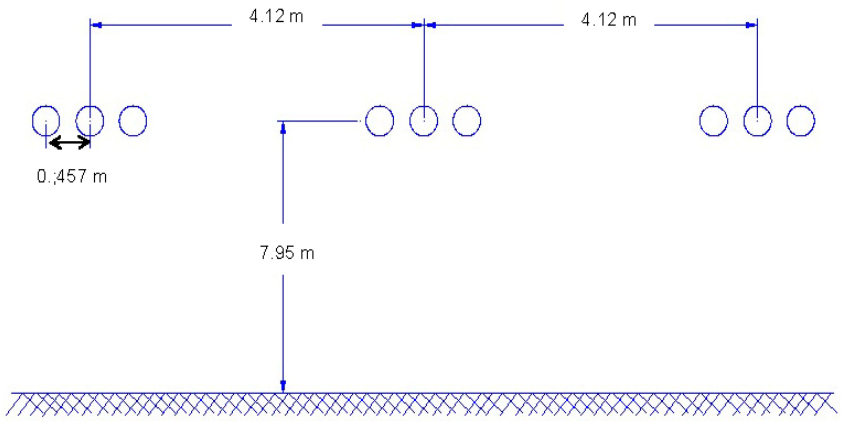

Figure I.4—Conductor configurations for corona calculations

I.2.3.1 Allowable voltage gradient

From Annex D, the corona onset voltage gradient (E_c), kV/cm, rms is given by the following equations:

$$E_c = m E_0 D_a \left(1 + \frac{C}{\sqrt{D_a r_e}}\right)$$

$$D_a = \left(\frac{273 + T_0}{273 + T}\right)\frac{P}{P_0}$$

To calculate the onset voltage gradient, the data in Table I.6 are required.

Copyright © 2010 IEEE. All rights reserved.
Copyright The Institute of Electrical and Electronics Engineers, Inc.
Provided by IHS under license with IEEE
No reproduction or networking permitted without license from IHS
Order Number: 02120914
Sold to:EGAT [700166108393] - VARRIS.Y@EGAT.CO.TH,
Not for Resale,2016-09-15 03:57:47 UTC

Table I.6—Physical data of the *Sagebrush* conductor

Data	Data description	Value
E_0	Empirical constant	21.1 kV/cm (rms value)
A	Altitude (substation elevation)	0.4 km
C	Empirical constant	0.301 cm^{-1}
T	The temperature of the ambient air (summer)	40 °C
T_o	The temperature used in the determination of the empirical constants E_0 and C	25 °C
r	Conductor radius	2.195 cm
m	Surface or roughness factor	0.3—0.85 for this example use 0.85
s	Bundle conductor spacing	0.457 m
g	Equal to 1 for bundle of 1,2,3 subconductors	1
r_e	Bundle conductor equiv. radius	See calculation below
D_a	Relative air density factor	See calculation below

$$r_e = r\left(g \times \frac{s}{r}\right)^{\frac{n-1}{n}} = 2.195 \times \left(1 \times \frac{45.7}{2.195}\right)^{2/3} = 16.6 \text{ cm}$$

$$\frac{P}{P_0} = 1 - \frac{A}{10} = 1 - \frac{0.4}{10} = 0.96$$

$$D_a = \left(\frac{273 + T_0}{273 + T}\right)\frac{P}{P_0} = \left(\frac{273 + 25}{273 + 40}\right)0.96 = 0.914$$

$$E_c = m E_0 D_a \left(1 + \frac{C}{\sqrt{D_a r_e}}\right) = 0.85 \times 21.1 \times 0.914\left(1 + \frac{0.301}{\sqrt{0.914 \times 16.6}}\right) = 17.7 \text{ kV/cm}$$

I.2.3.2 Maximum voltage gradient E_m

The following information is required to calculate the maximum voltage gradient E_m that can develop on the surface of bundle conductor.

Maximum line to ground operating voltage V_1:

$$V_1 = \frac{230}{\sqrt{3}} \times 1.1 = 146.1 \text{kV}$$

The equivalent distance from center of conductor to ground plane for three-phase h_e in cm is calculated using D = 412 cm and h = 795 cm.

$$h_e = \frac{hD}{\sqrt{4h^2 + D^2}} = \frac{795 \times 412}{\sqrt{4 \times (795)^2 + (412)^2}} = 199.4 \text{ cm}$$

Copyright © 2010 IEEE. All rights reserved.

Copyright The Institute of Electrical and Electronics Engineers, Inc.
Provided by IHS under license with IEEE
No reproduction or networking permitted without license from IHS

Order Number: 02120914
Sold to:EGAT [700166108393] - VARRIS.Y@EGAT.CO.TH,
Not for Resale,2016-09-15 03:57:47 UTC

The average voltage gradient E_a kV/cm is calculated using $n = 3$, $r_c = 16.6$ cm, $V_1 = 146.07$, and $r = 2.195$ cm.

$$E_a = \frac{V_1}{nr\ln\left(\frac{2h_e}{r_e}\right)} = \frac{146.1}{3\times 2.195\times \ln\left(\frac{2\times 199.4}{16.6}\right)} = 6.98 \text{ kV/cm}$$

$$E_m = \frac{h_e}{h_e - r_e}E_a = \frac{199.4}{199.4 - 16.6}\times 6.98 = 7.61 \text{ kV/cm}$$

I.2.3.3 Results on corona

Because the maximum voltage gradient E_m (7.61 kV/cm) is less than the calculated 17.7 kV/cm onset gradient voltage, we can conclude the design is acceptable.

I.2.4 Short circuit loading

The short circuit force calculation consists of calculating the forces applied to the structure during the short circuit, after the short circuit, and the pinch effect forced resulting from the bundle conductor clashes. The maximum resulting forces will be used for structure design calculations as follows. The forces will be calculated at both winter and summer temperature since their respective conditions are quite different. It is assumed that no ice is present on the conductors under short circuit conditions.

I.2.4.1 Short circuit force during fault current F_t

The following steps are used to calculate the short circuit force during short circuit current F_t and follow the procedure outlined in 11.3.5.

Characteristic electromagnetic load

From Table I.1, the necessary data is given by:

l = 48.8 m l_i = 2.0 m l_c = 44.7 m I_{k3} = 63 kA a = 4.12 m

$$F' = \frac{\mu_0}{2\pi}0.75\frac{I_{k3}^2}{a}\frac{l_c}{l} = \frac{1.257\times 10^{-6}}{2\pi}\times 0.75\times \frac{(63\times 10^3)^2}{4.12}\times \frac{44.7}{48.8} = 132.4 \text{ N/m}$$

Ratio of electromagnetic force to gravitational force

From Table I.4:

$$\overline{m} = 3.173 \text{ kg/m}$$

$$F_g = n\overline{m}g = 3\times 3.173\times 9.81 = 93.4 \text{ N/m}$$

Copyright © 2010 IEEE. All rights reserved.

Copyright The Institute of Electrical and Electronics Engineers, Inc.
Provided by IHS under license with IEEE
No reproduction or networking permitted without license from IHS

Order Number: 02120914
Sold to:EGAT [700166108393] - VARRIS.Y@EGAT.CO.TH,
Not for Resale,2016-09-15 03:57:47 UTC

$$r = \frac{F'}{F_g} = \frac{132.68}{93.38} = 1.42$$

Direction of resulting force exerted on conductor (F_{st})

Using the factor r angle δ_1 is calculated as:

$$\delta_1 = \arctan(r) = \arctan(1.42) = 54.8^o$$

Static tensile force

Sag (d) at winter temperature = 0.975m. Sag (d) at summer temperature = 1.80 m.

For winter temperature:

$$F_{st} = \frac{n\bar{m}gl^2}{8d} = \frac{3 \times 3.712 \times 9.81 \times 48.8^2}{8 \times 0.975} = 33354 \text{ N} = 33.4 \text{ kN}$$

For summer temperature:

$$F_{st} = \frac{n\bar{m}gl^2}{8d} = \frac{3 \times 3.173 \times 9.81 \times 48.8^2}{8 \times 1.80} = 15409 \text{ N} = 15.4 \text{ kN}$$

Natural period of conductor oscillation T

For winter temperature:

$$T = 2\pi\sqrt{0.8\frac{d}{g}} = 2\pi\sqrt{0.8 \times \frac{0.975}{9.81}} = 1.77 \text{ s}$$

For summer temperature:

$$T = 2\pi\sqrt{0.8\frac{d}{g}} = 2\pi\sqrt{0.8 \times \frac{1.804}{9.81}} = 2.41 \text{ s}$$

Period of oscillation during short circuit

For winter temperature:

$$T_{\text{res}} = \frac{T}{\sqrt[4]{1+r^2} \times \left[1 - \frac{\pi^2}{64} \times \left(\frac{\delta_1}{90^o}\right)^2\right]} = \frac{1.77}{\sqrt[4]{1+1.418^2} \times \left[1 - \frac{\pi^2}{64} \times \left(\frac{54.8}{90}\right)^2\right]} = 1.43 \text{ s}$$

Copyright © 2010 IEEE. All rights reserved.

Copyright The Institute of Electrical and Electronics Engineers, Inc.
Provided by IHS under license with IEEE
No reproduction or networking permitted without license from IHS

Order Number: 02120914
Sold to:EGAT [700166108393] - VARRIS.Y@EGAT.CO.TH,
Not for Resale,2016-09-15 03:57:47 UTC

For summer temperature:

$$T_{\text{res}} = \frac{T}{\sqrt[4]{1+r^2}\times\left[1-\frac{\pi^2}{64}\times\left(\frac{\delta_1}{90^o}\right)^2\right]} = \frac{2.41}{\sqrt[4]{1+1.418^2\times\left[1-\frac{\pi^2}{64}\times\left(\frac{54.8}{90}\right)^2\right]}} = 1.94\,\text{s}$$

Maximum swing angle δ_m

Theoretical maximum swing angle δ_k and the factor χ shall be calculated in order to calculate, the maximum swing angle.

From above and Table I.1, the following data are required:

T_{res}(winter) = 1.43 s T_{res}(summer) = 1.94 s T_{k1} = 0.1 s $\delta_1 = 54.8^o$

$$\delta_k = \begin{cases} \delta_1\left[1-\cos\left(360°\frac{T_{k1}}{T_{\text{res}}}\right)\right] & \text{for } 0 \le \frac{T_{k1}}{T_{\text{res}}} \le 0.5 \\ 2\times\delta_1 & \text{for } \frac{T_{k1}}{T_{\text{res}}} > 0.5 \end{cases}$$

For winter temperature:

$$\frac{T_{k1}}{T_{\text{res}}} = \frac{0.1}{1.43} = 0.0699 \le 0.5$$

For summer temperature:

$$\frac{T_{k1}}{T_{\text{res}}} = \frac{0.1}{1.94} = 0.0516 \le 0.5$$

For winter temperature:

$$\delta_k = \delta_1\left[1-\cos\left(360°\times\frac{T_{k1}}{T_{\text{res}}}\right)\right] = 54.8\times\left[1-\cos\left(360°\times(0.0699)\right)\right] = 5.20°$$

For summer temperature:

$$\delta_k = \delta_1\left[1-\cos\left(360°\times\frac{T_{k1}}{T_{\text{res}}}\right)\right] = 54.8\times\left[1-\cos\left(360°\times(0.0516)\right)\right] = 2.86°$$

Copyright © 2010 IEEE. All rights reserved.
Copyright The Institute of Electrical and Electronics Engineers, Inc.
Provided by IHS under license with IEEE
No reproduction or networking permitted without license from IHS
Order Number: 02120914
Sold to:EGAT [700166108393] - VARRIS.Y@EGAT.CO.TH,
Not for Resale,2016-09-15 03:57:47 UTC

$$\chi = \begin{matrix} 1-r\sin\delta_k & \text{for } 0 \le \delta_k \le 90° \\ 1-r & \text{for } \delta_k > 90° \end{matrix}$$

Since δ_k is less than 90° we have:

For winter temperature:

$$\chi = 1 - r\sin(\delta_k) = 1 - 1.418 \times \sin(5.20) = 0.872$$

For summer temperature:

$$\chi = 1 - r\sin(\delta_k) = 1 - 1.418 \times \sin(2.86) = 0.929$$

Based on the above values, δ_m is given by the following equation:

$$\delta_m = \begin{matrix} 1.25 \times \arccos\chi & \text{for } 0.766 \le \chi \le 1 \\ 10° + \arccos\chi & \text{for } -0.985 \le \chi \le 0.766 \\ 180° & \text{for } \chi \le -0.985 \end{matrix}$$

For winter temperature:

$$\delta_m = 1.25 \times \arccos(\chi) = 1.25 \times \arccos(0.977) = 36.6°$$

For summer temperature:

$$\delta_m = 1.25 \times \arccos(\chi) = 1.25 \times \arccos(0.929) = 27.2°$$

Flexibility norm of the conductor-insulator system

From Tables I.1 and I.4, the following data are required:

E_s = 68.9 Gpa E_i = 30 GPa A_s = 0.00114 m^2 A_i = 4.42 × 10^{-3} m^2
l_c = 44.74 m l_i = 2.03m l = 48.8 m

$$k_c = n\frac{E_s A_s}{l_c} = 3 \times \frac{68.9 \times 10^9 \times 0.00114}{44.74} = 5.27 \times 10^6$$

$$k_i = \frac{E_i A_i}{l_i} = \frac{3.00 \times 10^{10} \times 4.42 \times 10^{-3}}{2.03} = 6.53 \times 10^7$$

$$\frac{1}{k_{eq}} = \frac{1}{k_c} + \frac{2}{k_i} = \frac{1}{5.27 \times 10^6} + \frac{2}{6.53 \times 10^7} = 2.20 \times 10^{-7}$$

Copyright © 2010 IEEE. All rights reserved.

Copyright The Institute of Electrical and Electronics Engineers, Inc.
Provided by IHS under license with IEEE
No reproduction or networking permitted without license from IHS

Order Number: 02120914
Sold to:EGAT [700166108393] - VARRIS.Y@EGAT.CO.TH,
Not for Resale,2016-09-15 03:57:47 UTC

$$N = \frac{1}{k_{eq} \times l} = 2.204 \times 10^{-7} \times \frac{1}{48.8} = 4.52 \times 10^{-9} \text{ N}^{-1}$$

Stress factor of the conductor (ζ)

From Table I.1, the following data are required:

$n = 3$	$\overline{m} = 3.712$ kg/m (winter)	$l =$ 48.8 m
	$\overline{m} = 3.173$ kg/m (summer)	
$g = 9.8$ m/s^2	F_{st}(winter) = 33 354 N	
	F_{st}(summer) = 15 409 N	

For winter temperature:

$$\zeta = \frac{(ng\overline{m}\,l)^2}{24 \times F_{st}^3\ N} = \frac{(3 \times 9.81 \times 3.712 \times 48.8)^2}{24 \times (33354)^3 \times 4.52 \times 10^{-9}} = 7.06$$

For summer temperature:

$$\zeta = \frac{(ng\overline{m}\,l)^2}{24 \times F_{st}^3\ N} = \frac{(3 \times 9.81 \times 3.173 \times 48.8)^2}{24 \times (15409)^3 \times 4.52 \times 10^{-9}} = 52.3$$

Maximum tensile force during the short circuit

The maximum tensile force during the short circuit F_t is given by:

$$F_t = \begin{cases} F_{st}(1+\phi\psi) & \text{for } n = 1 \\ 1.1 \times F_{st}(1+\phi\psi) & \text{for } n \geq 2 \end{cases}$$

The parameter φ and ζ are determined by the following equations:

$$\phi = \begin{cases} 3 \times \left(\sqrt{1+r^2} - 1\right) & \text{for } T_{k1} \geq \dfrac{T_{\text{res}}}{4} \\ 3 \times \left(r \sin\delta_k + \cos\delta_k - 1\right) & \text{for } T_{k1} < \dfrac{T_{\text{res}}}{4} \end{cases}$$

The previously calculated data under will be used:

Winter temp.	$T_{\text{res}} = 1.43$ s	$T_{\text{res}}/4 = 0.358$ s	$\delta_k = 5.20^{\text{o}}$	$\zeta = 7.06$
Summer temp.	$T_{\text{res}} = 1.94$ s	$T_{\text{res}}/4 = 0.485$ s	$\delta_k = 2.86^{\text{o}}$	$\zeta = 52.3$
$T_{kl} = 0.1$ s	$r = 1.42$	F_{st}(winter) = 33 354 N	F_{st}(summer) = 15 409 N	

Since $T_{\text{res}}/4 > T_k$ for both winter and summer temperature, we obtain:

For winter temperature:

$$\varphi = 3 \times (r \sin\delta_k + \cos\delta_k - 1) = 3 \times (1.42 \times \sin(5.20) + \cos(5.20) - 1) = 0.374$$

Copyright © 2010 IEEE. All rights reserved.

Copyright The Institute of Electrical and Electronics Engineers, Inc.
Provided by IHS under license with IEEE
No reproduction or networking permitted without license from IHS

Order Number: 02120914
Sold to:EGAT [700166108393] - VARRIS.Y@EGAT.CO.TH,
Not for Resale,2016-09-15 03:57:47 UTC

For summer temperature:

$$\varphi = 3\times(r\sin\delta_k + \cos\delta_k - 1) = 3\times(1.42\times\sin(2.86) + \cos(2.86) - 1) = 0.209$$

Using φ and ζ, ψ can be calculated using the following equation:

$$\varphi^2\psi^3 + \varphi(2+\zeta)\cdot\psi^2 + (1+2\zeta)\psi - \zeta(2+\varphi) = 0$$

Since ψ has a value between 0 and 1, we find by iteration:

For winter temperature: $\psi = 0.914$

For summer temperature: $\psi = 0.989$

For $n \geq 2$, the tensile force is therefore equal to

$$F_t = \begin{array}{ll} F_{st}(1+\phi\psi) & \text{for } n = 1 \\ 1.1\times F_{st}(1+\phi\psi) & \text{for } n \geq 2 \end{array}$$

For winter temperature:

$$F_t = 1.1\times F_{st}(1+\varphi\psi) = 1.1\times 33354\times(1+0.374\times 0.914) = 49.2\times 10^3 \text{ N}$$

For summer temperature:

$$F_t = 1.1F_st(1+\varphi\psi) = 1.1\times 15409\times(1+0.209\times 0.989) = 20.5\times 10^3 \text{ N}$$

I.2.4.2 Maximum tensile force after the short circuit current has cleared when the conductor drops back

The following previously calculated data will be used:

Winter temp.	F_{st} = 33 354 N	ζ= 7.06	$\delta_m = 36.6^o$
Summer temp.	F_{st} = 15 409 N	ζ= 52.3	$\delta_m = 27.2^o$

For winter temperature:

$$F_f = 1.2\times F_{st}\sqrt{1+8\times\zeta\frac{\delta_m}{180^o}} = 1.2\times 33354\times\sqrt{1+8\times 7.06\times\frac{36.6}{180}} = 1.41\times 10^5 \text{ N}$$

For summer temperature:

$$F_f = 1.2\times F_{st}\cdot\sqrt{1+8\times\zeta\frac{\delta_m}{180^o}} = 1.2\times 15409\times\sqrt{1+8\times 52.3\times\frac{27.2}{180}} = 1.48\times 10^5 \text{ N}$$

--`,,,,,,`,```,,`,`,,`,-`-`,,`,,,`---
Copyright © 2010 IEEE. All rights reserved.

Copyright The Institute of Electrical and Electronics Engineers, Inc.
Provided by IHS under license with IEEE
No reproduction or networking permitted without license from IHS

Order Number: 02120914
Sold to:EGAT [700166108393] - VARRIS.Y@EGAT.CO.TH,
Not for Resale,2016-09-15 03:57:47 UTC

I.2.4.3 Maximum horizontal displacement of the span

To check clearances, the maximum horizontal displacement of a span will be calculated as follows.

The following previously calculated data will be used:

Winter temp.	F_t = 49.2 kN	F_{st} = 33.4 kN
Summer temp.	F_t = 20.5 kN	F_{st} = 15.4 kN
$N = 4.52 \times 10^{-9}$		

Elastic deformation to the change in tension

For winter temperature:

$$\varepsilon_{\text{ela}} = N(F_t - F_{st}) = 4.52\times10^{-9}\times(49.2\times10^{3} - 33354) = 7.16\times10^{-5}$$

For summer temperature

$$\varepsilon_{\text{ela}} = N(F_t - F_{st}) = 4.52\times10^{-9}\times(20.5\times10^{3} - 15409) = 2.30\times10^{-5}$$

Elastic deformation to thermal expansion ε_{th}

The following data will be used:

T_{res}(winter) = 1.43 s	T_{res}(summer) = 1.94 s	$c_{th} = 0.27 \times 10^{-18}$	A_s = 1.14E-03 m^2
Short circuit current	T_{k1} (fault clearing time) = 0.1 s	n = 3	$T_{\text{res}}/4$ = 0.0699 (winter)
I_{k3} = 63000A			$T_{\underline{res}}/4$ = 0.0516 (summer)

$$\varepsilon_{th} = \begin{cases} c_{th}\left[\dfrac{I_{k3}}{nA_s}\right]^2 \dfrac{T_{\text{res}}}{4} & \text{for } T_{k1} \geq T_{\text{res}}/4 \\ c_{th}\left[\dfrac{I_{k3}}{nA_s}\right]^2 T_{k1} & \text{for } T_{k1} < T_{\text{res}}/4 \end{cases}$$

Since T_{k1} is less than $T_{\text{res}}/4$ for both winter and summer conditions, ε_{th} is given by the following equation:

$$\varepsilon_{th} = c_{th}\left[\frac{I_{k3}}{n.As}\right]^2 T_{k1} = 0.27\times10^{-18}\left[\frac{63000}{3\times1.14\times10^{-3}}\right]\times0.1 = 9.16\times10^{-6}$$

For a ratio of electromagnetic force to gravitational force equal to 1.42, the factor C_f is equal to:

$$C_f = 0.97 + 0.1\times r = 0.97 + 0.1\times1.42 = 1.11$$

The factor C_D that allows for sag increase caused by the elastic and thermal elongation is given by:

Copyright © 2010 IEEE. All rights reserved.

Copyright The Institute of Electrical and Electronics Engineers, Inc.
Provided by IHS under license with IEEE
No reproduction or networking permitted without license from IHS

Order Number: 02120914
Sold to:EGAT [700166108393] - VARRIS.Y@EGAT.CO.TH,
Not for Resale,2016-09-15 03:57:47 UTC

Winter temp.	d = 0.975 m	$\varepsilon_{\text{elas}}$ = 7.16×10^{-5}	$\varepsilon_{th} = 9.16 \times 10^{-6}$
Summer temp.	d =1.80 m	$\varepsilon_{\text{elas}}$ = 2.30×10^{-5}	$\varepsilon_{th} = 9.16 \times 10^{-6}$

For winter temperature:

$$C_D = \sqrt{1+\frac{3}{8}\times\left[\frac{l}{d}\right]^2\left(\varepsilon_{\text{elas}}+\varepsilon_{th}\right)} = \sqrt{1+\frac{3}{8}\times\left[\frac{48.8}{0.975}\right]^2\times(7.16\times10^{-5}+9.16\times10^{-6})} = 1.04$$

For summer temperature:

$$C_D = \sqrt{1+\frac{3}{8}\times\left[\frac{l}{d}\right]^2\left(\varepsilon_{\text{elas}}+\varepsilon_{th}\right)} = \sqrt{1+\frac{3}{8}\times\left[\frac{48.8}{1.80}\right]^2\times(2.30\times10^{-5}+9.16\times10^{-6})} = 1.00$$

Strained conductor attached to the structure with 2 insulator chains (one on each side)

Winter temp.	C_D = 1.04	d = 0.0.975	δ_m = 36.6
Summer temp.	C_D = 1.00	d = 1.80	δ_m = 27.2
C_f = 1.11	δ_1 = 54.8		

The maximum horizontal displacement within a span b_h for $\delta_m < \delta_1$ is given by the following equation:

For winter temperature:

$$b_h = C_f C_D d \sin(\delta_m) = 1.11\times1.04\times0.975\times\sin(36.6) = 0.671 \text{ m}$$

For summer temperature:

$$b_h = C_f C_D d \sin(\delta_m) = 1.11\times1.00\times1.80\times\sin(27.2) = 0.913 \text{ m}$$

Minimum clearance due to fault condition is given by

For winter temperature:

$$a_{\min} = a - 2\times b_h = 4.12 - 2\times0.671 = 2.78 \text{ m}$$

For summer temperature:

$$a_{\min} = a - 2\times b_h = 4.12 - 2\times0.913 = 2.29 \text{ m}$$

Copyright © 2010 IEEE. All rights reserved.

Copyright The Institute of Electrical and Electronics Engineers, Inc.
Provided by IHS under license with IEEE
No reproduction or networking permitted without license from IHS

Order Number: 02120914
Sold to:EGAT [700166108393] - VARRIS.Y@EGAT.CO.TH,
Not for Resale,2016-09-15 03:57:47 UTC

I.2.4.4 Maximum tensile force caused by the pinch effect

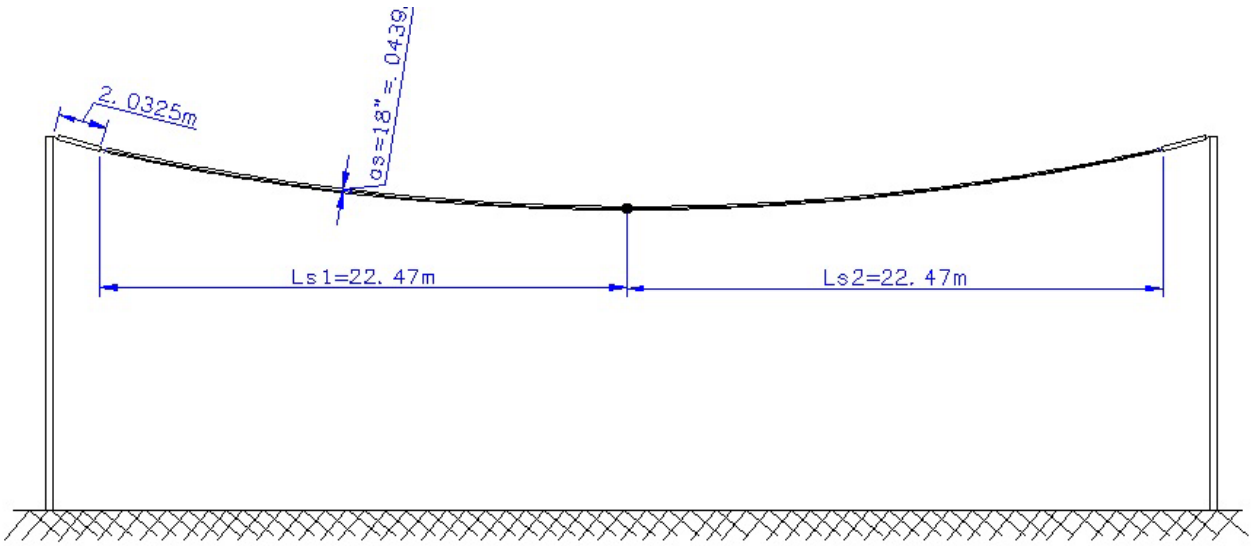

Figure I.5—Strain bus

This example requires the use of bundle conductors that consist of three conductors for the bus due to load current requirements. Spacers are used to minimize wind-induced motions, such as subconductor oscillation and Aeolian vibration, so that no conductor damage results to keep the subconductors from entangling due to galloping, ice unloading, and fault currents.

If the clearance between subconductors and the configuration of the spacers is such that the subconductors of the bundle effectively clash during a short circuit, the maximum tensile force due to the pinch effect F_{pi} may be ignored in contrast to the maximum tensile force F_t during the short circuit for regular bundle configurations of up to four subconductors.

Subconductors are considered to clash effectively, that is without significant pinch effect if the clearance a_s between the midpoints of adjacent subconductors, as well as the distance l_s between two adjacent spacers, fulfills either of the following two equations:

$$a_s / d_s \leq 2 \quad \text{and} \quad l_s \geq 50 \times a_s \quad \text{(condition 1)}$$

or

$$a_s / d_s \leq 2.5 \quad \text{and} \quad l_s \geq 70 \times a_s \quad \text{(condition 2)}$$

For this example, the following data from Table I.1 and Table I.4 is:

$d_s = 0.0438$ m $\quad a_s = 0.457$ m $\quad l_{s1} = l_{s2} = 22.37$ m

Copyright © 2010 IEEE. All rights reserved.

Copyright The Institute of Electrical and Electronics Engineers, Inc.
Provided by IHS under license with IEEE
No reproduction or networking permitted without license from IHS

Order Number: 02120914
Sold to:EGAT [700166108393] - VARRIS.Y@EGAT.CO.TH,
Not for Resale,2016-09-15 03:57:47 UTC

Check of condition 1:

$a_s / d_s \le 2$ and $l_s \ge 50 a_s$

$0.457 / 0.0438 = 10.4 \ge 2$

and

$l_s = 22.37 \le 50 \times 0.457 = 22.9$

Based on above, the conductors do not clash effectively.

Check of condition 2:

$a_s / d_s \le 2.5$ and $l_s \ge 70 a_s$

$0.457 / 0.0438 = 10.4 \ge 2.5$

and

$l_s = 22.47 \le 70 \times 0.457 = 32.0$

Based on both conditions, *the conductors do not clash effectively*. As a result, the maximum tensile force caused by the pinch effect F_{pi} shall be calculated.

The pinch effect force is given by the following equations:

The short circuit current force is given by

$$F_v = (n-1)\frac{\mu_o}{2\pi}\left(\frac{I_{k3}}{n}\right)^2 \frac{l_s}{a_s}\frac{\nu_2}{\nu_3}$$

The factor v_2 is determined by first calculating the factor v_1. The following data are required to calculate the factor v_1:

$N = 3$ $\quad \mu_0 = 1.257 \times 10^{-6}$ $\quad I_{k3} = 63\,000$ A $\quad \overline{m} = 3.173$ kg/m

$a_s = 0.457$ m $\quad d_s = 0.00438$ m $\quad \kappa = 1.8$ from Equation (54) with $X/R = 0.076$, $f = 60$ Hz

$$\nu_1 = f\frac{1}{\sin(\frac{180^o}{n})}\times\sqrt{\frac{(a_s - d_s)\overline{m}}{\frac{\mu_o}{2\pi}\left(\frac{I_{k3}}{n}\right)^2\frac{n-1}{a_s}}} = 60\frac{1}{\sin\left(\frac{180}{3}\right)}\times\sqrt{\frac{(0.457-0.0438)\times 3.173}{\frac{1.257\times10^{-6}}{2\pi}\left(\frac{63000}{3}\right)^2\times\frac{3-1}{0.457}}} = 3.03$$

For $\kappa = 1.8$ and $\nu_1 = 3.03$ from Figure 25, we obtain $\boldsymbol{\nu_2 = 1.7}$.

From Figure 26 with $a_s/d_s = 10.4$, we obtain $\boldsymbol{\nu_3 = 0.29}$. The short circuit current force is therefore given by:

$$F_v = (n-1)\frac{\mu_o}{2\pi}\left(\frac{I_{k3}}{n}\right)^2\frac{l_s}{a_s}\frac{\nu_2}{\nu_3} = 2\times(\frac{1.257\times10^{-6}}{2\pi}\left(\frac{63000}{3}\right)^2\times\frac{22.37}{0.457}\times\frac{1.7}{0.29} = 5.06\times10^4 \text{ N/m}$$

Copyright © 2010 IEEE. All rights reserved.

Copyright The Institute of Electrical and Electronics Engineers, Inc.
Provided by IHS under license with IEEE
No reproduction or networking permitted without license from IHS

Order Number: 02120914
Sold to:EGAT [700166108393] - VARRIS.Y@EGAT.CO.TH,
Not for Resale,2016-09-15 03:57:47 UTC

The strain factors ε_{st} characterizing the contraction of the bundle are calculated using the following data:

F_{st} = 33 354 N (winter) F_{st} = 15 409 N (winter) $N = 4.52 \times 10^{-9}$ a_s = 0.457 m
d_s = 0.0438 m

Fo winter temperature:

$$\varepsilon_{st} = 1.5 \times \frac{F_{st}\, l_s^2\, N}{\left(a_s - d_s\right)^2}\left(\sin\frac{180^o}{n}\right)^2 = 1.5 \times \frac{33354 \times 22.37^2 \times 4.52 \times 10^{-9}}{\left(0.457 - 0.0438\right)^2} \times \left(\sin\frac{180}{3}\right)^2 = 0.497$$

For summer temperature:

$$\varepsilon_{st} = 1.5 \times \frac{F_{st}\, l_s^2\, N}{\left(a_s - d_s\right)^2}\left(\sin\frac{180^o}{n}\right)^2 = 1.5 \times \frac{15409 \times 22.37^2 \times 4.52 \times 10^{-9}}{\left(0.457 - 0.0438\right)^2} \times \left(\sin\frac{180}{3}\right)^2 = 0.230$$

The strain factor ε_{pi} is calculated by the following equation:

$$\varepsilon_{pi} = 0.375 \times \frac{F_v l_s^3 N}{\left(a_s - d_s\right)^3} \times \left(\sin\frac{180^o}{n}\right)^3 = 0.375 \times \frac{5.06 \times 10^4 \times 22.37^3 \times 4.52 \times 10^{-9}}{\left(0.457 - 0.0438\right)^3} \times \left(\sin\frac{180}{3}\right)^3 = 8.84$$

The bundle configuration is determined according to the parameter j defined as follows:

For winter temperature:

$$j = \sqrt{\frac{\varepsilon_{pi}}{1 + \varepsilon_{st}}} = \sqrt{\frac{8.84}{1 + 0.497}} = 2.43$$

For summer temperature:

$$j = \sqrt{\frac{\varepsilon_{pi}}{1 + \varepsilon_{st}}} = \sqrt{\frac{8.84}{1 + 0.230}} = 2.68$$

Since $j \geq 1$, the subconductors clash and F_{pi} is given by:

$$F_{pi} = F_{st}\left(1 + \frac{\nu_e}{\varepsilon_{st}}\xi\right)$$

where ξ is given by the real solution of $\xi^3 + \varepsilon_{st} \times \xi^2 - \varepsilon_{pi} = 0$, where ξ shall fall within the range $j^{2/3} \leq \xi \leq j$, with j given above.

For ε_{st} (winter) = 0.497, we obtain $\boldsymbol{\xi = 1.91}$, which falls within the range above with j = 2.43.

For ε_{st} (summer) = 0.230, we obtain $\boldsymbol{\xi = 1.98}$, which falls within the range above with j = 2.68.

Copyright © 2010 IEEE. All rights reserved.
Copyright The Institute of Electrical and Electronics Engineers, Inc.
Provided by IHS under license with IEEE
No reproduction or networking permitted without license from IHS
Order Number: 02120914
Sold to:EGAT [700166108393] - VARRIS.Y@EGAT.CO.TH,
Not for Resale,2016-09-15 03:57:47 UTC

To determine v_e, we first determine v_4:

$$v_4 = \frac{a_s - d_s}{d_s} = \frac{0.457 - 0.0438}{0.0438} = 9.43$$

v_e is given by the following.

For winter temperature:

$$v_e = \frac{1}{2} + \left[\frac{9}{8} \times n(n-1) \frac{\mu_o}{2\pi} \left(\frac{I_{k3}}{n} \right)^2 N v_2 \left(\frac{l_s}{a_s - d_s} \right)^4 \frac{\left(\sin \frac{180^o}{n} \right)^4}{\xi^3} \left\{ 1 - \frac{\arctan \sqrt{v_4}}{\sqrt{v_4}} \right\} - \frac{1}{4} \right]^{1/2} =$$

$$v_e = \frac{1}{2} + \left[\frac{9}{8} \times 3(3-1) \times \frac{1.257 \times 10^{-6}}{2\pi} \left(\frac{63000}{3} \right)^2 \times 4.52 \times 10^{-9} \times 1.7 \times \left(\frac{22.37}{0.413} \right)^4 \times \frac{\left(\sin \frac{180}{3} \right)^4}{1.91^3} \times \left\{ 1 - \frac{\arctan \sqrt{9.43}}{\sqrt{9.43}} \right\} - \frac{1}{4} \right]^{\frac{1}{2}}$$

$$v_e = 1.78$$

For summer temperature:

$$v_e = \frac{1}{2} + \left[\frac{9}{8} \times 3(3-1) \times \frac{1.257 \times 10^{-6}}{2\pi} \left(\frac{63000}{3} \right)^2 \times 4.52 \times 10^{-9} \times 1.7 \times \left(\frac{22.37}{0.413} \right)^4 \times \frac{\left(\sin \frac{180}{3} \right)^4}{1.98^3} \times \left\{ 1 - \frac{\arctan \sqrt{9.43}}{\sqrt{9.43}} \right\} - \frac{1}{4} \right]^{\frac{1}{2}}$$

$$v_e = 1.70$$

Using the following data

Winter temp.	$v_e = 1.78$	F_{st}= 33 354 N	ξ = 1.91	ε_{st} = 0.497
Summer temp	v_e = 1.70	F_{st} = 15 409 N	ξ = 1.98	ε_{st} = 0.230

we obtain the pinch effect force as

For winter temperature:

$$F_{pi} = F_{st} \left(1 + \frac{v_e}{\varepsilon_{st}} \xi \right) = 33354 \times \left(1 + \frac{1.78}{0.497} \times 1.91 \right) = 2.62 \times 10^5 \text{ N}$$

Copyright © 2010 IEEE. All rights reserved.

Copyright The Institute of Electrical and Electronics Engineers, Inc.
Provided by IHS under license with IEEE
No reproduction or networking permitted without license from IHS

Order Number: 02120914
Sold to:EGAT [700166108393] - VARRIS.Y@EGAT.CO.TH,
Not for Resale,2016-09-15 03:57:47 UTC

For summer temperature:

$$F_{pi} = F_{st}\left(1+\frac{\nu_e}{\varepsilon_{st}}\xi\right) = 15\,409\times\left(1+\frac{1.70}{0.230}\times 1.98\right) = 2.41\times 10^5\ \text{N}$$

In the above calculations, one spacer is used in the middle of the span. Removing the spacer would allow the bundle conductors to clash effectively, without pinch effect.

I.2.4.5 Ice load

Refer to 11.1.3. The ice load data necessary for the calculations are given in Table I.7.

Table I.7—Ice load data

Data	Value
Ice weight divided by volume w_I	8820 N/m^3
Uniform radial ice thickness r_I	0.0127 m
Conductor outside diameter D_o	0.0438 m
Span length	44.74 m
Number of conductors per phase	3

The ice weight by unit length on a single conductor is given by:

$$F_I = \pi\, w_I\, r_I\,(D_o + r_I) = \pi \times 8820 \times 0.0127 \times (0.0438 + 0.0127) = 20.0\ \text{N/m}$$

This ice unit weight corresponds to an additional linear mass of 20/9.81 = 2.04 kg/m. By comparison, the linear mass of the conductor without ice is 3.71 kg/m under winter temperature. The total linear mass of the conductor under winter temperature with ice is therefore 3.71 + 2.04 = 5.75 kg/m. Assuming as a first and conservative approximation that the change of sag under the additional weight of ice is negligible (that is, the sag remains at the previously calculated value of 0.975 m), the final tension with ice for a single conductor is given as:

$$H = \frac{\bar{m}\times g\times l^2}{8\times D} = \frac{5.75\times 9.81\times 48.8^2}{8\times 0.975} = 17\,222\ \text{N} = 17.2\ \text{kN}$$

So that the tension for a bundle of three conductors from the additional weight of ice is equal to:

H_{ice} = 3 x 17.2 = **51.7 kN**

The total vertical load from the weight of ice on a single phase bundle is given by:

$$F_{\text{ice\_vertical}} = 3\times 20.0\times 44.74 = 2684\ \text{N}$$

The supporting structure has to be designed to support the above load for all three phases; assuming that the supporting structures at both ends are at the same height, each support will take for each phase half the vertical load calculated above. Note that this vertical load is in addition to the vertical load from the weight of the conductor itself.

Copyright © 2010 IEEE. All rights reserved.

Copyright The Institute of Electrical and Electronics Engineers, Inc.
Provided by IHS under license with IEEE
No reproduction or networking permitted without license from IHS

Order Number: 02120914
Sold to:EGAT [700166108393] - VARRIS.Y@EGAT.CO.TH,
Not for Resale,2016-09-15 03:57:47 UTC

I.2.4.6 Wind load

Refer to 11.2. The wind load data necessary for calculations is given in Table I.8.

Table I.8—Wind load data

Data	Value
Extreme wind speed V	112 km/h = 31.1 m/s
Wind speed with ice V_I	48 km/h = 13.3 m/s
Conductor height above ground	9.75 m
Conductor outside diameter	0.0438 m
Uniform radial ice thickness r_I	0.0127 m
Constant C in SI units	0.613
Force coefficient C_f (11.2.3)	1.2
Surface roughness	D
Exposure category	D
Exposure factor K_z [Table 7 or Equation (10)]	1.18
Gust factor response factor G_f (Table 11)	0.82
Importance factor I (11.2.6)	1.15
Bus span	44.7 m

The wind load by unit length will be calculated for the extreme wind speed (without ice) and the wind speed with ice.

For the extreme wind speed, the horizontal load by unit length on a single conductor is given by:

$$F_W = CV^2 D_o C_f K_Z G_f I = 0.613 \times (31.1)^2 \times 0.0438 \times 1.0 \times 1.18 \times 0.82 \times 1.15 = 28.9 \text{ N/m}$$

For wind with ice, the horizontal load by unit length on a single conductor is given by:

$$F_{WI} = CV_I^2 \left(D_o + 2 \times r_I\right) C_f K_Z G_f I = 0.613 \times (13.3)^2 \times (0.0438 + 2 \times 0.0127) \times 1.0 \times 1.18 \times 0.82 \times 1.15 = 8.35 \text{ N/m}$$

Since the extreme wind speed gives a higher unit load than the wind speed without ice, the load from the extreme wind speed will be used in design of the supporting structure.

The total horizontal load from the wind on a single phase bundle is given by:

$$F_{\text{wind\_horizontal}} = 3 \times 28.9 \times 44.7 = 3876 \ N = 3.88 \text{ kN}$$

The supporting structure has to be designed to support the above load for all three phases; assuming that the supporting structures at both ends are at the same height, each support will take for each phase half the horizontal load calculated above.

Copyright © 2010 IEEE. All rights reserved.

Copyright The Institute of Electrical and Electronics Engineers, Inc.
Provided by IHS under license with IEEE
No reproduction or networking permitted without license from IHS

Order Number: 02120914
Sold to:EGAT [700166108393] - VARRIS.Y@EGAT.CO.TH,
Not for Resale,2016-09-15 03:57:47 UTC

I.2.5 Summary of results

I.2.5.1 Design force for insulator selection

The selection of a proper insulator will be made according to the maximum tensile force acting on a single bundle of conductors (one phase). The maximum calculated tensile forces from the different loads are summarized in Table I.9, in kN. Here it is assumed that the short circuit forces and additional ice loading do no happen concurrently.

Table I.9—Calculated tensile forces on a single insulator (from one bundle)

Force	Winter	Summer
Static tensile load from weight alone F_{st}	33.4 kN	15.4 kN
Static tensile load from additional weight of ice H_{ice}	51.7 kN	—
Maximum tensile force during the short circuit F_t	49.2 kN	20.5 kN
Maximum tensile force after the short circuit when the conductor drops back F_f	141 kN	148 kN
Maximum tensile force caused by the pinch effect F_{pi} if bundle conductors clashes	262 kN	241 kN

The maximum tensile force is therefore caused by the pinch effect under winter temperature and should be used in selecting the proper insulator. This force could be reduced as discussed by allowing the conductors to clash effectively.

I.2.5.2 Design forces for supporting structures

The supporting structures and their anchorages should be designed such that they can safely withstand the vertical forces from the weight of the conductor (with or without ice), the horizontal forces from the short circuit forces, as well as the lateral load from the wind. The resulting loads are summarized in Table I.10 for one bundle (one phase) and are also given for each support as some should be divided by 2 as shared by both supports. Since three bundles are used, the design should be made considering the application of three times such forces on the supporting structures.

Table I.10—Calculated loads by bundle on one support

Force	Direction	Calculated force for one bundle	Net force by bundle on one support
Static tensile load from weight alone F_{st}	Horizontal	33.4 kN	33.4 kN
Static tensile load from additional weight of ice H_{ice}	Horizontal	51.7 kN	51.7 kN
Maximum tensile force caused by the pinch effect-F_{pi} if bundle conductors clashes	Horizontal	262 kN	262 kN
Total vertical load from weight of ice	Vertical	2.68 kN	1.34 kN
Total lateral load from wind	Lateral	3.88 kN	1.94 kN

Copyright © 2010 IEEE. All rights reserved.

Copyright The Institute of Electrical and Electronics Engineers, Inc.
Provided by IHS under license with IEEE
No reproduction or networking permitted without license from IHS

Order Number: 02120914
Sold to:EGAT [700166108393] - VARRIS.Y@EGAT.CO.TH,
Not for Resale,2016-09-15 03:57:47 UTC